

This file is part of the following work:

**Goldsworthy, Nisha Caretta (2024) *Implications of small body size: ecology and life-history of small and short-lived coral reef fishes of the genus Trimma*. PhD Thesis, James Cook University.**

Access to this file is available from:

<https://doi.org/10.25903/c9kv%2Dvn19>

Copyright © 2024 Nisha Caretta Goldsworthy

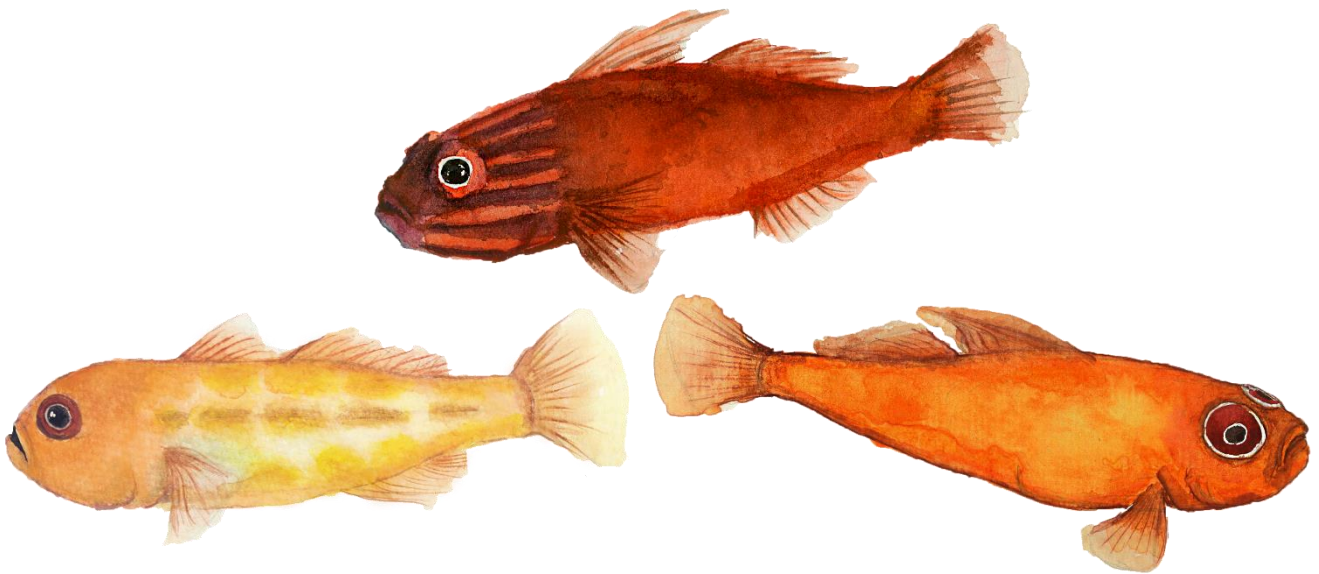
The author has certified to JCU that they have made a reasonable effort to gain permission and acknowledge the owners of any third party copyright material included in this document. If you believe that this is not the case, please email

[researchonline@jcu.edu.au](mailto:researchonline@jcu.edu.au)

# Implications of Small Body Size: Ecology and Life-History of Small and Short-Lived Coral Reef Fishes of the Genus *Trimma*

---

Nisha Caretta Goldsworthy  
BSc, Victoria University of Wellington



A thesis submitted for the degree of Doctor of Philosophy

College of Science and Engineering,  
and the Australian Research Council Centre of Excellence for Coral Reef Studies  
James Cook University

## Acknowledgements

---

The seed of this PhD was first planted on a cold, rainy day in Wellington, New Zealand. I was huddled in a lecture, with my trusty beanie and frosty toes, and that's when it hit me: "I can't endure this cold any longer!" So, with a quick Google search for "tropical marine biology university," James Cook University emerged. "I'll give it a shot!" I thought.

Behind every thesis is an army of supporters. I am immensely thankful to supervisors Geoff Jones, Maya Srinivasan and Patrick Smallhorn-West. Geoff, you granted me the freedom to explore my ideas while providing invaluable guidance. Being one of your last students was an honour and thank you for your wise words of ecological wisdom. Maya, you are an exceptional teacher, a powerful woman, and a fun friend. I aspire to be like you when I grow up 😊. Pat, your unwavering encouragement and positivity carried me through many hurdles. I'm forever grateful for my special supervisory team.

I acknowledge and pay my respects to the elders past and present of the Bindal and Wulgurukaba People, the traditional custodians of the Townsville region where I have lived and worked for the duration of my PhD.

I had the privilege of undertaking my fieldwork in the magical reefs of Kimbe Bay, Papua New Guinea. I express my gratitude to the traditional owners of the Kilu-Tamare reefs for allowing access to your pristine waters. To Jerry and Ricky, our boat drivers and walking GPS's of Kimbe Bay - your local knowledge of the waters and dedication to the team were remarkable. Thank you to the Mahonia Na Dari Research station team, who made research possible in this breathtaking location. Kudos to Somei Jonda for keeping it together, even when half of the Australian government came to your doorstep. I wish to extend my thanks to the Benjamin family and Walindi Plantation Resort for their warm welcome and for facilitating

access to the reefs. Thank you to all the wonderful people we met in Papua New Guinea. To Lau, who was the loveliest and most welcoming lady. Everyone misses you so much, Lau. To Martha and Keat for their constant banter after a long day in the field. Papua New Guinea will forever hold a special place in my heart and the hospitality we were shown by the local people was unforgettable.

This journey wouldn't have been possible without the contributions of these amazing volunteers: Amy Coppock, Kelsey Webber, and Marta Panero, your fish-catching skills were truly impressive! Lachlan Drane and Ronja Schuetz-Steyer, for all your hard work and your ability to turn disasters into fun moments. I will never forget this field trip and the great times we had, visa troubles aside. Jessica Zacharuk and Martina Zucchi, thank you for your plankton identification skills and your courage to analyse the stomach contents of a 20 mm fish.

My gratitude extends to those who offered their expertise and advice: Jake Lowe, Gemma Galbraith, Murray Logan, and Derek Ogle for help with statistics; Sterling Tebbet and Mike Mixalitsis for providing their expert eco-morphology advice; Mark O'Callaghan and Kyle Hillcoat for all things otoliths, Lit-Chien Cheah for histology skills; Philip Munday and Rick Winterbottom for insights into everything gobies. There are many others who have lent their advice throughout this PhD.

To the incredible Jones Lab and Keppels 3 team – including Maya Srinivasan, Lachlan Drane, Ben Cresswell, Gemma Galbraith, Amy Coppock, Tess Jenkins, Patrick Smallhorn-West, Saul Gonzalez-Murcia, Hugo Harrison, Daniella Ceccarelli, Brock Bergseth, Jake Lowe, Maren Toor, and, of course, Geoff Jones himself. The unwavering support of these individuals made me realize that I could indeed complete a PhD despite my doubts. Every return from a Keppels field trip left me bursting with renewed inspiration. Gemma, a special thanks to you



for sharing my enthusiasm for a frog meme and for your knack for making the PhD journey feel less intimidating!

To all my whānau, especially mum, dad, Jayan, Savita, and auntie Madhu. It is by mere chance that I was birthed into a loving, inspirational family that is supportive of all my crazy decisions from day one. I thank my lucky stars each day for all of you. To my 90-year-old Grandad “you’ve all done well you lot...none of you are junkies”. I’m grateful his standards weren’t overly demanding. Love you Grandad! To my wonderful friends, both those I’ve known before and those I’ve met on this journey who have played unique roles. I would specifically like to mention Lauren Huet, my soul sister, for being my number one supporter while I was tirelessly measuring otolith rings in the lounge during COVID lockdown. I couldn’t have done it without you! Last (but definitely not least!) to JUJU! You are my best friend. Thank you for showing me the beauty of the world in a way I have never seen before.

*Tēnā rawa atu koutou!*



## Statement of the Contribution of Others

---

Prof. Geoffrey Jones, Dr. Maya Srinivasan, and Dr. Patrick Smallhorn-West provided supervision for this thesis. Supervisors contributed to shaping the research ideas and offered guidance, intellectual insights, and editorial support. I was responsible for formulating the research questions, gathering, and analysing all data, and composing all the chapters. All research endeavours were carried out in accordance with the James Cook University Animal Ethics Guidelines (approval number A2665 and A2872) under a research visa allocated to Professor Geoffrey Jones and Nisha Goldsworthy issued by the government of Papua New Guinea. Local permissions were granted by: Mrs. Cecilie Benjamin (Chair of the Board, Mahonia Na Dari Research and Conservation Centre, Kilu) and Mr. Thomas Koi, (Village Elder and representative of the Local Marine Management Committee, Kilu).

For Chapter 3 (published in the *Journal of Fish Biology*), Prof. Philip Munday contributed to the initial project conceptualisation and methodology and provided editorial advice and Lit-Chien Cheah provided laboratory assistance. For Chapters 4 and 5, Dr. Gemma Galbraith contributed to the development of ideas and provided statistical assistance.

This research was funded by

- the Australian Research Council Centre of Excellence in Coral Reef Studies research allocation to GPJ (CE0561435).
- College of Science and Engineering Research Training Grant
- The Julia Cooper Memorial Wildlife Research Bursary
- The Joyce and George Vaughan Bequest Scholarship
- Australian Government Research Training Program Fee Offset Scholarship

## General Abstract

---

Small body size can significantly impact an animal's fundamental ecological and life history traits. Coral reefs host a wide size range of fishes, from the smallest vertebrates on Earth that are less than 20 mm as adults, to those exceeding 1000 mm in length. Body size may influence the habitat use, life history traits including reproductive strategies and growth, and trophic dynamics of coral reef fishes. Understanding the implications of small body size on such ecology and life history characteristics is important as it can directly impact functional roles of organisms on coral reefs.

Small cryptic coral reef fishes that occupy benthic habitats are known as cryptobenthic reef fishes (CRFs). CRFs can be incredibly diverse, abundant, and have important functional roles. Such fishes may exhibit short lifespans, linear growth, early maturation, and high mortality, leading to a fast generational turnover and high productivity over time. Additionally, many of these fishes are planktivorous and convert microscopic prey into biomass which can be funnelled to larger consumers. As a result, CRFs have the potential to be a vital ecosystem component. However, the ecological significance of CRFs is often overlooked as they have low standing biomass and are difficult to conduct research on due to their small size. Consequently, little is known about the fundamental ecology and life history of most CRF species.

The genus *Trimma* is among the smallest and shortest-lived CRFs. The small body size of these Indo-Pacific fishes may impact their life history and ecology, and potentially affect their functional roles. Nonetheless, little is known about these characteristics. **This thesis therefore aims to assess the habitat, life history, and trophic ecology of cryptobenthic coral reef fishes of the genus *Trimma*.** The study site of this thesis was Kimbe Bay, Papua New Guinea, a biodiverse area that holds a diverse array of *Trimma* species. The top three most

abundant species, *Trimma benjamini*, *T. capostriatum*, and *T. yanoi*, were selected as study subjects. This is the first study on *Trimma* in this location.

The thesis is structured into four main data chapters. **Chapter 2** used a combination of active visual search transects and observational behavioural studies to answer the question: *How do ecologically similar Trimma species partition habitats and does this occur at small spatial scales?* Factors reef location (inshore vs offshore), reef aspect (slope vs wall) and depth (4, 6 and 10 m) had significant effects on the distribution of each species but impacted each species' abundance differently. Furthermore, there were differences in population clustering among the three species, which may have an influence on the varying habitat preferences of *Trimma*. Habitat variations among species were also found on small scales, where there were differences in the microhabitats that each species was present on. Accordingly, spatial overlap of the studied species was minimal and there were few interactions among the target *Trimma* species. This chapter demonstrates how closely related, physiologically similar, or ecologically alike CRFs can partition habitats and coexist at small scales, potentially contributing to their diversity.

I used otolith microstructure and gonad histology in **Chapter 3** to answer the question *What life history constraints and reproductive strategies do Trimma possess?* Each species exhibited extremely high mortality rates, short maximum lifespans, long pelagic larval phases relative to lifespan, and a reduced time available to reproduce. All mature individuals had bisexual gonads including both ovarian and testicular portions, with only one sex being active at the same time in most individuals. These gonad structures were consistent with rapid bidirectional sex change. Chapter 3 showcases the life history hurdles that small CRFs encounter and illustrates how efficient reproductive strategies could benefit them, given these limitations.

**Chapter 4** asked the question *What are the larval, juvenile, and adult growth patterns, and generational turnover rates of Trimma?* This chapter used back-calculation growth models and the life history stages determined in Chapter 3. The three *Trimma* species had short lifespans and high population turnover. Growth was rapid in the larval phase, slowed in the juvenile phase, and slowed further in adulthood. However, decelerations in growth following maturity were minimal compared to larger fishes, with a considerable proportion of growth still occurring in the adult phase. These atypical life history traits could be linked with high mortality and ecological roles as productive food sources for reef dwellers.

Finally, **Chapter 5** asked *What are the food sources, feeding methods, and predation pressures of Trimma? Do Trimma possess morphological traits that may assist feeding or predator avoidance?* I examined stomach composition, undertook observational studies, and measured several eco-morphological traits. Most individuals were actively feeding at high rates, consuming mainly pelagic zooplankton (molluscs and gastropod veligers, and copepods). *Trimma* gape and eye morphology were suitable for obtaining such prey. Complete predation was not observed, but *Trimma* displayed antipredator responses to fishes of the family Labridae. In addition, *Trimma* possessed characteristics that could make them difficult to see or capture, including cryptic body colours, an elongated body shape, and low caudal fin aspect ratio. Chapter 5 sheds light on the potential trophic roles of *Trimma* in importing energy from the pelagic environment and transferring it to predatory organisms.

Altogether, this thesis suggests that species of the genus *Trimma* exhibit unique ecology and life history strategies that are not seen in larger fishes. These traits may be a product of their small maximum body size and could have implications for biodiversity, energy productivity, and energy transfer on Indo-Pacific coral reefs. My research also underscores the necessity for further investigations aimed at establishing links between life history and ecology.

The summation of these results adds to a growing body of research suggesting that small fishes may have important functional roles and therefore should be considered in the management and conservation of present and future coral reefs.

## Table of Contents

---

Acknowledgements.....	1
Statement of the Contribution of Others.....	4
General Abstract.....	5
Table of Contents.....	9
List of Tables.....	12
List of Figures.....	14
Chapter 1: General Introduction.....	18
1.1 Implications of body size for animal ecology and life history.....	18
1.2 Coral reef fishes.....	19
1.3 Cryptobenthic reef fishes.....	20
1.4 Habitat use and partitioning.....	21
1.5 Life history constraints and reproductive characteristics.....	22
1.6 Growth patterns across life history stages.....	23
1.7 Trophodynamics.....	24
1.8 The genus <i>Trimma</i> .....	24
1.9 Current knowledge and research gaps of <i>Trimma</i> ecology and life history.....	25
1.10 Aims and Questions.....	26
Chapter 2: Same-same but different: Habitat use and partitioning of three cryptobenthic coral reef fishes of the genus <i>Trimma</i> .....	30
2.1 Abstract.....	30
2.2 Introduction.....	31
2.3 Methods.....	35
2.3.1 Study sites.....	35
2.3.2 Visual surveys.....	35
2.3.3 Simulating population clustering.....	36
2.3.4 Behavioural observations.....	38
2.3.5 Data analysis.....	38
2.4 Results.....	41
2.4.1 Broad scale spatial patterns.....	42
2.4.2 Population clustering.....	45
2.4.3 Microhabitat.....	47
2.4.4 Interspecific interactions among the <i>Trimma</i> species examined.....	49
2.5 Discussion.....	50

Chapter 3: Life history constraints, short adult lifespan, and reproductive strategies in coral reef gobies of the genus <i>Trimma</i> .....	58
3.1 Abstract .....	58
3.2 Introduction.....	59
3.3 Materials and Methods.....	63
3.3.1 Species, specimen collection and ethical statement.....	63
3.3.2 Body size, longevity, and mortality .....	63
3.3.3 Pelagic Larval Duration .....	65
3.3.4 Maturation.....	65
3.3.5 Reproduction.....	66
3.4 Results.....	67
3.4.1 Body size, longevity, and mortality .....	67
3.4.2 Pelagic larval duration .....	71
3.4.3 Maturation.....	71
3.4.4 Reproduction.....	74
3.5 Discussion.....	75
Chapter 4: Growth strategies across life history stages and generational turnover of cryptobenthic coral reef fishes of the genus <i>Trimma</i> .....	83
4.1 Abstract .....	83
4.2 Introduction.....	84
4.3 Methods.....	88
4.3.1 Study site, specimen collection and sample processing .....	88
4.3.2 Otoliths processing and determination of age and increment measurements .....	89
4.3.3 Establishing age at life history milestones and generational turnover.....	89
4.3.4 Assessing the otolith-somatic growth (OSG) relationship.....	90
4.3.5 Back-calculation of lengths at previous ages.....	91
4.3.6 Population growth curves .....	91
4.3.7 Back calculation model selection .....	92
4.3.8 Growth throughout larval, juvenile, and adult life history stages.....	92
4.4 Results.....	93
4.4.1 Body size, age, and generational turnover .....	93
4.4.2 Validating age at settlement using increment widths.....	93
4.4.3 Assessing the otolith-somatic growth (OSG) relationship.....	94
4.4.4 Back-calculation of lengths at previous ages.....	94
4.4.5 Population growth curves .....	94
4.4.6 Back calculation model selection .....	95



4.4.7 Growth throughout larval, juvenile, and adult life history stages.....	100
4.5 Discussion.....	102
Chapter 5: Trophic dynamics of three small and short-lived coral reef fishes of the genus <i>Trimma</i> .....	108
5.1 Abstract.....	108
5.2 Introduction.....	109
5.3 Methods.....	113
5.3.1 Study site, specimen collection, and sample processing .....	113
5.3.2 Observational studies .....	114
5.3.3 Dietary composition.....	115
5.3.4 Morphological traits.....	115
5.3.5 Data processing and analysis .....	115
5.4 Results.....	118
5.4.1 Proportion actively feeding, feeding rate, and pelagic vs. benthic contributions .....	119
5.4.2 Dietary composition.....	120
5.4.3 Interferences.....	122
5.4.4 Morphological traits.....	124
5.5 Discussion.....	127
Chapter 6: Conclusions and Future Directions .....	137
References.....	144
Appendix 1: Supplementary Information for Chapter 2 .....	177
Appendix 2: Supplementary Information for Chapter 3 .....	196
Appendix 3: Supplementary Information for Chapter 4 .....	197
Appendix 4: Supplementary Information for Chapter 5 .....	207

## List of Tables

---

Table 2.1: Optimum models from a series of generalised linear models and generalised linear mixed effect models selected by AIC. Left to right: response variable, fixed effects of optimum model, random effects of optimum model, and optimal probability distribution with the appropriate link function.....	41
Table 2.2: Estimated cluster size (mean number of individuals per cluster), cluster density (mean number of individuals per m <sup>2</sup> in a cluster), and proportion of individuals considered solitary (%) for species <i>Trimma benjamini</i> , <i>T. capostriatum</i> and <i>T. yanoi</i> . Values represent the estimated modelled means, with 95% lower confidence levels (LCL) and 95% upper confidence levels (UCL) derived from the model distribution in Table 2.1, shown in brackets below estimated means. <i>n</i> = sample size. ....	46
Table 2.3: Percentage of individuals that engaged in interactions with an individual of a different <i>Trimma</i> species (i.e., chased or were chased by another <i>Trimma</i> ), and species that the interaction occurred with. Confidence intervals below proportions were derived from a Binomial distribution (McKeon et al., 2012).....	50
Table 3.1: Results for <i>Trimma benjamini</i> ( <i>n</i> = 129), <i>T. capostriatum</i> ( <i>n</i> = 102) and <i>T. yanoi</i> ( <i>n</i> = 122) showing a) Maximum recorded lifespan (days) and body size ( <i>L<sub>s</sub></i> , mm), b) Daily mortality estimated by Hoenig's equation, the Chapman-Robson estimator and catch-curve regression estimator and c) Age (days) and length (mm, proportion of max <i>L<sub>s</sub></i> ) at maturity. *mean ± 95% confidence intervals .....	68
Table 4.1: Estimated generational turnover (days) and number of generations per year for <i>Trimma benjamini</i> ( <i>n</i> = 129), <i>T. capostriatum</i> ( <i>n</i> = 102), and <i>T. yanoi</i> ( <i>n</i> = 122).....	97
Table 4.2: Proportion of growth that occurred in larval, juvenile, and adult life history phases relative to total growth. Values are derived from the Body Proportional Hypothesis optimum growth equations (Figure 4.4).....	101

Table 5.1: Dietary composition of *Trimma benjamini*, *T. capostriatum*, and *T. yanoi*. Mean relative numerical abundance (%N), mean relative size (%S), relative frequency of occurrence (%F), and the index of relative importance (%IRI) of each food group. n = 15 individuals per species ..... 120

## List of Figures

---

Figure 2.1: Above) Map of Kimbe Bay, West New Britain, Papua New Guinea, and the three inshore and three offshore study sites. Below) *In situ* photographs of *Trimma benjamini* (left), *T. capostriatum* (centre), and *T. yanoi* (right). .....37

Figure 2.2: Modelled mean counts per 20 X 1 m transect of a) *Trimma benjamini*, b) *T. capostriatum*, and c) *T. yanoi* individuals at different reef locations (inshore, offshore) reef aspects (slope, wall) at varying depths (4, 6, 10 m)  $\pm$  95% confidence intervals. Models have taken variation in abundance among sites into account where necessary. n = 108 transects. .44

Figure 2.3: Mean proportions of individuals present per m<sup>2</sup> quadrat in each microhabitat category for *Trimma benjamini*, *T. capostriatum*, and *T. yanoi*. Bars represent 95 % confidence intervals, derived from a Binomial distribution (McKeon et al., 2012). .....46

Figure 2.4: a) Area-proportional Euler diagram showing the proportion of m<sup>2</sup> quadrats occupied by lone species (*Trimma benjamini*, *T. capostriatum* and *T. yanoi*, shown by non-overlapping regions) relative to the proportion of m<sup>2</sup> quadrats occupied by multiple species (shown by overlapping regions). Total estimated overlap of each species is illustrated in square boxes. Values represent the modelled means, with 95% lower and upper confidence levels derived from a Binomial distribution shown in brackets below means. b) Proportion of individuals present in the same microhabitats in m<sup>2</sup> quadrats where species co-existed. Error bars display the 95% confidence intervals derived from a Binomial distribution (McKeon *et al.*, 2012). .48

Figure 2.5: Conceptual diagram summarising 1) Partitioning of broad scale habitats (i.e., reef location, aspect, depth). Points and arrows indicate the area each species occurred in greatest abundance. 2) Microhabitat partitioning. 1 and 2 combined resulted in 3) Minimal spatial overlap, co-existence of species, and territorial behaviour in rare cases of habitat overlap. Teal = *Trimma benjamini*, purple = *T. capostriatum*, yellow = *T. yanoi*. .....57

Figure 3.1: a) *Trimma yanoi* otolith showing daily growth increments and a change in optical density pre- and post-settlement. Arrows indicate settlement mark. Not all pre-settlement

increments are visible in this focal plane. b) Frequency distribution of pelagic larval duration (PLD) in *Trimma benjamini* (n = 129), *T. capostriatum* (n = 102) and *T. yanoi* (n = 122). ...69

Figure 3.2: 10-day age-frequency catch curve regression for the estimation of instantaneous mortality ( $Z$ ) for a) *Trimma benjamini* (n = 129), b) *T. capostriatum* and c) *T. yanoi* (n = 122). White points show ascending limb values which were not included in the analysis and black points show descending limb values that were included in the analysis. ....70

Figure 3.3: Number of days and percentage of maximum lifespan (mean  $\pm$  95% confidence intervals) spent in each life stage (pelagic larvae, juvenile and adult) for *Trimma benjamini* (n = 129), *T. capostriatum* (n = 102) and *T. yanoi* (n = 122). Dotted and dashed lines represent settlement and maturity, respectively. ....72

Figure 3.4: Proportional frequency distributions of the sexual phase-specific age and length structure of a) *Trimma benjamini* (n = 129), b) *T. capostriatum* (n = 102) and c) *T. yanoi* (n = 122). Estimated age and length at maturity trajectory is shown by solid logistic regression lines and the associated 95% confidence intervals are shown by dashed lines. ....73

Figure 3.5: Gonadal structures of a & b) Female, c) Male, d) Simultaneous hermaphrodite, e) Transitional, and f & g) Juvenile phases in *Trimma benjamini* (a, d & f), *T. capostriatum* (c) and *T. yanoi* (b, e, & g). *O* ovary, *T* testis, *AGS* accessory gonadal structure, *GB* gas bladder, *DT* digestive tract, *PV* previtellogenic oocyte, *V* vitellogenic oocyte, *HV* hydrated vitellogenic oocyte, *AV* atretic vitellogenic oocyte, *SD* sperm ducts filled with spermatozoa, *GS* germ cells. n = 129 *Trimma benjamini*, 102 *T. capostriatum* and 122 *T. yanoi*. Scale bar 200  $\mu$ m. ....76

Figure 4.1: a) Photograph of a whole processed *Trimma yanoi* otolith. b) Enlarged image showing daily growth increments from the otolith primordium to edge. Circled and enlarged is the settlement region. Arrow points to the settlement mark. Note that not all rings are visible at these magnifications. c) Widths of growth increments measured in a straight line 90 degrees from the longest axis. d) Mean increment width ( $\pm$  95% confidence intervals) at each increment number from the settlement-mark (i.e., settlement = 0 indicated by the dashed line. ....96

Figure 4.2: Age (days) and standard length (mm) frequency distributions in *Trimma benjamini*, *T. capostriatum* and *T. yanoi*. Dashed line represents the mean. ....97

Figure 4.3: Relationship between otolith radius and somatic growth (OSG relationship). Displayed are the best fitting models for each species: a second – degree polynomial in *T. benjamini* and *T. yanoi* and a generalised linear model in *T. capostriatum*. .....98

Figure 4.4: a & b) Modelled population growth curves across larval, juvenile, and adult life history stages for *Trimma benjamini*, *T. capostriatum*, and *T. yanoi*. Solid regression lines and shaded ribbons represent polynomial mixed-effects models of the 4th degree  $\pm$  95% confidence intervals (model equations for each species are displayed in a box). Dashed and dotted lines represent the age at settlement and maturity for each species, respectively. a) Displays growth curves fitted to individual fish growth trajectories back-calculated using the Body Proportional Hypothesis model. b) Illustrates growth curves against the ages (days) and standard lengths (mm) of individuals at the time of capture. Residual plots depict the deviations between the population growth model and observed ages and lengths at capture, with lines showing a locally weighted regression smoother applied to these residuals. ....99

Figure 4.5: a) Mean back-calculated growth rate (mm/day  $\pm$  95% confidence intervals) in larvae, juvenile, and adult life history phases, derived from the Body Proportional Hypothesis optimum population growth equations (Figure 4.4). b) Pairwise comparisons showing the mean difference (mm/day  $\pm$  95% confidence intervals) in growth between each life history phase. In a and b, species *Trimma benjamini*, *T. capostriatum* and *T. yanoi* are represented by different colours..... 101

Figure 5.1: a) Proportion of individuals that were actively feeding during the observation period. Error bars represent the 95 % confidence intervals derived from a Binomial distribution (logit link) (McKeon et al., 2012). b) Mean feeding rate per minute  $\pm$  95% Negative Binomial confidence intervals. c) Predicted proportion of feeding events that were pelagic, where food items were captured from the water column. 95 % confidence intervals were derived from a Binomial distribution (McKeon et al., 2012). For a and b,  $n = 369$  *T. benjamini*, 167 *T. capostriatum*, and 259 *T. yanoi* individuals. For c,  $n = 2152$  *T. benjamini*, 974 *T. capostriatum*, and 1178 *T. yanoi* feeding events. .... 118

Figure 5.2: a) Proportion of individuals (%) that were interfered with by a conspecific, Labridae, or other fish during the observation period. Error bars represent the 95% confidence intervals derived from a Binomial distribution (McKeon et al., 2012).  $n$  represents the number

of individuals in each category. b) Mean feeding rate per minute ( $\pm$  95% Negative Binomial distribution derived confidence intervals) for each interference category. c) Pairwise comparisons showing the mean differences ( $\pm$  95% confidence intervals) of the feeding rate of individuals that experienced interferences compared to those that did not. Ratio represents fold differences, where mean values and confidence levels crossing 1 hence indicate no significant difference. For a and b shapes represent the interference category. For a, b, and c, colour represents each species *Trimma benjamini* (n = 369), *T. capostriatum* (n = 166), and *T. yanoi* (n = 259)..... 123

Figure 5.3: a) Macro images of *Trimma benjamini*, *T. capostriatum*, and *T. yanoi* heads. Scale bars = 1 mm. b) Biplots of the relative horizontal gape plotted with relative eye diameter measurements, as a percentage of standard length. Dashed lines represent the mean value for each morphological trait, and points represents the relative eye and gape measurement of each individual fish. 95% confidence intervals are shown in brackets below the mean values. n = 94 *T. benjamini*, 74 *T. capostriatum*, and 99 *T. yanoi*. c) Biplot containing information for each species in a plotted on a singular graph. Plus symbol represents the mean morphological trait measurements for each species. Solid lines dividing the biplot represents overall average for fishes. Crecent moon and sun represents the nocturnal and diurnal average for fishes retrieved from Goatley and Bellwood (2009). Top left quadrat holds individuals with a larger eye and smaller mouth than the average for fishes, top right contains individuals with a larger eye and mouth than average, bottom left contains individuals with a smaller eye and mouth than average, and bottom right has individuals with a smaller eye and larger mouth than average. .... 125

Figure 5.4: a) Images of live *Trimma benjamini*, *T. capostriatum*, and *T. yanoi*. Graph below images shows the mean elongation values ( $L_S$ /maximum body depth) of each species b) Macro images of *Trimma benjamini*, *T. capostriatum*, and *T. yanoi* caudal fins. Graph below images shows the mean caudal fin aspect ratios (fin height<sup>2</sup> / fin area) of each species. For a and b, error bars represent the 95% confidence intervals derived from a gaussian distribution. Scale bars = 2 mm. .... 126

Figure 5.5: Conceptual image of *T. benjamini in situ* displaying how body colour can assist with crypsis by camouflage with the substratum (right), or at depths (9 m, left) where low frequency and long wavelength colours are filtered. .... 134

## Chapter 1: General Introduction

---

### 1.1 Implications of body size for animal ecology and life history

Body size is an important trait among animals that can influence many fundamental ecological and evolutionary parameters (Hanken & Wake, 1993; Marzluff & Dial, 1991; May, 1978; Peters, 1983; Roff, 1992). Animals with large body sizes exhibit distinct life history features relative to their smaller counterparts (Calder, 1984; Peters, 1983). Large animals tend to have traits such as reduced mortality rates, prolonged lifespans, delayed maturation, and long generation times (Calder, 1984; Roff, 1992; Stearns, 1992). Many are rare and threatened keystone species and are therefore often viewed as the most important components of ecosystems, and consequently receive substantial research focus and funding (Tensen, 2018).

In contrast, smaller-bodied animals experience high mortality rates, rapid and/or continuous growth patterns, shorter lifespans, and increased reproductive effort early in life (Calder, 1984; Roff, 1992; Stearns, 1992). Although often overlooked due to their size, small animals can occupy many small niches compared to larger animals and can be extremely diverse at local scales (Hutchinson & MacArthur, 1959; Schoener, 1974). In addition, small animals have life history strategies that result in rapid turnover rates and high productivity over time (Marzluff & Dial, 1991; May, 1978) and are often important links within food webs, connecting microscopic food to higher trophic levels (Brandl *et al.*, 2018; Yodzis, 2001). As such, small animals may play critical, albeit underappreciated, roles in many ecosystems, which can have implications for conservation and management efforts (Brandl *et al.*, 2019; Scudder, 2017). However, understanding these processes first requires a foundational knowledge of the ecology and life history of organisms in these environments, including an animal's habitat use, reproductive strategies, growth patterns and trophic dynamics (Odum,



1971), all of which are fundamentally linked to body size (Calder, 1984; Roff, 1992; Stearns, 1992).

## 1.2 Coral reef fishes

Coral reefs are among the most diverse and ecologically complex systems on Earth (Alfaro *et al.*, 2007; Roberts *et al.*, 2002). There is an increasing urgency to understand the ecology of organisms on coral reefs (Bellwood *et al.*, 2003; Villéger *et al.*, 2017), which are highly threatened due to a combination of anthropogenic and natural environmental disturbances (Bruno *et al.*, 2007; Hoegh-Guldberg *et al.*, 2007; Hughes *et al.*, 2003; Pratchett *et al.*, 2011). The fish fauna are vital constituents of ecosystem functioning on coral reefs (Hoegh-Guldberg *et al.*, 2019), and there are upwards of 6,300 known species that reside in these habitats (Brandl *et al.*, 2018). Among teleost fishes, body size varies significantly, spanning from the smallest and shortest-lived vertebrate on Earth, *Eviota sigillata*, which grows to a mere 20 mm and has a maximum lifespan of 59 days (Depczynski & Bellwood, 2005a), to large species such as *Bolbometopon muricatum*, which can reach lengths of up to 1200 mm and live for over 30 years (Andrews *et al.*, 2015; Taylor *et al.*, 2018). Although collectively coral reef fishes represent a well-examined group of organisms, current knowledge of them is skewed, with greater understanding of larger or visually prominent species than their smaller or cryptic counterparts (Bellwood *et al.*, 2020). For example, research on conspicuous Pomacentridae and Chaetodontidae families accounted for more than 46% of studies. Less than 9% of studies included the families Gobiidae and Blennidae, which are among the smallest fishes on the reef (Bellwood *et al.*, 2020). Despite this, there is increasing evidence to suggest small and cryptic fishes have important ecological roles (Brandl *et al.*, 2019; Depczynski & Bellwood, 2003).

### 1.3 Cryptobenthic reef fishes

Small fishes with adult body sizes of <50 mm, benthic habitats, and cryptic traits are known as cryptobenthic reef fishes (CRFs) (Brandl et al., 2018; Goatley & Brandl, 2017). The diversity of this group is remarkable. CRFs encompass an estimated 2799 species, accounting for 44% of all documented fishes, including numerous species that remain undescribed (Brandl et al., 2018). CRFs are also highly abundant on coral reefs, and make up an average of 50% of the total fish abundance on the Great Barrier Reef and up to 95% in the Gulf of California Galland *et al.* (2017). CRF diversity, abundance, and several aspects of their habitat use, reproductive strategies, growth patterns, and trophodynamics suggest CRFs could be important components of energy and nutrient transfer on coral reefs (Brandl et al., 2019).

CRFs have not always been recognised as significant in the past and continue to be subjects of subconscious study biases due to their small body size and cryptic appearance (Bellwood et al., 2020). As a result of these traits, it is challenging to estimate abundances when surveying fish assemblages unless searching for particular species (Ackerman & Bellwood, 2000; Munday *et al.*, 1997). Standard underwater visual census is the most common technique used to survey fish assemblages and can underestimate the number of CRF species and density by up to 91% (Ackerman & Bellwood, 2000; Willis, 2001). This can lead to inaccurate conclusions that CRFs have low abundances and consequently, they are often removed from studies (Ackerman & Bellwood, 2000). In addition, CRFs have low standing biomass as a result of their small body sizes (Ackerman & Bellwood, 2000; Morais & Bellwood, 2019). Many studies use standing biomass to measure productivity (Morais & Bellwood, 2019; terHorst & Munguia, 2008). However, biomass does not reflect how productive organisms are, as it does not consider life history traits (e.g., longevity, growth and mortality), which significantly influences productivity (Morais & Bellwood, 2019, 2020).

These biases can result in the misleading assumption that CRFs are insignificant energy contributors to coral reefs (Ackerman & Bellwood, 2000; Bellwood et al., 2020; Morais & Bellwood, 2019) and accordingly, CRFs remain among the least understood group of coral reef inhabitants (Brandl et al., 2018). Little is known about the fundamental ecology and life history of most species that fall into this group. This lack of knowledge is problematic as it likely causes us to miss key components of ecosystem functioning (Brandl et al., 2019).

#### **1.4 Habitat use and partitioning**

Intense competition for essential resources such as habitat or food can arise when these commodities are limited (Connell, 1983; Schoener, 1983). Niche partitioning of spatial resources can alleviate competition among species with similar ecological characteristics (Ross, 1986), which can sustain biodiversity by enabling the coexistence of sympatric species (Chesson, 2000; Connell, 1978; MacArthur, 1958; Schoener, 1974). Following the trends of larger fishes, CRFs may partition spatial resources based on factors such as across continental shelves (Goatley *et al.*, 2016), among reef zones (Depczynski & Bellwood, 2005b), among regions with varying topography (Glavicic *et al.*, 2016), and among depths (Tornabene *et al.*, 2016). However, unlike their larger counterparts, CRFs may also partition habitats on very small spatial scales as a result of their small body size and close contact with benthic structures (Brandl et al., 2018). Some CRFs partition habitats by occupying a single type of coral exclusively (Dirnwöber & Herler, 2007; Munday, 2001; Munday et al., 1997). Others have preferences for different substratum types or reef structures (Clarke, 1994; Depczynski & Bellwood, 2004; Doll *et al.*, 2021; Herler, 2007; Tornabene *et al.*, 2013; Wilson *et al.*, 2013). Within select CRF genera, intricate habitat partitioning has been connected to their high levels of diversity by enabling the co-existence of species (Herler *et al.*, 2011; Munday & Jones, 1998; Munday *et al.*, 2004).

### 1.5 Life history constraints and reproductive characteristics

Small body size may come with a suite of life history constraints that have the potential to impact reproductive ability. Many CRFs face the challenges of reduced longevity of less than one year and extreme natural mortality every day (Depczynski & Bellwood, 2006; Hernaman & Munday, 2005a, 2005b). In addition, CRFs face two critical life milestones that can result in a reduced time available for reproduction. The first of these is the pelagic larval duration (PLD), which occurs in most coral reef fishes preceding settlement onto the reef (Leis & McCormick, 2002). The second is the juvenile stage, which occurs post-settlement onto the reef and prior to the age at maturity (Hernaman & Munday, 2005b). The PLD and juvenile life history stages of CRFs are exclusively devoted to growth and development rather than reproduction. Both may constitute a substantial portion of their short lives (Depczynski & Bellwood, 2006; Hernaman & Munday, 2005b; Leis & McCormick, 2002).

CRFs may have reproductive characteristics that could be beneficial for overcoming high mortality and a limited time available for reproduction (Benvenuto *et al.*, 2017; Brandl *et al.*, 2019; Munday *et al.*, 2010). Some CRFs have the ability to change sex in both directions, from female to male and vice versa (Munday *et al.*, 2010), which can be inferred by the structure of their gonads. This is known as bidirectional sex change and is rare among larger coral reef fishes, but highly prevalent in CRFs (Kuwamura *et al.*, 2020). Bidirectional sex change is frequently observed in habitat-specialist CRFs, which may face limited opportunities to establish new partners after losing a mate, and movement between habitats is too risky (Munday *et al.*, 1998). In other CRFs, bidirectional patterns of sex change might be an advantage where high and unpredictable mortality may result in the constant change of social structure in polygynous hierarchies (Munday *et al.*, 2010).

## 1.6 Growth patterns across life history stages

Growth patterns differ substantially both among animal species and across life stages of individuals, and can have an impact on population dynamics (Peters, 1983). Some animals have determinate growth, where they reach their adult body size early in life and stop growing following maturity, while others have indeterminate growth and continue to grow throughout their lifespan (Lincoln *et al.*, 1982; Sebens, 1987). Most coral reef fishes have a pelagic larval phase, a juvenile phase and an adult phase, and growth patterns vary across these stages (Anderson, 1988; Leis & McCormick, 2002; Sale, 2002). Most fishes have fast larval growth, which slows after settlement onto the reef (Beeken *et al.*, 2021; Leis & McCormick, 2002). Coral reef fishes often exhibit rapid larval growth, as faster growing larvae have an increased likelihood of successful recruitment and survival (Depczynski & Bellwood, 2006; Goatley & Bellwood, 2016). In the CRFs studied, growth tends to differ from larger fishes by having unique patterns of continuous growth at linear or near linear rates following maturity (Beeken *et al.*, 2021; Depczynski & Bellwood, 2006; Winterbottom *et al.*, 2011; Winterbottom & Southcott, 2008). This contrasts with larger fishes, where growth slows substantially or stops completely in adulthood (Choat & Robertson, 2002). In addition to growth, body size can impact population regeneration, where small body size and continuous growth is generally associated with fast turnover rates (Depczynski & Bellwood, 2006). The larval, juvenile, and adult growth patterns and generational turnover of CRFs might have implications for their ecological function as productive and highly regenerative food sources for other reef animals (Ackerman & Bellwood, 2000; Beeken *et al.*, 2021; Brandl *et al.*, 2018; Brandl *et al.*, 2019; Depczynski & Bellwood, 2006; Depczynski *et al.*, 2007; Galland *et al.*, 2017; Winterbottom *et al.*, 2011).

## 1.7 Trophodynamics

Understanding the ecological roles of animals can be facilitated by identifying their trophic niche, which includes determining their feeding ecology and the predators that consume them (Mouillot *et al.*, 2013; Silvertown, 2004). The trophic roles of CRFs could be particularly significant due to several features of their ecology and life history. First, CRFs generally have high energy requirements that require increased food intake relative to their body size (Brandl *et al.*, 2018), and their high abundances combined with continuous growth, short lifespans, efficient reproduction, and fast turnover rates contribute to high biomass productivity over time (Brandl *et al.*, 2019; Depczynski *et al.*, 2007; Goldsworthy *et al.*, 2022; Morais & Bellwood, 2019). Finally, CRFs play a role in multiple trophic pathways, exploiting resources unavailable to higher trophic levels, and are important prey for larger predators due to their small body size (Depczynski & Bellwood, 2003; Goatley *et al.*, 2017; Goldsworthy *et al.*, 2022). As such, CRFs could be important for energy production and transfer within coral reef ecosystems, with one study demonstrating they account for almost 60% of consumed reef fish biomass (Brandl *et al.*, 2019). A comprehensive analysis of trophic dynamics in CRFs is achieved through methods like gut content analysis, observational studies, and morphological trait analysis, each helping to elucidate aspects of their prey acquisition and predator avoidance (Bierwagen *et al.*, 2018; Goatley & Bellwood, 2009).

## 1.8 The genus *Trimma*

The genus *Trimma* (family Gobiidae) is a highly diverse group of CRFs with 105 species currently documented (Winterbottom, 2019; Winterbottom *et al.*, 2014). These colourful but cryptic fishes are found exclusively on Indo-Pacific coral reefs, spanning from South Africa and the Red Sea in the west to Easter Island in the east. *Trimma* is divided into two groups: benthic species, which perch on the substratum, and epibenthic species that school

close to the benthos where they seek refuge when exposed to predators. In addition to high diversity, *Trimma* is also incredibly abundant, especially in the coral triangle. Along with a similar genus *Eviota*, *Trimma* is a dominant CRF associated with hard substrata (Winterbottom, 2019). Perhaps the most salient characteristic of this group is their small body size. Members of the genus *Trimma* grow to a maximum total length of less than 30 mm (Winterbottom et al., 2011; Winterbottom & Southcott, 2008), which has given rise to their common name ‘pygmy goby’. The small body size of *Trimma* may have implications for their life history, ecology, and essentially their functional roles. However, due to research biases associated with small-bodied cryptic fishes, there are few studies regarding these subjects, with the exception of mating systems and sex change (Winterbottom, 2019).

### **1.9 Current knowledge and research gaps of *Trimma* ecology and life history**

There is limited information available on the habitat use of the genus *Trimma*, with a few community studies of CRFs concluding that they inhabit coral-rock caves (Depczynski & Bellwood, 2004; Herler, 2007). Two studies determined the life stages, mortality, and growth of *Trimma benjamini* and *T. nasa* from Palau specimens, which revealed extreme mortality, long pelagic larval phases relative to lifespans, and largely linear growth following maturity (Winterbottom et al., 2011; Winterbottom & Southcott, 2008). Moreover, since 1990, multiple studies on *Trimma* have revealed diverse mating systems and sex change patterns (Sunobe & Nakazono, 1990, 1993). Studies have shown that polygyny (Fukuda, Tanazawa, *et al.*, 2017; Sunobe & Nakazono, 1990), monogamy (Fukuda, Manabe, *et al.*, 2017), and multimale groups (Tomatsu *et al.*, 2018) occur in the genus, and both gonochorism and bidirectional sex change have been exhibited (Fukuda, Tanazawa, *et al.*, 2017; Manabe *et al.*, 2007; Manabe *et al.*, 2008; Sakurai *et al.*, 2009; Sunobe *et al.*, 2005; Sunobe & Nakazono, 1993; Sunobe *et al.*, 2017). This is the most well-known topic of *Trimma* biology, especially for *T. okinawae*

(Winterbottom, 2019). Finally, one study examined the feeding ecology of *T. caudomaculata* and *T. caesiura* (Saeki *et al.*, 2005) while another community-wide study included *T. caesiura* and *T. striata* (Depczynski & Bellwood, 2003). Both studies concluded that the selected species were planktivorous and consumed predominantly copepods (Depczynski & Bellwood, 2003; Saeki *et al.*, 2005).

For a genus characterised by high diversity, abundance, and potentially significant ecological roles, there exists a notable lack of research, particularly concerning key aspects of *Trimma* habitat, life history, and trophodynamics. Accordingly, I have identified four main subjects that are lacking research, which extends not only to the genus *Trimma* but also to CRFs in general. These gaps in the research encompass:

- How closely related, physiologically analogous, and ecologically similar species partition habitats.
- The relationship between life history constraints and reproductive characteristics.
- Growth patterns across all three life history stages, particularly noting the insufficient knowledge regarding pre-settlement growth patterns.
- The roles of CRFs as both micro-consumer and prey species.

Gaining a better understanding of the habitat use and partitioning, life history constraints and reproductive characteristics, growth patterns across life history stages, and trophic niches of dominant CRFs such as *Trimma* can significantly enhance insights into their ecological roles on coral reefs (Brandl *et al.*, 2019; Depczynski *et al.*, 2007).

## 1.10 Aims and Questions

The overarching aim of this thesis was to assess **the habitat, life history and trophic ecology of cryptobenthic coral reef fishes of the genus *Trimma***. The study site for this thesis



was Kimbe Bay, West New Britain Province, Papua New Guinea (5.1667° S, 150.5000° E). Kimbe Bay is located in the Indo-Pacific coral triangle, which is a region of extreme species diversity. It was designated as a Mission Blue World Hope Spot in 2020, a recognition that underscores the area's critical importance to ocean health. Collaborations between G. P. Jones, colleagues, students, and Mahonia Na Dari Conservation and Research Centre have resulted in numerous peer-reviewed papers regarding marine ecology in this region over the last 40 years. This location also holds a diverse community of *Trimma* species, though no studies have been conducted on the genus in this region. To address the objectives, three *Trimma* species; *T. benjamini*, *T. capostriatum*, and *T. yanoi*, were used as a case study. These species were selected as they are a highly abundant *Trimma* species in this region, based on an initial pilot study and a 22-year data set by P. L. Munday monitoring the abundance of CRFs in Kimbe Bay. The local abundance of the three species suggests they have potential to be an ecological significant species in this region. The three *Trimma* species selected are closely related and appear similar at first glance in terms of their body size and general ecology such as habitats and feeding methods (Winterbottom, 2019; Winterbottom et al., 2014).

The thesis contains four data chapters that were written as manuscripts for publication in peer-reviewed journals, which have since been reconfigured and incorporated into the thesis. I planned the methodology and sampling design, undertook the field and laboratory work, analysed the data, and wrote all chapters. Manuscripts have been shared with and edited by my thesis supervisory team (Maya Srinivasan, Patrick Smallhorn-West, and Geoffrey Jones) and other co-authors for selected sections (Lit-Chien Cheah and Philip Munday)

**Chapter 2** addressed the question: *How do ecologically similar Trimma species partition habitats and does this occur at small spatial scales?* To answer these questions, I assessed variances in each species distributions across differing spatial scales: at varying

distances from the shore, across distinct reef areas characterised by different reef aspects, and at different depths. Additionally, I identified if there were variations in *Trimma* microhabitats to determine if niches were partitioned at fine spatial scales. Finally, I observed the level of interactions within the genus to determine if spatial separation of niches resulted in few interactions among the *Trimma* species examined.

**Chapter 3** asked: *What life history constraints and reproductive strategies do Trimma have?* To address this, I determined the length of each life history stage by uncovering overall longevity, pelagic larval duration, and age at maturity. I also estimated daily natural mortality. Finally, I assessed gonad structure to infer their sex change and reproductive characteristics. I discussed the potential benefits of these strategies for the life-history challenges these small-bodied fishes encounter.

In **Chapter 4**, I addressed the questions: *What are the larval, juvenile, and adult growth patterns, and generational turnover rates of Trimma?* Herein I used the life history parameters determined in Chapter 3 and constructed growth trajectories that transitioned through each life history stage. This was accomplished by the back-calculation of fish lengths at ages prior to capture, fitting population growth models to back-calculated data sets, and differentiating these models to determine growth rates. I discussed these growth patterns and compared them to larger-bodied fishes. I also estimated the generational turnover of *Trimma* using the age at maturity and maximum age.

Finally, in **Chapter 5**, I asked *What are the food items consumed, food origin, feeding methods, and predation pressures of Trimma? Do Trimma possess morphological traits that may assist feeding or predator avoidance?* This chapter used several methods to achieve insights into the trophic niches of the *Trimma* species studied. I examined ingestion rate, dietary composition and origin, potential predators, and measured morphological features that could

be beneficial for capturing prey and predator avoidance. I described how these features might contribute to the ecological roles of *Trimma* in coral reef ecosystems

## Chapter 2: Same-same but different: Habitat use and partitioning of three cryptobenthic coral reef fishes of the genus *Trimma*.

---

### 2.1 Abstract

Partitioning critical resources can alleviate competition among species, allow coexistence and contribute to biodiversity. The mechanisms driving habitat partitioning within the small-bodied and highly diverse genus *Trimma* remain unclear. The main aim of this study was to uncover habitat use and partitioning of *T. benjamini*, *T. capostriatum*, and *T. yanoi* that may enable their coexistence on coral reefs in Kimbe Bay, Papua New Guinea, using a combination of active visual search transects and behavioural observations. The spatial distributions of each species were distinct. Reef aspect played a significant role, with *T. yanoi* and *T. benjamini* being most abundant on the reef wall, while *T. capostriatum* predominantly favoured the reef slope at offshore locations. Generally, there were variations in abundance among depths in all species, though there were exceptions for specific reef aspects. Reef location (inshore vs offshore) influenced the distribution of *T. yanoi* and *T. capostriatum*, but not *T. benjamini*. Population clustering was also examined due to its influence on habitat. *T. yanoi* formed the largest clusters of 9 individuals on average, followed by *T. benjamini* with 7 individuals on average. *T. yanoi* clusters had 1.5 times the population density per m<sup>2</sup> quadrat compared to *T. benjamini*. In contrast, *T. capostriatum* exhibited the smallest cluster sizes and densities, with the highest proportion (30%) of solitary individuals. At small spatial scales, coexistence was observed in 34.5 – 52% of m<sup>2</sup> quadrats. Within 1 m<sup>2</sup> quadrats where species coexisted, there were differences in the microhabitat that each species commonly occupied, resulting in minimal overlap of microhabitats (9.2- 18.2%) . Accordingly, interactions between *Trimma* species were rare, involving less than 1% of individuals. These findings exemplify

how small reef fish can effectively partition habitats even when closely related, with almost identical body size and morphology.

## 2.2 Introduction

Biodiversity is the foundation of resilient ecosystems (Naeem & Li, 1997). It supports important ecological processes such as productivity and nutrient cycling and increases overall resistance to disturbances such as climate change and biological invasions (Chapin III *et al.*, 2000; Hooper *et al.*, 2005; Naeem *et al.*, 2000). Ecological partitioning is acknowledged as a fundamental mechanism for sustaining biodiversity (Chesson, 2000; Connell, 1978; MacArthur, 1958; Schoener, 1974). In densely populated areas, essential resources like space or food may be limited, leading to intense competition for these critical resources (Connell, 1983; Schoener, 1983). Niche partitioning can reduce competition for these resources and enable the coexistence of sympatric species that occupy similar ecological niches (Chesson, 2000; Ross, 1986). However, species that are closely related or physiologically similar may exhibit ecological niches with only minor distinctions. Consequently, niche partitioning of these species may be subtle and difficult to detect (Gause, 1934; Shpigel & Fishelson, 1989).

Ecological partitioning is fundamental on tropical coral reefs, which serve as habitats for over 6,000 species of coral reef fish (Bonin *et al.*, 2015; Brandl *et al.*, 2018). As such, ecologically similar coral reef fishes may partition space by having different distributions, which can vary across scales. For example, distributions can vary on broad spatial scales including across continental shelves (Goatley *et al.*, 2016; Hoey & Bellwood, 2008), and on local scales such as among reef zones (Arias-González *et al.*, 2006; Depczynski & Bellwood, 2005b; Eurich, 2018), among areas of reef that differ topographically (Brokovich *et al.*, 2006; Jankowski *et al.*, 2015), and among depths (Arias-González *et al.*, 2006; Jankowski *et al.*, 2015;

Srinivasan, 2003; Tornabene et al., 2016). These distributions are determined by a range of abiotic and biotic factors such as water movement (Fulton & Bellwood, 2005; Greenfield & Greenfield, 1982; Wilson, 2001), light levels (Brokovich *et al.*, 2008), habitat differences (Arias-González et al., 2006; Jankowski et al., 2015), competition (Eurich *et al.*, 2018; Munday *et al.*, 2001), and food availability (Böhm & Hoeksema, 2017; Wilson, 2001), all of which may vary across different spatial gradients and drive a species' distribution. However, differences in spatial distributions alone may still result in habitat overlap (Eurich et al., 2018; Gardiner & Jones, 2005; Meekan *et al.*, 1995). In this case, finer scale spatial partitioning, such as minor differences in diet and habitat preferences, may occur (Eurich et al., 2018)

Cryptobenthic reef fishes (CRFs) are abundant on coral reefs and contribute significantly to reef fish diversity (Depczynski & Bellwood, 2005a). Individuals of this group are typically <50 mm as adults, are behaviourally or physically cryptic, and are closely associated with benthic habitats (Goatley & Brandl, 2017). There is increasing recognition of the important roles these fish play in energy flow within ecosystems, due to life history traits such as short lifespans and high population turnover (Brandl et al., 2019; Depczynski & Bellwood, 2003). Moreover, CRFs account for 50% of individuals and 40% of species present in sections of the Great Barrier Reef (Ackerman & Bellwood, 2000), and 95% of individuals and 40% of species in the Gulf of California (Galland et al., 2017). Accordingly, multiple species are often located in close proximity on the reef (Depczynski & Bellwood, 2004; Herler, 2007). Like larger fishes, partitioning of spatial resources among CRFs can occur at a range of spatial scales, (e.g., reef location, zone or depth; Glavicic et al., 2016; Goatley et al., 2016; Wilson, 2001). However, habitat partitioning can also occur at very fine spatial scales, as these tiny fishes are able to inhabit numerous small and distinct habitats that are not accessible to their larger counterparts (Brandl et al., 2018). For example, some CRFs are known to partition habitats very finely by being highly specialised on particular coral species (Dirnwöber &

Herler, 2007; Munday, 2001; Munday et al., 1997), having varying preferences for certain reef microhabitat types at a fine scale (Depczynski & Bellwood, 2004; Doll et al., 2021; Herler, 2007; Tornabene et al., 2013), or utilising shelter holes of different sizes or positions (Clarke, 1994; Wilson et al., 2013). Among some CRF genera, diversity has been linked to the ability to exploit a diverse range of microhabitats on small scales (Herler et al., 2011; Munday & Jones, 1998; Munday et al., 2004).

Despite the many examples of fine scale habitat partitioning among CRFs, there is still evidence for microhabitat overlap among many CRF species, especially those within the same genus (Depczynski & Bellwood, 2004; Doll et al., 2021). In areas of spatial overlap, CRFs may exploit different dietary resources, to allow them to co-exist (Brandl, Casey, *et al.*, 2020; Saeki et al., 2005). However, there is limited information available regarding coexistence mechanisms among CRFs with similar diet and microhabitat requirements (but see Wilson et al., 2013). In such cases, it could be valuable to explore other microhabitat characteristics that might contribute to this fine scale spatial partitioning, such as microhabitat structure (Depczynski & Bellwood, 2004). Certain larger fish species display a preference for specific reef structures (Jankowski et al., 2015; Jones & Syms, 1998), and therefore a similar pattern may be seen in CRFs at a smaller scale. However, the role of small-scale microhabitat structure in habitat partitioning among CRFs is less known (but see Depczynski & Bellwood, 2004). Moreover, for species that live in clusters, preferred microhabitats may be influenced by factors such as population density (Kane *et al.*, 2009). Species that are predominantly solitary, have sparse clusters, or live in dense clusters may occupy microhabitats with distinct characteristics, as these different microhabitats support a varying number of individuals (Troyer *et al.*, 2018). This emphasises the importance of considering population clustering alongside habitat differences (Kane et al., 2009).

The genus *Trimma* (family Gobiidae) is an abundant and extremely diverse group of CRFs on Indo-Pacific coral reefs, consisting of 105 species (Winterbottom, 2019). Members of this genus attain a tiny body size of <30 mm. Some *Trimma* species are benthic, perching on the reef substratum, and often live in groups in small caves in the reef (Depczynski & Bellwood, 2004; Herler, 2007; Winterbottom, 2019). The benthic group of *Trimma* is of particular interest regarding niche segregation, as many species co-occur within apparently similar habitats (Depczynski & Bellwood, 2004; Herler, 2007) and utilise similar feeding strategies (Goldsworthy, unpublished data). The mechanisms behind *Trimma* species' coexistence, despite their ecological similarities, are currently unknown.

The aim of this study was to identify differences in distributions and habitat use of three *Trimma* species (*Trimma benjamini*, *T. capostriatum* and *T. yanoi*) that may enable them to coexist on coral reefs in Kimbe Bay, Papua New Guinea. These species are the most common *Trimma* in this location. All share similar life history characteristics; being small, having short lifespans, and exhibiting high daily mortality rates (Goldsworthy et al., 2022). Furthermore, the three species are closely related and ecologically similar (Winterbottom, 2019; Winterbottom et al., 2014). Herein, I investigated differences in *Trimma* species distribution across different spatial scales: 1) among reefs different distances from shore (inshore vs offshore); 2) among areas of reef with differing aspect (slope vs wall); and 3) among depths. I also examined fine scale variations in *Trimma* population clustering and microhabitat use, and finally examined the level of behavioural interactions between *Trimma* species. Following trends in other CRFs, it was expected that variations in distribution may be seen on both broad and fine spatial scales. Where distribution overlap occurs, there may be fine-scale differences in their microhabitat. If microhabitats displayed unique characteristics, I predicted that few interactions may occur among *Trimma* species. This study explored further mechanisms that may enable the coexistence of ecologically similar CRFs.



## 2.3 Methods

### 2.3.1 Study sites

Kimbe Bay (Figure 2.1) is situated in the coral triangle, and has a high diversity of reef fish species, including eight described species of benthic *Trimma*. Surveys were conducted at six reefs located at two distances from shore: three inshore reefs (Hanging Gardens, Limuka, and Lady Di) located approximately 0.8-1.3 km from shore and three offshore reefs (Vanessa's Reef, Joy's Reef and Donna's Reef) located approximately >2.5 km from shore (Figure 2.1). These reefs have sheer walls on the windward side and shallower reef slopes on the leeward side.

### 2.3.2 Visual surveys

Visual surveys were conducted during November – December 2019 between 08:00 and 16:00 at two areas of each reef with differing aspects (reef slope on the leeward side and vertical reef wall on the windward side), and at three depths (4, 6, and 10 m), using three 20 x 1 m transects at each reef aspect-depth combination. A total of 108 transects were surveyed.

Each transect was laid along the reef following the depth contour, and the surveyor waited five minutes before commencing surveys, allowing any disturbed fish to emerge. The surveyor swam down the transect, undertaking a thorough visual search of the area, including searching every cave and crevice with a torch. The selected approach was non-invasive in nature. Alternative methods, such as the use of clove oil stations, would not have been ethically viable for targeting just three species, as it would inadvertently cause harm to the numerous other cryptobenthic organisms in the area. The following was recorded for each individual of *T. benjamini*, *T. caopstriatum* and *T. yanoi* present within 0.5 m on either side of the transect tape: the distance along the transect, the microhabitat type of the area occupied, and whether it was solitary or part of a cluster of conspecifics. The microhabitats recorded incorporated a

combination of different substrata and small-scale topography. Microhabitats included flat reef, vertical reef, sloping inwards reef, sloping outwards reef, and overhanging reef – all of which were covered composed of live coral rock (coral rock colonised by encrusting substrata such as turf algae, crustose coralline algae, encrusting sponges, or encrusting corals) (Yuen *et al.*, 2009), complex sponge, soft coral, ascidian, branching coral, foliose coral, and mounding coral. A fish was considered solitary if it had no conspecifics present within a 1 m radius around the point where it was situated. If one or more conspecifics were present within a 1 m radius, this was considered part of a cluster.

### **2.3.3 Simulating population clustering**

To simulate population clustering, a density clustering algorithm was utilised. A data matrix was created for each species containing a unique value for each distance along each transect to use as the X variable, a dummy Y variable of the value 1 for each individual. The data matrix was entered into the `dbSCAN()` function in the DBSCAN package in R. The model assumed that a cluster required a minimum of two individuals, and that individuals of the same species located within one meter of each other were considered part of the same cluster. Cluster size was derived from the output of the density clustering algorithm. Cluster density per m<sup>2</sup> was estimated by  $\frac{\text{Cluster size}}{\text{Cluster ground cover (m)}}.$

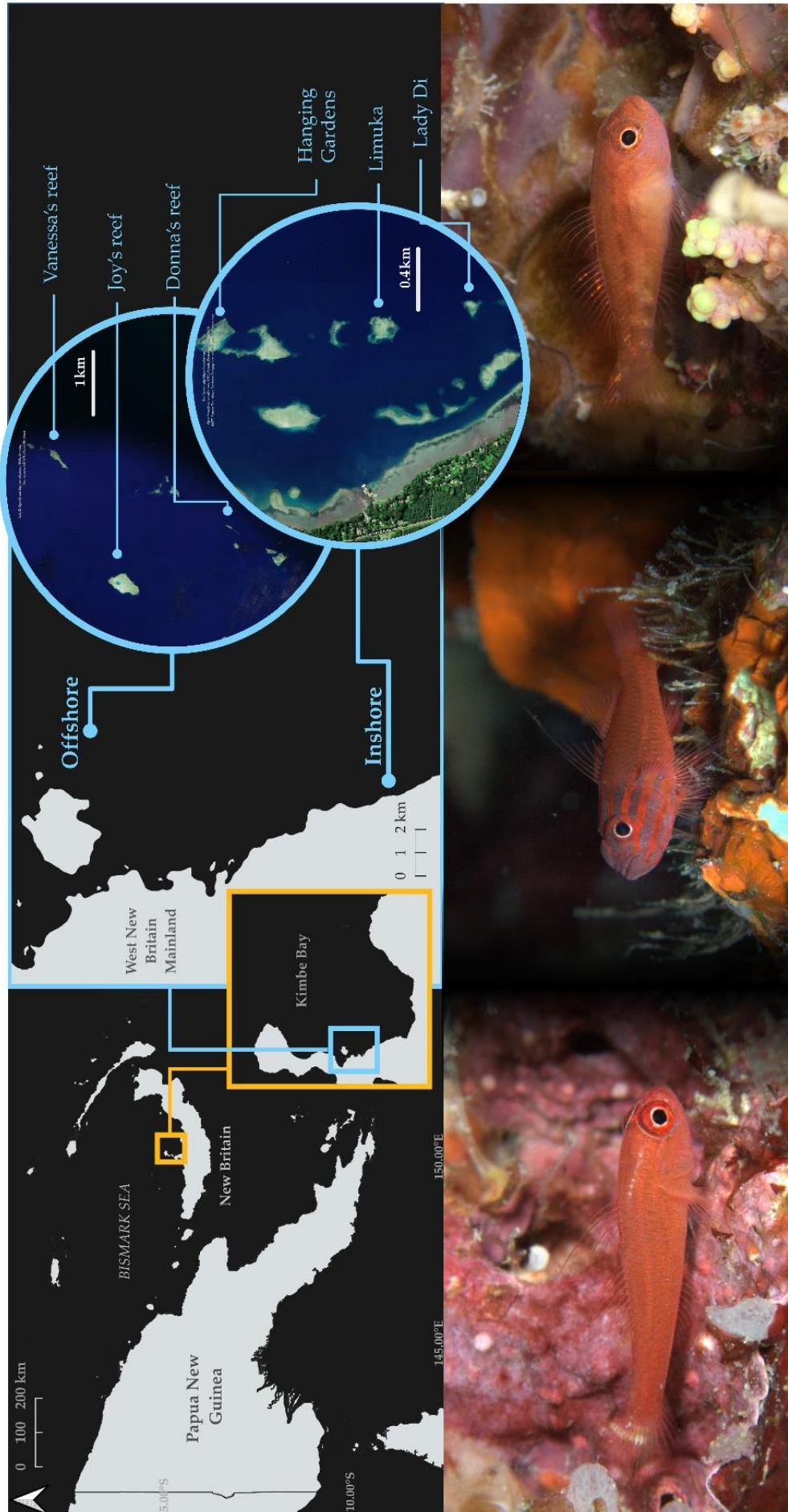


Figure 2.1: Above) Map of Kimbe Bay, West New Britain, Papua New Guinea, and the three inshore and three offshore study sites. Below) *In situ* photographs of *Trimma benjamini* (left), *T. capostriatum* (centre), and *T. yanoi* (right).

### **2.3.4 Behavioural observations**

To determine the level of interactions among the target *Trimma* species, behavioural observations of 369 *T. benjamini*, 167 *T. capostriatum* and 259 *T. yanoi* individuals were conducted in December 2022. The time gap between the surveys and these observations was due to not being able to travel to the study site during the COVID-19 pandemic. Each fish was observed for two minutes, and the number of times it interacted with individuals of another *Trimma* species was recorded.

### **2.3.5 Data analysis**

To compare broad scale spatial patterns, clustering, and microhabitat differences among the 3 species and to determine the level of interspecific interactions, a series of generalised linear models (glms) and generalised linear mixed effect models (glmms) were constructed for each topic.

To assess variation in the abundance of each species between inshore and offshore reefs, between reef slopes and walls and among depths, models for each species contained the fixed effects of reef location, reef aspect, and depth, and incorporated a three-way interaction term between the variables. Random effects of site and transect number were incorporated into the model only if accounting for variation among these effects significantly improved the model fit. The data were evaluated against Poisson, Negative Binomial, and Tweedie distributions to determine which distribution and link function was optimal. *T. capostriatum* and *T. yanoi* contained zero count factor levels and therefore a small constant of 0.1 was added to all categories prior to model fitting (Logan, 2010). The optimum model for each species was chosen by evaluation of the Akaike Information Criterion (AIC) (Sakamoto *et al.*, 1986), where the lowest AIC scores indicated a better fitting model, provided a difference of 2 AIC units and that residual distributions were satisfactory. If the difference in AIC scores was not significant

by 2 units, the model with the lowest consumed degrees of freedom was selected. Modelling of broad scale spatial patterns was conducted separately for each species. Significant interactions of fixed effects were determined by applying the `aov()` function to each optimum model. Significant interactions were untangled by exploring pairwise comparisons (Logan, 2010).

Cluster size, cluster density, and proportion of solitary individuals were each modelled by a series of glms and glmms as a function of species. The random effects of transect number and site were tested to determine if they significantly improved the models for each topic. When modelling cluster size, individual cluster number was also assessed as a random effect. The optimum model was selected, informed by AIC. Pairwise comparisons were used to assess the significance and scale of population clustering differences.

To examine differences among species at the microhabitat level, each transect was divided into 1 m<sup>2</sup> quadrats. Only 1 m<sup>2</sup> quadrats occupied by *Trimma* were utilised. Different transects, which consisted of multiple 1 m<sup>2</sup> quadrats, were pooled for analysis. To analyse the microhabitat that each species was predominantly located in, the category “Flat reef” was removed due to only two observations in this group. Complex sponge, soft coral, ascidian, branching coral, and foliose coral were consolidated into a category labelled "Other 3D substrata" due to minimal observations of individuals present in these microhabitats. The proportion of individuals in each microhabitat category per 1 m<sup>2</sup> quadrat was modelled among species. These proportions were weighted by the total number of individuals in each 1 m<sup>2</sup> quadrat. The random effects of site and transect number were considered to determine if there was any variation among them and the optimum model was selected by AIC.

To quantify distribution overlap on a small scale, the proportion of m<sup>2</sup> quadrats that were occupied by each lone species and each combination of co-existing species was modelled

via a presence-absence matrix with a series of glms and glmms with a Binomial family (logit link) which tested for variation among sites and transects. Optimum models were selected by AIC. An area proportion Euler diagram was formulated from this output using the `eulerr` package in R.

Microhabitat overlap was quantified where species coexisted within the same  $m^2$  quadrat. The binary response of whether heterospecific individuals were present in the same vs different microhabitat category was modelled by glms and glmms with a Binomial family (logit link). Variability among sites and transects was assessed as random effects, and the optimum model was selected by AIC.

Models to determine the level of interactions among the target *Trimma* species included the binary response of whether or not each individual of each species engaged in interactions with another *Trimma* species. The random effect of site was considered to determine if significant variability among sites existed.

All statistical analyses were conducted in R studio. All glms and glmms were constructed using the `glmmTMB` package in R and optimal models determined by AIC were assessed for suitability by examining the distribution of residuals (Logan, 2010).

## 2.4 Results

Table 2.1: Optimum models from a series of generalised linear models and generalised linear mixed effect models selected by AIC. Left to right: response variable, fixed effects of optimum model, random effects of optimum model, and optimal probability distribution with the appropriate link function.

	Response	Fixed effects	Random effects	Distribution
<b>a) Broad-scale spatial patterns</b>				
<i>Trimma benjamini</i>	No. individuals per 20 X 1 m	<ul style="list-style-type: none"> <li>○ Location</li> <li>○ Aspect</li> <li>○ Depth</li> </ul>	Site	Tweedie (log link)
<i>Trimma capostriatum</i>	No. individuals per 20 X 1 m + 0.1	<ul style="list-style-type: none"> <li>○ Location</li> <li>○ Aspect</li> <li>○ Depth</li> </ul>	Site	Negative Binomial (log link)
<i>Trimma yanoi</i>	No. individuals per 20 X 1 m + 0.1	<ul style="list-style-type: none"> <li>○ Location</li> <li>○ Aspect</li> <li>○ Depth</li> </ul>	None	Negative Binomial (log link)
<b>b) Population clustering</b>				
Cluster size	Size of cluster	<ul style="list-style-type: none"> <li>○ Species</li> </ul>	Cluster number	Poisson (log link)
Cluster density	Density of cluster (per m <sup>2</sup> )	<ul style="list-style-type: none"> <li>○ Species</li> </ul>	Transect number	Negative Binomial (log link)
Proportion solitary	Solitary vs not solitary	<ul style="list-style-type: none"> <li>○ Species</li> </ul>	Transect number	Binomial (logit link).
<b>c) Microhabitat-scale patterns</b>				
Microhabitat	Proportion per m <sup>2</sup> quadrat (weighted by the total per m <sup>2</sup> quadrat)	<ul style="list-style-type: none"> <li>○ Microhabitat categories</li> <li>○ Species</li> </ul>	None	Binomial (logit link)
Distribution overlap	Proportion of m <sup>2</sup> quadrats	<ul style="list-style-type: none"> <li>○ Lone species and co-existing species categories (i.e., B, C, Y, B&amp;C, B&amp;Y,</li> </ul>	None	Binomial (logit link)

			C&Y and B&C&Y)*		
Microhabitat overlap	Proportion of individuals per m <sup>2</sup> quadrat that inhabited the same microhabitat category (overlap) vs different (no overlap)	○	Co-existing species category (i.e., B&C, B&Y, C&Y)*	None	Binomial (logit link)
<b>d) Interactions among <i>Trimma</i></b>					
Interactions	Proportion of individuals that interacted vs did not interact with another <i>Trimma</i> species	○	Species	None	Binomial (logit link)

\*B = *Trimma benjamini*, C = *T. capostriatum*, Y = *T. yanoi*

#### 2.4.1 Broad scale spatial patterns

A total of 2146 *T. benjamini*, 384 *T. capostriatum* and 1303 *T. yanoi* individuals were surveyed in 108 transects. For each species, the optimum broad scale spatial pattern models contained the fixed effects of location, aspect, and depth (Table 2.1a). For *T. benjamini*, the optimum model featured the random effect of site and utilised a Tweedie distribution (log-link) (Table 2.1a, Table A1. 1a). The optimum model for *T. capostriatum* accounted for variations among sites and had a Negative Binomial distribution (log-link) (Table 2.1a, Table A1. 2a). In *T. yanoi*, the optimum model did not include random effects and the Negative Binomial distribution had the best fit (log link) (Table 2.1a, Table A1. 2).

The distribution of each species was uniquely impacted by the factors location, aspect, and depth (Figure 2.2). *T. benjamini* abundance did not significantly differ between inshore and offshore reef locations (Figure 2.2a, Table A1. 1b). When exploring differences in *T. benjamini* abundance between reef aspects, there were significantly higher abundances on reef



wall regions than reef slopes at all locations and depths, with an average of between 22.5 - 41.1 (3.4 – 20 times) more individuals on the reef wall vs the reef slope on average (Figure 2.2a, Table A1. 1c). The effect of depth depended on the aspect of the reef (Table A1. 1b), with 21.6 more individuals or 1.9 times the abundance on average at 6 m compared to 4 m on the reef wall (Figure 2.2a, Table A1. 1c). There were no significant differences between other depths on the reef wall and slope (Figure 2.2a, Table A1. 1c).

For *T. capostriatum*, there was a significant interaction between variables location and aspect (Table A1. 2b). There were 3.2 more individuals or 1.8 times more individuals on average observed at offshore reef slopes compared to inshore reef slopes (Figure 2.2b, Table A1. 2c). In offshore locations, *T. capostriatum* was more associated with the reef slope than the reef wall, where there were 6.9 more individuals on average compared to the reef wall (Figure 2.2b, Table A1. 2c). In contrast, there were on average 3.7 fewer individuals observed at offshore reef walls compared to inshore reef walls (Figure 2.2b, Table A1. 2c). There was a significant interaction between variables aspect and depth (Table A1. 2b) An increase in *T. capostriatum* abundance with depth was exhibited on the reef slope, with 1.8 and 1.7 times the abundance at 10 m than at 6 m and 4 m, respectively (Figure 2.2b, Table A1. 2c). On the reef wall, there were no significant differences in *T. capostriatum* counts among depths (Figure 2.2b, Table A1. 2c).

There were no *T. yanoi* individuals observed on the reef slope (Figure 2.2c). For this species, the effect of location and depth was dependent on the reef aspect (Table A1. 3b). On the reef wall, there were significantly more individuals observed at offshore compared to inshore locations (Figure 2.2c, Table A1. 3c). There was an increase in abundance with depth on the reef wall, with 11 and 7.4 times more individuals at 10 m and 6 m, respectively, than at 4 m (Figure 2.2c, Table A1. 3c). Significantly more individuals were observed on the reef wall

compared to the reef slope at depths of 10 m and 6 m (Figure 2.2c, Table A1. 3c). However, due to few individuals occurring in shallow regions, there was no significant difference between the reef wall and slope at 4 m (Figure 2.2c, Table A1. 3b). There was no significant three-way interaction among variables location, aspect, and depth for any species (Table A1. 1b, Table A1. 2b, Table A1. 3b)

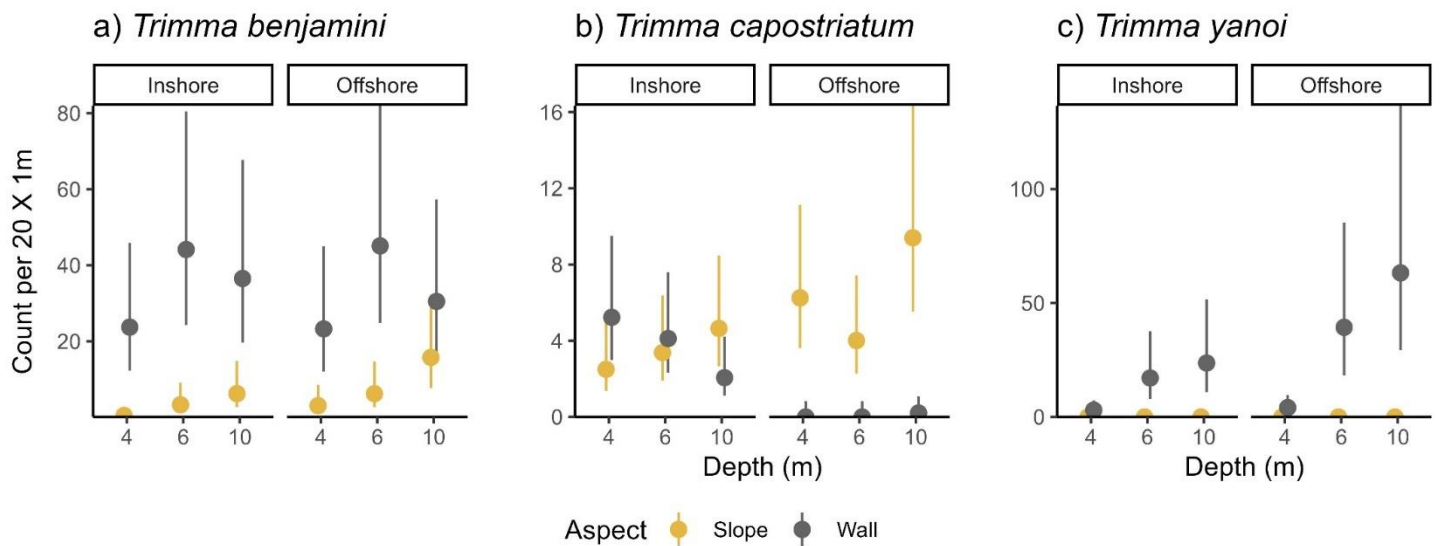


Figure 2.2: Modelled mean counts per 20 X 1 m transect of a) *Trimma benjamini*, b) *T. capostriatum*, and c) *T. yanoi* individuals at different reef locations (inshore, offshore) reef aspects (slope, wall) at varying depths (4, 6, 10 m)  $\pm$  95% confidence intervals. Models have taken variation in abundance among sites into account where necessary. n = 108 transects.

### 2.4.2 Population clustering

A clumped distribution was apparent in all three *Trimma* species examined, with a high proportion of 1 m<sup>2</sup> quadrats along the transect having either zero individuals or high densities of individuals. The density clustering algorithm estimated that 242, 83 and 107 clusters of *T. benjamimi*, *T. capostriatum* and *T. yanoi* (respectively) were present over the 108 transects surveyed (Figure A1. 1, Figure A1. 2, Figure A1. 3).

The optimum model to estimate mean cluster size among species had the random effect of each cluster, with variable intercept and variable slope parameters for each species, and had a Poisson family (log link) (Table 2.1b, Table A1. 4a). *T. yanoi* had the largest average cluster size of 9 individuals, which was 1.3 times greater on average than *T. benjamimi* clusters which had an average of 7 individuals (Table 2.2, Table A1. 4b). *T. capostriatum* had the smallest cluster sizes of 3 individuals (Table 2.2, Table A1. 4b).

The optimum model to estimate mean cluster density among species accounted for variation among transects (with variable intercepts and fixed slope parameters for each species) and had a Negative Binomial family with a log link (Table 2.1b, Table A1. 5a). *T. yanoi* clusters had 1.5 times the average density of *T. benjamimi* clusters (Table 2.2, Table A1. 5b). *T. capostriatum* had the smallest cluster size and density (Table 2.2, Table A1. 5b).

Finally, to estimate the proportion of solitary individuals, the optimum model had the random effect of transect number with variable intercept and slope parameters for each species, with a Binomial family (logit link) (Table 2.1b, Table A1. 6a). *T. benjamimi* and *T. yanoi* species both had a low proportion (< 2%) of solitary individuals, while 30.7 % of *T. capostriatum* individuals were considered solitary, which is a significantly higher proportion than the other two species (Table 2.2, Table A1. 6b).

Table 2.2: Estimated cluster size (mean number of individuals per cluster), cluster density (mean number of individuals per m<sup>2</sup> in a cluster), and proportion of individuals considered solitary (%) for species *Trimma benjamini*, *T. capostriatum* and *T. yanoi*. Values represent the estimated modelled means, with 95% lower confidence levels (LCL) and 95% upper confidence levels (UCL) derived from the model distribution in Table 2.1, shown in brackets below estimated means. *n* = sample size.

		<i>Trimma benjamini</i>	<i>Trimma capostriatum</i>	<i>Trimma yanoi</i>
	Cluster size	6.9 (6.2, 7.7) <i>n</i> = 242	3.3 (2.9, 3.8) <i>n</i> = 83	9.0 (7.5, 10.6) <i>n</i> = 107
Mean (95% LCL, 95% UCL)	Cluster density (m <sup>2</sup> )	4.0 (3.6, 4.3) <i>n</i> = 242	2.2 (1.9, 2.6) <i>n</i> = 83	5.9 (5.2, 6.6) <i>n</i> = 107
	Proportion solitary (%)	1.9 (0.8, 4.2) <i>n</i> = 2146	30.7 (23.0, 39.7) <i>n</i> = 384	0.4 (0.1, 1.3) <i>n</i> = 1303

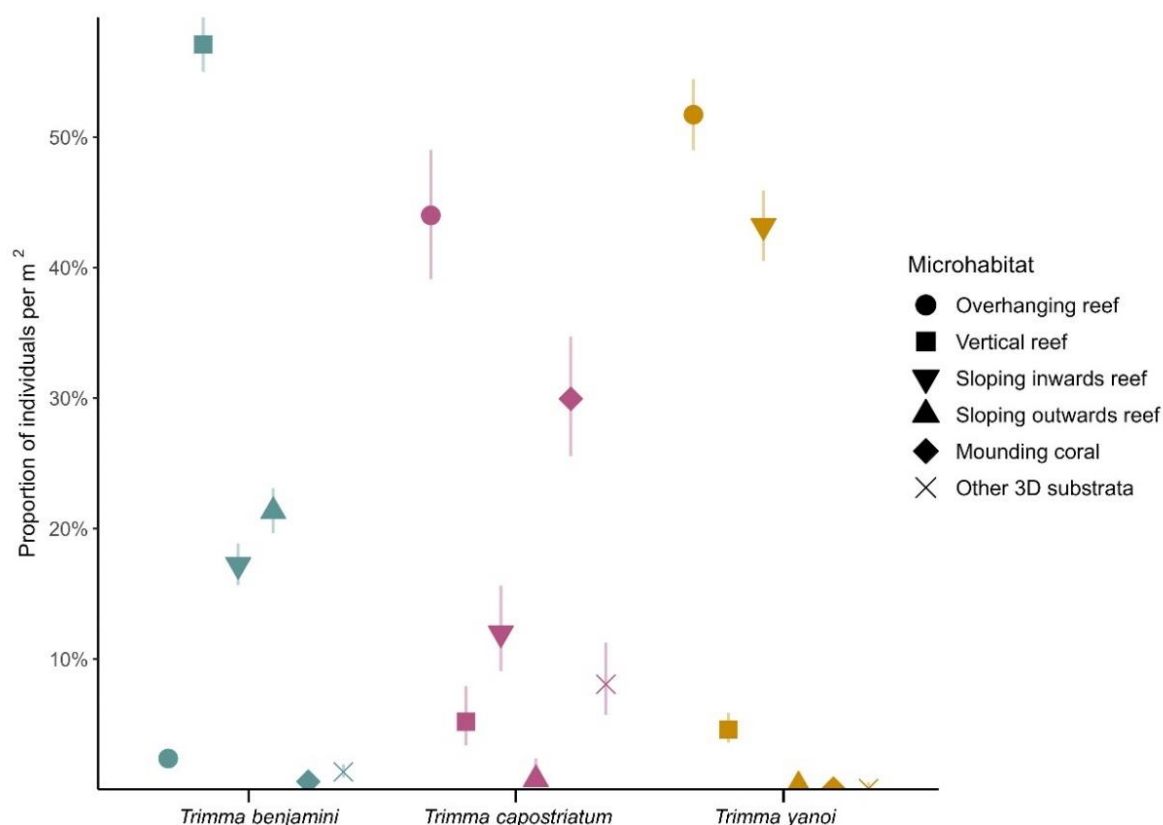


Figure 2.3: Mean proportions of individuals present per m<sup>2</sup> quadrat in each microhabitat category for *Trimma benjamini*, *T. capostriatum*, and *T. yanoi*. Bars represent 95 % confidence intervals, derived from a Binomial distribution (McKeon et al., 2012).

### 2.4.3 Microhabitat

Models to estimate the predominant microhabitat characteristics of each species did not include random effects of site or transect number and had a Binomial distribution with a logit link (Table 2.1c, Table A1. 7a). The predominant microhabitat category that individuals were found in varied substantially among species (Figure 2.3, Table A1. 7b). *T. benjamimi* occurred in the highest proportions in vertical reef microhabitats (57.1%) followed by sloping outwards reef (21.3%) and sloping inwards reef (17.2%), with <4.5% occurring in the other three categories (Figure 2.3, Table A1. 7c). Conversely, *T. capostriatum* occurred mostly in overhanging reef microhabitats (44%) followed by mounding corals (30%) with <26% of individuals present in the other categories (Figure 2.3, Table A1. 7c). Similar to *T. capostriatum*, *T. yanoi* occurred in highest proportions overhanging reef microhabitats (51.7%) but also commonly occupied sloping inwards reef (43.2%). 5% of individuals on average were present in the other two categories (Figure 2.3, Table A1. 7c).

The optimum models to quantify spatial overlap at the m<sup>2</sup> quadrat level, and microhabitat overlap of co-existing species had a Binomial distribution (logit link), and did not include the random effects of site or transect number (Table 2.1c, Table A1. 8, Table A1. 9). *T. benjamimi*, *T. capostriatum*, and *T. yanoi* were the sole species 46.5%, 17%, and 11.9% of occupied 1 m<sup>2</sup> quadrats, respectively, and each species experienced 34.5% (*T. benjamimi*), 42.9% (*T. capostriatum*) and 52% (*T. yanoi*) of overlap with another *Trimma* (Figure 2.4a)

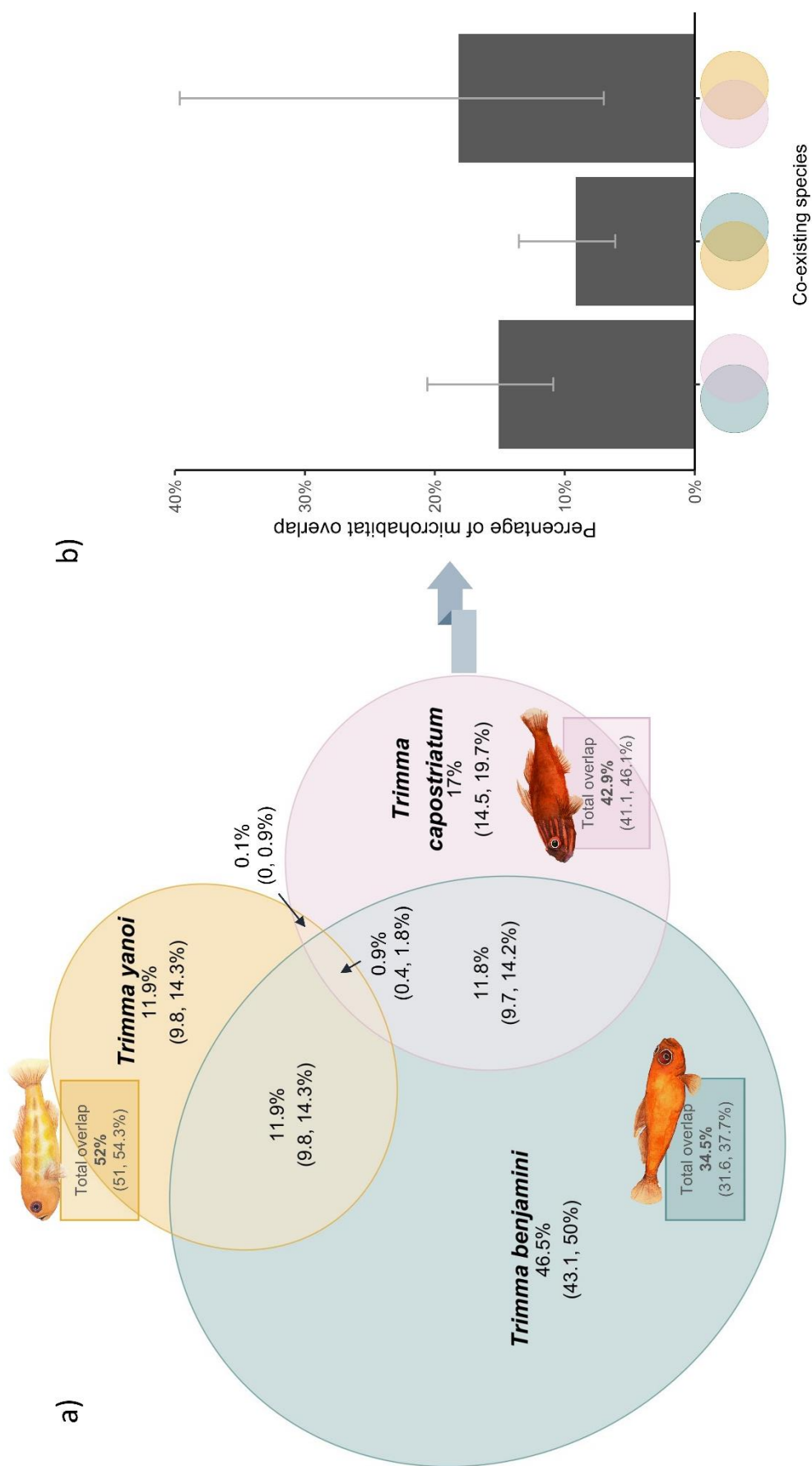


Figure 2.4: a) Area-proportional Euler diagram showing the proportion of  $m^2$  quadrats occupied by lone species (*Trimma benjamini*, *T. capostriatum* and *T. yanoi*, shown by non-overlapping regions) relative to the proportion of  $m^2$  quadrats occupied by multiple species (shown by overlapping regions). Total estimated overlap of each species is illustrated in brackets below means. Values represent the modelled means, with 95% lower and upper confidence levels derived from a Binomial distribution shown in brackets below means. b) Proportion of individuals present in the same microhabitats in  $m^2$  quadrats where species co-existed. Error bars display the 95% confidence intervals derived from a Binomial distribution (McKeon *et al.*, 2012).

*T. benjamini* and *T. capostriatum* co-existed in 12.8% of occupied 1 m<sup>2</sup> quadrats (Figure 2.4a). 15.1% of coexisting individuals were present in the same microhabitats, while 83.9% occupied differing microhabitats (Figure 2.4b). *T. benjamini* and *T. yanoi* co-existed in 12.7% of 1 m<sup>2</sup> quadrats (Figure 2.4a). Within these coexisting regions, a small proportion (9.2%) shared the same microhabitat while most individuals (90.8%) occupied microhabitat that were distinct (Figure 2.4b). Co-existence of *T. capostriatum* and *T. yanoi* was seldom at 1% (Figure 2.4a). 18.2% of individuals occupied the same microhabitats and 81.8% occupied alternate ones (Figure 2.4b). However, the sample size was small due to very few co-occurring *T. capostriatum* and *T. yanoi* individuals and this may affect the reliability of predictions regarding microhabitat overlap between these species.

#### **2.4.4 Interspecific interactions among the *Trimma* species examined**

The optimum model to estimate the level of interspecific interactions among the focal *Trimma* species had a Binomial distribution (logit link) and did not include the random effect of site (Table 2.1d, Table A1. 10). Interspecific interactions were low for all species, with 0.3 – 0.6% of individuals engaging with an individual of another *Trimma* species (Table 2.3). *T. benjamini* interacted with both *T. capostriatum* and *T. yanoi*. *T. yanoi* and *T. capostriatum* did not interact with one another (Table 2.3). These interactions were chasing behaviours and were assumed to be territorial.

Table 2.3: Percentage of individuals that engaged in interactions with an individual of a different *Trimma* species (i.e., chased or were chased by another *Trimma*), and species that the interaction occurred with. Confidence intervals below proportions were derived from a Binomial distribution (McKeon et al., 2012).

Species observed	Number of individuals observed	Interactions among <i>Trimma</i> species examined (% of individuals)	Species that interactions occurred with
<i>Trimma benjamini</i>	369	0.3% (0.1, 1.1%)	<i>Trimma capostriatum</i> and <i>Trimma yanoi</i>
<i>Trimma capostriatum</i>	167	0.6% (0.1, 2.4%)	<i>Trimma benjamini</i>
<i>Trimma yanoi</i>	259	0.4% (0.1, 1.5%)	<i>Trimma benjamini</i>

## 2.5 Discussion

The three *Trimma* species exhibited notable differences in niches across various spatial scales. These differences were evident in spatial partitioning based on broad scale spatial factors, including variations in species' abundance between inshore and offshore reefs, between reef slopes and reef walls, and among the three depths investigated. Additionally, population clustering of individuals differed among species, both in terms of the number of individuals and density of clusters. Microhabitat differentiation was also apparent on a small scale. Consequently, minimal interspecific interactions were observed among the three species. Here, I discuss drivers of these differences and how they may enable the coexistence of species, potentially facilitating the extreme diversity of CRFs.

Reef aspect and depth had varying effects on the distribution of each species. Differences in distribution and abundance of *Trimma* may be attributed to variations in underlying habitat types, which is influenced by reef aspect and depth (Brokovich et al., 2006; Jankowski et al., 2015; Srinivasan, 2003). *T. yanoi* exhibited a highly selective presence for



deep regions of the reef wall. Here, they were found in large aggregations, predominantly inhabiting overhanging or sloping inward reef microhabitats. These cave structures are found mainly on the reef wall at depths, and such habitats are uncommon in shallower regions or reef slopes (Depczynski & Bellwood, 2004). A similar trend is shown in *Chromis delta* and *Pictichromis paccagnellae*, which highlights the same preference for cave entrances and overhangs and are hence confined to reef walls (Jankowski et al., 2015). *T. benjamini* also preferred the reef wall over the reef slope. This species exhibited preferences for vertical reef microhabitats which are commonly found on the reef wall and appeared to be less impacted by more complex habitat structures like caves. In contrast to the other two species, *T. caopstriatum* was the only species that was predominantly reef slope associated, and the only species commonly associated with mounding corals which aligns with the observation that mounding corals are prominently found on the reef slope (Jankowski et al., 2015). Although underlying habitat is known to drive reef fish distributions, it may only partially explain these patterns (Brokovich et al., 2006). Hence, drivers of distribution are likely to encompass a combination of other biotic or abiotic factors that are interrelated with reef aspect and depth (Jankowski et al., 2015; Srinivasan, 2003). For example, exposure to water motion (Fulton & Bellwood, 2005), light filtration (Brokovich et al., 2008), food availability (Wilson, 2001), predation success (Stewart & Jones, 2001), and competition with other species (Clarke, 1989) can all vary with depth and/or reef aspect (Jankowski et al., 2015). However, as these variables were not assessed, the underlying mechanisms involved here are yet to be determined.

Reef location did not influence *T. benjamini* abundance, but it did for the other two species. There was a higher abundance of *T. yanoi* individuals on offshore reef walls compared to inshore reef walls. For *T. caopstriatum*, there were more individuals on inshore reef walls than offshore reef walls and more individuals on offshore reef slopes than inshore reef slopes. Nearshore reefs may be exposed to a variety of coastal processes that have less effect in

offshore regions. Terrestrial runoff can alter environmental conditions by elevating dissolved inorganic nutrients, particulate organic matter, and suspended sediments in the water and by reducing light levels as a result of turbidity (Fabricius, 2005). These factors can impact the composition of coral reef fish assemblages, leading to variations in species composition between inshore and offshore reefs (Fabricius, 2005; Goatley et al., 2016; Moustaka *et al.*, 2018; Orpin & Ridd, 2012). Cross-shelf differences are evident in CRFs on the Great Barrier Reef. Goatley et al. (2016) determined that each reef location was characterised by a single species of goby that dominated the area in terms of abundance. Although the findings did not show this for *T. benjamini*, the effect of reef location may be stronger at a broader scale (i.e., if offshore sites were further from the shore).

While the findings indicated differences in distributions at broad spatial scales, there was still overlap even at small spatial scales, with each species experiencing 34.5 – 52% of overlap with another *Trimma* species at the 1 m<sup>2</sup> quadrat scale. Examining coral reef fish distributions at the reef scale or greater is often insufficient to reveal complete spatial segregation. To achieve this, analysis of finer habitat partitioning becomes necessary (Eurich et al., 2018). This is especially important for CRFs due to their small body sizes (Depczynski & Bellwood, 2004). The *Trimma* species examined have small body sizes of <25 mm (Goldsworthy et al., 2022; Winterbottom et al., 2011), and accordingly may have the ability to exploit many small and different microhabitats within the same area of the reef (Brandl et al., 2018). Many studies have investigated microhabitat partitioning in CRFs (Herler, 2007). For instance, within the genus *Gobiodon*, an intricate level of niche partitioning is evident, where different species of this genus inhabited distinct species of *Acropora* corals (Dirnwöber & Herler, 2007; Munday et al., 1997). Additionally, within the genus *Pleurosicya*, *P. micheli* predominantly inhabited massive corals, whereas *P. prognatha* occupied a range of *Acropora* species (Herler, 2007). Pygmy gobies of the genus *Eviota* are present in a broad range of

microhabitats where different species exhibit distinct preferences for coral, sand, rubble, and coral rock (Brandl et al., 2018; Doll et al., 2021; Herler, 2007; Tornabene et al., 2013).

For the *Trimma* examined in this study, there were disparities in the structure of the microhabitat that each species was predominantly found in, with 81.8 – 90.8% of co-existing individuals present in different microhabitats. *T. yanoi* was predominantly found in dense aggregations in overhanging or sloping inward reef microhabitats covered in encrusting substrata, which are cave-like environments. *T. capostriatum* also frequented overhanging reef microhabitats or was found solitary or in smaller clusters in cavities underneath mounding corals that may simulate a small cave-like environment. Marine caves are biodiversity hotspots on the reef (Slattery et al., 2013). These structurally complex habitats provide a refuge for many coral reef fishes (Jones & Syms, 1998; S. K. Wilson et al., 2009). Protective habitats, such as caves, may be beneficial for many CRFs due to their small size and consequent susceptibility to predation (Depczynski & Bellwood, 2006; Depczynski & Bellwood, 2004; Goldsworthy et al., 2022; Winterbottom et al., 2011). Alongside this, caves are rich in nutrients (Kötter et al., 2001; Slattery et al., 2013). *Trimma* predominantly feed on zooplankton (Depczynski & Bellwood, 2003; Saeki et al., 2005) and caves contain aggregates of zooplankton that use these structures to shelter from currents (Emery, 1968). Furthermore, heterogeneous environments can be present within caves, with high habitat rugosity and differing light levels with distance from entrances. Such differences may therefore allow the separation of spatial resources, which can reduce interspecific interactions where species co-occur (Chave, 1978; Depczynski & Bellwood, 2004). Though this may be applicable to *T. yanoi* and *T. capostriatum*, both of which showed high occurrences in cave-like microhabitats, they co-existed together in less than 1% of occupied m<sup>2</sup> quadrats and were not seen interacting with one another. In conclusion, overhanging reef structures may be desirable habitats, as they are nutrient rich and provide diverse and protective environments for many small fishes.

However, not all species showed a preference for cave-like microhabitats. *T. benjamini* predominantly inhabited vertical reef microhabitats covered in encrusting substrata and was not commonly observed in overhanging reef microhabitats. Factors influencing differing microhabitat preferences of small CRFs may be similar to processes occurring at larger scales (Depczynski & Bellwood, 2004), including trade-offs between food availability (Wilson, 2001), competition (Stewart & Jones, 2001), and group organisation (Kane et al., 2009). Plankton composition is known to differ between caves and open areas (Emery, 1968), thus perhaps differences in microhabitat is driven by varying dietary preferences (Brandl, Casey, et al., 2020). Moreover, since caves are important habitats for many species of fish (Chave, 1978; Depczynski & Bellwood, 2004), there is likely to be high competition for resources such as space, and therefore interspecific competition may drive others out of these optimal habitats (Munday et al., 2001). Finally, the clustering patterns of each species might have an influence on which microhabitats are used by each species (Kane et al., 2009; Troyer et al., 2018). For example, cavities underneath mounding corals may only be able to support the small aggregations of *T. capostriatum* and would not be able to support the larger cluster sizes and densities seen in *T. yanoi* or *T. benjamini*. Factors driving spatial separation based on small-scale habitats may be an interplay of these influences and remain open for further investigation.

Despite the structural differences in microhabitats seen, this study of three *Trimma* species reveals a notable consistency. One common feature among the frequently inhabited areas is the prevalence of coral rock covered with encrusting species like crustose coralline algae, turf algae, encrusting corals, and encrusting sponges. This preference may be attributed to the suitability of coral rock for the growth of encrusting organisms, rendering it a prevalent substratum type (Satheesh & El-Sherbiny, 2022). Given *Trimma*'s association with hard substrata, their presence on live coral rock may be primarily attributed to its availability (Winterbottom, 2019). However, these species might also actively select this substratum for

several other possible reasons. Firstly, encrusting organisms on coral rock may offer slightly elevated perches from which *Trimma* can efficiently capture food, which is a behaviour documented in these fishes (Depczynski & Bellwood, 2004; Winterbottom, 2019). Secondly, the encrusting substratum matrix, crevices, and holes in live coral rock may provide additional hiding opportunities by providing more 3D complexity and therefore may increase crypsis (Mallela, 2007; Marshall *et al.*, 2019). In essence, the microhabitats characterised by coral rock and encrusting organisms offer a multifaceted environment that meets both the foraging and sheltering needs of *Trimma* species.

Differences seen at broader spatial scales in combination with those at a fine scale, resulted in little spatial overlap among the three *Trimma* species (Figure 2.5). Each species had compartmentalised habitats even if they co-occurred less than a meter apart. Species coexistence may be enhanced by the high habitat rugosity of coral rock covered in encrusting organisms. This structural complexity presents a multiplicity of refugia, including holes and crevices, potentially facilitating multiple species to coexist within constrained spatial domains (Depczynski & Bellwood, 2004; Herler, 2007; Mallela, 2007). When these species did encounter one another, interspecific territorial chasing behaviours were demonstrated (Figure 2.5). However, because they barely overlapped spatially, these incidents were rare, occurring in <1% of individuals observed in each species. Such spatial differentiation may serve as a mechanism for enabling high CRFs diversity at small spatial scales (Ahmadi *et al.*, 2018; Herler *et al.*, 2011; Munday & Jones, 1998; Munday *et al.*, 2004). There are over 6000 species of coral reef fishes, and it is estimated that 44% of these are CRFs (Brandl *et al.*, 2018). In the genus *Trimma*, there are currently 105 species (Winterbottom, 2019) and this number could surpass 200 species when accounting for genetic differences, which would make them the most speciose genus of coral reef fishes (Winterbottom *et al.*, 2014). While it has been suggested that niche partitioning plays a partial role in the diversity of *Trimma* (Herler *et al.*, 2011),

further investigation is required to establish a definitive link between these two phenomena. However, studying CRFs has additional challenges of tiny body size and camouflage within benthic habitats. Standard underwater visual census has low detectability of CRFs, and many studies that do not account for this are missing a large portion of reef diversity (Ackerman & Bellwood, 2000). Although several necessary precautions have been taken to minimise this bias ethically as outlined in the methodology, the abundance of fishes (particularly those < 14 mm standard length) may have been underestimated.

Understanding drivers of niche partitioning and diversity in CRFs is important due to their potentially critical ecological roles in coral reef energy transfer (Brandl et al., 2019; Depczynski & Bellwood, 2003). In the event of species loss, ecosystems with greater diversity have a lower risk of losing important functional roles (Naeem & Li, 1997). Moreover, considering the effects of climate change and the decline of Scleractinia corals, numerous coral-associated CRFs are at risk (Brandl et al., 2018). Therefore, it becomes crucial to understand habitats, niche partitioning and diversity in CRFs that have a lower association with corals (Doll et al., 2021), including *Trimma*. The summation of my results is an example of how ecologically, functionally, and phylogenetically similar species can simultaneously co-exist, which may allow for high levels of diversity to exist at small scales.

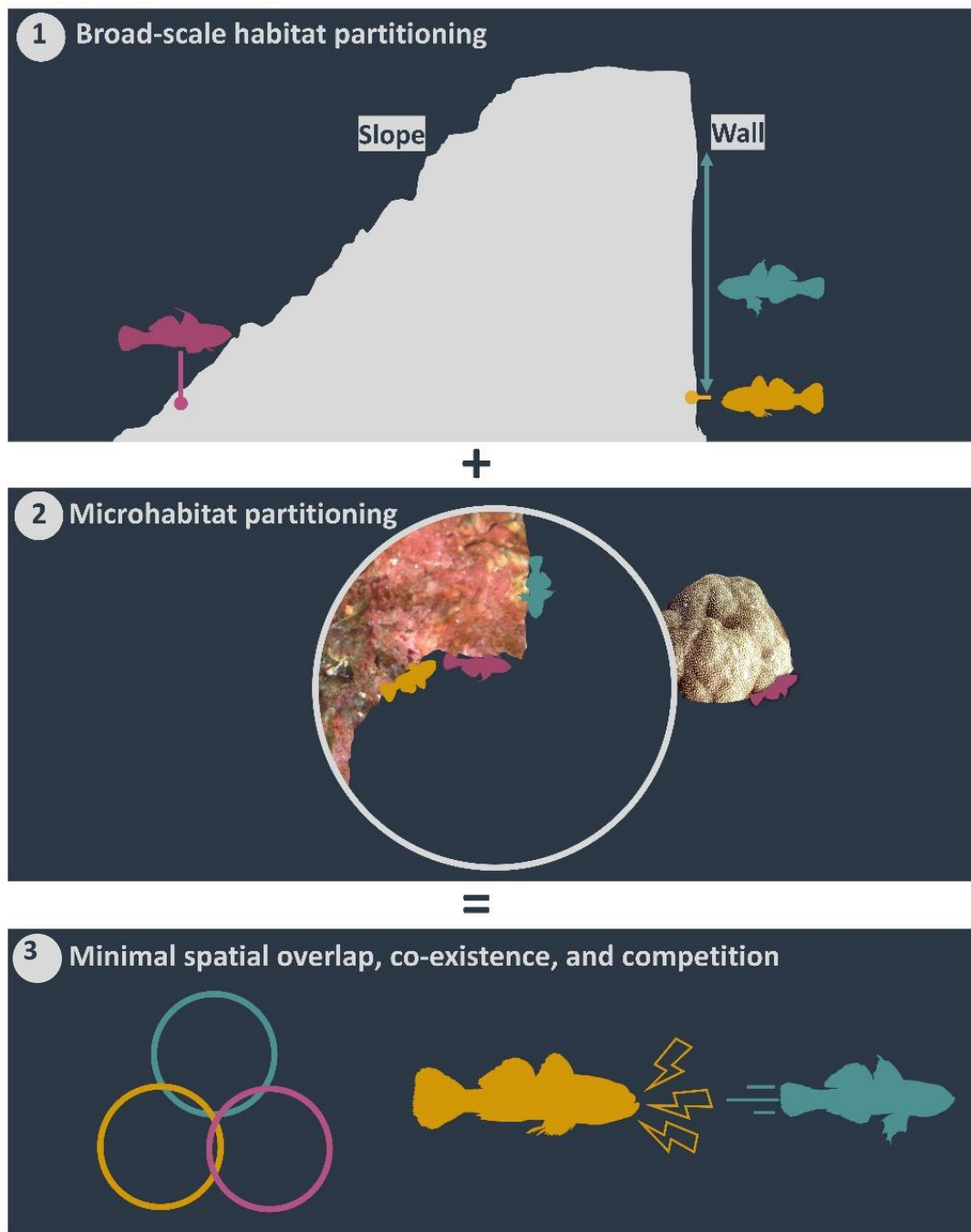


Figure 2.5: Conceptual diagram summarising 1) Partitioning of broad scale habitats (i.e., reef location, aspect, depth). Points and arrows indicate the area each species occurred in greatest abundance. 2) Microhabitat partitioning. 1 and 2 combined resulted in 3) Minimal spatial overlap, co-existence of species, and territorial behaviour in rare cases of habitat overlap. Teal = *Trimma benjamini*, purple = *T. capostriatum*, yellow = *T. yanoi*.

### Chapter 3: Life history constraints, short adult lifespan, and reproductive strategies in coral reef gobies of the genus *Trimma*

---

#### Published as

Goldsworthy, N. C., Srinivasan, M., Smallhorn-West, P., Cheah, L.-C., Munday, P. L., & Jones, G. P. (2022). Life history constraints, short adult lifespan and consequences for reproduction in coral reef gobies of the genus *Trimma*. *Journal of Fish Biology*.  
<https://doi.org/10.1111/jfb.15161>

#### 3.1 Abstract

Body size influences many life history traits, with small-bodied animals tending to have short lifespans, high mortality, and greater reproductive effort early in life. This study investigated the life history traits and reproductive strategies of three small-bodied coral reef gobies of the genus *Trimma*: *Trimma benjamini*, *T. capostriatum* and *T. yanoi*. All *Trimma* species studied attained a small body size of <25 mm, had a short lifespan of <140 days, and experienced high estimated daily mortality of 3.0 – 6.7%. Furthermore, the pelagic larval phase accounted for 25.3 – 28.5% of the maximum lifespan, and maturation occurred between 74.1 and 82.1 days at 15.2 – 15.8 mm, leaving only 35-43% of the total lifespan as a reproductively viable adult. All mature individuals had gonad structures consistent with bidirectional sex change, with bisexual gonads including both ovarian and testicular portions separated by a thin wall of connective tissue. In the female and male phase, only ovaries or testes were mature, while gonadal tissue of the non-active sex remained. One *T. benjamini* individual and one *T. yanoi* individual had ovarian and testicular tissue active simultaneously. These results highlight the life history challenges small CRFs face on their path to reproduction and reproductive strategies that could be beneficial in fishes with high and unpredictable mortality and short reproductive lifespans.



### 3.2 Introduction

Body size has broad ecological and evolutionary implications for animals, impacting on their diversity, abundance, ecological specialization and life history traits (Hanken & Wake, 1993; Marzluff & Dial, 1991; May, 1978; Peters, 1983; Roff, 1992). Large-bodied organisms tend to exhibit prolonged lifespans, reduced mortality, and late maturation. In contrast, small-bodied animals tend to exhibit short lifespans and high mortality, resulting in limited time available to reproduce and the selection for greater reproductive effort earlier in life (Calder, 1984; Roff, 1992; Stearns, 1992). Small animals must adopt strategies to develop quickly and reproduce early and successfully before their short life ends (Fisher *et al.*, 2013). However, for small species, there may be ecological and physiological constraints on how short development and maturation times can be (Bernardo, 1993; Charnov *et al.*, 2001; Roff, 1992).

On coral reefs, fishes that occupy benthic habitats and are small bodied (i.e., <50 mm) are known as cryptobenthic reef fishes (CRFs., Goatley & Brandl, 2017). The majority of coral reef fish species have a small body size (Munday & Jones, 1998) and they can be highly abundant on coral reefs (Ackerman & Bellwood, 2000; Galland *et al.*, 2017). While considerable attention has been given to the ecological implications of small body size, including diversity, abundance, habitat specialization, and predation risk (Jones *et al.*, 2002; Munday & Jones, 1998), much less is known about CRF life history strategies to compensate for high mortality and short lifespan. There is increasing evidence which shows CRFs have vital ecological roles in maintaining coral reef energy flow, providing 60% of consumer biomass through their extraordinarily fast-paced life history dynamics (Brandl *et al.*, 2019; Depczynski *et al.*, 2007). However, a fast-paced life history requires time to transition from the larval stage, time to reach reproductive maturity and to reproduce successfully. How extremely small coral reef fishes partition their life history is poorly understood.

CRFs are faced with several obstacles throughout their life that potentially limit their ability to survive and reproduce. Firstly, the small body size of CRFs is associated with reduced longevity compared to larger coral reef fishes, and hence a small maximum window for reproduction (Depczynski & Bellwood, 2006). Second, CRFs also experience high mortality rates as a result of their small size (Depczynski & Bellwood, 2006; Goatley & Bellwood, 2016; Goatley et al., 2017; Winterbottom et al., 2011). Mortality in reef fishes decreases exponentially after reaching a size threshold of ~43 mm (Goatley & Bellwood, 2016). Many CRFs thus experience high mortality throughout their entire lives as this threshold is never surpassed (Depczynski & Bellwood, 2006; Winterbottom et al., 2011), leading to an increased chance of perishing before reaching reproductive maturity.

In addition to a short lifespan and high mortality, CRFs encounter two main physiological constraints which reduce their reproductive lifetime, the first being the length of their pelagic larval duration (PLD). Reef fishes have a two-part life cycle, comprising a pelagic larval phase before settlement onto the reef (Leis & McCormick, 2002). PLD is broadly similar across most reef fish species, despite vast differences in overall longevity (Depczynski & Bellwood, 2006). For example, *Bolbometopon muricatum* can live up to 37 years (Andrews et al., 2015) and has a PLD of just 25 days (Taylor et al., 2018), representing 0.2% of the maximum lifespan. By contrast, the pygmy goby, *Trimma nasa*, lives <90 days and has a PLD of 34 days, representing 38.7% of its lifespan (Winterbottom & Southcott, 2008). PLD may be constrained among fishes to attain a critical size or developmental stage before settlement onto the reef (Beeken et al., 2021; Depczynski & Bellwood, 2006). Consequently, PLD, which is a considerable time in early life not available for reproduction, potentially makes up a large proportion of the maximum lifespan of CRFs.

The second physiological constraint for CRFs is their length/age at maturity. According to life history theory, early maturation should be selected for in small-bodied individuals with high mortality rates to increase the probability that individuals will survive until they reproduce (Ricklefs, 2010; Roff, 1992; Stearns, 1992). However, early maturation has disadvantages associated with maturing at a smaller body size. For example, female fecundity is low with a small body size, or a larger body size may be selected for where intraspecific competition is present (Hernaman & Munday, 2005b; Wong *et al.*, 2008). As a result, CRFs are faced with a dilemma regarding the best overall reproductive strategy to adopt, either: i) mature early to increase the overall chance of surviving to reproduce (e.g., Depczynski & Bellwood, 2006), or ii) delay maturation and attain a larger body size to improve size related reproductive outputs (e.g., Kunishima *et al.*, 2021). Delaying maturation, however, further reduces the reproductive time available to CRFs and could be a risky strategy when mortality rates remain high throughout life.

Many coral reef fishes are capable of enhancing lifetime reproductive outputs by employing various sex change strategies (Benvenuto *et al.*, 2017). The size-advantage model (SA model, Ghiselin, 1969; Warner, 1975) suggests protogyny will be favoured in polygynous groups, where large males achieve the highest reproductive success as a result of intrasexual competition for mates or breeding sites. Conversely, protandry is favoured where male body size does not affect reproductive success and larger individuals have a higher reproductive success as females, due to the positive relationship between body size and fecundity (Ghiselin, 1969; Warner, 1975). In addition, bidirectional sex change can occur in polygynous groups, where a large female can transition to male when the dominant male is lost. Reverse sex change can occur if a single male infiltrates a group with a larger male (Manabe *et al.*, 2007). In small fishes with high and erratic mortality rates, a male may abruptly lose every female in his harem. A solitary male may have an indefinite window for reproduction due to the high likelihood of

predation, and delays in locating new breeding partners may significantly reduce his reproductive value. By becoming female and reproducing in an established group, his reproductive outputs may be higher than remaining male and waiting for a new harem to form (Munday et al., 2010).

Sex change comes at a cost of time and energy taken to convert the gonads from one sex to another, which can place further pressure on reproduction (Munday & Molony, 2002). Some CRFs have minimised these costs by evolving bisexual gonads with female and male tissues, containing developed tissues of the active sex, and regressed tissues of the non-functional sex (Sunobe & Nakazono, 1993). This avoids entire gonad reconstruction and allows for rapid sex change, thus saving time and energy (Munday et al., 2010; Yamaguchi & Iwasa, 2017), which may be beneficial in species when social conditions experienced by males might change dramatically and unpredictably and when a delay in finding a new partner could result in a substantial loss of reproductive output (Munday et al., 2010).

The genus *Trimma* (family *Gobiidae*) is a group of hyper-diverse Indo-Pacific CRFs, consisting of 105 species (Winterbottom, 2019). These small-bodied fishes have a standard length ( $L_s$ ) of <30 mm and are among the smallest vertebrates on Earth. Despite extensive research describing mating systems and sex change strategies of *Trimma* (Fukuda, Manabe, et al., 2017; Fukuda & Sunobe, 2020; Fukuda, Tanazawa, et al., 2017; Kobayashi *et al.*, 2005; Manabe et al., 2007; Manabe et al., 2008; Sakurai et al., 2009; Sunobe & Nakazono, 1990; Sunobe et al., 2017; Tomatsu et al., 2018), there have been limited attempts to describe other aspects of their ecology and life history (but see Winterbottom et al., 2011; Winterbottom & Southcott, 2008). Consequently, little is known about the challenges *Trimma* face on their path to reproduction. Given their small body size, it is expected that *Trimma* species may also experience traits associated with other small-bodied fishes, such as: i) reduced longevity; ii)

high mortality rates; iii) long PLD relative to lifespan and iv) early or delayed maturation, depending on the presence of advantages favouring either strategy. A combination of i-iv can lead to a short reproductive life. In this study, I investigate these life-history obstacles and reproductive strategies in three species of *Trimma*: *Trimma benjamini*, *T. capostriatum* and *T. yanoi*.

### **3.3 Materials and Methods**

#### ***3.3.1 Species, specimen collection and ethical statement***

*Trimma* is speciose and abundant genus on Indo-Pacific coral reefs and adjacent habitats. All three species studied here are sedentary benthic species which perch on hard substrata, as opposed to hovering in the water column above the benthos like several other members of this genus. A total of 353 individuals (129 *T. benjamini*, 102 *T. capostriatum*, 122 *T. yanoi*) were collected between November and December 2019 from inshore and offshore reefs in Kimbe Bay, Papua New Guinea. All individuals were captured on SCUBA using a fine-mesh (2 mm) hand net and clove oil anaesthetic solution (5:1, ethanol: clove oil), and euthanized by immersion in an ice slurry (50% water, 50% ice) immediately after surfacing. Fish collections were compliant with James Cook University Ethics Approval A2665 and were collected under a research visa allocated to Professor Geoffrey Jones issued by the government of Papua New Guinea. Permissions were granted by: Mrs. Cecilie Benjamin (Chair of the Board, Mahonia Na Dari Research and Conservation Centre, Kilu) and Mr. Thomas Koi, (Village Elder and representative of the Local Marine Management Committee, Kilu).

#### ***3.3.2 Body size, longevity, and mortality***

Fresh specimens were blotted dry and measured to 0.5 mm  $L_s$ . The head of each fish was removed from the body by sectioning between the operculum and pectoral fins and was

preserved in 70% ethanol. Fish age and PLD were determined using sagittal otoliths, which were removed from the brain cavity, cleaned with water, and stored dry in vials. Thermoplastic glue (Crystalbond 509™) was used to mount otoliths sulcus-down on glass slides. The surface of each otolith was polished using 9, 3 and 0.3  $\mu\text{m}$  lapping film to obtain a thin, flat section of a whole otolith with growth rings clearly visible from the otolith primordium to edge. Sections were coated in immersion oil to improve microstructure clarity and photographed at 200x and 400x magnification with an Olympus EP50 digital camera attached to a BX43 Olympus microscope. Growth rings were counted in ImageJ (Schneider *et al.*, 2012) from the core outwards, beginning at the first increment which was assumed to be deposited at hatching (Winterbottom *et al.*, 2011). Although this could not be validated experimentally for *Trimma*, growth increments were assumed to be daily deposits, as seen in ecologically similar CRFs (e.g. Depczynski & Bellwood, 2006; Depczynski & Bellwood, 2005a; Hernaman & Munday, 2005a; Longenecker & Langston, 2005; Vigliola & Meekan, 2009; Winterbottom *et al.*, 2011; Winterbottom & Southcott, 2008). For each individual, two counts of each otolith were made on separate occasions and the mean was calculated. If the initial counts differed by >10% of the mean, a third count was made. The average of the closest two counts were then taken assuming all were within 10% of the mean, and this value represented the age of the fish in days. The maximum lifespan was defined as the fish with the greatest number of rings in each species (Winterbottom *et al.*, 2011).

Natural daily mortality was estimated by three methods and was calculated separately for each species. The first method calculated mortality rate according to Hoenig's equation, which is derived from experimental evidence over a broad range of marine taxa ( $r^2 = 0.82$ ):  $\ln Z = 1.46 - 1.01 \ln T_{max}$ .  $Z$  is the instantaneous mortality rate and  $T_{max}$  the maximum age (Hoenig, 1983). Secondly, mortality was calculated with the Chapman and Robson estimator using the frequency of individuals in 10-day age-class bins. This model is based on the concept that the

descending section of the catch-at-age data followed a geometric probability distribution, which was used to estimate the survival ( $S$ ) parameter.  $Z$  was calculated from these estimates of  $S$ , where  $S = e^{-Z}$  (Chapman & Robson, 1960; Winterbottom et al., 2011). Finally, mortality was calculated using the catch curve regression estimator (Dunn *et al.*, 2002) by fitting a linear regression to the descending section of a 10-day age frequency plot after log transformation to obtain estimates of  $Z$ . Estimates of  $Z$  from the Chapman and Robson estimator and the catch curve regression estimator were converted to daily mortality using  $\frac{(1-e^{-Z})}{10}$  and expressed as a percentage.

### 3.3.3 *Pelagic Larval Duration*

Settlement was determined by a change in contrast from more opaque (pre-settlement) to less opaque (post-settlement) and/or a decrease in increment width in each otolith (Figure 3.1A) (Wilson & McCormick, 1999). The number of rings pre-settlement indicated the PLD, and the maximum post-settlement lifespan was the difference between the PLD and maximum age. Differences in mean PLD among species were assessed using a one-way ANOVA and post-hoc Tukey HSD test.

### 3.3.4 *Maturation*

Length and age at maturity were defined as the  $L_S$  and age at which 50% of specimens were sexually mature females (sex determined by gonad structure, see below). Estimations of maturity were obtained by fitting a logistic regression function to the proportional frequency of juveniles to females in 1 mm  $L_S$  class intervals and 10-day age class intervals (Lowe *et al.*, 2021). Individual logistic regression curves were fitted for each species, and 95% confidence intervals were determined using a Gaussian error distribution (Antle *et al.*, 1970). For each species, time spent as a juvenile was calculated as the difference between the mean PLD and

the age at maturity, and time spent as a reproductively viable adult was taken as the difference between the age at maturity and the maximum lifespan. Finally, the dimensionless ratio  $\frac{\text{length at maturity}}{\text{maximum } L_s}$  was calculated for each species, which shows the proportional lengths that are expended before and after maturation (Tsikliras & Stergiou, 2014).

### **3.3.5 Reproduction**

Reproductive phases and strategies were assessed by histological examination of the gonads. After capture of specimens, abdomen sections were dissected just anterior to the anus and were placed in a formaldehyde 4%, acetic acid 5%, calcium chloride 1.3% (FAACC) fixative for three days, then transferred to 70% ethanol. At the time of processing, abdomens were placed in a tissue processor, embedded in paraffin wax with the body cavity facing down, sectioned to 5  $\mu\text{m}$  using a microtome, mounted on glass microscope slides, and stained with Mayer's Haematoxylin and Young's eosin-erythrosine (H&E). 5 - 15 sections were taken per specimen, separated by 50-200  $\mu\text{m}$  to ensure an adequate representation of each gonad was captured. Histological samples were examined under a high-power microscope with transmitted light.

Ovaries and testes were classed as mature or undeveloped according to Sunobe et al. (2005) and Sakurai et al. (2009). Ovaries were classed as mature when the most advanced oocyte present in the gonads was vitellogenic or hydrated, and undeveloped when ovaries contained only previtellogenic oocytes. Testes were classed as mature when consisting of expanded sperm ducts containing many free spermatozoa, and a developed, lobed and secreting accessory gonadal structure (AGS) attached to each testis was evident (Cole, 1990). Testes were classed as undeveloped when spermatozoa were absent or present in small amounts with no sperm ducts evident, and the testes associated AGS was undeveloped and was non-lobed



and non-secreting. The term bisexual refers to a gonad structure consisting of both ovarian and testicular tissue, and does not refer to bisexual function (Lowe et al., 2021).

### 3.4 Results

#### 3.4.1 *Body size, longevity, and mortality*

*T. benjamini*, *T. capostriatum*, and *T. yanoi* exhibited small body sizes ( $L_s$ ) of  $17.2 \pm 0.5$  mm (mean  $\pm$  95% confidence interval),  $17.6 \pm 0.6$  mm and  $15.8 \pm 0.7$  mm, and reached a maximum  $L_s$  of 24 mm, 24.5 mm and 22 mm, respectively (Table 3.1a, Figure A2. 1). All species were short-lived, with maximum ages of 130 days, 137.5 days and 126.5 days in *T. benjamini*, *T. capostriatum*, and *T. yanoi*, respectively (Table 3.1a, Figure A2. 1).

Daily mortality estimates obtained from the focal *Trimma* species were high, ranging from 3.2 – 5.4% in *T. benjamini*, 3.0 – 6.7% in *T. capostriatum*, and 3.2 – 4.4% in *T. yanoi* (Table 3.1b). Specimens younger than 95 days in *T. benjamini*, 105 days in *T. capostriatum* and 85 days in *T. yanoi* were not included in the Chapman-Robson and Catch curve analysis (Figure 3.2), as their frequency suggests they may have been under sampled (Winterbottom et al., 2011).

Table 3.1: Results for *Trimma benjamini* (n = 129), *T. capostriatum* (n = 102) and *T. yanoi* (n = 122) showing a) Maximum recorded lifespan (days) and body size ( $L_s$ , mm), b) Daily mortality estimated by Hoenig's equation, the Chapman-Robson estimator and catch-curve regression estimator and c) Age (days) and length (mm, proportion of max  $L_s$ ) at maturity. \*mean  $\pm$  95% confidence intervals

		<i>Trimma benjamini</i> n = 129	<i>Trimma capostriatum</i> n = 102	<i>Trimma yanoi</i> n = 122
<b>a) Body size and lifespan</b>	Maximum lifespan (days)	130.0	137.5	126.5
	Maximum $L_s$ (mm)	24.0	24.5	22.0
<b>b) Daily mortality</b>	Hoenig's equation (%)	3.2	3.0	3.2
	Chapman-Robson estimator (%) *	5.4 $\pm$ 1.0	6.1 $\pm$ 0.6	4.4 $\pm$ 1.1
	Catch-curve regression (%)*	5.1 $\pm$ 2.8	6.7 $\pm$ 3.0	4.4 $\pm$ 2.8
<b>c) Maturity</b>	Age at maturity (days)*	74.1 $\pm$ 3.1	82.1 $\pm$ 3.4	81.7 $\pm$ 3.4
	Length at maturity (mm)*	15.4 $\pm$ 0.7	15.2 $\pm$ 0.9	15.8 $\pm$ 0.4
	(proportion of max $L_s$ )*	0.64 $\pm$ 0.03	0.62 $\pm$ 0.04	0.72 $\pm$ 0.02

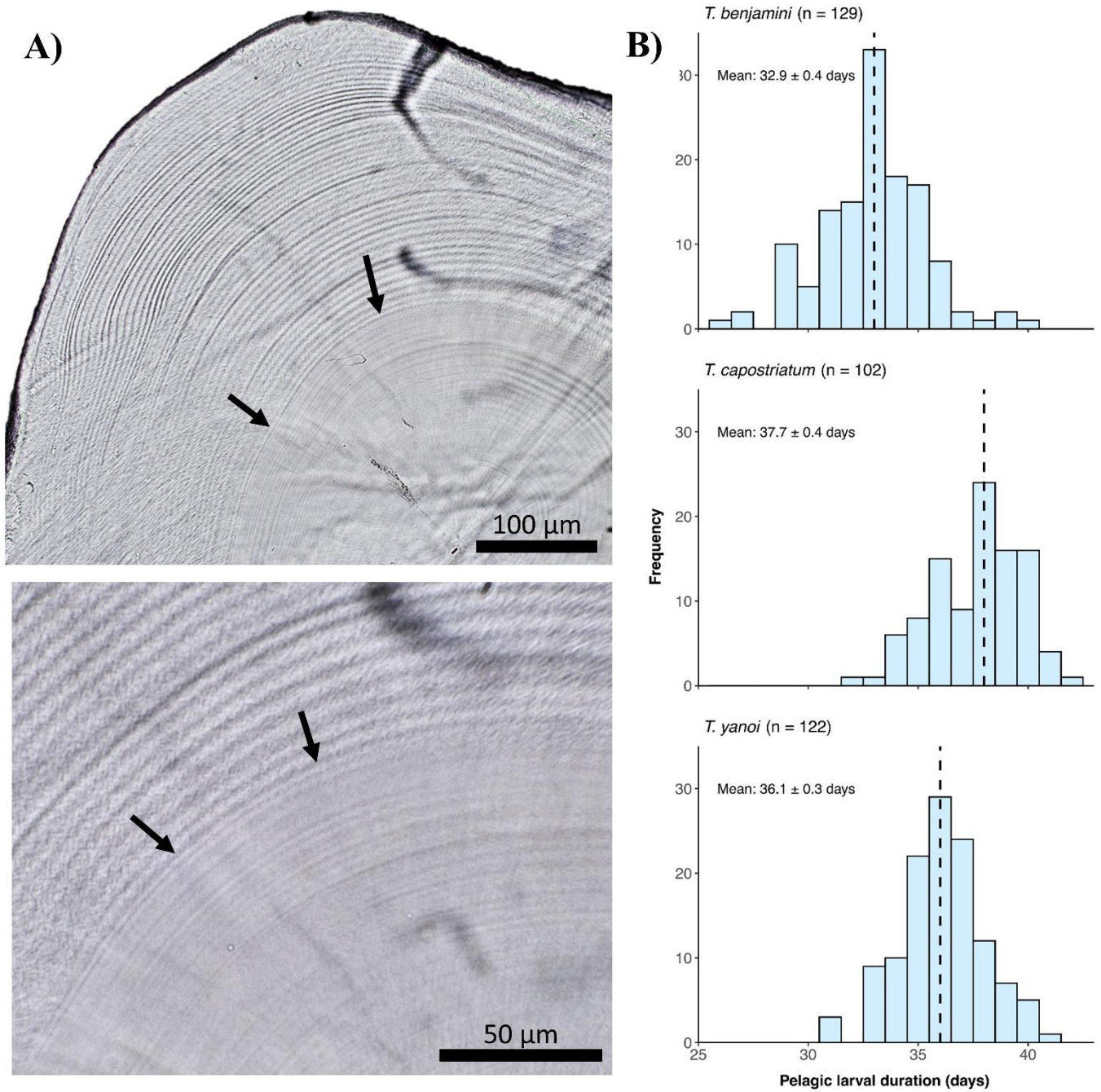


Figure 3.1: a) *Trimma yanoi* otolith showing daily growth increments and a change in optical density pre- and post-settlement. Arrows indicate settlement mark. Not all pre-settlement increments are visible in this focal plane. b) Frequency distribution of pelagic larval duration (PLD) in *Trimma benjamini* (n = 129), *T. capostriatum* (n = 102) and *T. yanoi* (n = 122).

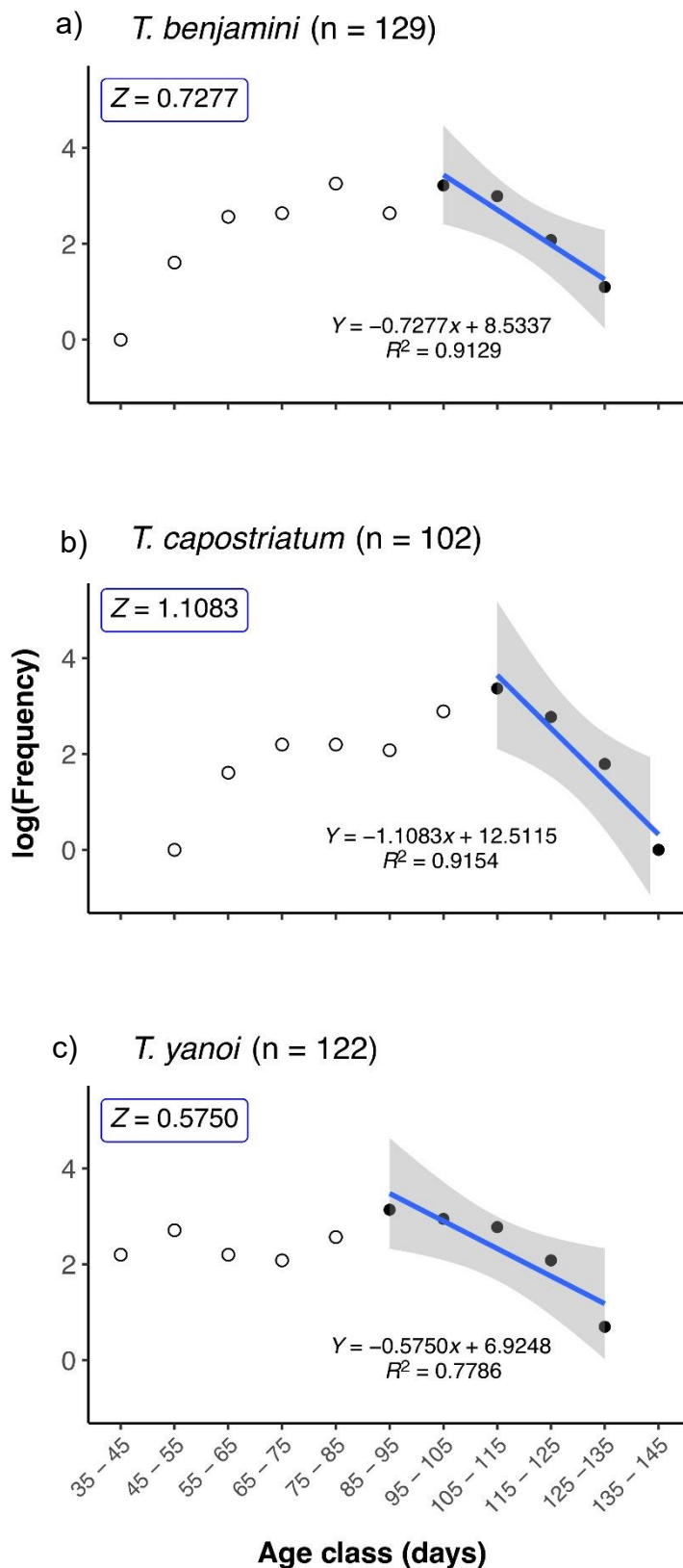


Figure 3.2: 10-day age-frequency catch curve regression for the estimation of instantaneous mortality ( $Z$ ) for a) *Trimma benjamini* (n = 129), b) *T. capostriatum* and c) *T. yanoi* (n = 122). White points show ascending limb values which were not included in the analysis and black points show descending limb values that were included in the analysis.

### 3.4.2 Pelagic larval duration

Clear settlement marks were able to be determined in all individuals (Figure 3.1A). PLD differed significantly among the three species ( $F_{(2, 350)} = 148.72$ ,  $p < 0.001$ ) and ranged from 26 – 40 days in *T. benjamini*, 32 – 42 days in *T. capostriatum* and 31 – 41 days in *T. yanoi* (Figure 3.1B). The mean PLD (32.9 – 37.7 days) represented over  $\frac{1}{4}$  of the maximum lifespan in all species (Figure 3.3). Accordingly, the post-settlement lifespan in each species was less than 100 days (Figure 3.3).

### 3.4.3 Maturation

Length at maturity (Figure 3.4) was similar for all three species (15.2 – 15.8 mm) and ranged from 0.62 – 0.72 as a proportion of the maximum  $L_s$  (Table 3.1c). *T. benjamini* matured the earliest at 74.1 days, followed by *T. capostriatum* and *T. yanoi*, which matured at similar ages of 82.1 and 81.7 days, respectively (Table 3.1c, Figure 3.4).

Thus, mean duration as a reproductively redundant juvenile in the species examined was 41.1–45.7 days, representing 31.7 – 36.1% of the maximum lifespan (Figure 3.3). The mean reproductive window was therefore a narrow 44.8 – 55.9 days, representing 35.4 – 43.0% of the maximum lifespan (Figure 3.3).

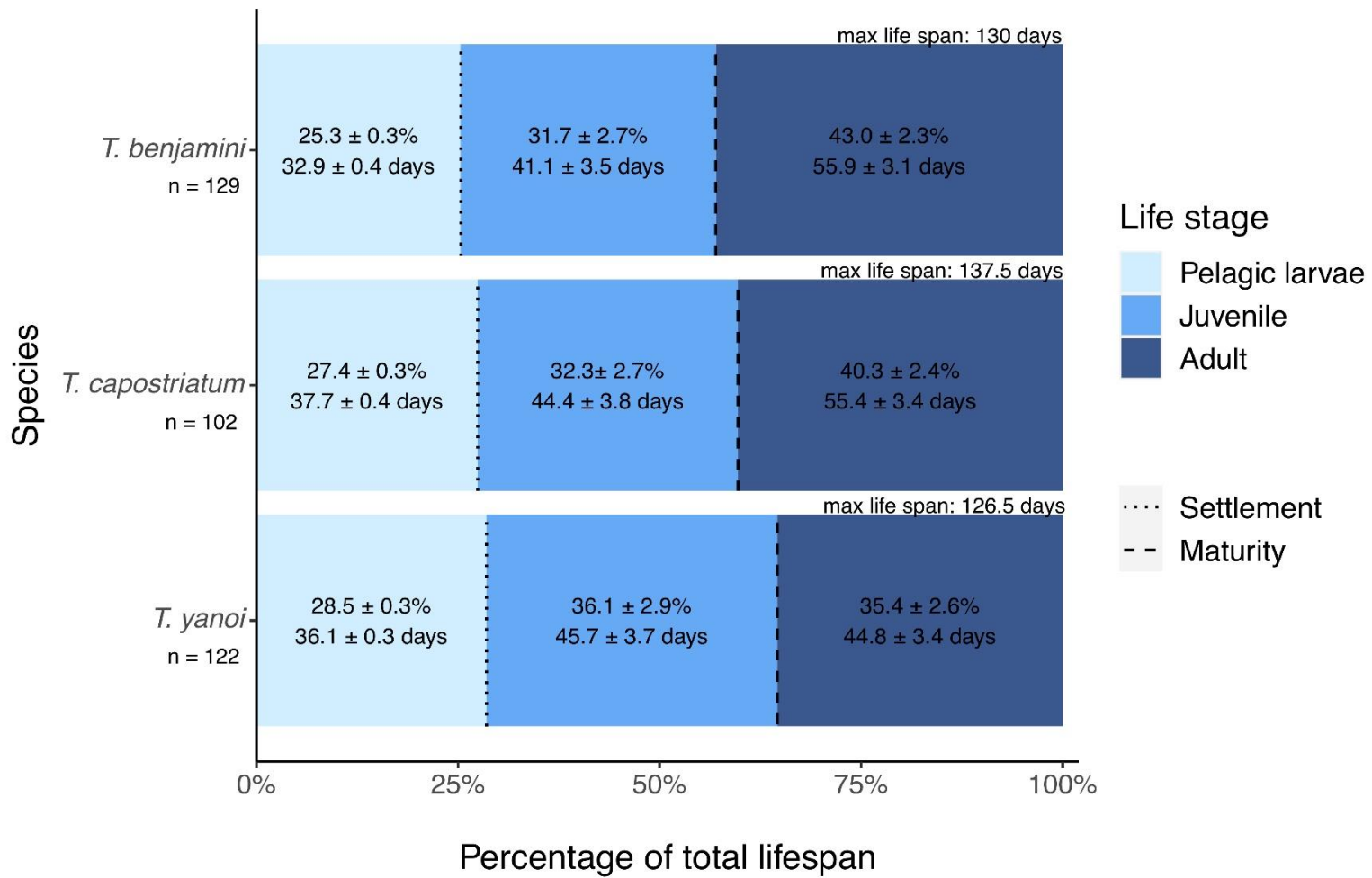


Figure 3.3: Number of days and percentage of maximum lifespan (mean  $\pm$  95% confidence intervals) spent in each life stage (pelagic larvae, juvenile and adult) for *Trimma benjamini* (n = 129), *T. capostriatum* (n = 102) and *T. yanoi* (n = 122). Dotted and dashed lines represent settlement and maturity, respectively.

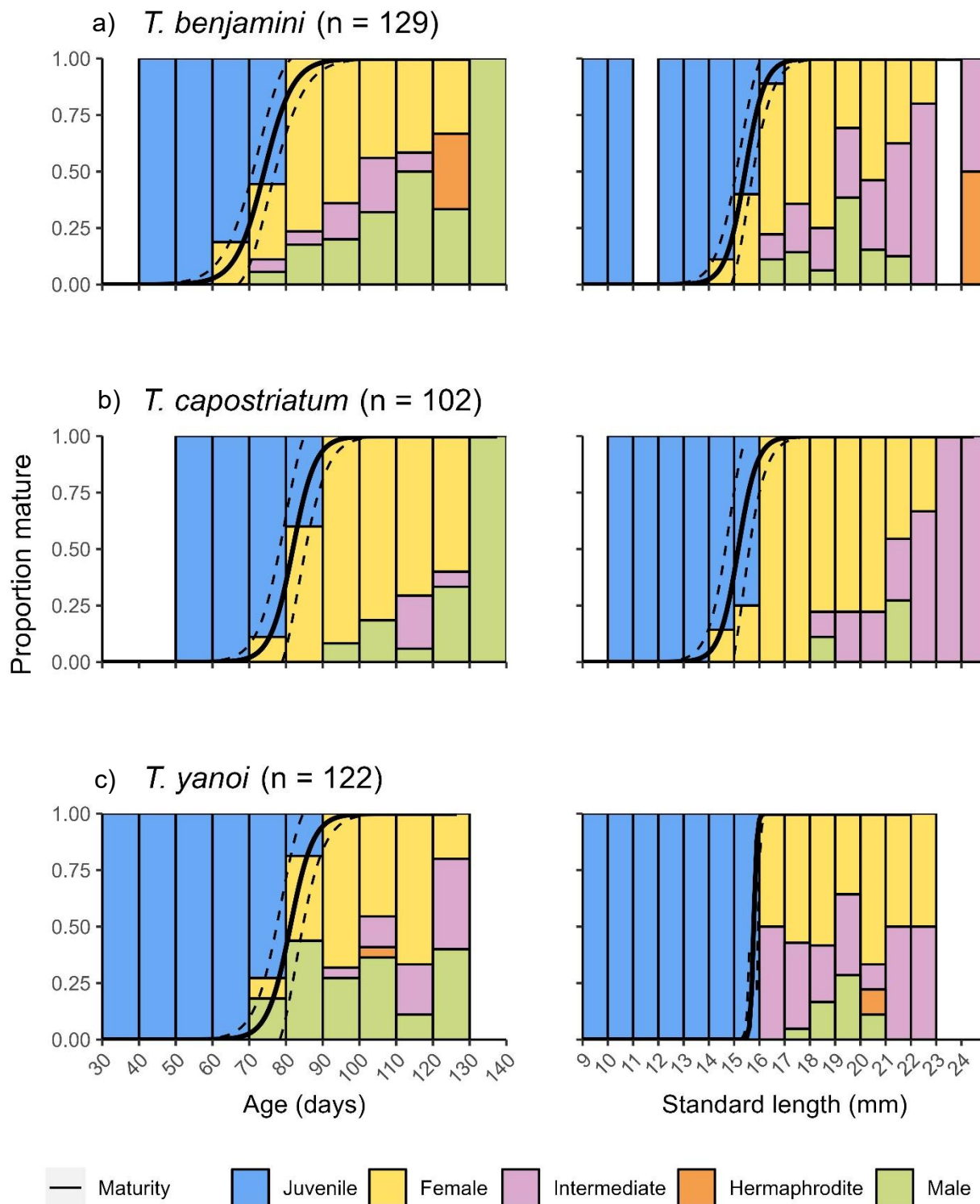


Figure 3.4: Proportional frequency distributions of the sexual phase-specific age and length structure of a) *Trimma benjamini* (n = 129), b) *T. capostriatum* (n = 102) and c) *T. yanoi* (n = 122). Estimated age and length at maturity trajectory is shown by solid logistic regression lines and the associated 95% confidence intervals are shown by dashed lines.

#### 3.4.4 Reproduction

In total, 353 *Trimma* gonads (129 *T. benjamini*, 102 *T. caopstriatum* and 122 *T. yanoi*) were analysed histologically. Aside from juveniles with undifferentiated gonadal cells, all individuals had bisexual gonads, which consisted of both ovarian and testicular portions, partitioned by a thin wall of connective tissue, and an accessory gonadal structure (AGS) connected to each testis. This gonad arrangement was the same in all species. In female and male phase specimens, only ovaries or testes were mature at a single point in time, while gonadal tissue of the non-active sex remained. 55 (*T. benjamini*), 61 (*T. caopstriatum*) and 39 (*T. yanoi*) individuals were female phase, evident by mature ovaries and undeveloped testes. The testes consisted of spermatogonia, spermatocytes spermatids, and few spermatozoa, indicating that spermatogenesis continued in the female phase. However, no sperm ducts were evident and the AGS was undeveloped and was non-lobed and non-secreting (Figure 3.5a, 5b). 25 (*T. benjamini*), 14 (*T. caopstriatum*), and 26 (*T. yanoi*) specimens were male phase. These individuals had mature testes and undeveloped ovaries, which consisted of a small section containing few previtellogenic oocytes (Figure 3.5c). The male: female sex ratios were 1: 2.2 in *T. benjamini*, 1: 4.4 in *T. caopstriatum* and 1: 1.5 in *T. yanoi*. Two specimens (1 each of *T. benjamini* and *T. yanoi*) had both mature ovaries and testes simultaneously and were thus labelled as a simultaneous hermaphrodite (referring to gonad structure and not necessarily function, Figure 3.5d). 13 *T. benjamini*, 5 *T. caopstriatum* and 8 *T. yanoi* individuals had ovaries and testes at intermediate levels of development and were thus labelled as transitional phase. Gonads in this phase consisted of ovaries with degenerating atretic oocytes and testes with proliferating spermatogenic tissue or degenerating spermatogenic tissue and proliferating oocytes. The AGS was lobed but non-secreting or secreting small amounts (Figure 3.5e). 35 (*T. benjamini*), 22 (*T. caopstriatum*) and 48 (*T. yanoi*) specimens had no mature ovarian or testicular tissue present and were classified as juveniles. Gonads of these individuals were



either bisexual, with ovaries that contained previtellogenic oocytes, testes with spermatogonia, and an undeveloped AGS (Figure 5f), or consisted entirely of undifferentiated gonadal germ cells (Figure 3.5g).

### 3.5 Discussion

The findings in this study indicate that the most prominent feature of *Trimma spp.* life histories is an extreme constraint on the time available for reproduction. All three species examined, were characterised by small body size, short lifespan, and high mortality, relatively long PLD, time taken to mature after settlement, and bisexual gonad development. Only 35 – 43% of the total lifespan was available for reproduction. Together, these life-history characteristics imply the genera is constrained both by a large proportion of lifespan unavailable to reproduce and high mortality owing to their small size. These results conform to a previous study by Winterbottom et al. (2011) examining the life history characteristics of *T. benjamini*.

The *Trimma* species in this study are among the smallest and shortest-lived fishes on coral reefs, with all individuals examined having a  $L_s$  of less than 25 mm and living less than 140 days. Small body size comes with many constraints including a short lifespan, high mortality risk, a long PLD relative to lifespan and consequently, a short reproductive life. Since the age of coral reef fishes ranges from 59 days in *Eviota sigillata* (Depczynski & Bellwood, 2006) to 81 years in *Macolor macularis* (Taylor et al., 2021), *Trimma* were at the lower end of the spectrum, which is also seen in other small CRFs (e.g., Beeken et al., 2021; Depczynski et al., 2007; Longenecker & Langston, 2005). Consequently, the maximum window available for reproduction is very narrow.

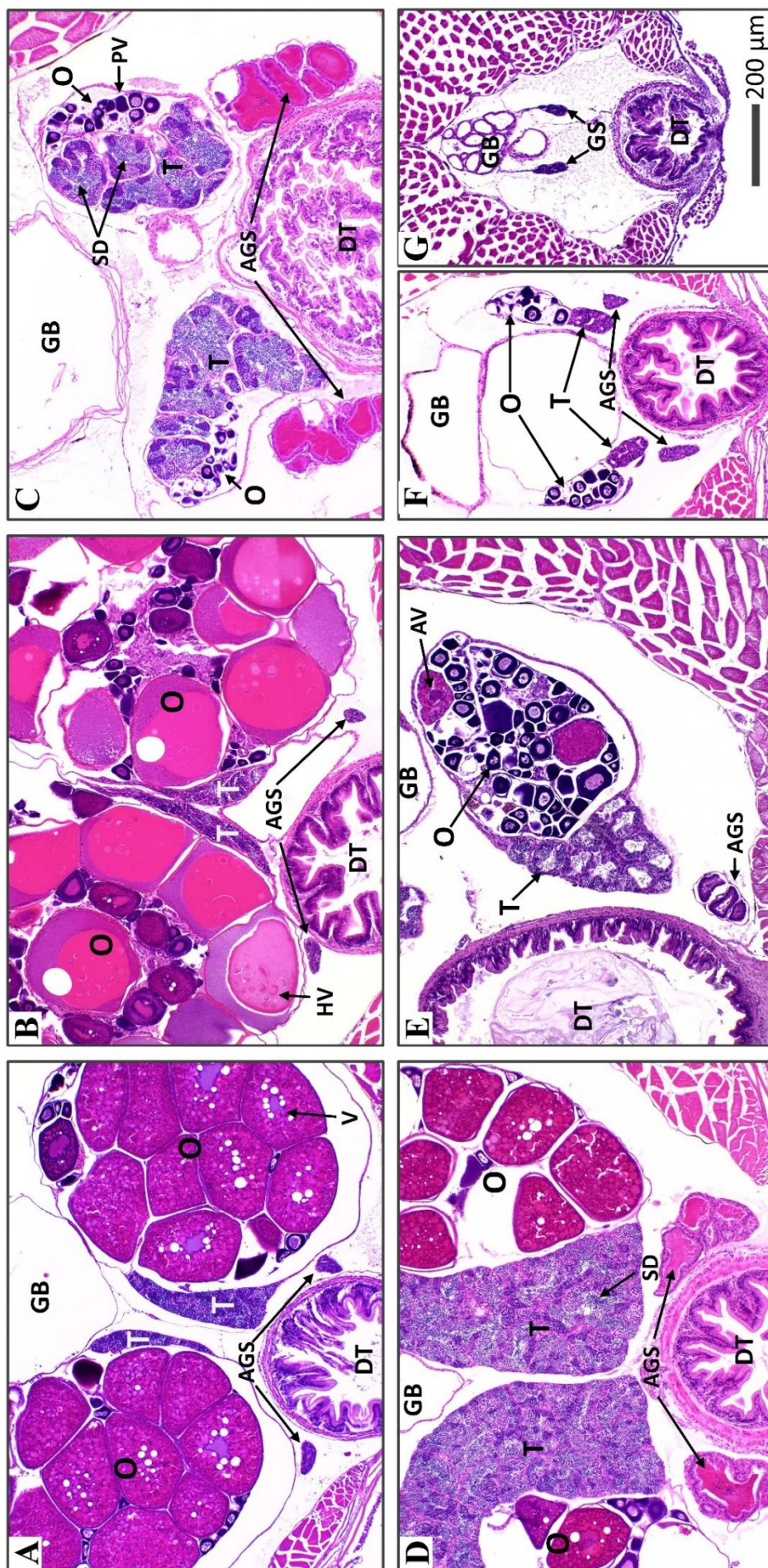


Figure 3.5: Gonadal structures of a & b) Female, c) Male, d) Simultaneous hermaphrodite, e) Transitional, and f & g) Juvenile phases in *Trimma benjamini* (a, d & f), *T. capostriatum* (c) and *T. yanoi* (b, e, & g). O ovary, T testis, AGS accessory gonadal structure, GB gas bladder, DT digestive tract, PV previtellogenic oocyte, V vitellogenic oocyte, HV hydrated vitellogenic oocyte, AV atretic vitellogenic oocyte, SD sperm ducts filled with spermatozoa, GS germ cells. n = 129 *Trimma benjamini*, 102 *T. capostriatum* and 122 *T. yanoi*. Scale bar 200 µm.

Estimated daily mortality of 3.0 – 6.7% per day is comparable to high mortality rates seen in other small-bodied CRFs (Depczynski & Bellwood, 2006). With a small body size of <25 mm, *Trimma* species never reach the size threshold of ~43 mm where mortality in larger species has been observed to decline. Consequently, *Trimma* remain at high risk of mortality throughout their entire life. Predation is assumed to be the main cause of mortality in CRFs, however, Goatley et al. (2017) propose predation rates are variable as a result of habitat or behavioural differences between species. *Trimma* species inhabit exposed reef slopes and drop offs on coral reefs, where they predominantly perch on hard substrata (Winterbottom, 2019), and may be victims of predation due to limited sheltering opportunities (Brandl et al., 2018). Moreover, the average size difference between predator and prey is strikingly small at 12.1 mm (Goatley et al., 2017). Therefore, *Trimma* species may be subject to predation by not only large fishes, but small ones too.

The PLDs of the three *Trimma* species examined represented a substantial proportion of their maximum lifespan (>25%), which is high, compared with the <1% demonstrated by many larger coral reef fishes (Depczynski & Bellwood, 2006). Yet, spending over a quarter of the lifespan as pelagic larvae is not unique to *Trimma* and is seen in other CRFs such as the genera *Coryphopterus* (Beeken et al., 2021), *Eviota* (Depczynski & Bellwood, 2006) and *Enneapterygius* (Longenecker & Langston, 2005). An extensive PLD to allow growth to a sufficient size may be a strategy to decrease extreme mortality of small recruits (Beeken et al., 2021). Some fishes that settle into protective habitats with lower post-settlement mortality have a reduced PLD (Depczynski & Bellwood, 2006). For example, *Amphiprion melanopus* settle directly into anemone hosts that provide protection from predators, experience short PLDs of <15 days, and are capable of settlement at <7 mm (Job & Bellwood, 2000). In contrast, *Trimma* species mainly settle onto hard substrata on exposed reef slopes and drop offs, which are not well protected (Winterbottom, 2019), and may suggest a minimum size threshold to reduce



post-recruitment mortality (Depczynski & Bellwood, 2006; Goatley & Bellwood, 2016). Accordingly, the PLD reduces the post-settlement life of *Trimma* to just 90-100 days, during which they need to complete metamorphosis, find a suitable home, grow, mature, and reproduce.

Maturation in the *Trimma spp.* examined was fast compared to most fishes. For example, mean age and lengths at maturity of Mediterranean Actinopterygii were 2.2 years and 207 mm, respectively, with maximum maturity at 12 years in *Epinephelus marginatus* (Tsikliras & Stergiou, 2015) and 2,235 mm in *Xiphias gladius* (Tsikliras & Stergiou, 2014). The ability for *Trimma* to rapidly mature in 74.1 – 82.1 days at 15.2 – 15.8 mm allows them to complete reproduction despite extremely short lifespans. However, length at maturity as a proportion of the maximum  $L_s$  was 0.62 – 0.72 in the three *Trimma* species, which was notably later than the average of 0.59 (SD = 0.122, n = 471) for Actinopterygii (Tsikliras & Stergiou, 2014). Several CRFs with short lifespans mature earlier than this average, which is consistent with life history theory. For example, *Eviota queenslandica* mature at 0.51 of the maximum length and 0.42 in *Eviota melasma* (Depczynski & Bellwood, 2006). However, like the *Trimma* species examined, some CRFs mature later than this average. For example *Eviota sigillata* mature at 0.62 of the maximum length (Depczynski & Bellwood, 2006). Maturation in such fishes can occur later than the average for several reasons. Firstly, fecundity may be low near the minimum body size threshold for maturation, due to female fecundity declining with decreasing body cavity size as they produce and carry fewer eggs (Hernaman & Munday, 2005b). At the same time, reproduction is energetically costly and may come at the risk of heightened mortality as a result of increased foraging activity to fuel reproduction. It may therefore be beneficial for these small fishes to delay reproduction to attain a larger size where fecundity is greater (Audzijonyte & Richards, 2018). Additionally, intrasexual competition may favour a delay in maturation. Harem polygyny is the most common mating system

recorded in *Trimma* (Sunobe et al., 2017), where larger males achieve a higher level of reproductive success than smaller males due to being more competitive for mates or territory (Fukuda & Sunobe, 2020; Fukuda, Tanazawa, et al., 2017; Manabe et al., 2008; Sakurai et al., 2009; Sunobe & Nakazono, 1990; Sunobe et al., 2017). Moreover, females in polygynous groups may compete for breeding resources such as breeding sites, food, and paternal care by males. Accordingly, small subordinate females may be largely excluded from breeding, thus favouring maturation at a larger size (Wong et al., 2008). Delaying maturation therefore may have several benefits, however, it severely decreases the time these fishes have as reproductively viable adults to just 45-56 days. It also exposes them to increased risk of mortality before any reproduction is achieved.

Sex change strategies can be inferred by gonad structure (Lowe et al., 2021; Sunobe et al., 2017). The high number of individuals with gonads in a transitional state indicate that sex change may occur frequently in the three species examined here. Excluding the two individuals with simultaneous hermaphrodite phase gonads, all mature individuals had testes or ovaries active at any one time, while the tissue of the non-functional sex was retained, as has been described previously (Cole, 1990; Fukuda, Tanazawa, et al., 2017; Manabe et al., 2008; Sakurai et al., 2009; Sunobe & Nakazono, 1993; Sunobe et al., 2017). In protandrous species, bisexual gonads occur in initial phase males, which have an inactive ovarian portion. However, ovarian tissue completely displaces testicular tissue after transition to the female phase, leaving no remaining testicular tissue (Chang & Yueh, 1990; Law & Sadovy de Mitcheson, 2017; Sunobe et al., 2016). In the initial female phase of protogynous species, some individuals have small sections of germ cells or spermatogonia, while others contain no spermatogenic tissue. In all species, no ovarian tissue is retained after sexual transition (Bhandari et al., 2003; Nakamura et al., 1989; Sundberg et al., 2009). Retention of bisexual gonads in both female and male phases indicates that the *Trimma* species examined are always potentially capable of

functioning as either female or male and thus likely exhibit bidirectional sex change (Munday et al., 2010; Sunobe et al., 2017).

Bidirectional sex change is reported as rare in coral reef fishes (Yamaguchi & Iwasa, 2018), occurring in just 4.1% of known hermaphroditic species outside of the *Gobiidae* (16 of 395 species., Kuwamura et al., 2020). However, it is the most common type of hermaphroditism in the *Gobiidae*, with approximately 75% of known hermaphroditic gobies (50 of 66 species) displaying sex change in both directions (Kuwamura et al., 2020). In polygynous *T. okinawae*, sex change is induced by a change in social status (Kobayashi et al., 2009), where individuals become the sex that will result in the highest reproductive success in accordance with the size-advantage hypothesis of sex change (Munday et al., 2006). The loss of the dominant male from a polygynous group can result in the largest female changing sex to become the dominant male (Manabe et al., 2007; Sunobe & Nakazono, 1993) and reverse sex change from male to female occurs when all females in a group disappear, and the resultant bachelor male enters a group with a larger residing male (Manabe et al., 2007). The *Trimma* species examined have female biased sex ratios indicating polygyny is a likely mating system (Winterbottom et al., 2011), and therefore the benefits of bidirectional sex change in these species may be akin to other polygynous members of the genus. Bidirectional sex change can be valuable when a male's social circumstances may change drastically and unexpectedly and when a delay in selecting new mates may cause a significant decrease in reproductive output. Due to high and unpredictable mortality in the three *Trimma* species examined, the loss of individuals and changes to mating circumstances is likely a common phenomenon. Thus, the ability to change sex in both directions depending on the social circumstances present may increase overall reproductive value.

Possessing ovarian and testicular portions in both female and male phase individuals can avoid entire gonad reconstruction and may allow for rapid sex change in small gobies with short lifespans and high mortality rate (Munday et al., 2010; Munday & Molony, 2002; Yamaguchi & Iwasa, 2017). In contrast, the *Trimma* species examined retain ovarian and testicular portions in both male and female phases. Sex change in *Trimma* involves the tissue of one sex rapidly proliferating while tissue of the other sex degenerates, and total gonad repurposing is avoided (Sunobe et al., 2005). Sex change can occur in as little as four days (female to male) and six days (male to female) in *T. okinawae*. (Sunobe & Nakazono, 1993; Yamaguchi, 2016). Bisexual gonads in both male and female phases is seen in other small fishes with short reproductive lifespans and high mortality, such as the genera *Eviota* (Maxfield & Cole, 2019a; Schemmel & Cole, 2016), *Lythrypnus* (Maxfield & Cole, 2019b; Muñoz-Arroyo et al., 2019), *Bryaninops* (Munday et al., 2002), *Priolepis* (Manabe et al., 2013), and multiple other *Trimma* species (Sunobe et al., 2017). High and unpredictable mortality can mean that an individual's social circumstances can quickly change. Therefore, rapid change from one sex to another may be an advantage with the limited reproductive period these fishes experience (Munday et al., 2010; Yamaguchi, 2016; Yamaguchi & Iwasa, 2017).

One *T. benjamini* individual and one *T. yanoi* individual exhibited gonads with both active ovarian and testicular regions, which has not been observed in this genus before. This gonadal structure may indicate rare occurrences of simultaneous hermaphroditism, where individuals can function as both female and male simultaneously (Sakakura et al., 2006; Tuset et al., 2005). Alternatively, it could represent a period where individuals are capable of acting as both female and male during sexual transition. This could maximise the available reproductive time, as individuals can remain reproductively active rather than being reproductively redundant for the duration of the sex change process. However, in other species of *Trimma* the tissue of one sex degenerates while the tissue of the other sex proliferates, and

there is no evidence of simultaneous hermaphroditism during this process (Sunobe et al., 2005). Periods of simultaneous hermaphroditism during sex change may be a rare occurrence, or happen quickly, which may explain why this stage has not been captured in previous studies. Moreover, having the gonad structure of a simultaneous hermaphrodite does not necessarily mean they function as one. For example, most *Lythrypnus zebra* individuals have a gonad structure comparable to that of a simultaneous hermaphrodite, despite functioning as a single sex (Munday et al., 2010; St. Mary, 1996). Further population histological studies in *Trimma* are warranted to confirm if these rare individuals are functional or non-functional simultaneous hermaphrodites, or if this phenomenon occurs only during sex change.

Despite the life history constraints associated with small body size, small-bodied fishes persist. Furthermore, the majority of reef fishes are small, with the average length being just 45 mm (Bellwood *et al.*, 2017). There may be several reasons for this, including the ability to exploit a range of small habitats, increased agility, low energy demands per individual, and the ability to grow and reproduce quickly, leading to a high rate of population increase (Blanckenhorn, 2000; Brandl et al., 2018; Brandl et al., 2019; Depczynski & Bellwood, 2006; Winterbottom et al., 2011). Here, I demonstrate that an expanding number of small CRF's maintain a dual-gonad arrangement, which may be advantageous to maximise reproductive potential in species where a short reproductive life is combined with high and unpredictable rates of mortality that can dramatically and unpredictably alter social living conditions that individuals experience.



## Chapter 4: Growth strategies across life history stages and generational turnover of cryptobenthic coral reef fishes of the genus *Trimma*

---

### 4.1 Abstract

Somatic growth influences survival and reproduction, with flow on effects on population dynamics and energy fluxes within ecosystems. Small-bodied cryptobenthic reef fishes may contribute significantly to productivity due to their life history traits including growth rates and rapid generational turnover. However, comprehensive studies on growth that encompass all stages of life are rare. This study investigated growth patterns across life history stages and generational turnover rates in three *Trimma* species that are abundant on Indo-Pacific coral reefs: *Trimma benjamini*, *T. capostriatum*, and *T. yanoi*. The *Trimma* species examined had small body sizes of <25 mm and short lifespans of less than 140 days, potentially enabling them to produce over three generations annually. Three growth models were compared (Modified Fry Model, Body Proportional Hypothesis, and the Biological Intercept Model) to back-calculate growth at ages prior to capture, and the Body Proportional Hypothesis statistically performed the best in each species. Each species displayed similar growth patterns, with growth rates varying across different life history stages. Growth was most rapid during the pelagic larval phase, averaging 0.2 mm per day. The size at settlement was small, ranging from 7.6 to 8.4 mm. Growth was initially rapid post-settlement but gradually slowed, averaging 0.16 to 0.17 mm per day during the juvenile stage. In the adult phase growth was non-asymptotic, averaging approximately 0.15 mm per day, with 31.3% to 37.0% of total growth occurring during this stage. Growth decreased by 8.6% – 11.7% following maturation, which is minor compared to the patterns observed in larger fish species. My findings support the expanding literature suggesting cryptobenthic reef fishes exhibit unique life history traits that could be associated with their small maximum body size.

## 4.2 Introduction

There is a wide diversity of growth strategies in the animal kingdom that have important implications for a species' life history, behaviour and ecology (Peters, 1983). Somatic growth is the increase in body size or weight over time and is a critical trait that influences individual survival and reproduction, which has important implications for population dynamics and energy fluxes in ecosystems (Anderson, 1988; Barneche *et al.*, 2018; Brown *et al.*, 1993; Savage *et al.*, 2004). Divergent growth strategies are associated with fundamental trade-offs in life history evolution. Rapid growth is often associated with early maturation, high reproductive effort, short lifespan, and small body size, while slow growers may spread their breeding over long lives and reach large body sizes (Calder, 1984; Roff, 1992; Stearns, 1992). Many animals grow to their maximum body size early in life (determinate growth), while others, such as many fishes, continue to grow throughout their lives (indeterminate growth) (Lincoln *et al.*, 1982; Sebens, 1987). Growth rates may also differ within a species as they adopt distinct growth strategies across various life history stages (Borgstein *et al.*, 2020; Roff, 1992; Stamps *et al.*, 1998; Stearns, 1992). Determining when and why animals grow fast, slow, or not at all is critical to understanding their overall life history, population dynamics and turnover, and their ecosystem roles.

Coral reef fishes have complex life histories that involve a short pelagic larval duration (PLD), an immature juvenile stage, and a reproductive adult stage (Jones & McCormick, 2002; Jones *et al.*, 2002; Leis & McCormick, 2002; Sale, 2002). Growth of fishes is likely to change as they transition between life history stages, and is generally fastest in the larval stage, slower in the juvenile stage, and decelerates or ceases altogether in the adult phase (Anderson, 1988). Rapid larval growth is usually selected for under natural selection, as larvae with accelerated growth and development have an increased chance of survival and successful recruitment

(Depczynski & Bellwood, 2006; Goatley & Bellwood, 2016). Growth in the juvenile phase generally slows following settlement onto the reef due to protective habitats, larger body size, and decreased naivety to predators (Beeken et al., 2021; Depczynski & Bellwood, 2006; Leis & McCormick, 2002; Winterbottom et al., 2011; Winterbottom & Southcott, 2008). Finally, most adult fishes experience asymptotic growth, where energy previously allocated to somatic growth is utilised in reproduction (Roff, 1992; Stamps et al., 1998; Stearns, 1992). However, while this may apply to some fishes, there is evidence that growth may persist linearly beyond maturity in some fish species (Beeken et al., 2021; Depczynski & Bellwood, 2006; Winterbottom et al., 2011; Winterbottom & Southcott, 2008).

Knowing the timing of life history stages specific to different species is a crucial prerequisite to understanding growth changes that occur throughout these stages. Sagittal otoliths are calcified structures found within the brain cavity of fishes. These structures offer valuable insights into the timing of different life history phases (Choat & Robertson, 2002; Goldsworthy et al., 2022; Wilson & McCormick, 1999). Sagittal otoliths accumulate increments either annually or daily in older and younger fish, respectively, and can therefore be used to determine fish age and lifespan (Choat & Robertson, 2002). Additionally, otoliths contain a settlement mark that defines the age boundary between the larval and juvenile stages. This mark is characterised by a decrease in otolith increment width and/or optical contrast after settlement (Goldsworthy et al., 2022; Wilson & McCormick, 1999). The age at maturation can be determined by fitting a logistic regression to the proportion of immature individuals versus mature females, which establishes the boundary between the juvenile and adult stages (Goldsworthy et al., 2022; Hernaman & Munday, 2005b; Lowe et al., 2021). The maximum age, determined by the fish with the greatest number of rings in each species, provides insights

into the duration of the adult phase (Goldsworthy et al., 2022; Winterbottom & Southcott, 2008). A holistic overview of growth can be attained by modelling growth during these phases.

Examining the relationship between fish age and length at capture is the most utilised technique to model growth (Choat & Robertson, 2002; Green *et al.*, 2009; Ogle, 2016). Yet, it can be difficult to collect specimens in the early life history stages and is therefore mainly restricted to establishing post-settlement (Gwinn *et al.*, 2010; Vigliola & Meekan, 2009). Alternatively, the early life history growth of fishes can be reconstructed at ages prior to capture using historical evidence held in the otoliths. This is achieved by the application of back-calculation models to otolith increment width measurements to determine lengths at previous ages (Francis, 1990; Vigliola & Meekan, 2009). These models assume that there is a relationship between otolith growth and somatic growth (OSG), so it is essential that this relationship is assessed beforehand (Vigliola & Meekan, 2009). There are several back-calculation methods which have been reviewed by Vigliola and Meekan (2009) who determined that the Modified Fry back calculation model was the most appropriate in general. However, other studies have shown that the optimal model varies depending on the species examined (Smedstad & Holm, 1996; Starrs *et al.*, 2013; Vigliola *et al.*, 2000; J. A. Wilson *et al.*, 2009). As poorly fitting models can lead to incorrect interpretations of growth, it is therefore important where possible to validate these methods either experimentally (e.g. Roemer & Oliveira, 2007), or by comparing back-calculated datasets to ages and lengths at capture (e.g. Starrs et al., 2013). This is especially essential for fishes that may not conform to the general trends in growth seen across different life history stages.

The cryptobenthic reef fishes (CRFs) are among the smallest and shortest lived vertebrates on the planet; many with maximum adult body length of <50 mm and maximum lifespan of <150 days (Depczynski & Bellwood, 2003). Although these fishes exhibit the same three life history stages of most coral reef fishes, CRFs have distinct traits that may be associated with small body size that are atypical to their larger counterparts. These traits include extreme mortality, reduced longevity, a long PLD relative to lifespan, early maturation, a short reproductive life, and fast generational turnover rates (Depczynski & Bellwood, 2006; Hernaman & Munday, 2005a, 2005b; Winterbottom et al., 2011; Winterbottom & Southcott, 2008). Additionally, many CRFs have unique growth patterns during certain life history stages. Like larger fishes, CRFs tend to have rapid larval growth, then growth slows in the juvenile stage (Beeken et al., 2021). What distinguishes CRFs is their capacity to sustain continued growth throughout adulthood, in contrast to the majority of other fishes, where growth generally slows substantially after reaching reproductive maturity (Depczynski & Bellwood, 2006; Hernaman & Munday, 2005a, 2005b; Winterbottom et al., 2011; Winterbottom & Southcott, 2008). However, current literature of growth strategies in CRFs is mainly limited to post-settlement growth, with few studies encompassing growth across all life history stages, including larval, juvenile, and adult growth (but see Beeken et al., 2021). These strategies have clear implications for the high turnover of CRF populations and their functional roles as productive sources of nutrition for other reef organisms (Ackerman & Bellwood, 2000; Beeken et al., 2021; Brandl et al., 2018; Brandl et al., 2019; Depczynski & Bellwood, 2006; Depczynski et al., 2007; Galland et al., 2017; Winterbottom et al., 2011).

This aim of this study was to analyse growth during the larval, juvenile, and adult life history stages in three cryptobenthic goby species of the genus *Trimma* in Kimbe Bay, Papua New Guinea (5.1667° S, 150.5000° E). *Trimma* is a speciose genus of Indo-Pacific CRFs,

currently containing 105 species (Winterbottom, 2019). Several *Trimma* species are present in Kimbe Bay, which is situated in the biodiverse Indo-Pacific Coral Triangle. *Trimma benjamini*, *T. capostriatum* and *T. yanoi* are among the benthic group of *Trimma* species that perch on hard substrata and are highly abundant on coral reefs in Kimbe Bay (Goldsworthy et al., 2022; Winterbottom, 2019; Winterbottom et al., 2011). No studies have been conducted to evaluate the growth of CRFs in this biodiversity hotspot. Body size and age distributions were examined in all three species, where small body size was predicted to be associated with rapid growth, short lifespan, and fast generational turnover. Three different otolith back-calculation methods were also assessed, with the expectation that the Modified Fry model would most appropriately describe ontogenetic changes in growth trajectories of *Trimma*. As is common in most coral reef fishes, the hypothesis was that growth would be (1) most rapid in the larval stage; (2) remain rapid immediately following settlement due to the naivety and small size at settlement, then decrease throughout the juvenile stage; and (3) continuous during adulthood, as seen in some other CRFs.

## 4.3 Methods

### 4.3.1 Study site, specimen collection and sample processing

Sampling was conducted during November and December 2019 at reefs in Kimbe Bay, Papua New Guinea (5.1667° S, 150.5000° E). 129 *T. benjamini*, 102 *T. capostriatum*, and 122 *T. yanoi* specimens were collected at random on SCUBA using a fine hand net and 5:1 ethanol: clove oil anaesthetic solution. Fish were humanely euthanized by immersion in a 50% water, 50% ice slurry shortly after surfacing. Specimens were blotted dry then measured to 0.5 mm standard length ( $L_s$ ). The head of each fish was sectioned from the body. Heads were preserved in 70% ethanol, and bodies were fixed in a formaldehyde 4%, acetic acid 5%, calcium chloride

1.3% (FAACC) solution for three days, then transferred to 70% ethanol (Goldsworthy et al., 2022).

#### **4.3.2 Otoliths processing and determination of age and increment measurements**

Otoliths were removed from the brain cavity, cleaned, and fixed to glass slides using Crystalbond 509™ thermoplastic glue with the convex side facing downwards. The surface of each otolith was polished using lapping film and water on a glass plate until a thin section was achieved (Figure 4.1a). Otoliths were coated in immersion oil, viewed on a BX43 Olympus microscope, and photographed at 200x and 400x magnification with an Olympus EP50 digital camera. ImageJ software (Schneider et al., 2012) was used to count growth increments from the otolith primordium to edge (Figure 4.1b). Two counts of each otolith were undertaken, and the mean of these two counts was used. A third count was conducted if the two initial counts differed by >10% of the mean. The mean of the closest two counts was then used, provided that all 3 counts were within 10% of the mean. This value corresponded to the age of the fish in days, as growth increments were assumed to be deposited daily as with other CRFs (e.g., Depczynski & Bellwood, 2006; Depczynski & Bellwood, 2005a; Hernaman & Munday, 2005a; Hernaman *et al.*, 2000; Longenecker & Langston, 2005; Winterbottom et al., 2011).

The widths of otolith increments were measured using ImageJ software (Schneider et al., 2012) in a straight trajectory 90° from the longest axis, as this was the trajectory with the greatest microstructure clarity in all otoliths (Figure 4.1c). Unmeasurable otoliths were omitted from the analysis. Otolith radius was taken as the total of all increment widths in each otolith.

#### **4.3.3 Establishing age at life history milestones and generational turnover**

As described in Goldsworthy et al. (2022), the PLD (mean  $\pm$  95% confidence interval) was  $32.9 \pm 0.4$  days in *T. benjamini*,  $37.7 \pm 0.4$  days in *T. capostriatum*, and  $36.1 \pm 0.3$  days in

*T. yanoi*. This study builds on Goldsworthy et al. (2022) by validating the age at settlement using otolith growth increments. The average width of each growth increment was plotted against the age in days, with the expectation that these increments would decrease after the settlement mark, as a result of the transition from the pelagic larval stage to benthic life (Wilson & McCormick, 1999). The age at maturity (AM) for *T. benjamini*, *T. capostriatum* and *T. yanoi* was  $74.1 \pm 3.1$ ,  $82.1 \pm 3.4$ , and  $81.7 \pm 3.4$  days, respectively (Goldsworthy et al., 2022). Maximum age ( $T_{max}$ ) was defined as the age of the individual with the greatest number of growth rings for each species.

Generational turnover was calculated from AM and  $T_{max}$  for each species using the formula (Table A3. 1.1):

$$GT = AM \pm \left( \frac{T_{max} - AM}{2} \right)$$

This equation estimated the number of days required for a new generation to be produced (Depczynski & Bellwood, 2006). The potential number of generations produced annually was calculated by dividing 365 by the generational turnover.

#### **4.3.4 Assessing the otolith-somatic growth (OSG) relationship**

To examine the nature of the OSG relationship, two different models were fit to the radius at length data for each species in R (R Core Team, 2021). A generalised linear model (Table A3. 1.2) was used to determine if a linear relationship existed, and second-degree polynomial model (Table A3. 1.3) was used to establish if curvature existed. Akaike information criterion (AIC, Table A3. 1.4) was used to determine the model of best fit. A difference in AIC scores of  $> 2$  units indicated variation in model fit and a lower AIC score indicated a better fitting model. If AIC scores were within  $< 2$  units of one another, the most conservative model was used.



#### 4.3.5 *Back-calculation of lengths at previous ages*

Three back-calculation methods were then applied to the otolith increment data to estimate fish  $L_s$  at previous ages: the experimental version of the Modified Fry model (MF model, Table A3. 1.5) (Vigliola et al., 2000), the Biological Intercept model (BI model, Table A3. 1.6) (Campana, 1990), and the Body Proportional Hypothesis model (BPH model, Table A3. 1.7) (Francis, 1990). These three models were chosen as they were recommended by Vigliola and Meekan (2009) in a comprehensive review of back-calculation methods in fishes. Back-calculation methodology was used to determine growth as it produces more reliable estimates of growth than using otolith radius alone. Back-calculations were performed in R using the `backCalc()` function in the `RfishBC` package (Ogle, 2019; R Core Team, 2021).

#### 4.3.6 *Population growth curves*

Following back-calculations, polynomial mixed effect models of degrees 1-10 (Table A3. 1.3) were fitted to back-calculated  $L_s$  for each species and back-calculation method to create population growth curves. Polynomial models were chosen over the traditional Von Bertalanffy model as they are suitable for fishes where growth shows linearity (Ogle *et al.*, 2017), which is demonstrated in CRFs such as *Trimma* (Depczynski & Bellwood, 2006; Winterbottom et al., 2011; Winterbottom & Southcott, 2008). In each polynomial model, growth ( $L_s \sim \text{age}$ ) was incorporated as a fixed factor to estimate population level effects, and individual fish were included as a random factor, with variable intercept and slope parameters to estimate variability among individuals. This method also accounts for the longitudinal and autocorrelated nature of datasets generated from back-calculations, which originate from multiple observations per otolith (Ogle et al., 2017; Vigliola & Meekan, 2009). K-fold cross-validation (with  $K = 10$  folds) was utilised to calculate the average mean squared error (MSE) for each polynomial model, to identifying the degree of polynomial that demonstrated both

conservatism and a satisfactory fit. A lower cross-validated MSE indicated a superior model fit, where a difference exceeding 0.01 was deemed significant (Berrar, 2018). Using the optimum polynomial model, mean back-calculated  $L_S$  and 95% confidence intervals were made for the entire age range of each species using the `emmeans` package in R (Lenth, 2021). This was conducted for each species and back-calculation model, resulting in a population growth curve that transitioned through larval, juvenile, and adult life history phases for the MF, BI, and BPH models.

#### **4.3.7 Back calculation model selection**

To determine which of the MF, BI or BPH methods best described growth in each species, population growth curves were compared to the observed  $L_S$  at capture. This could not be undertaken for larval growth due to no individuals captured, measured, and aged in the larval phase, however, I assumed that models that adequately described post-settlement growth also described larval growth. Residuals were calculated as *back calculated  $L_S$  -  $L_S$  at capture* and were plotted with fish age to examine the fit of each back-calculation method over the range of observed ages. A locally weighted regression smoother was added to assist with uncovering patterns in the residuals. Residuals were squared and summed (RSS) and averaged to return the MSE, where lower RSS and MSE values provided further evidence of a better fitting population growth curve.

#### **4.3.8 Growth throughout larval, juvenile, and adult life history stages**

Body size at settlement and maturity for each species was estimated from age at settlement and maturity using the optimum population growth model equation. For each species, the proportion of growth that occurred in each phase relative to the total growth was determined by:

$$\begin{aligned} \text{Larval phase:} & \quad \frac{L_s \text{ at settlement}}{\text{Maximum } L_s} \\ \text{Juvenile phase:} & \quad \frac{L_s \text{ at maturity} - L_s \text{ at settlement}}{\text{Maximum } L_s} \\ \text{Adult phase:} & \quad \frac{L_s \text{ at maturity} - \text{Maximum } L_s}{\text{Maximum } L_s} \end{aligned}$$

Where maximum  $L_s$  was defined as the maximum  $L_s$  on the growth curve

Growth rate ( $G_i$ , mm/day) was determined by differentiating the optimum population growth model selected (Table A3. 1.8) and applying the derived equation across the entire range of ages for each species (Vigliola et al., 2000). Differences in the in mean daily growth rate among life history stages was subsequently analysed with a generalised linear model (Table A3. 1.2) and significance of these differences were assessed by pairwise comparisons.

## 4.4 Results

### 4.4.1 Body size, age, and generational turnover

Each species attained a small adult body size.  $L_s$  of specimens ranged from 9.5 – 24 mm (mean  $\pm$  95% confidence interval = 17.2  $\pm$  1.1 mm) in *T. benjamini*, 10.5 – 24.5 mm (17.6  $\pm$  1.2 mm) in *T. caopstriatum* and 9 – 22 mm (15.6  $\pm$  1.3 mm) in *T. yanoi* (Figure 4.2). As predicted, these fishes exhibited short lifespans and fast generational turnover. Age ranged from 43 – 130 days (87.8  $\pm$  6.9 days) in *T. benjamini*, 52.5 – 137.5 days (99.5  $\pm$  7.6 days) in *T. caopstriatum* and 37.5 – 126.5 (82.7  $\pm$  8.7 days) in *T. yanoi* (Figure 4.2). Generational turnover ranged from 102 – 110 days (Table 4.1) and thus each species potentially produces 3.3 – 3.6 generations every year (Table 4.1).

### 4.4.2 Validating age at settlement using increment widths

The increment widths and otolith radii of 128 *T. benjamini*, 95 *T. capostriatum* and 116 *T. yanoi* individuals were measured. The settlement mark was determined in all individuals (Figure 4.1b). As expected, increment widths increased leading up to settlement, reached a peak near settlement, and then decreased significantly after settlement as individuals transitioned from pelagic to benthic life (Figure 4.1d).

#### **4.4.3 Assessing the otolith-somatic growth (OSG) relationship**

There was a positive OSG relationship in all species examined. This relationship was best described by a 2<sup>nd</sup> degree polynomial model in *T. benjamini*, generalised linear model in *T. capostriatum*, and a 2<sup>nd</sup> degree polynomial model in *T. yanoi* (Figure 4.3, Table A3. 2). Nonetheless, curvature in the OSG relationship of *T. benjamini* and *T. yanoi* was weak, and a generalised linear model still provided a good fit (Table A3. 2). A largely linear OSG relationship confirmed the use of the experimental version of the MF model, and linear versions of the BI and BPH models.

#### **4.4.4 Back-calculation of lengths at previous ages**

Back calculations were applied successfully to 128 *T. benjamini*, 95 *T. capostriatum*, and 116 *T. yanoi* using the MF, BI and BPH models (Table A3. 1.5, Table A3. 1.6, Table A3. 1.7), resulting in a total of 11,125 (*T. benjamini*), 9,384 (*T. capostriatum*), and 9,449 (*T. yanoi*) back calculated standard lengths for each back calculation model. Each individual fish in the sample exhibited a unique growth trajectory that spanned its entire age range (Figure 4.4a, Figure A3. 2a, Figure A3. 3a).

#### **4.4.5 Population growth curves**

For each species, a 3<sup>rd</sup> degree polynomial model was identified as optimal for back-calculated datasets generated by the MF model (Figure A3. 1, Table A3. 3, Figure A3. 2). For

back calculated datasets generated by the BI model, polynomial models of the 4<sup>th</sup> degree were selected for each species (Figure A3. 1, Table A3. 3, Figure A3. 3). 4<sup>th</sup> degree polynomial models were also selected for each species for back calculated datasets generated by the BPH model (Figure A3. 1, Table A3. 3, Figure 4.4).

#### **4.4.6 Back calculation model selection**

The BPH model provided the most accurate trajectory of growth in all species (Figure 4.4, Table A3. 4). Back-calculated  $L_s$  generated by the BPH model and analysed by polynomial mixed effect models of the 4<sup>th</sup> degree followed closely to the  $L_s$  of captured individuals, visualised by minimal patterning in the residuals vs. age plots (Figure 4.4b). In addition, the BPH model had slightly lower RSS and MSR values than the BI model, and significantly lower values than MF model in all species examined (Table A3. 4), providing additional evidence that the BPH model produced the best representation of growth. The MF model severely overestimated  $L_s$  at the lower end of the post settlement age spectrum, and underestimated  $L_s$  in the older ages, demonstrated by a diagonal distribution of residuals (Figure A3. 2, Table A3. 4). The BI model provided the next best fit after the BPH model, showing comparable results but slightly greater deviations from ages and lengths at capture (Figure A3. 3, Table A3. 4).

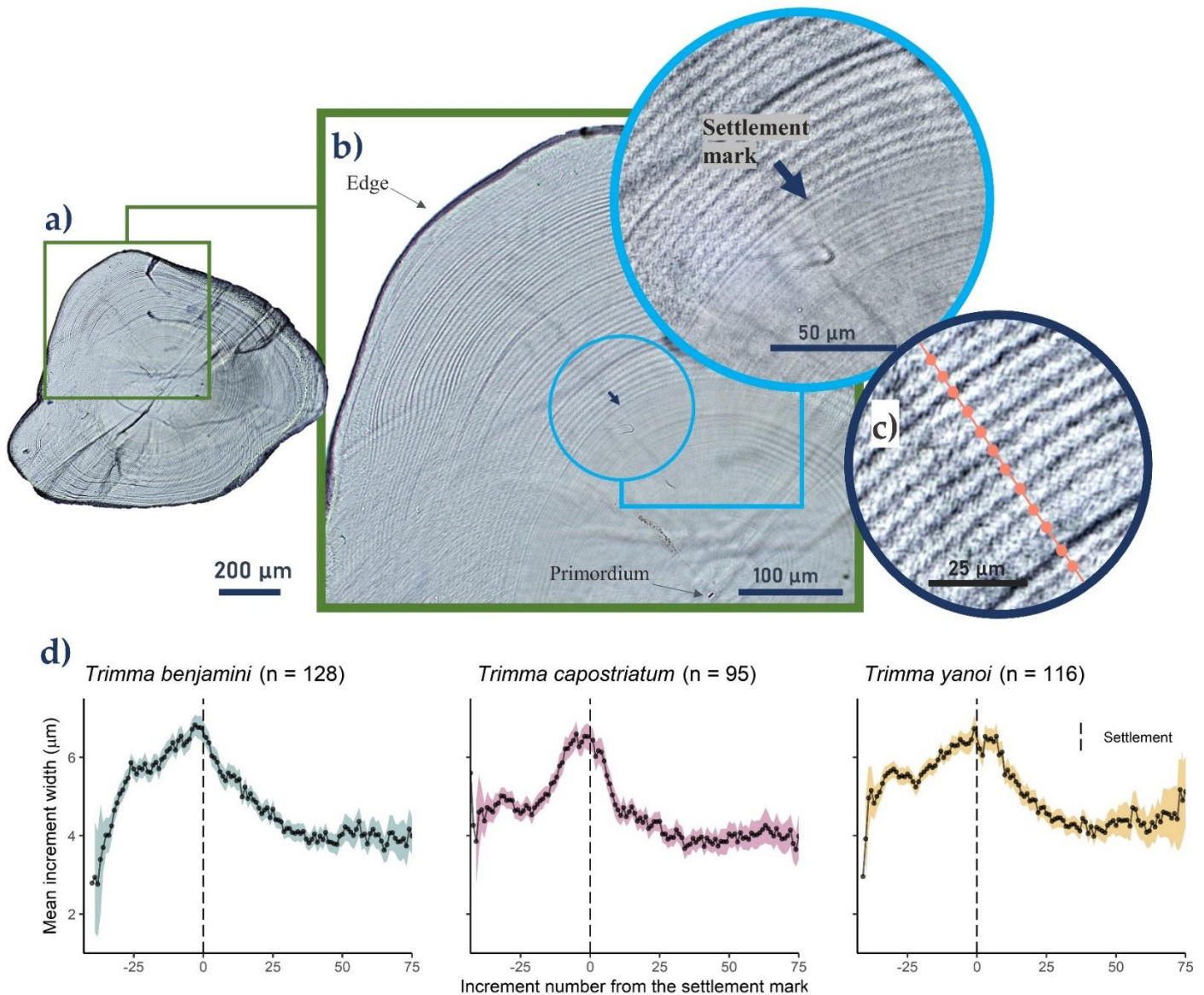


Figure 4.1: a) Photograph of a whole processed *Trimma yanoi* otolith. b) Enlarged image showing daily growth increments from the otolith primordium to edge. Circled and enlarged is the settlement region. Arrow points to the settlement mark. Note that not all rings are visible at these magnifications. c) Widths of growth increments measured in a straight line 90 degrees from the longest axis. d) Mean increment width ( $\pm$  95% confidence intervals) at each increment number from the settlement-mark (i.e., settlement = 0 indicated by the dashed line).

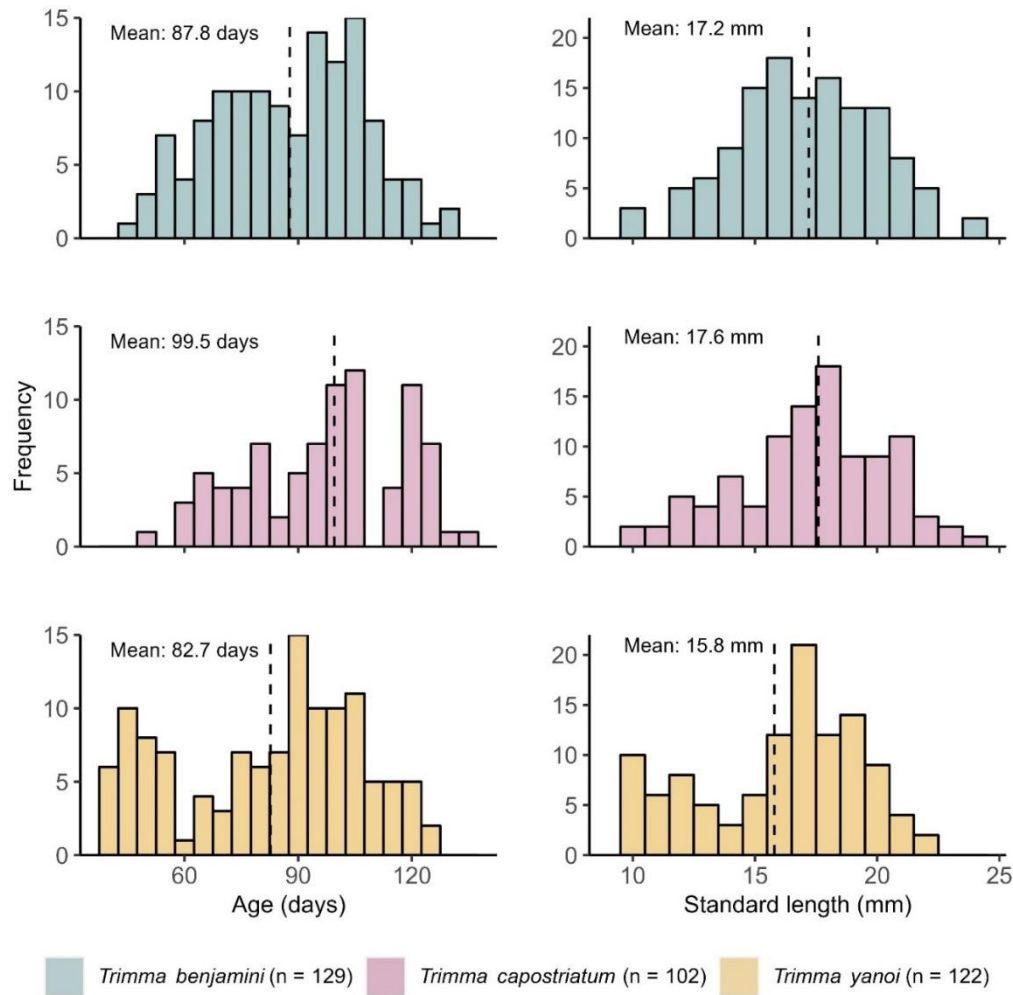


Table 4.1: Estimated generational turnover (days) and number of generations per year for *Trimma benjamini* (n = 129), *T. capostriatum* (n = 102), and *T. yanoi* (n = 122)

	Generational turnover (days)	Generations per year
	Mean ± 95% confidence interval	
<i>Trimma benjamini</i>	102 ± 1.5	3.58 ± 0.1
<i>Trimma capostriatum</i>	109.8 ± 1.7	3.32 ± 0.1
<i>Trimma yanoi</i>	104.1 ± 1.7	3.51 ± 0.1

Figure 4.2: Age (days) and standard length (mm) frequency distributions in *Trimma benjamini*, *T. capostriatum* and *T. yanoi*. Dashed line represents the mean.

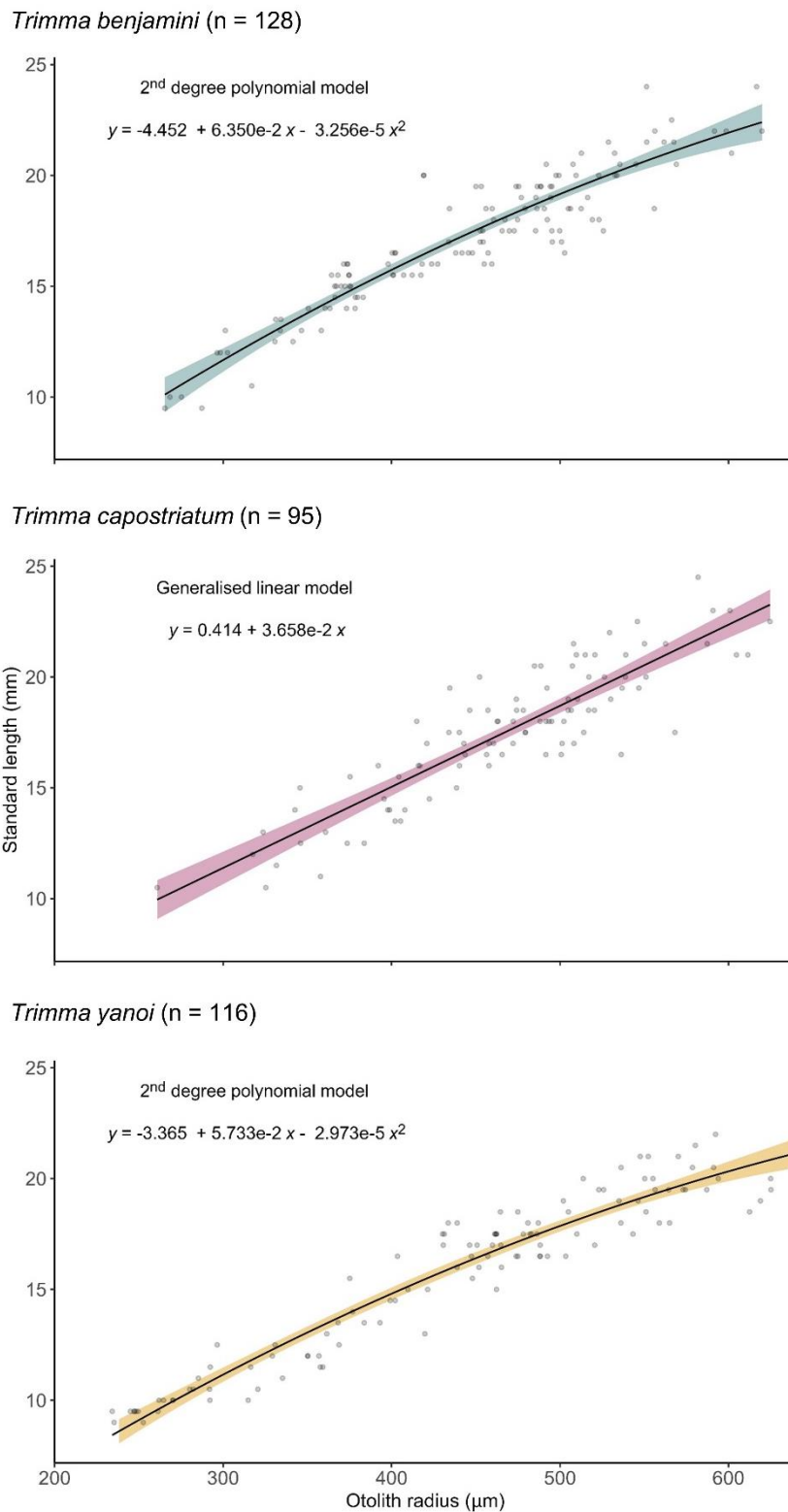


Figure 4.3: Relationship between otolith radius and somatic growth (OSG relationship). Displayed are the best fitting models for each species: a second – degree polynomial in *T. benjamini* and *T. yanoi* and a generalised linear model in *T. capostriatum*.



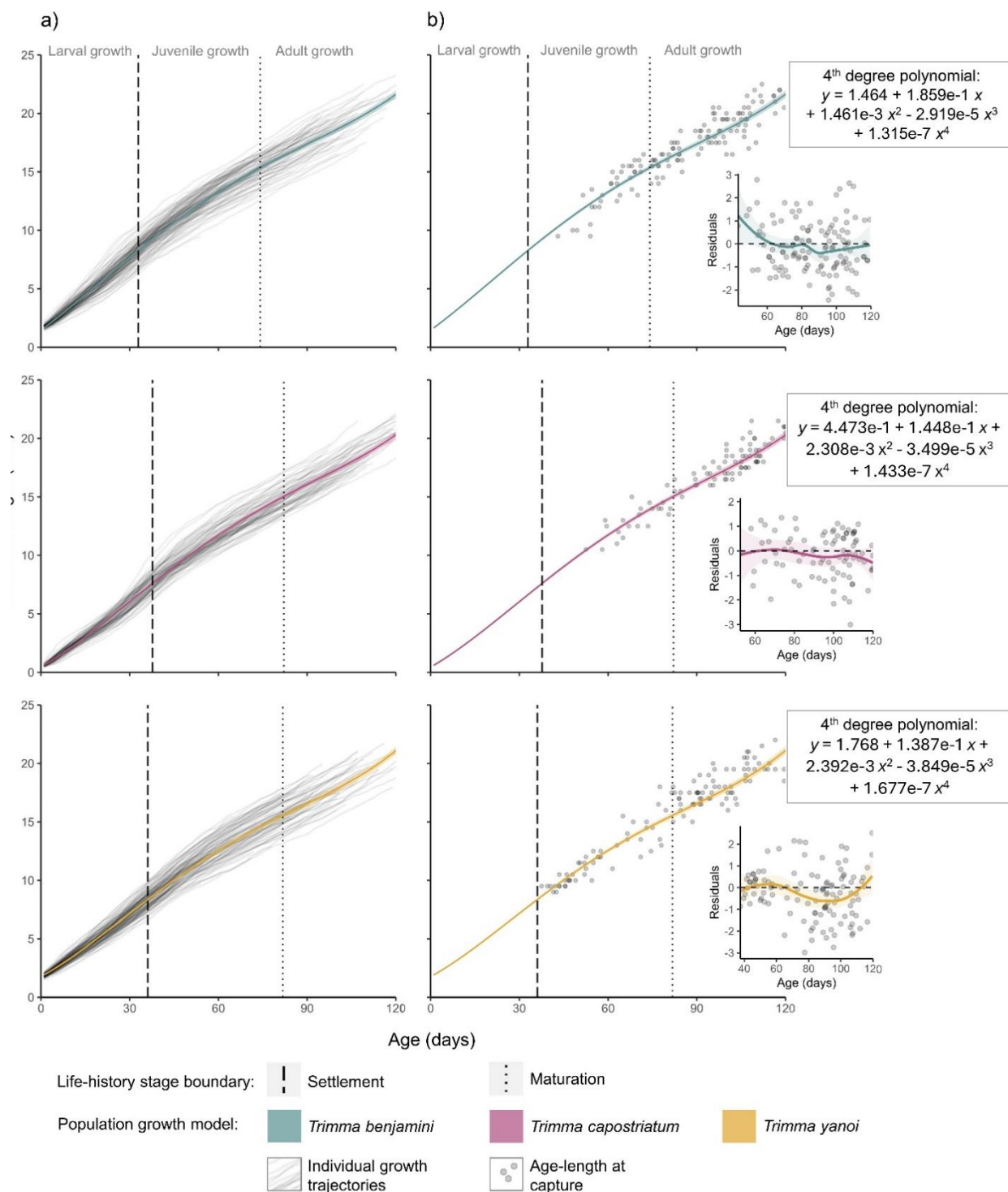


Figure 4.4: a & b) Modelled population growth curves across larval, juvenile, and adult life history stages for *Trimma benjamini*, *T. capostriatum*, and *T. yanoi*. Solid regression lines and shaded ribbons represent polynomial mixed-effects models of the 4<sup>th</sup> degree  $\pm$  95% confidence intervals (model equations for each species are displayed in a box). Dashed and dotted lines represent the age at settlement and maturity for each species, respectively. a) Displays growth curves fitted to individual fish growth trajectories back-calculated using the Body Proportional Hypothesis model. b) Illustrates growth curves against the ages (days) and standard lengths (mm) of individuals at the time of capture. Residual plots depict the deviations between the population growth model and observed ages and lengths at capture, with lines showing a locally weighted regression smoother applied to these residuals.

#### 4.4.7 Growth throughout larval, juvenile, and adult life history stages

The larval phase accounted 31.3% - 38% of total growth (Table 4.2). As hypothesised, out of all the life history phases, growth curves were the steepest in the larval phase (Figure 4.4), where growth was 0.207 mm/day on average in each species (Figure 4.5a).

$L_s$  at settlement was on average  $8.3 \pm 0.2$  mm in *T. benjamini*,  $7.6 \pm 0.2$  mm in *T. capostriatum*, and  $8.4 \pm 0.2$  mm in *T. yanoi*. 29.8%, - 31.8% of growth occurred in the juvenile phase (Table 4.2). In all species, Juvenile growth was high immediately after settlement, and gradually decreased as the juvenile stage progressed (Figure 4.4). Growth in the juvenile stage was 0.171, 0.160 and 0.162 mm/day on average in *T. benjamini*, *T. capostriatum* and *T. yanoi*, respectively (Figure 4.5a). The growth rate of juvenile *T. benjamini* was 0.036 mm/day slower compared to larval growth, representing a 17.4% decrease. For *T. capostriatum*, juvenile growth rates were 0.047 mm/day slower than larval growth, corresponding to a decrease of 22.8%. *T. yanoi* also showed a decrease in growth during the juvenile stage, with growth rates being 0.045 mm/day or 21.7% slower compared to larval growth (Figure 4.5b).

Body size at maturity was  $15.3 \pm 0.4$  mm in *T. benjamini*,  $15.0 \pm 0.4$  mm in *T. capostriatum* and  $15. \pm 0.4$  mm in *T. yanoi*. The adult phase accounted for 31.3% - 37.0% of growth (Table 4.2), and growth rates were 0.151, 0.146, and 0.148 mm/day in *T. benjamini*, *T. capostriatum* and *T. yanoi*, respectively (Figure 4.5a). Growth was approximately linear throughout the adult life history phase and did not reach a plateau (Figure 4.4). In contrast to juvenile growth, the adult growth decreased by an average of 11.7% (0.020 mm/day) in *T. benjamini*, 8.8% (0.014 mm/day) in *T. capostriatum*, and 8.6% (0.014 mm/day) in *T. yanoi* (Figure 4.5b).

Table 4.2: Proportion of growth that occurred in larval, juvenile, and adult life history phases relative to total growth. Values are derived from the Body Proportional Hypothesis optimum growth equations (Figure 4.4).

	Proportion of growth (%) in each life history phase		
	Larvae	Juvenile	Adult
<i>Trimma benjamini</i>	35.4	29.8	34.8
<i>Trimma capostriatum</i>	38.0	30.7	31.3
<i>Trimma yanoi</i>	31.3	31.8	37.0

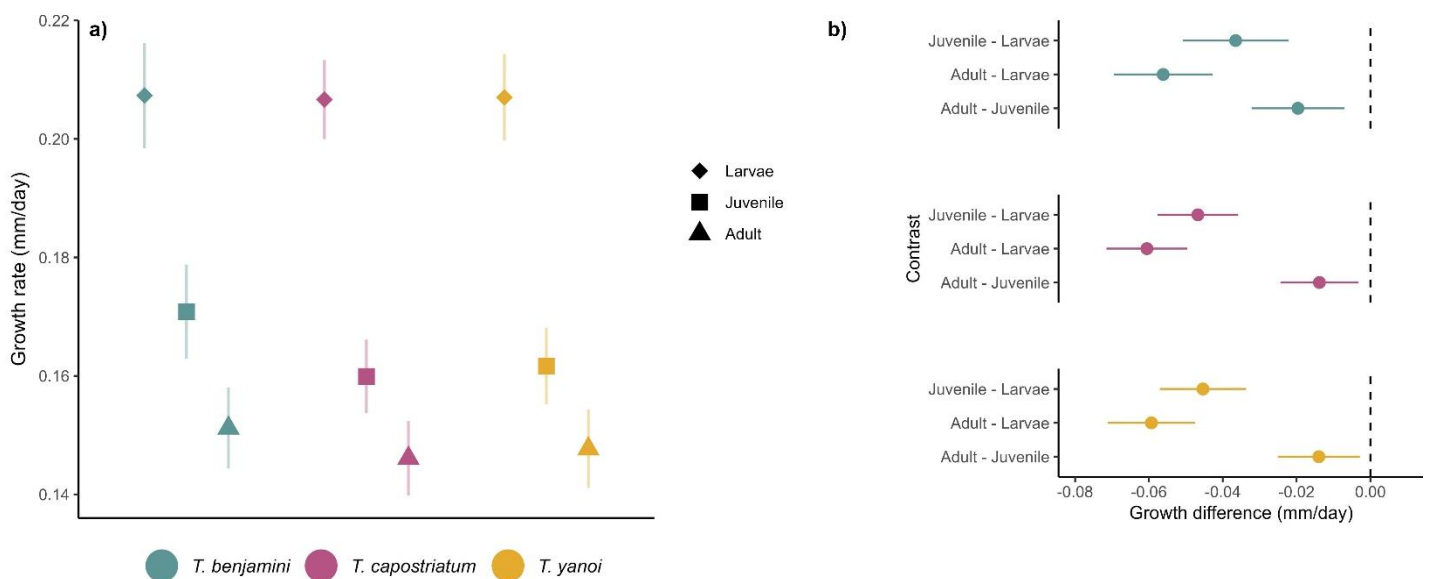


Figure 4.5: a) Mean back-calculated growth rate (mm/day  $\pm$  95% confidence intervals) in larvae, juvenile, and adult life history phases, derived from the Body Proportional Hypothesis optimum population growth equations (Figure 4.4). b) Pairwise comparisons showing the mean difference (mm/day  $\pm$  95% confidence intervals) in growth between each life history phase. In a and b, species *Trimma benjamini*, *T. capostriatum* and *T. yanoi* are represented by different colours.

#### 4.5 Discussion

These findings contribute to a growing body of evidence that suggests CRFs, such as *Trimma*, exhibit extreme life history traits that are unique from their larger counterparts. The *Trimma* species examined were characterised by distinct traits that could be related to their small body size of <25 mm, including reduced longevity of <140 days and the ability to produce over three generations annually. Each species exhibited similar growth patterns, where growth varied across different life history stages. As expected, the highest growth rates were observed during the pelagic larval phase. Size at settlement was small at 7.6-8.4 mm, and growth slowed gradually following settlement. Adult growth was non-asymptotic, with 31.3% - 37.0% of total growth occurring in this phase, and minor reductions ( $\leq 12\%$ ) in growth occurring after maturation relative to patterns seen in larger fishes. The following sections discuss the significance of such life history traits and the flow on implications for CRF survival and energy fluxes on coral reefs.

Larval growth in the *Trimma* species examined was the fastest out of all life history stages, which is commonly observed among coral reef fishes (Leis & McCormick, 2002). Rapid larval growth may reduce the high mortality rates experienced in this stage (Anderson, 1988). Larval fish face mortality rates of over 99% due factors such as predation and starvation, which can be attributed partially to body size (Leis & McCormick, 2002; Shima *et al.*, 2021). Smaller larvae face increased vulnerability due to a higher number of predators capable of consuming them (Wilson & Meekan, 2002). In addition, smaller larvae have reduced prey availability and lower feeding success as a result of their small body and oral gape size (Pepin, 2023). Hence, faster increases in larval body size can lead to greater survivorship and decreased mortality, which consequently may result in improved recruitment onto the reef (Bergenius *et al.*, 2002; Leis & McCormick, 2002; Wilson & Meekan, 2002). Successful

recruitment from the plankton, mediated by larval growth, is necessary for the stability or growth of coral reef fish populations (Wilson & Meekan, 2002). However, this may be especially important for CRFs due to additional life history pressures (Lefèvre *et al.*, 2016). CRFs have high lifetime mortality mainly due to their small body size (Depczynski & Bellwood, 2006; Goldsworthy *et al.*, 2022; Winterbottom *et al.*, 2011), which is offset by high population turnover rates of 3 – 4 and 4 – 8 generations produced per year in *Trimma* and *Eviota* (Depczynski & Bellwood, 2006), respectively. Therefore, in order to maintain stable populations, small fish species require a higher occurrence of successful recruitment events compared to larger species (Lefèvre *et al.*, 2016). When confronted with environmental changes that affect larval growth, such as alterations in food availability (Platt *et al.*, 2003), predator abundance (Anderson, 1988), temperature (Pepin, 1991), hydrodynamics (China & Holzman, 2014), or disruptions in lunar light emission (Shima *et al.*, 2021), the population dynamics of small fish species may be more rapidly affected compared to their larger counterparts (Brandl *et al.*, 2018; Goatley *et al.*, 2016).

Upon settlement, juvenile growth remained high immediately, then gradually declined as the juvenile stage advanced. This pattern was expected, considering that small and inexperienced recruits remain highly vulnerable to predation (Almany & Webster, 2006; Doherty *et al.*, 2004). The small size at settlement, ranging from 7.7 – 8.4 mm, exposes them to a suite of predators. Additionally, fresh recruits often lack the skills and traits to effectively evade predators, as they are confronted with new reef predators that have different attack techniques compared to pelagic predators previously encountered in the larval stage. (Goatley & Bellwood, 2016; McCormick & Holmes, 2006). In such circumstances, mortality rates in this life history stage can exceed 60% (Almany & Webster, 2006). Increases in growth during this phase can be an advantage, where 1 mm increases can reduce gape-limited predators and potentially extend their lifespan by approximately 11 days (Goatley & Bellwood, 2016).

However, this phase of heightened mortality and rapid growth is typically short-lived. As fishes encounter predation of conspecifics, they learn to avoid specific predators using visual and olfactory cues (McCormick & Holmes, 2006; McCormick & Manassa, 2008). Therefore, while the initial juvenile period is marked by extreme mortality and rapid growth, it may gradually subside as the fish grow and learn strategies escape predation (Goatley & Bellwood, 2016).

Growth in each species did not plateau in adulthood, with 31.3% - 37.0% of the total growth occurring in this phase, and minor (8.6% – 11.7%) reductions in growth rates compared to the juvenile phase. Growth is determinate in many larger coral reef fishes such as lutjanids and acanthurids. These fishes exhibit rapid linear growth during early life history, where growth almost stops completely after maturation (Audzijonyte & Richards, 2018; Munday & Molony, 2002). Herein, just 20% to 40% of growth occurs during the final 75% of the lifespan, as energy once utilised in somatic growth is directed to reproduction (Choat & Robertson, 2002). In other larger fishes such as *Plectropomus spp.*, somatic growth takes place across a broader size range and decreases slowly following maturity and spawning (Fukuda & Sunobe, 2020; Fukuda, Tanazawa, et al., 2017; Manabe et al., 2008; Sakurai et al., 2009; Sunobe & Nakazono, 1990; Sunobe et al., 2017; Wong et al., 2008). CRFs such as *Trimma* and *Eviota* display contrasting growth patterns (Depczynski & Bellwood, 2006; Winterbottom et al., 2011; Winterbottom & Southcott, 2008). The growth curves suggest that 77% – 83 % of growth occurs in the last 75% of life of life. It is noteworthy that these CRFs can continue to grow substantially and reproduce simultaneously, as reproduction requires significant energy to find mates and sustain mature gonads (McCormick, 1998; Winterbottom et al., 2011).

Non-asymptotic growth in the three *Trimma* species may be beneficial in the presence of life history hardships, such as reproductive limitations and extreme mortality. Continuous growth may be advantageous with higher reproductive success that occurs with increasing body size. For example, increases in female body size can lead to a larger clutch size (Depczynski

& Bellwood, 2006; Wootton, 1998) and larger individuals of both sexes may exhibit greater dominance when there is competition present (Fukuda & Sunobe, 2020; Fukuda, Tanazawa, et al., 2017; Manabe et al., 2008; Sakurai et al., 2009; Sunobe & Nakazono, 1990; Sunobe et al., 2017; Wong et al., 2008). Increases in the body size of *Trimma* and corresponding reproductive advantages throughout their lives may be beneficial due to their short reproductive lifespans of <50 days and the need to reproduce efficiently (Goldsworthy et al., 2022). Such growth patterns may be achievable by consuming an energy rich diet, increasing feeding rates or attaining food items that require less energy to forage (McCormick, 1998; Winterbottom et al., 2011).

Alongside reproductive benefits, this phenomenon may be an advantage with extreme lifetime mortality on coral reefs. It is well established that early life history stages fishes exhibit linear growth to account for the heavy predation rates that come with a small body size (Anderson, 1988; Goatley & Bellwood, 2016; Shima & Findlay, 2002; Wilson & Meekan, 2002). This theory may be applied to CRFs throughout all life history stages as a result of their small size. The growth curves suggest the *Trimma* examined mature at 15 – 15.5 mm and attain a maximum size of < 25 mm, which is consistent with previous literature (Goldsworthy et al., 2022; Winterbottom et al., 2011). Goatley and Bellwood (2016) demonstrate that mortality rates decrease drastically after reaching a size threshold of 43 mm. However, the *Trimma* species examined, along with many other CRFs, never reach this size limit where mortality declines and growth asymptotes (Depczynski & Bellwood, 2006; Goldsworthy et al., 2022; Winterbottom et al., 2011; Winterbottom & Southcott, 2008). Thus, *Trimma* remain at elevated risk of predation throughout their lives. Although predation is difficult to capture *in situ*, there are several points to support this, including: i) increased longevity of CRFs in the absence of predators (Randall & Delbeek, 2009), ii) reproductively active individuals present even at maximum longevities (Depczynski & Bellwood, 2006; Goldsworthy et al., 2022; Winterbottom et al., 2011; Winterbottom & Southcott, 2008), iii) exhibition of extreme

mortality rates of up to 8% per day and short lifespans <140 days (Depczynski & Bellwood, 2006; Goldsworthy et al., 2022; Winterbottom et al., 2011; Winterbottom & Southcott, 2008), and finally, iv) CRFs are consumed by any predator that is able to catch them (Goatley et al., 2017), which invites the possibility that these fishes are important prey species on coral reefs (Brandl et al., 2018).

Surprisingly, the BPH back calculation model followed by the BI model outperformed the MF model in all species, contrary to the expectation that the MF model would be superior (Vigliola & Meekan, 2009). Indeed, the MF model produced the best estimates of size in *Elacatinus evelynae* and *E. prochilos* (J. A. Wilson et al., 2009) and *Diplodus sargus*, *D. vulgaris* and *D. puntazzo* (Vigliola et al., 2000). However, there are exceptions where other methods were adequate. For example, the best estimates of size was obtained by the BI and Time-varying Growth models in early life history *Mogurnda adspersa* (Starrs et al., 2013), and the Age Effect model in *Salvelinus leucomaenis* (Morita & Matsuishi, 2001). Starrs et al. (2013) explain that fishes with longer lifespans and more complex OSG relationships may be more suitably modelled by the MF model, whereas simpler methods may be better where the OSG relationship is near linear. Therefore, the superior performance of the simple BPH model may be attributed to the linear or near-linear OSG relationships observed in the examined *Trimma* species. This highlights the need for a review of the most appropriate back-calculation model in small and short-lived coral reef fishes with atypical growth patterns compared to larger fishes.

Extreme life history characteristics associated with a small adult body size of three *Trimma* species are prevalent among other CRFs, and highlight their potential to be large players in energy flow on coral reefs (Beeken et al., 2021; Brandl et al., 2019; Depczynski & Bellwood, 2006; Depczynski et al., 2007; Winterbottom et al., 2011; Winterbottom & Southcott, 2008). With >3 generations produced annually and continuous growth throughout



life, CRFs such as *Trimma* may be a continuous and regenerative source of nutrients and energy for other reef consumers (Brandl et al., 2018; Depczynski & Bellwood, 2003; Depczynski et al., 2007; Morais & Bellwood, 2020). Investigating the spawning dynamics of *Trimma* should be a focus of future research, as a comprehensive understanding of these patterns is crucial to for population dynamics and their ecosystem implications. When CRF life history traits and population dynamics are considered, it is estimated juveniles and adults can deliver productivity of up to  $2.31 \text{ kg ha}^{-1} \text{ d}^{-1}$  on healthy coral reefs, (Brandl, Johansen, *et al.*, 2020; Morais & Bellwood, 2019, 2020), and account for almost 60% of fish biomass consumed on the reef (Brandl et al., 2019). Determining growth across life history stages is a step towards underpinning the ecosystem importance of *Trimma* on coral reefs. Future studies can progress and build upon this to better understand the many ecosystem processes that are influenced by growth.

## Chapter 5: Trophic dynamics of three small and short-lived coral reef fishes of the genus *Trimma*

---

### 5.1 Abstract

Small animals may have the ability to convert microscopic food into biomass, a form of energy that is accessible to larger predators. Small-bodied cryptobenthic reef fishes (CRFs) exploit a variety of food items and may be important food sources for other coral reef dwellers. However, knowledge regarding the trophic niches of small and abundant CRFs of the genus *Trimma* is lacking. The aim of this study was to investigate the trophic dynamics of *Trimma benjamini*, *T. capostriatum*, and *T. yanoi* by examining their feeding behaviour, food items consumed, food origins (benthic or pelagic), trophic interactions, and ecological morphology. The majority of individuals (79.7% to 93.4%) were actively engaged in feeding at a rate of 2.8 to 3.2 events per minute. These species consumed pelagic items >99% of the time, where identifiable stomach content revealed a diet consisting mostly of Mollusca larvae (Gastropoda and Bivalvia 32% - 48.3%) and Copepoda (14.2 – 28.9 %), though there were high amounts of unidentifiable dietary items. The physical attributes of *Trimma*, such as gape and eye morphology, were well-suited for capturing small and mobile prey. Though complete predation was not observed, 10.2% to 18.5% of *Trimma* individuals noticeably avoided fishes of the family Labridae and experienced a significant decrease in feeding rate of 45.2% to 80.8% at these times. Interferences by conspecifics or other fish species did not lead to a reduction in feeding rate. *Trimma* had morphological traits that included cryptic colouration, an elongated body shape, and a reduced caudal fin aspect ratio, which might be beneficial for predator avoidance. This study suggests that *Trimma* may play ecological roles in importing energy from the pelagic environment and potentially transferring it to predatory organisms.

## 5.2 Introduction

The trophic niche refers to the place of an organism within the environment, regarding both its food sources and the predators that consume it (Silvertown, 2004). It is an important part of determining the functional group of a species (Mouillot et al., 2013), and provides insights into resource utilisation, species interactions, nutrient and energy flow, and the ecological roles of organisms (Bierwagen et al., 2018; Hairston & Hairston, 1993; Odum, 1968; Rigler, 1975). There are multiple trophic pathways within ecosystems that interact to form complex food webs (Yodzis, 2001). Among these are the dynamics that occur between predator and prey groups. Predators exert cascading effects throughout the food web, regulating the population dynamics and behaviour of prey species (Gaynor *et al.*, 2019; Terborgh & Estes, 2013), while prey contribute energy and nutrients to fuel higher trophic levels (Terborgh & Estes, 2013). Most organisms occupy intermediate positions in the trophic web and can be both predator and prey (Weber & Lundgren, 2009). Small animals occupying such positions can have the ability to utilise resources that are inaccessible to higher trophic levels. These organisms may act as important links in the chain where they convert microscopic prey into biomass that can be utilised by larger predators (Brandl et al., 2018; Yodzis, 2001).

Coral reefs host upwards of 6000 species of fish that are heavily involved in the movement of energy and nutrients (Brandl et al., 2018; Sale, 2002). Increasing threats to these biodiverse systems have directed attention to determining the trophic niches of fishes, which is a key component in understanding the ecological roles they play (Bellwood et al., 2003; Bierwagen et al., 2018; Eurich *et al.*, 2019). Determining dietary items and whether food is derived predominantly from the pelagic or benthic environment is of particular importance. Benthic feeders may be involved in nutrient and energy recycling of reef associated material (de Goeij *et al.*, 2013; Marnane & Bellwood, 2002), consuming items such as benthic

invertebrates, detritus, coral, and algae (Bellwood et al., 2003; Depczynski & Bellwood, 2003; Eurich et al., 2019; Marnane & Bellwood, 2002). Alternatively, planktivores may consume items such as pelagic phytoplankton, copepods, or larvae entering the reef (Brandl et al., 2019; Depczynski & Bellwood, 2003; Hamner *et al.*, 1988; Morais & Bellwood, 2019; Saeki et al., 2005). Food derived from the pelagic environment constitutes the most productive trophic pathway (Morais & Bellwood, 2019) and may contribute to net energy gain on the reef (Clarke, 1999; Emery, 1968; Hamner et al., 1988; Winterbottom et al., 2011). However, many fishes have flexible diets, and a single species can contribute to multiple trophic functions (Eurich et al., 2019; Morais & Bellwood, 2019).

Furthermore, the role of fishes as potential prey for other organisms is important to understand when examining the trophic niches of fishes (Silvertown, 2004). Predation stands as a fundamental process on coral reefs, playing a critical role in the transfer of energy from one organism to another (Mihalitsis & Bellwood, 2021). In the presence of potential predators, prey individuals may exhibit antipredator behaviour as the flight response is activated (Brown *et al.*, 1999). The threat-sensitivity hypothesis suggests that prey species will make trade-offs between avoiding predators and other activities (e.g., foraging), depending on the level of predator threat imposed (Helfman, 1989). This may result in decrease in activity levels, increased shelter use, and lowered feeding rates as survival becomes the priority, overshadowing the need to forage for food (Catano *et al.*, 2016; Lönnstedt & McCormick, 2013; Rizzari *et al.*, 2014).

A combination of multiple methods may be used to achieve a holistic analysis of trophic dynamics (Bierwagen et al., 2018). Analysis of stomach content paired with observations of predator-prey interactions can identify food items consumed, origin of prey (i.e., benthic or pelagic), determine feeding behaviour, and identify potential predators (Bierwagen et al., 2018;

Choat *et al.*, 2004; Depczynski & Bellwood, 2003; Fox *et al.*, 2009; Savino & Stein, 1989). In addition, these methods may be supplemented with the measurement of morphological traits. Fishes may possess physical characteristics that have been linked to the performance of several functions, including food acquisition or predator avoidance (Goatley & Bellwood, 2009; Mihalitsis *et al.*, 2021; Tebbett *et al.*, 2018). Mouth and eye size can influence the ability of fishes to capture prey (Goatley & Bellwood, 2009). The horizontal mouth gape of a fish sets a limit on the size of prey it can consume. Fishes with larger mouths can therefore access a wider range of potential prey, enhancing feeding opportunities (Goatley & Bellwood, 2009; Mihalitsis & Bellwood, 2017). Larger eyes may increase the ability of a fish to perceive prey in low-light conditions or improve visual acuity, enabling fishes to capture microscopic prey with greater precision (Goatley & Bellwood, 2009). Furthermore, body colour, body shape and fin aspect ratio (the relationship of fin area to fin height) are all morphological attributes that may assist with predator avoidance. Benthic fishes that are susceptible to predation may have a colouration that is cryptic underwater (Depczynski & Bellwood, 2004; Marshall *et al.*, 2019), elongated bodies that facilitate manoeuvring through narrow spaces or remaining compressed against the benthos (Friedman *et al.*, 2020; Herler, 2007; Mihalitsis *et al.*, 2021), and low fin aspect ratios that have been linked to quick bursts of swimming and manoeuvrability (Luciani *et al.*, 2005). Such traits may be amplified in fishes with a small adult body size (Depczynski & Bellwood, 2004; Herler, 2007). These fishes have high mortality levels throughout all life history stages (Goldsworthy *et al.*, 2022) as their small size makes them available to a wide range of predators (Brandl *et al.*, 2018; Goatley & Bellwood, 2016).

Fishes with a maximum adult body length of less than 50 mm, benthic lifestyles, and cryptic characteristics are known as cryptobenthic reef fishes (CRFs) (Brandl *et al.*, 2018; Goatley & Brandl, 2017). The trophodynamics of this group is gaining research interest for several reasons. Firstly, CRFs possess the ability to exploit various trophic modes, including

predatory, herbivorous, and detritivorous pathways (Depczynski & Bellwood, 2003). CRFs have high energy requirements due to their small size, with exponentially greater mass-specific metabolisms compared to larger fishes with similar lifestyles, resulting in increased food uptake (Brandl et al., 2018). Additionally, CRFs are numerically abundant, exhibit continuous growth patterns, have short lifespans, and fast generational turnover rates, making them highly productive over time (Depczynski et al., 2007; Morais & Bellwood, 2019). The small size of CRFs also subject them to extreme mortality due to predation, underscoring their significance as potential prey species (Goatley et al., 2017; Goldsworthy et al., 2022). For these reasons among others, CRFs may act as productive “trophic bridges” between microscopic food and larger predators, with emerging evidence suggesting they are important conduits of energy and nutrient transfer on coral reefs (Brandl et al., 2019). However, the small size of CRFs leads to low biomass on the reef, which has historically led to their trophic contributions to coral reef ecosystems being undervalued (Ackerman & Bellwood, 2000). Consequently, the fundamental ecology, including the trophic niches, of most CRF species is not known (Winterbottom, 2019).

The genus *Trimma* (family Gobiidae) represents a remarkably diverse group of CRFs, encompassing 105 species (Winterbottom, 2019). Members of this genus attain a small body size of <30 mm, live less than 140 days, and have extreme daily mortality (Goldsworthy et al., 2022; Winterbottom et al., 2011; Winterbottom & Southcott, 2008). *Trimma* is highly abundant on Indo-Pacific coral reefs, and several species adopt a benthic lifestyle where they perch on hard substrata, predominantly in coral rock caves or reef walls (Depczynski & Bellwood, 2004; Goldsworthy, unpublished data; Herler, 2007). There is evidence to suggest that some members of this genus are planktivores, feeding primarily on copepods (Depczynski & Bellwood, 2003; Saeki et al., 2005) however, this knowledge is restricted to a few species and locations. For such a diverse, abundant, and potentially ecologically important group in the Indo-Pacific region, further knowledge of *Trimma* trophodynamics is necessary.

The aim of this study was to examine the trophic ecology of three *Trimma* species: *Trimma benjamini*, *T. capostriatum* and *T. yanoi* on coral reefs in Kimbe Bay, Papua New Guinea. Herein, stomach content analysis, direct observational studies, and the measurements of specific morphological traits were used to determine: 1) the proportion and feeding rate of actively feeding individuals and the benthic vs pelagic feeding methods; 2) dietary composition; 3) morphological features *Trimma* possess that may be beneficial for capturing prey; and 4) potential predators and how *Trimma* may avoid predation. Since *Trimma* likely have high mass-specific metabolic demands due to their small body size, it was expected that the majority of individuals would be actively feeding and ingesting food at a high rate. I predicted that they may be consuming pelagic and microscopic food items from previous research on other *Trimma* species. However, food items consumed may differ as no studies have examined *Trimma* diets in this location. If indeed *Trimma* species are consuming plankton at a high rate, I expected that they will have morphological traits that may be advantageous for capturing small and mobile food items. Finally, due to their small size and high mortality, *Trimma* may be subjected to predation pressure from other animals, possess specific morphological traits that could be beneficial for evading predators, and display anti-predator responses in the presence of threats.

## 5.3 Methods

### 5.3.1 Study site, specimen collection, and sample processing

Large samples of each species (120 *T. benjamini*, 82 *T. capostriatum*, and 131 *T. yanoi*) were collected between 08:00 and 16:00 (06/12/2022 – 10/12/2022) across six different reefs in Kimbe Bay, Papua New Guinea (5.1667° S, 150.5000° E). Fish were collected via random encounter with clove oil anaesthetic solution (5:1 ethanol: clove oil) and a 2 mm hand net on SCUBA. After surfacing, fish were immediately euthanised in a slurry of ice (1:1 ice: water).

Samples were transported to the laboratory, where they were blotted dry and photographed perpendicular to the camera alongside a measurement scale. Fish heads were sectioned from the body and photographed alongside a scale, with mouths spread open without any distortion, and directly facing the camera. All photographs were taken using the super-macro function of an Olympus TG 6 camera. Specimens were preserved in 70% ethanol after being photographed.

### 5.3.2 *Observational studies*

To investigate feeding behaviour and identify potential predators, observational studies were conducted between 08:00 and 16:00. 369 *T. benjamini*, 167 *T. capostriatum*, and 259 *T. yanoi* were observed and were selected by haphazard encounters over a variety of depths between 4 m and 10 m. Each individual was observed for two minutes, and the following behaviour was recorded. To identify feeding modes, the number of times each individual engaged in feeding strikes, and whether they fed from the pelagic or benthic environment was recorded. A pelagic feeding event was defined by an individual making rapid advances from their position on the substratum to capture prey suspended in the water column. A benthic feeding event was noted when an individual selected an item from the reef substratum. When benthic feeding modes were exhibited, the type of substratum each individual fed from was recorded (turf or crustose coralline algae-covered rock, encrusting sponge, encrusting coral).

To determine potential predators, whether an individual under observation experienced interferences by other animals was also documented. In this study, an interference was defined as aggressive behaviour exhibited by intruder-like animals within the territories of the observed *Trimma*. Interferences were documented at the family level and were subsequently grouped for analysis according to sample size. The final analysis comprised three interference categories: "Conspecifics", "Labridae", and "Other" which encompassed individuals of the families Pomacentridae, Blennidae, and other Gobiidae.



### **5.3.3 Dietary composition**

A subsample of 15 individuals per species were selected randomly from the sample pool to analyse stomach content. For each specimen selected, stomachs were removed from the body cavity, dissected, and emptied into zooplankton counting trays containing 70% ethanol. The entire content of the stomach was examined with a binocular microscope and the numerical abundance of each of the following food groups were recorded: Copepods, Mollusc larvae (Bivalvia and Gastropod), unidentifiable animal fragments, plant matter, unidentifiable digested material. Other animal food items were incorporated into one category “other animal” due to minimal observations of other animals in the stomachs.

### **5.3.4 Morphological traits**

Body length, eye diameter, horizontal mouth gape, body depth, and tail area and height were measured from photographed specimens in image J (Schneider et al., 2012) for all specimens. Body length was measured as standard length ( $L_S$ ). Eye diameter was taken as the largest anterior–posterior measurement of the eye. Horizontal gape was taken as the largest horizontal measurement of the fish’s open mouth. Eye diameter and horizontal gape were divided by  $L_S$  to get relative measurements to remove the effect of fish size (Goatley & Bellwood, 2009). Body depth was determined by the maximum vertical measurement of the body, excluding fins.  $L_S$  was divided by body depth to determine the body elongation index (Claverie & Wainwright, 2014). Caudal fin aspect ratio was determined by fin height squared, divided by fin area (Sambilay, 1990). Only caudal fins with fully extended rays were measured. Live macro photos of each species were taken in situ to display these traits in action.

### **5.3.5 Data processing and analysis**

The proportion of actively feeding individuals, feeding rate per minute, and pelagic relative to benthic contributions were modelled separately among species using a series of

generalised linear models (glms) and generalised linear mixed effect models (glmms). These models assessed the random effects of site and depth and/or tested different statistical distributions to determine the optimum model for each response variable.

Throughout this study, optimum models were selected by Akaike Information Criterion (AIC., Sakamoto et al., 1986). Lower AIC scores indicated superior model fit, given a minimum difference of two AIC units, along with satisfactory residual distributions. All glms and glmms in this study were conducted in R (R Core Team, 2021) using the `glmmTMB` package (Brooks *et al.*, 2017). Model assumptions were assessed using residual distributions (Hartig, 2021).

Analysis of stomach content incorporated the frequency of occurrence, relative numerical abundance, and the relative size of each food group for each species (Hyslop, 1980; Saeki et al., 2005). Frequency of occurrence of each food group was calculated for each species by:  $\%F = \frac{N_i}{N} \times 100$  where: %F = Frequency of occurrence of a specific food group,  $N_i$  = number of stomachs containing a specific food group, and N = total number of stomachs containing food in the sample (Loto *et al.*, 2021). Numerical abundance of each food group was modelled using a glm with a Negative Binomial family for each species and each food item was expressed as a percentage of the total mean abundances. Sizes of each food group were derived from a subsample of food items that were photographed alongside a measurement scale. Lengths and widths of food items were measured in image J and were multiplied together to get the approximate size of each food item. For each species, the mean size of each food group was modelled using a glm with a gaussian distribution and was expressed as a percentage of the total to get relative sizes. A modified version of the index of relative importance for each food group for each species was calculated as  $IRI = (\%N + \%S) \times \%F$ , where IRI = the index of relative importance, %N = relative numerical abundance, %S = relative size, and %F =

relative frequency of occurrence (Hyslop, 1980; Saeki et al., 2005; Sagar *et al.*, 2019). This formula has been adapted in this study to include relative sizes instead traditional methods that use relative weights or volumes. This is because sizes were determined from two-dimensional photographs and therefore height was not measured to calculate volume, and food items were microscopic and therefore could not be weighed efficiently.

To identify potential predators, firstly, the proportion of individuals in interference categories ‘Conspecifics’, ‘Labridae’, and ‘Other’ was modelled by glms and glmms (including site and depth effects) with a Binomial family (logit link) for each species separately. The same was done to model the feeding rate per minute in each category compared to individuals that did not experience interferences, however comparing the fit of Gaussian (identity link), Poisson (log link), and Negative Binomial (log link) distributions to determine the most suitable model. For *T. capostriatum*, categories “Other” and “Conspecific” were removed prior to analysis due to  $\leq 1$  individual present in these categories, and hence models were run separately for each species due to empty factor levels. Mean feeding rates of individuals in each interaction category was compared to the mean feeding rate of individuals that did not interact using pairwise comparisons.

To analyse morphological trait measurements, mean eye diameter, horizontal gape, elongation, and caudal fin aspect ratio were estimated for each species using multiple glms. Mean measurements for each trait were compared among species using pairwise comparisons. Relative eye diameter and horizontal gape measurements were combined into a biplot, with the diurnal, nocturnal and overall relative eye and horizontal gape averages for fishes retrieved from Goatley and Bellwood (2009). Here, the mean relative eye diameters were 7.8 mm, 11.7 mm, and 8.4 mm and mean relative horizontal gape measurements were 6.6 mm, 10.4 mm, and 7.2 mm for diurnal fishes, nocturnal fishes, and for fishes overall, respectively.

## 5.4 Results

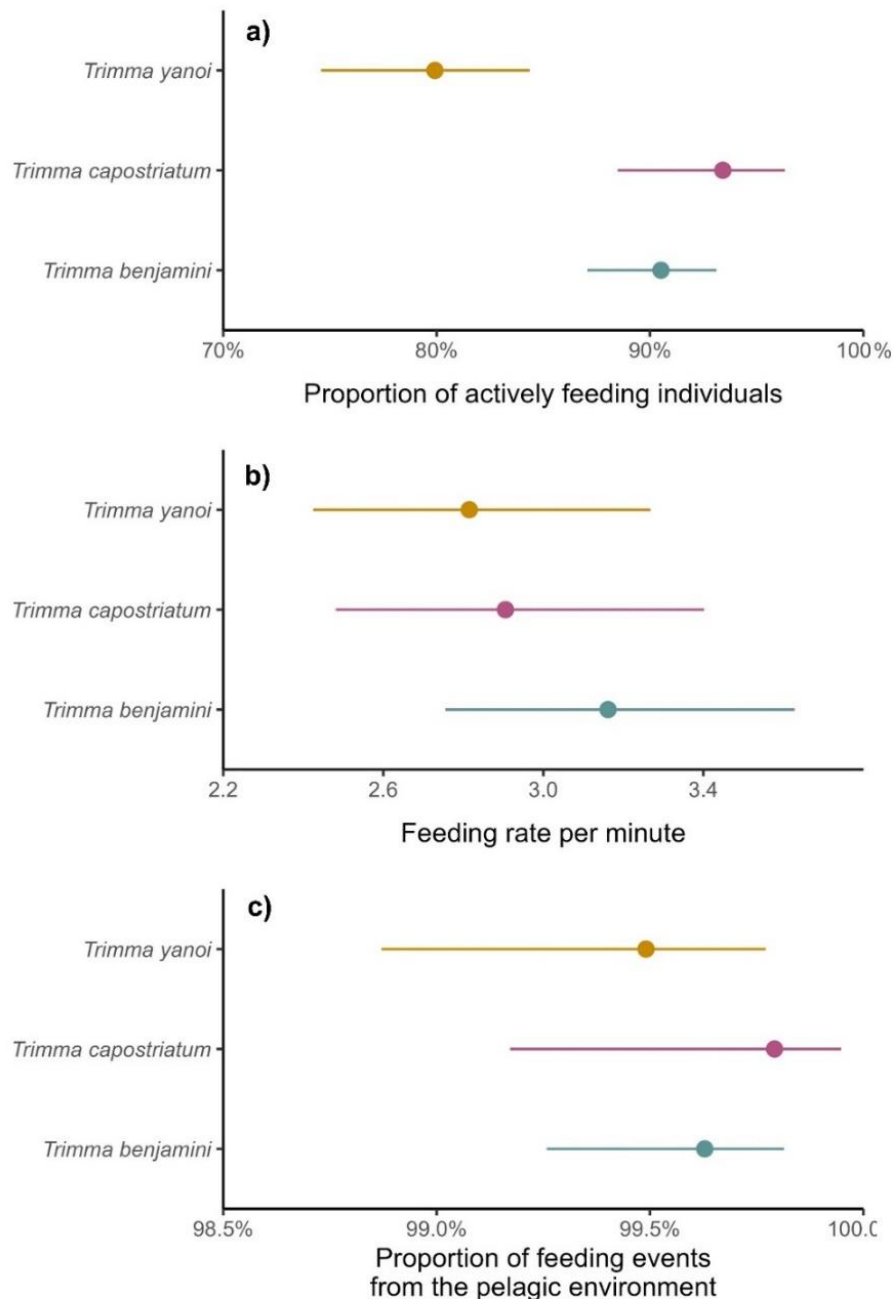


Figure 5.1: a) Proportion of individuals that were actively feeding during the observation period. Error bars represent the 95 % confidence intervals derived from a Binomial distribution (logit link) (McKeon et al., 2012). b) Mean feeding rate per minute  $\pm$  95% Negative Binomial confidence intervals. c) Predicted proportion of feeding events that were pelagic, where food items were captured from the water column. 95 % confidence intervals were derived from a Binomial distribution (McKeon et al., 2012). For a and b,  $n = 369$  *T. benjamini*, 167 *T. capostriatum*, and 259 *T. yanoi* individuals. For c,  $n = 2152$  *T. benjamini*, 974 *T. capostriatum*, and 1178 *T. yanoi* feeding events.

#### 5.4.1 *Proportion actively feeding, feeding rate, and pelagic vs. benthic contributions*

A total of 2152 feeding events were observed in *T. benjamini*, 974 in *T. capostriatum* and 1178 in *T. yanoi* individuals. To determine the proportion of actively feeding individuals in each species, the optimum model had a Binomial family (logit link) and no random effects (Table A4. 1). Most individuals (79.9 - 93.4%) were actively feeding during the observation period (Figure 5.1a).

The optimum model to determine feeding rate among species accounted for variance among sites and utilised Negative Binomial distribution (Table A4. 2). The mean feeding rate of actively feeding individuals was similar among species at 2.8 - 3.2 feeding events per minute (Figure 5.1b), and reached a maximum of 11.5, 10, and 13 feeding events per minute in *T. benjamini*, *T. capostriatum*, *T. yanoi*, respectively.

To estimate the proportion of feeding events that were pelagic relative to benthic for each species, the optimal model did not include random effects and a Binomial family with a logit link (Table A4. 3). Majority of feeding events were pelagic (>99.5%, Figure 5.1c), where individuals were perched on the substratum and made rapid advances to grab a microscopic food item that was suspended in the water column. <0.5% of feeding events were benthic and involved an individual selecting a food item from the reef substratum (Table A4. 4). In *T. benjamini*, 6 benthic feeding events were from turf algae-covered coral rock, one feeding event was from encrusting coral, and one from an encrusting sponge. In *T. capostriatum*, both benthic feeding events were from encrusting sponge. In *T. yanoi* all 6 feeding events were from turf algae-covered coral rock. In all benthic feeding observations, whether the benthic substratum itself was ingested or if the individual picked an item (e.g., benthic invertebrate) off the substratum was unknown.

#### 5.4.2 Dietary composition

According to the index of relative importance (IRI), mollusc veligers were the most important food group for each species, accounting for 32- 48.3 % of the diet. Within the mollusc complex, bivalve larvae accounted for 13% - 24.1% of the diet and gastropod larvae comprised 19 – 24.2% of the diet (Table 5.1). Copepods were a significant food group, accounting for 14.2 – 28.9 % of the diet (Table 5.1). The importance of animals other than mollusc and copepods was low at 1.3% – 1.7% (Table 5.1). The *Trimma* species examined were predominantly carnivorous, and plant material made up a low proportion (0% - 4.8%) of the diet in each species (Table 5.1). There was a large volume of unidentifiable material. Animal fragments comprised 3.2% – 22.3% of the diet, and unidentifiable digested material had a high IRI in each species, comprising 15.5 – 23% of the (Table 5.1). While numerical abundances were relatively low in this group (8.4 – 12%), the mean relative size of this food group was the largest in each species at 27.6 - 33.3% (Table 5.1).

Table 5.1: Dietary composition of *Trimma benjamini*, *T. capostriatum*, and *T. yanoi*. Mean relative numerical abundance (%N), mean relative size (%S), relative frequency of occurrence (%F), and the index of relative importance (%IRI) of each food group. n = 15 individuals per species

Species	Food items	Numerical abundance (%N)	Size of food group (%S)	Frequency of occurrence (%F)	%IRI
<i>Trimma benjamini</i>	Copepod	25.2	14.9	91.7	<b>21.6</b>
	Bivalvia larvae (Mollusca)	18.3	22.7	100.0	<b>24.1</b>
	Gastropoda larvae (Mollusca)	26.8	22.5	83.3	<b>24.2</b>
	Other animal	3.5	5.5	25.0	<b>1.3</b>
	Plant material	10.1	0.7	75.0	<b>4.8</b>

	Unidentifiable animal fragments	6.9	0.4	75.0	<b>3.2</b>
	Unidentifiable digested material	9.1	33.3	83.3	<b>20.8</b>
<hr/>					
<i>Trimma capostriatum</i>	Copepod	30.2	14.5	81.8	<b>28.9</b>
	Bivalvia larvae (Mollusca)	7.3	15.3	72.7	<b>13.0</b>
	Gastropoda larvae (Mollusca)	19.6	24.6	54.5	<b>19.0</b>
	Other animal	0.6	17.7	9.1	<b>1.3</b>
	Plant material	0.0	0.0	0.0	<b>0.0</b>
	Unidentifiable animal fragments	34.1	0.3	81.8	<b>22.3</b>
	Unidentifiable digested material	8.4	27.6	54.5	<b>15.5</b>
<hr/>					
<i>Trimma yanoi</i>	Copepod	17.3	9.4	91.7	<b>14.2</b>
	Bivalvia larvae (Mollusca)	22.3	21.1	83.3	<b>20.9</b>
	Gastropoda larvae (Mollusca)	15.9	28.5	91.7	<b>23.5</b>
	Other animal	2.8	6.0	33.3	<b>1.7</b>
	Plant material	6.0	1.6	50.0	<b>2.2</b>
	Unidentifiable animal fragments	23.7	0.4	83.3	<b>11.6</b>
	Unidentifiable digested material	12.0	33.0	100.0	<b>26.0</b>
<hr/> <hr/>					

### 5.4.3 Interferences

The optimum models to determine the proportion of individuals in each interference category had no random effects for each species and utilised a Binomial (logit link) distribution (Table A4. 5). All individuals made reactions when interfered with by intruders, either by hiding or darting to another location on the substratum. 15.2% of *T. benjamini* observed were interfered with by individuals of the family Labridae, 1.5% by conspecifics, and 5.4% by other fish species. 10.2% of *T. capostriatum* were interfered with by labrids and <1% by another fish species. No *T. capostriatum* individuals were interfered with by conspecifics. 18.5% of *T. yanoi* individuals were interfered with by labrids, 4.2% by conspecifics, and 2.3% by other species (Figure 5.2a).

No complete predation events were witnessed during the observation period. Interferences by labrids were assumed to be attempted predation events, where labrids were actively searching the reef substratum and made rapid advances for *Trimma* individuals, prompting them to retreat into cervices/ holes in the reef. Interferences by conspecifics or other fishes were territorial chasing behaviours.

The optimum models used to determine the feeding rate of individuals in different interference categories varied by species. The optimum model for *T. benjamini* included no random effects, while the model for *T. capostriatum* accounted for variation among sites, and the model for *T. yanoi* considered depth variations. In each species, a Negative Binomial distribution with a log link was used (Table A4. 6a).

The mean feeding rates of those interfered with by labrid individuals was 1.5, 1.7, and 0.5 feeding events per minute in *T. benjamini*, *T. capostriatum*, and *T. yanoi*, respectively (Figure 5.2b). On average, this represented significant percentage decreases of 53.1% in *T. benjamini*, 45.2% in *T. capostriatum*, and 80.8% in *T. yanoi* when compared to the mean



feeding rate of individuals that did not experience interferences (Figure 5.2c, Table A4. 6b). For each species, there was no significant difference in the mean feeding rate of individuals that were interfered with by conspecifics or other fish species when compared to individuals that did not experience interferences (Figure 5.2c, Table A4. 6b)

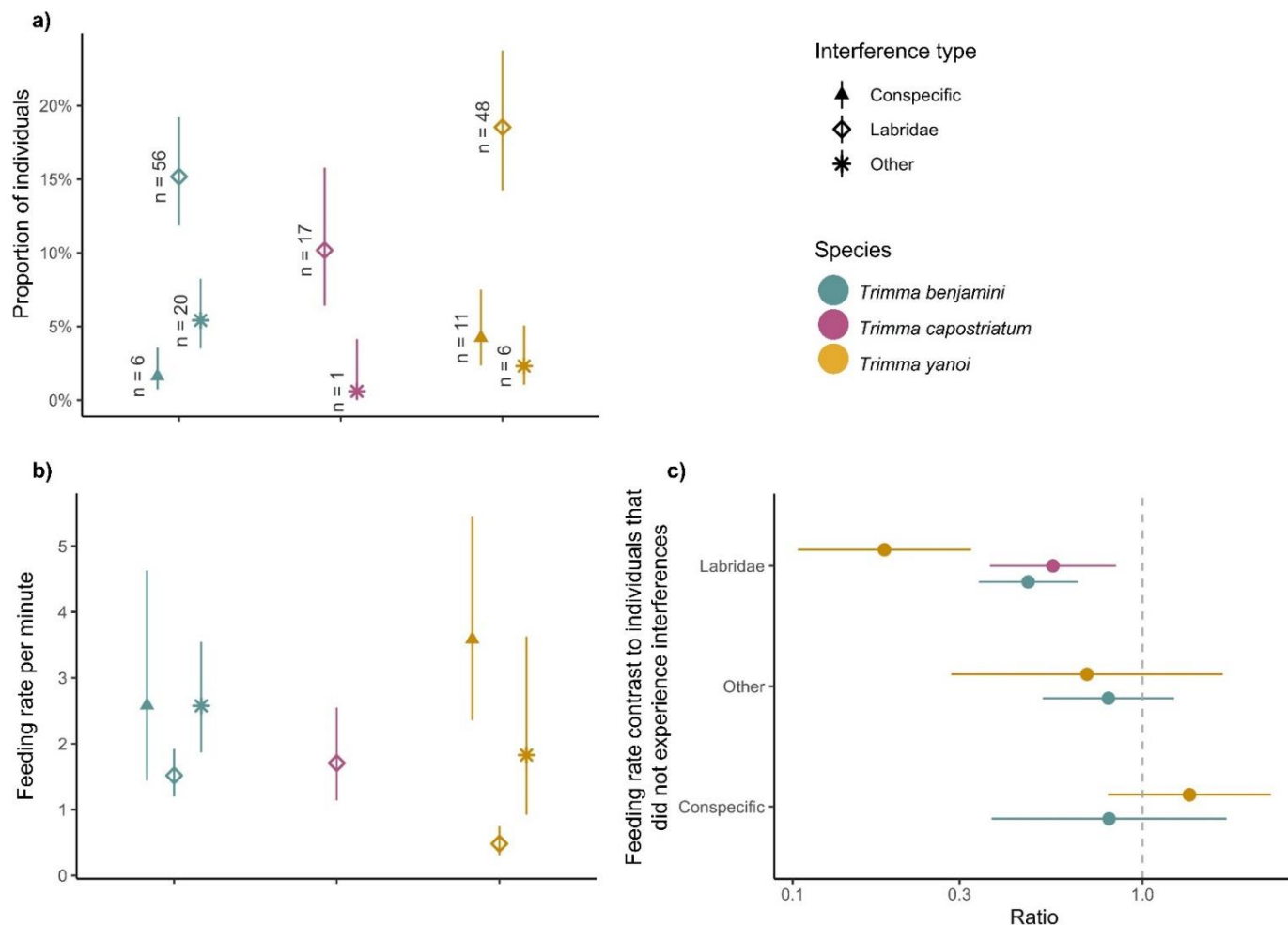


Figure 5.2: a) Proportion of individuals (%) that were interfered with by a conspecific, Labridae, or other fish during the observation period. Error bars represent the 95% confidence intervals derived from a Binomial distribution (McKeon et al., 2012). n represents the number of individuals in each category. b) Mean feeding rate per minute ( $\pm$  95% Negative Binomial distribution derived confidence intervals) for each interference category. c) Pairwise comparisons showing the mean differences ( $\pm$  95% confidence intervals) of the feeding rate of individuals that experienced interferences compared to those that did not. Ratio represents fold differences, where mean values and confidence levels crossing 1 hence indicate no significant difference. For a and b shapes represent the interference category. For a, b, and c, colour represents each species *Trimma benjamini* (n = 369), *T. capostriatum* (n = 166), and *T. yanoi* (n = 259).

#### 5.4.4 Morphological traits

The optimum model to determine traits mean relative horizontal gape, elongation index and caudal fin aspect ratio had a gaussian (identity link) distribution and accounted for variation among sites. Mean relative eye diameter was also modelled under a gaussian (identity link) distribution but had no random effects (Table A4. 7a).

Eye diameter ranged from 1.4 – 2.8 mm in *T. benjamini*, 1.0 – 2.6 mm in *T. capostriatum*, and 1.0 – 2.7 mm in *T. yanoi*. Mean eye diameter ranged from 11.7 – 13.1% of the  $L_S$  (Figure 5.3a, Figure 5.3b). Horizontal gape ranged from 0.9 – 1.8 mm in *T. benjamini* and 0.8 – 2.0 mm in *T. capostriatum* and *T. yanoi*. Relative horizontal gape measurements were between 7.7 – 9% of the  $L_S$  (Figure 5.3b). *T. benjamini* and *T. capostriatum* had a similar relative eye and horizontal gape sizes, while *T. yanoi* had a significantly larger relative eye and horizontal gape size than *T. benjamini* and *T. capostriatum* (Table A4. 7b). Each species had a larger relative eye size and average - larger relative horizontal gape size than the overall average for fishes (eye 8.4, gape 7.2: Goatley & Bellwood, 2009). Mean measurements of the species examined were closer to the nocturnal average measurements (eye 11.7, gape 10.4: Goatley & Bellwood, 2009) than the diurnal average measurements (eye 7.8, gape 6.6: Goatley & Bellwood, 2009), despite being active during the day (Figure 5.3c).

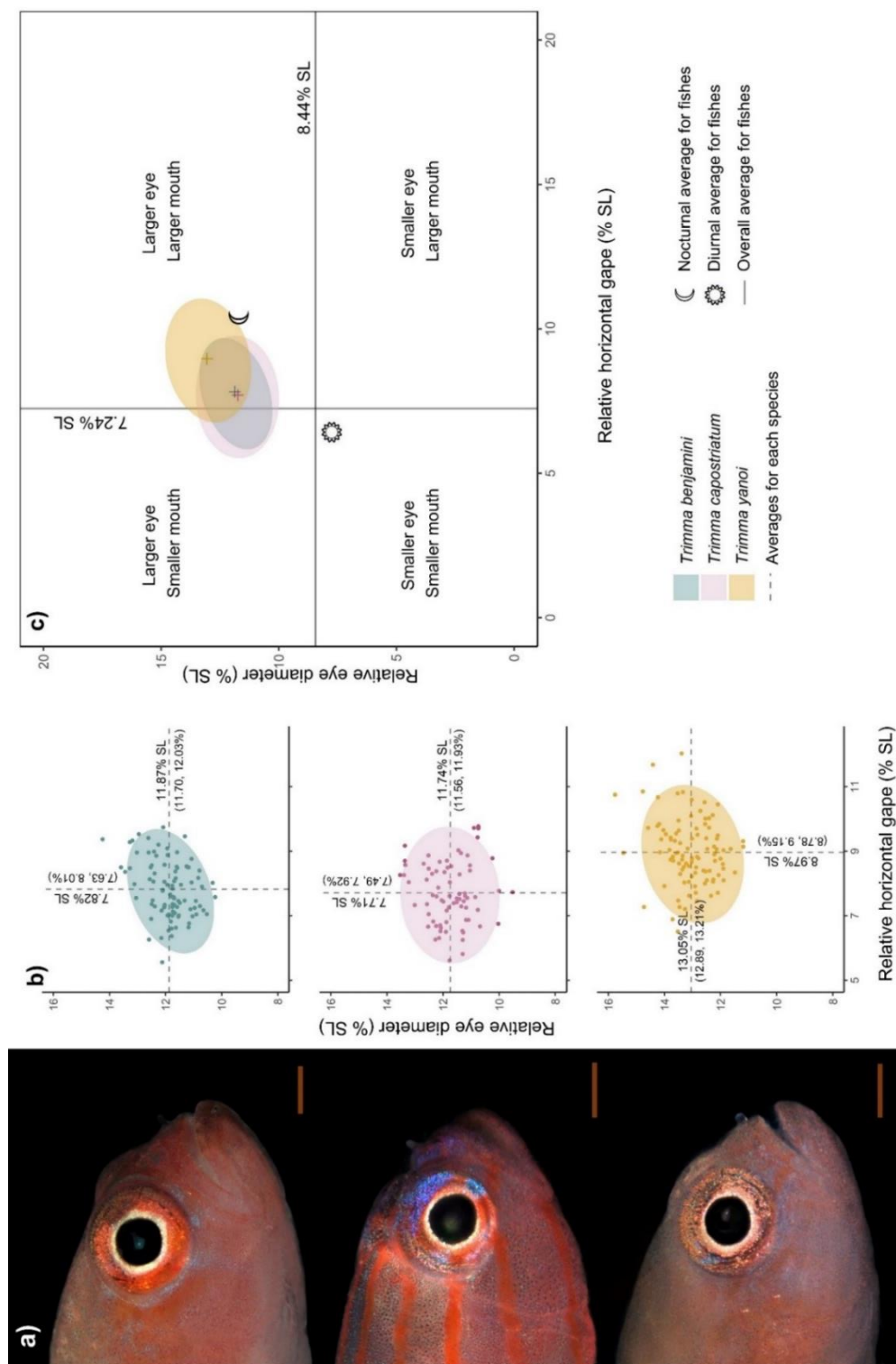


Figure 5.3: a) Macro images of *Trimma benjamini*, *T. capostriatum*, and *T. yanoi* heads. Scale bars = 1 mm. b) Biplot of the relative horizontal gape plotted with relative eye diameter measurements, as a percentage of standard length. Dashed lines represent the mean value for each morphological trait, and points represent the relative eye and gape measurement of each individual fish. 95% confidence intervals are shown in brackets below the mean values.  $n = 94$  *T. benjamini*, 74 *T. capostriatum*, and 99 *T. yanoi*. c) Biplot containing information for each species in a plotted on a singular graph. Plus symbol represents the mean morphological trait measurements for each species. Solid lines dividing the biplot represents overall average for fishes. Crescent moon and sun represents the nocturnal and diurnal average for fishes retrieved from Goatley and Bellwood (2009). Top left quadrant holds individuals with a larger eye and smaller mouth than the average for fishes, top right contains individuals with a larger eye and mouth than average, bottom left contains individuals with a smaller eye and larger mouth than average, and bottom right has individuals with a smaller eye and larger mouth than average.

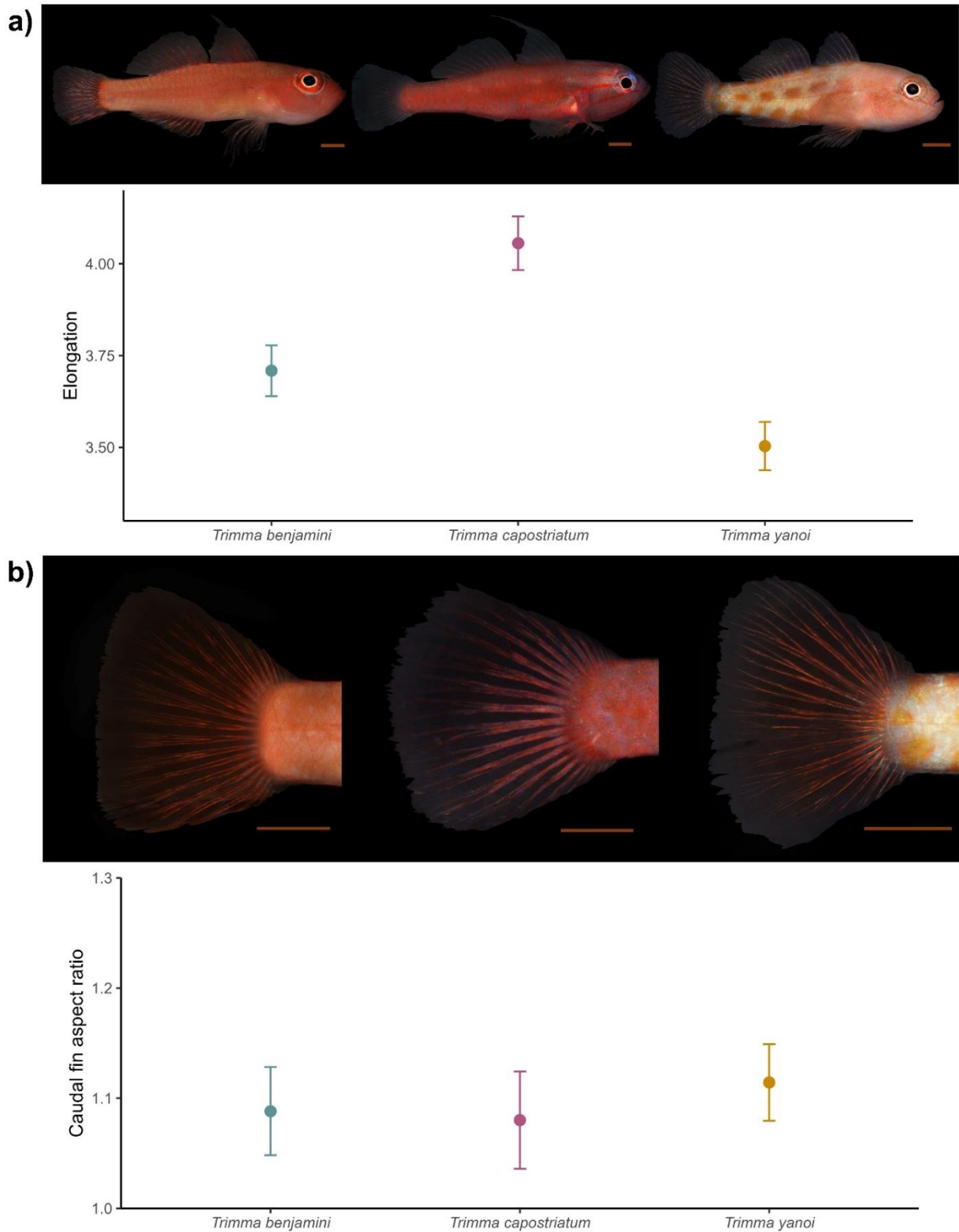


Figure 5.4: a) Images of live *Trimma benjamini*, *T. capostriatum*, and *T. yanoi*. Graph below images shows the mean elongation values ( $L_s$  /maximum body depth) of each species b) Macro images of *Trimma benjamini*, *T. capostriatum*, and *T. yanoi* caudal fins. Graph below images shows the mean caudal fin aspect ratios (fin height<sup>2</sup> / fin area) of each species. For a and b, error bars represent the 95% confidence intervals derived from a gaussian distribution. Scale bars = 2 mm.

Body colour of the *Trimma* examined consisted of warm, low frequency, and long wavelength colours. The body of *T. benjamini* individuals was red-orange, *T. capostriatum* individuals were red-pink, and *T. yanoi* was a combination of yellow and orange (Figure 5.4a). Body shape was elongated in all species.  $L_S$  was an average of 3.7, 4.1 and 3.5 times the maximum body depth in *T. benjamini*, *T. capostriatum*, and *T. yanoi*, respectively. *T. capostriatum* had the most elongated shape, and was 9.4% more elongated than *T. benjamini*, and 15.8% more elongated than *T. yanoi*. *T. benjamini* was 5.9% more elongated than *T. yanoi* (Figure 5.4a, Table A4. 7b). Caudal fins were paddle shaped, with low mean caudal fin aspect ratios of 1.1 in all species (Figure 5.4b, Table A4. 7b).

## 5.5 Discussion

This study aimed to investigate the trophic niches of *T. benjamini*, *T. capostriatum*, and *T. yanoi* by determining their feeding behaviour, food items consumed, food origin (benthic or pelagic), trophic interactions, and ecological morphology. The majority of individuals (79.7% to 93.4%) were actively feeding, displaying a rapid feeding rate of 2.8 to 3.2 bouts per minute. The identifiable dietary items of these species in Kimbe Bay primarily consisted of the larvae of molluscs, with bivalve and gastropod larvae accounting for 32% to 48.3%, and copepods which accounted for 14.2% to 28.9 % of the diet according to the IRI values, though there was a high proportion of unidentifiable dietary items. Almost all feeding events (<99%) involved prey acquisition from the pelagic environment. *Trimma* gape and eye morphological attributes were consistent with the effective capture of microscopic and mobile prey. Although no complete predation events were witnessed, 10.2% to 18.5% of *Trimma* observed experienced interferences by labrid individuals. Individuals interfered with by labrids showed a significant decrease in feeding rate of 44.5% to 81.7%, whereas those that were interfered with by conspecifics or other fishes did not have a lowered feeding rate. Additionally, specific attributes

of *Trimma* were identified that may aid in predator evasion, including cryptic colouration, an elongated body shape, and a low caudal fin aspect ratio. In the subsequent discussion, I delve into these findings and discuss their potential in determining the trophic function of *Trimma* on Indo-Pacific coral reefs.

A significant proportion of individuals actively engaged in high rate feeding on pelagic food items. With their small adult body size of <25 mm, the *Trimma* species examined are among the smallest vertebrate carnivores on the reef (Mihalitsis *et al.*, 2022), with high percentage occurrences of pelagic bivalve and gastropod veligers and copepods in their diets. Our results conform to a previous study on *Trimma caudomaculata* and *T. caesiura*, which fed primarily on copepods (Saeki *et al.*, 2005). Many CRFs rely on the consumption of zooplankton (Brandl *et al.*, 2018; Herler *et al.*, 2011), with crustaceans, including copepods, accounting for 45.6% of CRF diets (Brandl *et al.*, 2018). Bivalve and gastropod larvae are also significant prey, although to a lesser extent than crustaceans (Brandl *et al.*, 2018; Depczynski & Bellwood, 2003). In contrast, many CRFs are dependent on benthos where they consume detritus as a primary food source (Depczynski & Bellwood, 2003). Plankton feeding in *Trimma* may be related to their microhabitat use (Depczynski & Bellwood, 2004). Zooplankton often aggregate in large quantities, particularly in areas with low water motion such as cave structures (Emery, 1968), which are frequently inhabited by species like *Trimma* (Depczynski & Bellwood, 2004; Herler, 2007). *Trimma* species may utilise cave ceilings, openings, and reef walls as vantage points to capture prey (Depczynski & Bellwood, 2004). Therefore, zooplankton may be highly accessible for these fishes, and they may not be able to utilise detritus like other CRFs in benthic habitats (Herler *et al.*, 2011). In addition, these micro-invertebrates serve as an energy-rich and high-protein source of food (Brandl *et al.*, 2018; Herler *et al.*, 2011; Kotrschal & Thomson, 1986; Kramer *et al.*, 2013). Feeding on lower quality food, such as primary production, would require an even higher feeding rate to obtain enough energy, diverting attention from other

crucial life activities like predator avoidance and reproduction (Hernaman *et al.*, 2009). Clarke (1999) demonstrated that *Acanthemblemaria spinosa*, positioned in elevated locations on branching corals to capture pelagic Calanoid copepods, may play ecological roles in assimilating energy from the pelagic environment. Likewise, the *Trimma* species examined might also serve as significant micro-predators contributing to the energy influx onto the reef.

*Trimma* feeding mode is likely a reflection of their high energy requirements (Brandl *et al.*, 2018) and there are several factors that can contribute to these high energy needs. Firstly, small body size and high size-related metabolic demands. Following allometric scaling properties (West *et al.*, 1997), small organisms such as CRFs use exponentially more metabolic energy per unit of body mass relative to their larger counterparts of similar activity levels (Ackerman & Bellwood, 2000; Brandl *et al.*, 2018). Secondly, although the benthic predatory lifestyle of *Trimma* is considered to expend less energy than those that exhibit continuous swimming (Brandl *et al.*, 2018; Fu *et al.*, 2009), very few individuals were fully sedentary during observations. 10.2% to 18.5% of individuals were disturbed by labrids, which resulted in subsequent flight responses. Moreover, 79.7% to 93.4% of individuals were actively feeding, where they exhibited regular bouts of outward swimming from the reef to capture prey, averaging around three times per minute, and reaching a maximum of 13 times per minute. These frequent episodes of rapid swimming due to foraging effort or antipredator responses would require energy to perform (Helfman, 1989; Whiterod, 2013), which is amplified by the energetic costs of swimming in small fishes being high due to opposing hydrodynamic forces (Tokić & Yue, 2019). Additionally, Growth in these fishes does not asymptote in adulthood as typically seen in larger fishes and remains at near linear rates following maturation (Goldsworthy, unpublished data; Winterbottom *et al.*, 2011). Sustaining growth rates and carrying out reproduction simultaneously may be energetically demanding, as the latter requires energy to source mates and maintain reproductive structures (Audzijonyte & Richards,

2018; Munday & Molony, 2002). Finally, the *Trimma* species examined possess energetically expensive traits and behaviours. For example, large eyes relative to *Trimma* body size may impose significant costs, as the vertebrate retina is among the most metabolically demanding tissue, exhibiting energetic costs greater than the brain (Protas *et al.*, 2007). Additionally, ovarian structures in the gonads of functional males (Goldsworthy *et al.*, 2022), impose significant energetic costs to develop and maintain (Audzijonyte & Richards, 2018; Munday & Molony, 2002). Moreover, *Trimma* may exhibit parental care and mate guarding, which could also be costly and divert feeding attention (Fukuda, Manabe, *et al.*, 2017). Consequently, these factors, among others, may contribute to the high energy demands of these fishes, making them less tolerant of starvation periods, decreased food intake, or low-quality food (Brandl *et al.*, 2018; Depczynski & Bellwood, 2003).

*Trimma* exhibited morphological traits that may assist with the acquisition of their prey (Goatley & Bellwood, 2009). Each *Trimma* species possessed larger relative eye size than the average relative size for fishes. These measurements resembled the average size found in nocturnal fishes more closely than diurnal fishes, despite being active during the day. *Trimma* inhabit low-light environments, such as caves or steep reef structures (Depczynski & Bellwood, 2004; Herler, 2007). The relatively larger eye diameters of these fishes likely enhance the capacity of *Trimma* to perceive microscopic and mobile prey in these dark habitats (Goatley & Bellwood, 2009; Herler, 2007). Furthermore, each species displayed a slightly larger horizontal mouth gape relative to their size compared to the average, however, overall gape size was still small at 0.8 – 2.0 mm. As mouth gape limits prey size, this restricts their prey to microscopic items, such as zooplankton (Brandl *et al.*, 2018; Goatley & Bellwood, 2009; Mihalitsis & Bellwood, 2017). Alternatively, several studies have suggested that traits such as large eyes or gapes in small fishes may be related to the negative allometric relationship of these morphologies with increasing body size (Job & Bellwood, 2000; Santos-Santos *et al.*, 2015).



However, this may not be the case for CRFs in general, as they have diverse diets (Depczynski & Bellwood, 2003) and their morphologies reflect this variability in similar ways to their larger counterparts (Goatley & Bellwood, 2009).

In addition to their roles as micro-predators, *Trimma* might also be an important food source for other animals on the reef (Brandl et al., 2018; Winterbottom et al., 2011). This study suggested that interferences by labrid individuals were attempted predation events. Labrids continually patrolled the reef walls in Kimbe Bay and would rapidly approach a *Trimma* individual, prompting them to seek refuge in crevices or holes in the reef and re-emerge cautiously once the threat had passed. Individuals subjected to these events displayed a decreased feeding rate compared to those that did not experience interferences. This alteration of behaviour suggests that labrids may be potential predators of *Trimma* (Brown et al., 1999), however further experiments and observations are required to confirm this. Predators inducing shifts in prey behaviour is common across animal species, including coral reef fishes (Brown et al., 1999; Catano et al., 2016; Magnhagen, 1988). For example, large herbivorous fishes consumed 90% less food in the presence of predators, and made trade-offs between feeding and predator avoidance (Catano et al., 2016). Likewise, the *Trimma* species examined must reconcile the opposing, yet equally crucial requirements of evading predators and obtaining enough food to survive (Magnhagen, 1988; Ryer & Olla, 1998). Feeding methods and body size are among factors that can contribute to predation risk (Goatley & Bellwood, 2016; Goatley et al., 2017; Magnhagen, 1988). Momentary ventures away from the safety of the reef benthos is required for these *Trimma* species to capture pelagic prey. While *Trimma* generally stayed close to the reef, the frequent departures from secure habitats may expose them to predators (Balaban-Feld et al., 2019).

Though no complete predation events were witnessed, there are several points of evidence to suggest that *Trimma* and other CRFs are preyed upon. Firstly, *Trimma* have extreme mortality rates of 3-7 % per day (Goldsworthy et al., 2022; Winterbottom et al., 2011). Mortality in coral reef fishes declines exponentially following settlement as recruits learn to avoid predators and becomes low when a fish reaches 43 mm in length. However, with a body size of less than 25 mm, *Trimma* experience high mortality throughout their lives (Goatley & Bellwood, 2016). Their small body size also renders them available to a suite of predators (Mihalitsis & Bellwood, 2017), and ecologically similar CRFs are consumed opportunistically by any predator that can capture them (Goatley et al., 2017). Finally, CRFs have increased longevity in the absence of predators (Randall & Delbeek, 2009) and individuals are reproductively active even at maximum ages (Depczynski & Bellwood, 2006; Goldsworthy et al., 2022; Winterbottom et al., 2011; Winterbottom & Southcott, 2008). Accordingly, CRFs may account for 60% of consumed reef fish biomass (Brandl et al., 2019). However, predation is rarely seen and is difficult to quantify, as majority of piscivore stomachs are empty, events usually only last a few milliseconds, and predation rate is often non-uniform throughout the day (Mihalitsis et al., 2022). The lack of predation incidents during the observation period could be attributed to piscivory occurring during dusk, dawn, or at night (Danilowicz & Sale, 1999; Shoji *et al.*, 2017). For example, predatory *Cephalopholis cyanostigma* have crepuscular activity, with the highest number of feeding strikes at dusk (Bosiger & McCormick, 2014). This study demonstrates that *Trimma* live under constant threat of being consumed, and individuals that are not in optimal physical condition or lack vigilance may face increased risks to their survival.

In contrast, The *Trimma* species examined display several features that make them appear cryptic. The body colouration of the *Trimma* species examined consisted of red, orange, and yellow tones. These colours are cryptic by camouflage with the benthos which is frequently

coated in pink-red crustose coralline algae, or at depths where low frequency and long wavelength light is filtered, making these colours appear dull underwater (Figure 5.5) (Depczynski & Bellwood, 2004; Marshall et al., 2019). Each species also had an elongated body shape, which is a common shape in fishes (Claverie & Wainwright, 2014). In benthic species, elongation may be beneficial to remain inconspicuous to predators, as decreased dimensionality is more cryptic against the reef benthos (Herler, 2007; Mihalitsis et al., 2021). It could also be an advantage to enable movement through small crevices or holes in the reef matrix which *Trimma* frequent to escape predators (Depczynski & Bellwood, 2004; Friedman et al., 2020). Interestingly, despite having the lowest proportion of actively feeding individuals, *T. yanoi* exhibited a stockier body shape than the other two species, which could reflect variations in habitats (Herler, 2007). *T. yanoi* primarily inhabits large cave structures or sloping inward sections of the reef. The highly rugose and low light characteristics of large cave habitats may reduce the need for elongation in *T. yanoi* compared to the other species. In contrast, *T. benjamini* inhabits more open areas and *T. capostriatum* occupies smaller spaces, potentially favouring a depressed body shape due to crypsis and manoeuvrability, respectively (Depczynski & Bellwood, 2004). However, this is speculative, and further investigation is necessary to confirm these hypotheses. Finally, each species had a low mean caudal fin aspect ratio of 1.1, indicating a large fin area relative to its height. Paddle shaped tails seen in these species are common among CRFs and reflect their benthic lifestyle. While not well-suited for sustained swimming, paddle-shaped tails offer an advantage for quick bursts of acceleration (Luciani et al., 2005). This contrasts to pelagic fishes with higher fin aspect ratios, which are better suited for prolonged, continuous swimming (Magnuson, 1978). A combination of these eco-morphological traits, among others, might make healthy *Trimma* harder to detect or catch than species without these characteristics (Depczynski & Bellwood, 2004; Herler et al., 2011). Nonetheless, predation still imposes an intense and constant threat regardless of these traits

(Brandl et al., 2018; Goldsworthy et al., 2022). Moreover, while these traits may have advantages, it may not be the underlying cause of their evolution. Body colourations of other ecologically similar CRFs are not always red/orange (Winterbottom, 2019), and elongated body structures and paddle shaped caudal fins are common in many fishes (Claverie & Wainwright, 2014; Mihalitsis & Bellwood, 2019). Evolutionary adaptations are often multifaceted and elusive without concrete experimental evidence.

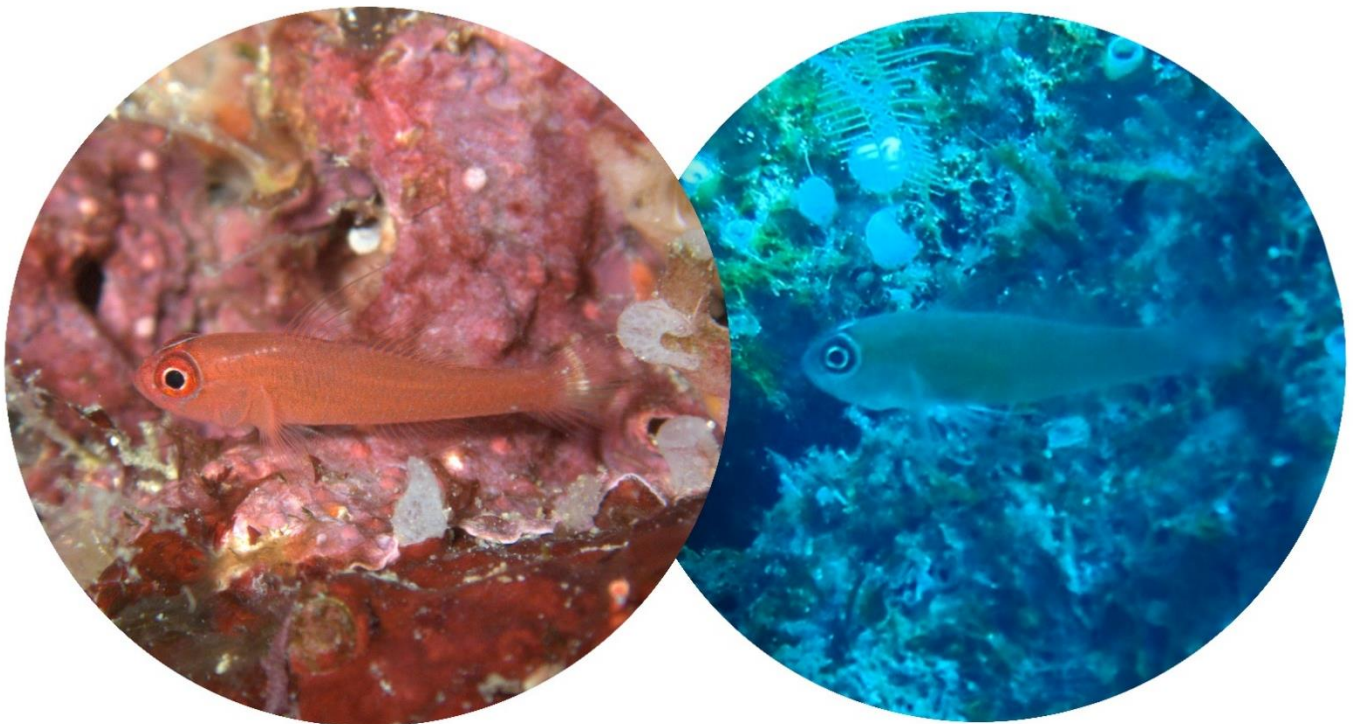


Figure 5.5: Conceptual image of *T. benjamini in situ* displaying how body colour can assist with crypsis by camouflage with the substratum (right), or at depths (9 m, left) where low frequency and long wavelength colours are filtered.

Stomach content analysis, while a valuable tool in understanding the dietary composition of fishes, has its limitations. One significant challenge is the occurrences of unidentifiable material within stomach contents, often in the form of heavily digested or fragmented items, which makes it difficult to precisely identify these items in the diet (Bierwagen et al., 2018; Sagar et al., 2019). DNA metabarcoding has the potential to address

this issue by providing more detailed genetic information on such items (Brandl, Casey, et al., 2020; Casey *et al.*, 2019), however a detailed DNA library is not yet available for use in Kimbe Bay. Additionally, stomach content analysis tends to be biased toward recently consumed food items. To mitigate these limitations, future research avenues could explore stable isotopes of both these fishes and end-members, which has lower resolution but offers insights into dietary assimilation over a more extended period, providing a more comprehensive understanding of an organism's diet when used alongside stomach content analysis (Bierwagen et al., 2018; Cocheret de la Moriniere *et al.*, 2003; Eurich et al., 2019).

The trophic dynamics of the *Trimma* species examined suggests significance as both micro-predators and potential prey for other animals within the reef ecosystem. These fishes likely contribute to the "wall of mouths," which captures incoming plankton and thus facilitates the influx of energy onto the reef (Clarke, 1999; Hamner et al., 1988). Notably, the small body size of *Trimma* positions them as possible prey for various piscivorous reef fishes (Goatley & Bellwood, 2016), thereby highlighting their potential to channel assimilated energy to higher trophic levels (Brandl et al., 2018). *Trimma* trophic dynamics in combination with high abundances on Indo-Pacific coral reefs (Winterbottom, 2019), continuous growth patterns (Goldsworthy, unpublished data; Winterbottom et al., 2011), efficient reproductive methods (Goldsworthy et al., 2022), and rapid generational turnover rates (Goldsworthy, unpublished data), may emerge them as a productive and replenishing source of nutrition for consumers. Nonetheless, further exploration is required to confirm the ecological function of *Trimma*. I suggest a Stable Isotope Analysis of prey end-members of *Trimma* from nearshore and offshore sources, a dietary analysis of potential predators of *Trimma* via stable isotope or DNA metabarcoding in combination with gut contents, and quantification of productivity within the genus (Brandl, Casey, et al., 2020; Morais & Bellwood, 2020; Winterbottom, 2019). Such studies could unveil the extent to which *Trimma* facilitate energy assimilation from the

plankton and its subsequent transfer to other organisms, ultimately determining the ecological roles and significance of the genus *Trimma* within coral reef ecosystems.

## Chapter 6: Conclusions and Future Directions

---

In my research, I have delved into the fundamental ecology and life history of the genus *Trimma*, identifying key components of their habitat, reproduction, growth, and trophic dynamics. The overarching aim of **Chapter 2** was to answer the question: *How do ecologically similar Trimma species partition habitats and does this occur at small spatial scales?* To summarise the main results of this chapter, separation of habitats occurred on broad spatial scales, with variation in distributions according to factors reef location, aspect, and depth. Coexistence was observed in many quadrats, but microhabitat differences minimized overlap, resulting in spatial separation on fine scales and rare interactions among *Trimma* species. Such spatial separation can allow for the coexistence of multiple ecologically similar species, potentially contributing to the exceptional local diversity within the genus.

**Chapter 3** aimed to answer: *What life history constraints and reproductive strategies do Trimma have?* In this chapter, I illustrated that the *Trimma* species were small-bodied, had short lifespans, and faced high daily mortality rates. The pelagic larval phase and juvenile phase comprised a significant portion of the maximum lifespan, leaving a short window available for reproduction. All mature individuals exhibited bidirectional sex change, with bisexual gonads. These findings shed light on the life history challenges *Trimma* face and how such reproductive strategies are beneficial for fishes with high mortality rates and short reproductive lifespans.

**Chapter 4** asked: *What are the larval, juvenile, and adult growth patterns, and generational turnover rates of Trimma?* Here, I demonstrated that growth was fastest in the larval phase, decreased in the juvenile stage, and slowed further in the adult phase, though growth differences among life history stages were small compared to the patterns seen in larger fishes. In addition, their short lifespans were coupled with high generational turnover rates.

Finally, the aim of **Chapter 5** was to answer the question: *What are the food items consumed, food origin, feeding methods, and predation pressures of Trimma? Do Trimma possess morphological traits that may assist feeding or predator avoidance?* I demonstrated *Trimma*'s ability to consume microscopic and planktonic food at a rapid rate and highlighted their position as potential prey for other reef-dwellers. The eye and gape morphology that *Trimma* possess may be beneficial for their feeding methods, while their cryptic colours, elongated body, and paddle shaped tails may be beneficial to evade predators.

Collectively, these findings suggest that *Trimma* is a potentially ecologically important group on Indo-Pacific coral reefs. The continuous growth, efficient reproduction, and short lifespans, paired with extreme natural mortality of *Trimma* result in exceptionally high population regeneration rates. When coupled with the high abundance of *Trimma* on coral reefs of the Indo-Pacific (Winterbottom, 2019), this likely contributes to substantial energy productivity over time (Brandl et al., 2019; Depczynski et al., 2007; Morais & Bellwood, 2019). Moreover, *Trimma* may play central ecological roles in importing energy and nutrients from the pelagic environment and its transfer to other reef organisms (Brandl et al., 2018; Depczynski & Bellwood, 2003; Goatley et al., 2017). All of these traits could be related to their small body size (Depczynski & Bellwood, 2006). There is increasing recognition of the functional roles of small-bodied CRFs in coral reef ecosystems, with CRFs constituting 60% of consumed fish biomass (Brandl et al., 2019). In the Indo-Pacific, the genus *Trimma* could make up a substantial proportion of this consumed biomass, as they are a dominant CRF in this area (Winterbottom, 2019). These contributions, which were not considered in the past, could have significant implications for the conservation and management of present and future coral reefs (Ackerman & Bellwood, 2000; Brandl et al., 2019; Winterbottom, 2019).



Despite representing a dominant and speciose genus, the ecological aspects of *Trimma*, beyond mating systems and sex change, have been relatively underexplored in existing literature (Winterbottom, 2019). Understanding features of *Trimma* ecology and life history, as demonstrated in this thesis, marks an essential step towards assessing their present and future ecological significance. Nevertheless, further quantification of *Trimma* ecology is imperative to grasp their niches and roles in an ecosystem and there are limitations to the present data. An initial limitation involves the unique challenges of studying CRFs, due to their small body size and cryptic nature. Standard underwater visual census methods regularly have low detectability of CRFs, potentially leading to an underestimation of their abundance and diversity (Ackerman & Bellwood, 2000). While I ensured that additional measures were made to minimize such biases, the abundance of fishes in the smaller size classes may have been underestimated. Furthermore, static mortality calculations used in this study, although widely employed for CRFs throughout the literature (Hernaman & Munday, 2005b; Winterbottom et al., 2011), remain estimates and likely vary across life history stages. Future research should investigate how mortality impacts CRFs throughout their life stages, particularly considering the exponential decrease in mortality after settlement as fishes learn to avoid predators (Goatley & Bellwood, 2016). This is a gap in the literature that is seldom addressed but could have wider implications for population dynamics. Understanding the ecological niche of *Trimma* species in Kimbe Bay requires more information on population dynamics, including individual reproductive success, spawning season, spawning interval, number of eggs per spawning bout, sex ratio, mating system, and timing and number of juvenile settlements. It is important to examine both population dynamics and community structure surrounding *Trimma* to comprehensively understanding their ecological roles.

In addition, I propose that future research should focus on furthering investigations into the trophodynamics of *Trimma*. Firstly, conducting stable isotope analysis on multiple *Trimma*

species across various regions of the Indo-Pacific could enhance insights into their trophodynamics (Winterbottom, 2019). Carbon and Nitrogen stable isotopes are being increasingly used in ecological studies. Although low resolution, it can assist with discerning broad groups of food items, trophic position, and the origins of food items, such as benthic versus pelagic and inshore versus offshore (Cocheret de la Moriniere et al., 2003; Eurich et al., 2019). For *Trimma*, examining isotope ratios of plankton samples from various nearshore and offshore sources, as well as assessing benthic invertebrates that migrate into the water column, can help determine whether the plankton consumed by *Trimma* originates from local or offshore sources. Such an investigation could shed light on whether *Trimma* species function as net importers of energy and nutrients onto the reef or contribute to nutrient recycling localised within the reef ecosystem (Winterbottom, 2019).

A future productivity study could quantify how much energy *Trimma* is contributing to reef ecosystems. There is increasing recognition that biomass is not adequate for measuring productivity as it disregards important life history characteristics (Morais & Bellwood, 2019, 2020; terHorst & Munguia, 2008). Morais and Bellwood (2020) developed a leading method for estimating productivity that incorporates both field data and life history characteristics. They have also provided an R package *rfishprod* that incorporates features for performing all calculations, predicting essential life-history information for fishes, or retrieving such data from FishBase if required. Productivity assessments for *Trimma* could be conducted at both healthy and degraded reef environments. This could emulate shifts in community composition and population levels that may result from habitat alterations associated with climate change (Morais & Bellwood, 2019).

Moreover, it may be beneficial to include larval dynamics in productivity quantifications. The dynamics of CRF larvae may contribute to coral reefs energy demands via

the extensive inputs of larval fishes from the pelagic environment (Brandl et al., 2019). The larval input from CRFs significantly surmounts larger reef fish larvae at nearshore reefs, which can be attributed to a high abundance of CRF adults, their success in converting gametes into larvae, and the retention of larvae close to natal reefs (Ackerman & Bellwood, 2000; Brandl et al., 2019; Galland et al., 2017). Their larval dynamics may contribute to the high levels of biomass produced by CRFs (Brandl et al., 2019). In addition, larval fish may supply extensive amounts of essential nutrients (carbon, nitrogen and phosphorous) to the reef, and can bolster productivity levels (Allgeier *et al.*, 2018). Yet, the dynamics of *Trimma* larvae, aside from larval growth examined in this thesis, is currently unknown and presents research challenges (Hogan *et al.*, 2017; Vigliola & Meekan, 2009). Nonetheless, as *Trimma* abundances are high on Indo-Pacific coral reefs (Winterbottom, 2019), it would be interesting to investigate their larval dynamics. Such information could be used to provide holistic estimates of productivity by including all life history stages (Brandl et al., 2019; Shima et al., 2021).

The final research suggestion I have concerns the involvement of *Trimma* in energy transfer to higher trophic levels via predation. Evidence suggesting that *Trimma* is subjected to predation arises from their elevated mortality rates, anti-predator behaviours, and the consumption of similar species in controlled aquaria settings (Goatley et al., 2017; Goldsworthy et al., 2022; Winterbottom et al., 2011). Accordingly, since direct predation was not observed in my research, conducting a comprehensive dietary investigation is warranted. It would be beneficial to include both a stomach content and stable isotope analysis on piscivorous species that roam the reef walls, which could determine if *Trimma* is being ingested and the specific species that are consuming them (Bierwagen et al., 2018; Eurich et al., 2019). This could be supplemented with diver or video observations of predation during nocturnal and crepuscular activity periods, which are times when many predators are most active (Bosiger & McCormick, 2014; Danilowicz & Sale, 1999; Shoji et al., 2017).

The multifaceted approach to study the trophodynamics of *Trimma* suggested here has potential to yield significant results. It has the capacity to quantify the overall energy production of *Trimma*, whether said energy is gained from offshore sources or recycled from local sources on the reef, and the extent of energy transfer to higher trophic levels (Brandl et al., 2018; Winterbottom, 2019). This research could clarify the connection between the ecology and life history traits of *Trimma*, as outlined in this thesis, and elucidate the functional significance of these fishes within coral reef ecosystems (Bierwagen et al., 2018).

Looking ahead, the ecological significance of the genus *Trimma* may increase with climate change. With their short generation times, CRFs like *Trimma* may possess a unique ability to adapt quickly to rising ocean temperatures (Munday et al., 2017). Moreover, a combination of both natural and anthropogenic environmental changes is causing the loss of Scleractinia corals, which drastically alters fish community structure and habitat complexity (Hoegh-Guldberg et al., 2007; Hughes et al., 2017; Jones et al., 2004). Given that many CRFs exhibit a high selectivity for corals, the loss or reduction of these habitats puts a substantial portion of CRF diversity at risk, which could have drastic ecological consequences (Bellwood et al., 2006; Brandl et al., 2018; Doll et al., 2021; Munday, 2004). On a brighter note, *Trimma* predominantly inhabit non-living coral rock. Intricate spatial partitioning in the genus may enable them to sustain high diversity in these non-coral habitats, and accordingly, they may be largely robust to climate-related habitat alterations (Tornabene et al., 2013). Consequently, the ecological roles of hard substrata-associated genera like *Trimma* may gain further importance with the evolving landscapes of coral reefs.

After spending a very long time contemplating three small fish species and exploring their incredible quirks, it has left me wondering about other animals that are small, and as a consequence, overlooked. *Trimma* is emblematic of a broader issue encompassing small

species being underrepresented, understudied, and undervalued in both the scientific community and everyday society. We as humans tend to favour the larger, more visually appealing, and charismatic members of the animal kingdom, inadvertently failing to notice the less conspicuous. It has become evident that studying these small species presents substantial challenges, as they tend to be cryptic, frustrating, and difficult to secure research funding for. However, this journey has proven immensely rewarding, exposing unique and intriguing findings at every turn. I now find myself seeking out and celebrating the underdogs of the animal kingdom, from tiny insects to little brown skinks. Great things indeed come in small packages, and their worthiness of our attention and effort cannot be overstated.

## References

---

- Ackerman, J. L., & Bellwood, D. R. (2000). Reef fish assemblages: A re-evaluation using enclosed rotenone stations. *MARINE ECOLOGY PROGRESS SERIES*, 206, 227-237. <https://doi.org/10.3354/meps206227>
- Ahmadia, G. N., Tornabene, L., Smith, D. J., & Pezold, F. L. (2018). The relative importance of regional, local, and evolutionary factors structuring cryptobenthic coral-reef assemblages. *CORAL REEFS*, 37, 279-293. <https://doi.org/10.1007/s00338-018-1657-2>
- Alfaro, M. E., Santini, F., & Brock, C. D. (2007). Do reefs drive diversification in marine Teleosts? Evidence from the pufferfishes and their allies (order Tetraodontiformes). *EVOLUTION*, 61(9), 2104-2126. <https://doi.org/10.1111/j.1558-5646.2007.00182.x>
- Allgeier, J. E., Speare, K. E., & Burkepile, D. E. (2018). Estimates of fish and coral larvae as nutrient subsidies to coral reef ecosystems. *ECOSPHERE*, 9(6), 1-10. <https://doi.org/10.1002/ecs2.2216>
- Almany, G. R., & Webster, M. S. (2006). The predation gauntlet: Early post-settlement mortality in reef fishes. *CORAL REEFS*, 25, 19-22. <https://doi.org/10.1007/s00338-005-0044-y>
- Anderson, J. T. (1988). A review of size dependant survival during pre-recruit stages of fishes in relation to recruitment. *JOURNAL OF NORTHWEST ATLANTIC FISHERY SCIENCE*, 8, 55-56.
- Andrews, A. H., Choat, J. H., Hamilton, R. J., & DeMartini, E. E. (2015). Refined bomb radiocarbon dating of two iconic fishes of the Great Barrier Reef. *MARINE AND FRESHWATER RESEARCH*, 66, 305- 316. <https://doi.org/10.1071/MF14086>
- Antle, C., Klimko, L., & Harkness, W. (1970). Confidence intervals for the parameters of the logistic distribution. *BIOMETRIKA*, 57(2), 397-402. <https://doi.org/10.1093/biomet/57.2.397>
- Arias-González, J. E., Done, T. J., Page, C. A., Cheal, A. J., Kininmonth, S., & Garza-Pérez, J. R. (2006). Towards a reefscape ecology: Relating biomass and trophic structure of

- fish assemblages to habitat at Davies Reef, Australia. *MARINE ECOLOGY PROGRESS SERIES*, 320, 29-41. <https://doi.org/10.3354/meps320029>
- Audzijonyte, A., & Richards, S. A. (2018). The energetic cost of reproduction and its effect on optimal life-history strategies. *THE AMERICAN NATURALIST*, 192(4), 150-162. <https://doi.org/10.1086/698655>
- Balaban-Feld, J., Mitchell, W. A., Kotler, B. P., Vijayan, S., Elem, L. T. T., Rosenzweig, M. L., & Abramsky, Z. (2019). Individual willingness to leave a safe refuge and the trade-off between food and safety: a test with social fish. *PROCEEDINGS OF THE ROYAL SOCIETY B*, 286(1907), 1-7. <https://doi.org/http://dx.doi.org/10.1098/rspb.2019.0826>
- Barneche, D. R., Allen, A. P., & Mumby, P. (2018). The energetics of fish growth and how it constrains food-web trophic structure. *ECOLOGY LETTERS*, 21(6), 836-844. <https://doi.org/10.1111/ele.12947>
- Beeken, N. S., Selwyn, J. D., & Hogan, J. D. (2021). Determining the life history strategy of the cryptobenthic reef gobies *Coryphopterus hyalinus* and *C. personatus*. *MARINE ECOLOGY PROGRESS SERIES*, 659, 161-173. <https://doi.org/10.3354/meps13573>
- Bellwood, D. R., Goatley, C. H. R., & Bellwood, O. (2017). The evolution of fishes and corals on reefs: form, function and interdependence. *BIOLOGICAL REVIEWS OF THE CAMBRIDGE PHILOSOPHICAL SOCIETY*, 92, 878-901. <https://doi.org/10.1111/brv.12259>
- Bellwood, D. R., Hemingson, C. R., & Tebbett, S. B. (2020). Subconscious biases in coral reef fish studies. *BIOSCIENCE*, 70(7), 621-627. <https://doi.org/10.1093/biosci/biaa062>
- Bellwood, D. R., Hoey, A. S., Ackerman, J. L., & Depczynski, M. (2006). Coral bleaching, reef fish community phase shifts and the resilience of coral reefs. *GLOBAL CHANGE BIOLOGY*, 12(9), 1587-1594. <https://doi.org/10.1111/j.1365-2486.2006.01204.x>
- Bellwood, D. R., Hoey, A. S., & Choat, J. H. (2003). Limited functional redundancy in high diversity systems: Resilience and ecosystem function on coral reefs. *ECOLOGY LETTERS*, 6(4), 281-285. <https://doi.org/10.1046/j.1461-0248.2003.00432.x>

- Benvenuto, C., Coscia, I., Chopelet, J., Sala-Bozano, M., & Mariani, S. (2017). Ecological and evolutionary consequences of alternative sex-change pathways in fish. *SCIENTIFIC REPORTS*, 7(9084), 1-12. <https://doi.org/10.1038/s41598-017-09298-8>
- Bergenius, M. A. J., Meekan, M. G., Robertson, D. R., & McCormick, M. I. (2002). Larval growth predicts the recruitment success of a coral reef fish. *OECOLOGIA*, 131, 521-525. <https://doi.org/10.1007/s00442-002-0918-4>
- Bernardo, J. (1993). Determinants of maturation in animals. *TRENDS IN ECOLOGY & EVOLUTION*, 8(5), 166-173. [https://doi.org/10.1016/0169-5347\(93\)90142-C](https://doi.org/10.1016/0169-5347(93)90142-C)
- Berrar, D. (2018). Cross-Validation. In *ENCYCLOPEDIA OF BIOINFORMATICS AND COMPUTATIONAL BIOLOGY* (Vol. 1, pp. 542–545). Elsevier. <https://doi.org/10.1016/B978-0-12-809633-8.20349-X>
- Bhandari, R. K., Komuro, H., Nakamura, S., Higa, M., & Nakamura, M. (2003). Gonadal restructuring and correlative steroid hormone profiles during natural sex change in protogynous honeycomb grouper (*Epinephelus merra*). *ZOOLOGICAL SCIENCE*, 20, 1399-1404. <https://doi.org/10.2108/zsj.20.1399>
- Bierwagen, S. L., Heupel, M. R., Chin, A., & Simpfendorfer, C. A. (2018). Trophodynamics as a tool for understanding coral reef ecosystems. *FRONTIERS IN MARINE SCIENCE*, 5(24), 1-13. <https://doi.org/10.3389/fmars.2018.00024>
- Blanckenhorn, W. U. (2000). The evolution of body size: what keeps organisms small? *THE QUARTERLY REVIEW OF BIOLOGY*, 75(4), 385-407. <https://doi.org/10.1086/393620>
- Böhm, T., & Hoeksema, B. W. (2017). Habitat selection of the coral-dwelling spinyhead blenny, *Acanthemblemaria spinosa*, at Curaçao, Dutch Caribbean. *MARINE BIODIVERSITY*, 47(1), 17-25. <https://doi.org/10.1007/s12526-016-0543-9>
- Bonin, M. C., Boström-Einarsson, L., Munday, P. L., & Jones, G. P. (2015). The prevalence and importance of competition among coral reef fishes. *ANNUAL REVIEW OF ECOLOGY AND SYSTEMATICS*, 46(1), 169-190. <https://doi.org/10.1146/annurev-ecolsys-112414-054413>



- Borgstein, N., Beltrán, D. M., & Prada, C. (2020). Variable growth across species and life stages in Caribbean reef Octocorals. *FRONTIERS IN MARINE SCIENCE*, 7(483), 1-11. <https://doi.org/10.3389/fmars.2020.00483>
- Bosiger, Y. J., & McCormick, M. I. (2014). Temporal links in daily activity patterns between coral reef predators and their prey. *PLOS ONE*, 9(10), 1-11. <https://doi.org/10.1371/journal.pone.0111723>
- Brandl, S. J., Casey, J. M., & Meyer, C. P. (2020). Dietary and habitat niche partitioning in congeneric cryptobenthic reef fish species. *CORAL REEFS*, 39(2), 305-317. <https://doi.org/10.1007/s00338-020-01892-z>
- Brandl, S. J., Goatley, C. H. R., Bellwood, D. R., & Tornabene, L. (2018). The hidden half: ecology and evolution of cryptobenthic fishes on coral reefs. *BIOLOGICAL REVIEWS*, 93, 1846-1873. <https://doi.org/10.1111/brv.12423>
- Brandl, S. J., Johansen, J. L., Casey, J. M., Tornabene, L., Morais, R. A., & Burt, J. A. (2020). Extreme environmental conditions reduce coral reef fish biodiversity and productivity. *NATURE COMMUNICATIONS*, 11, 1-14. <https://doi.org/10.1038/s41467-020-17731-2>
- Brandl, S. J., Tornabene, L., Goatley, C. H. R., Casey, J. M., Morais, R. A., Côté, I. M., Baldwin, C. C., Parravicini, V., Schiettekatte, N. M. D., & Bellwood, D. R. (2019). Demographic dynamics of the smallest marine vertebrates fuel coral reef ecosystem functioning. *SCIENCE*, 364, 1189-1192. <https://doi.org/10.1126/science.aav3384>
- Brokovich, E., Baranes, A., & Goren, M. (2006). Habitat structure determines coral reef fish assemblages at the northern tip of the Red Sea. *ECOLOGICAL INDICATORS*, 6(3), 494-507. <https://doi.org/10.1016/j.ecolind.2005.07.002>
- Brokovich, E., Einbinder, S., Shashar, N., Kiflawi, M., & Kark, S. (2008). Descending to the twilight-zone: changes in coral reef fish assemblages along a depth gradient down to 65 m. *MARINE ECOLOGY PROGRESS SERIES*, 371, 253-262. <https://doi.org/10.3354/meps07591>
- Brooks, M. E., Kristensen, K., van Benthem, K. J., Magnusson, A., Berg, C. W., Nielsen, A., Skaug, H. J., Maechler, M., & Bolker, B. M. (2017). glmmTMB balances speed and

- flexibility among packages for zero-inflated generalized linear mixed modeling. *THE R JOURNAL*, 9(2), 378-400.
- Brown, J. H., Marquet, P. A., & Taper, M. L. (1993). Evolution of body size: consequences of an energetic definition of fitness. *THE AMERICAN NATURALIST*, 142(4), 573-584. <https://doi.org/10.1086/285558>
- Brown, J. S., Laundré, J. W., & Gurung, M. (1999). The ecology of fear: Optimal foraging, game theory, and trophic interactions. *JOURNAL OF MAMMALOGY*, 80(2), 385-399. <https://doi.org/10.2307/1383287>
- Bruno, J. F., Selig, E. R., Casey, K. S., Page, C. A., Willis, B. L., Harvell, C. D., Sweatman, H., & Melendy, A. M. (2007). Thermal stress and coral cover as drivers of coral disease outbreaks. *PLOS BIOLOGY*, 5(6). <https://doi.org/10.1371/journal.pbio.0050124>
- Calder, W. A. (1984). *SIZE, FUNCTION, AND LIFE HISTORY*. Harvard University Press.
- Campana, S. E. (1990). How reliable are growth back-calculations based on otoliths? *CANADIAN JOURNAL OF FISHERIES AND AQUATIC SCIENCES*, 47, 2219–2227.
- Casey, J. M., Meyer, C. P., Morat, F., Brandl, S. J., Planes, S., Parravicini, V., & Mahon, A. (2019). Reconstructing hyperdiverse food webs: Gut content metabarcoding as a tool to disentangle trophic interactions on coral reefs. *METHODS IN ECOLOGY AND EVOLUTION*, 10(8), 1157-1170. <https://doi.org/10.1111/2041-210X.13206>
- Catano, L. B., Rojas, M. C., Malossi, R. J., Peters, J. R., Heithaus, M. R., Fourqurean, J. W., & Burkepile, D. E. (2016). Reefscapes of fear: Predation risk and reef heterogeneity interact to shape herbivore foraging behaviour. *THE JOURNAL OF ANIMAL ECOLOGY*, 85(1), 146-156. <https://doi.org/10.1111/1365-2656.12440>
- Chang, C.-F., & Yueh, W.-S. (1990). Annual cycle of gonadal histology and steroid profiles in the juvenile males and adult females of the protandrous black porgy, *Acanthopagrus schlegeli*. *AQUACULTURE*, 91, 179-196. [https://doi.org/10.1016/0044-8486\(90\)90187-R](https://doi.org/10.1016/0044-8486(90)90187-R)
- Chapin III, F. S., Zavaleta, E. S., Eviner, V. T., Naylor, R. L., Vitousek, P. M., Reynolds, H. L., Hooper, D. U., Lavorel, S., Sala, O. E., Hobbie, S. E., Mack, M. C., & Díaz, S.

- (2000). Consequences of changing biodiversity. *NATURE*, 405(6783), 234-242.  
<https://doi.org/10.1038/35012241>
- Chapman, D. G., & Robson, D. S. (1960). The analysis of a catch curve. *BIOMETRICS*, 16(3), 354-368. <https://doi.org/10.2307/2527687>
- Charnov, E. L., Turner, T. F., & Winemiller, K. O. (2001). Reproductive constraints and the evolution of life histories with indeterminate growth. *PROCEEDINGS OF THE NATIONAL ACADEMY OF SCIENCES*, 98, 9460-9464. <https://doi.org/10.1073/pnas.161294498>
- Chave, E. H. (1978). General ecology of six species of Hawaiian cardinalfishes. *PACIFIC SCIENCE* 32(3).
- Chesson, P. (2000). Mechanisms of maintenance of species diversity. *ANNUAL REVIEW OF ECOLOGY AND SYSTEMATICS*, 31, 343-366.  
<https://doi.org/10.1146/annurev.ecolsys.31.1.343>
- China, V., & Holzman, R. (2014). Hydrodynamic starvation in first-feeding larval fishes. *PROCEEDINGS OF THE NATIONAL ACADEMY OF SCIENCES*, 111(22), 8083-8088.  
<https://doi.org/10.1073/pnas.1323205111>
- Choat, J. H., Robbins, W. D., & Clements, K. D. (2004). The trophic status of herbivorous fishes on coral reefs: II. Food processing modes and trophodynamics. *MARINE BIOLOGY*, 145(3), 445-454. <https://doi.org/10.1007/s00227-004-1341-7>
- Choat, J. H., & Robertson, D. R. (2002). Age-based studies. In P. F. Sale (Ed.), *CORAL REEF FISHES : DYNAMICS AND DIVERSITY IN A COMPLEX ECOSYSTEM* (pp. 57-80).
- Clarke, R. D. (1989). Population fluctuation, competition and microhabitat distribution of two species of tube blennies, *Acanthemblemaria* (Teleostei: Chaenopsidae). *BULLETIN OF MARINE SCIENCE*, 44(3), 1174-1185.
- Clarke, R. D. (1994). Habitat partitioning by Chaenopsid Blennies in Belize and the Virgin Islands. *COPEIA*, 1994(2), 398-405. <https://doi.org/10.2307/1446987>

- Clarke, R. D. (1999). Diets and metabolic rates of four Caribbean tube blennies, genus *Acanthemblemaria* (Teleostei: Chaenopsidae). *BULLETIN OF MARINE SCIENCE*, 65(1), 185-199.
- Claverie, T., & Wainwright, P. C. (2014). A morphospace for reef fishes: Elongation is the dominant axis of body shape evolution. *PLOS ONE*, 9(11), 1-11.  
<https://doi.org/10.1371/journal.pone.0112732>
- Cocheret de la Moriniere, E., Pollux, B. A. J., Nagelkerken, I. A., & van der Velde, G. (2003). Ontogenetic dietary changes of coral reef fishes in the mangrove-seagrass-reef continuum: stable isotopes and gut-content analysis. *MARINE ECOLOGY PROGRESS SERIES*, 246, 279-289. <https://doi.org/10.3354/meps246279>
- Cole, K. S. (1990). Patterns of gonad structure in hermaphroditic gobies (Teleostei Gobiidae). *ENVIRONMENTAL BIOLOGY OF FISHES*, 28, 125-142.  
<https://doi.org/10.1007/BF00751032>
- Connell, J. H. (1978). Diversity in tropical rain forests and coral reefs. *SCIENCE*, 199(4335), 1302-1310. <https://doi.org/10.1126/science.199.4335.1302>
- Connell, J. H. (1983). On the prevalence and relative importance of interspecific competition: Evidence from field experiments. *THE AMERICAN NATURALIST*, 122(5), 661-696.  
<https://doi.org/10.1086/284165>
- Danilowicz, B. S., & Sale, P. F. (1999). Relative intensity of predation on the French grunt, *Haemulon flavolineatum*, during diurnal, dusk, and nocturnal periods on a coral reef. *MARINE BIOLOGY*, 133(2), 337-343. <https://doi.org/10.1007/s002270050472>
- de Goeij, J. M., van Oevelen, D., Vermeij, M. J. A., Osinga, R., Middelburg, J. J., de Goeij, A. F. P. M., & Admiraal, W. (2013). Surviving in a marine desert: The sponge loop retains resources within coral reefs. *SCIENCE*, 342(6154), 108-110.  
<https://doi.org/10.1126/science.1241981>
- Depczynski, M., & Bellwood, D. (2006). Extremes, plasticity, and invariance in vertebrate life history traits: insights from coral reef fishes. *ECOLOGY*, 87(12), 3119-3127.  
[https://doi.org/10.1890/0012-9658\(2006\)87\[3119:EPPIV\]2.0.CO;2](https://doi.org/10.1890/0012-9658(2006)87[3119:EPPIV]2.0.CO;2)

- Depczynski, M., & Bellwood, D. R. (2003). The role of cryptobenthic reef fishes in coral reef trophodynamics. *MARINE ECOLOGY PROGRESS SERIES*, 256, 183-191. <https://doi.org/10.3354/meps256183>
- Depczynski, M., & Bellwood, D. R. (2004). Microhabitat utilisation patterns in cryptobenthic coral reef fish communities. *MARINE BIOLOGY*, 145(3), 455-463. <https://doi.org/10.1007/s00227-004-1342-6>
- Depczynski, M., & Bellwood, D. R. (2005a). Shortest recorded vertebrate lifespan found in a coral reef fish. *CURRENT BIOLOGY*, 15(8), 288-289. <https://doi.org/10.1016/j.cub.2005.04.016>
- Depczynski, M., & Bellwood, D. R. (2005b). Wave energy and spatial variability in community structure of small cryptic coral reef fishes. *MARINE ECOLOGY PROGRESS SERIES*, 303, 283-293. <https://doi.org/10.3354/meps303283>
- Depczynski, M., Fulton, C., Marnane, M. J., & Bellwood, D. R. (2007). Life history patterns shape energy allocation among fishes on coral reefs. *OECOLOGIA*, 153, 111-120. <https://doi.org/10.1007/s00442-007-0714-2>
- Dirnwöber, M., & Herler, J. (2007). Microhabitat specialisation and ecological consequences for coral gobies of the genus *Gobiodon* in the Gulf of Aqaba, northern Red Sea. *MARINE ECOLOGY PROGRESS SERIES*, 342, 265-275. <https://doi.org/10.3354/meps342265>
- Doherty, P. J., Dufour, V., Galzin, R., Hixon, M. A., Meekan, M. G., & Planes, S. (2004). High mortality during settlement is a population bottleneck for a tropical surgeonfish. *ECOLOGY*, 85(9), 2422-2428. <https://doi.org/10.1890/04-0366>
- Doll, P. C., Munday, P. L., Bonin, M. C., & Jones, G. P. (2021). Habitat specialisation and overlap in coral reef gobies of the genus *Eviota* (Teleostei: Gobiidae). *MARINE ECOLOGY PROGRESS SERIES*, 677, 81-94.
- Dunn, A., Francis, R. I. C. C., & Doonan, I. J. (2002). Comparison of the Chapman–Robson and regression estimators of  $Z$  from catch-curve data when non-sampling stochastic error is present. *FISHERIES RESEARCH*, 59, 149-159. [https://doi.org/10.1016/S0165-7836\(01\)00407-6](https://doi.org/10.1016/S0165-7836(01)00407-6)

- Emery, A. R. (1968). Preliminary observations on coral reef plankton. *LIMNOLOGY AND OCEANOGRAPHY*, 13(2), 293-303.
- Eurich, J. G. (2018). *Processes underlying the fine-scale partitioning and niche diversification in a guild of coral reef damselfishes* James Cook University].
- Eurich, J. G., Matley, J. K., Baker, R., McCormick, M. I., & Jones, G. P. (2019). Stable isotope analysis reveals trophic diversity and partitioning in territorial damselfishes on a low-latitude coral reef. *MARINE BIOLOGY*, 166(2), 1-14.  
<https://doi.org/10.1007/s00227-018-3463-3>
- Eurich, J. G., McCormick, M. I., & Jones, G. P. (2018). Habitat selection and aggression as determinants of fine-scale partitioning of coral reef zones in a guild of territorial damselfishes. *MARINE ECOLOGY PROGRESS SERIES* 587, 201-215. <https://doi.org/10.3354/meps12458>
- Fabricius, K. E. (2005). Effects of terrestrial runoff on the ecology of corals and coral reefs; review and synthesis. *MARINE POLLUTION BULLETIN*, 50(2), 125-146.  
<https://doi.org/10.1016/j.marpolbul.2004.11.028>
- Fisher, D. O., Dickman, C. R., Jones, M. E., & Blomberg, S. P. (2013). Sperm competition drives the evolution of suicidal reproduction in mammals. *PROCEEDINGS OF THE NATIONAL ACADEMY OF SCIENCES* 110(44), 17910-17914.  
<https://doi.org/10.1073/pnas.1310691110>
- Fox, R. J., Sunderland, T. L., Hoey, A. S., & Bellwood, D. R. (2009). Estimating ecosystem function: contrasting roles of closely related herbivorous rabbitfishes (Siganidae) on coral reefs. *MARINE ECOLOGY PROGRESS SERIES* 385, 261-269. <https://doi.org/10.3354/meps08059>
- Francis, R. I. C. C. (1990). Back-calculation of fish length: a critical review. *JOURNAL OF FISH BIOLOGY*, 36(6), 883-902. <https://doi.org/10.1111/j.1095-8649.1990.tb05636.x>
- Friedman, S., Price, S., Corn, K., Larouche, O., Martinez, C., & Wainwright, P. (2020). Body shape diversification along the benthic–pelagic axis in marine fishes. *PROCEEDINGS OF THE ROYAL SOCIETY B*, 287(1931), 20201053.

- Fu, S., Zeng, L., Li, X., Pang, X., Cao, Z., Peng, J., & Wang, Y. (2009). The behavioural, digestive and metabolic characteristics of fishes with different foraging strategies. *JOURNAL OF EXPERIMENTAL BIOLOGY*, 212(14), 2296-2302. <https://doi.org/10.1242/jeb.027102>
- Fukuda, K., Manabe, H., Sakurai, M., Dewa, S.-i., Shinomiya, A., & Sunobe, T. (2017). Monogamous mating system and sexuality in the gobiid fish, *Trimma marinae* (Actinopterygii: Gobiidae). *JOURNAL OF ETHOLOGY*, 35(1), 121-130. <https://doi.org/10.1007/s10164-016-0499-z>
- Fukuda, K., & Sunobe, T. (2020). Group structure and putative mating system of three hermaphrodite gobiid fish, *Priolepis akihittoi*, *Trimma emeryi*, and *Trimma hayashii* (Actinopterygii: Gobiiformes). *ICHTHYOLOGICAL RESEARCH*, 67, 552–558. <https://doi.org/10.1007/s10228-020-00750-w>
- Fukuda, K., Tanazawa, T., & Sunobe, T. (2017). Polygynous mating system and field evidence for bidirectional sex change in the gobiid fish *Trimma grammistes*. *INTERNATIONAL JOURNAL OF PURE AND APPLIED ZOOLOGY*, 5(3), 92-99.
- Fulton, C. J., & Bellwood, D. R. (2005). Wave-Induced water motion and the functional implications for coral reef fish assemblages. *LIMNOLOGY AND OCEANOGRAPHY*, 50(1), 255-264. <https://doi.org/10.4319/lo.2005.50.1.0255>
- Galland, G. R., Erisman, B., Aburto-Oropeza, O., & Hastings, P. A. (2017). Contribution of cryptobenthic fishes to estimating community dynamics of sub-tropical reefs. *MARINE ECOLOGY PROGRESS SERIES*, 584, 175-184. <https://doi.org/10.3354/meps12364>
- Gardiner, N. M., & Jones, G. P. (2005). Habitat specialisation and overlap in a guild of coral reef cardinalfishes (Apogonidae). *MARINE ECOLOGY PROGRESS SERIES* 305, 163-175. <https://doi.org/10.3354/meps305163>
- Gause, G. F. (1934). *STRUGGLE FOR EXISTENCE*. Williams and Wilkins Company.
- Gaynor, K. M., Brown, J. S., Middleton, A. D., Power, M. E., & Brashares, J. S. (2019). Landscapes of fear: Spatial patterns of risk perception and response. *TRENDS IN ECOLOGY & EVOLUTION*, 34(4), 355-368. <https://doi.org/10.1016/j.tree.2019.01.004>



- Ghiselin, M. T. (1969). The evolution of hermaphroditism among animals. *THE QUARTERLY REVIEW OF BIOLOGY*, 44(2), 189-208. <https://doi.org/10.1086/406066>
- Glavicic, I., Paliska, D., Soldo, A., & Kovacic, M. (2016). A quantitative assessment of the cryptobenthic fish assemblage at deep littoral cliffs in the Mediterranean. *SCIENTIA MARINA*, 80(3), 329-337. <https://doi.org/10.3989/scimar.04307.23A>
- Goatley, C. H. R., & Bellwood, D. R. (2009). Morphological structure in a reef fish assemblage. *CORAL REEFS*, 28, 449-457. <https://doi.org/10.1007/s00338-009-0477-9>
- Goatley, C. H. R., & Bellwood, D. R. (2016). Body size and mortality rates in coral reef fishes: a three-phase relationship. *PROCEEDINGS OF THE ROYAL SOCIETY B*, 283(1841), 1-6. <https://doi.org/10.1098/rspb.2016.1858>
- Goatley, C. H. R., & Brandl, S. J. (2017). Cryptobenthic reef fishes. *CURRENT BIOLOGY*, 27(11), 452-454. <https://doi.org/10.1016/j.cub.2017.03.051>
- Goatley, C. H. R., González-Cabello, A., & Bellwood, D. R. (2016). Reef-scale partitioning of cryptobenthic fish assemblages across the Great Barrier Reef, Australia. *MARINE ECOLOGY PROGRESS SERIES*, 544, 271-280. <https://doi.org/10.3354/meps11614>
- Goatley, C. H. R., González-Cabello, A., & Bellwood, D. R. (2017). Small cryptopredators contribute to high predation rates on coral reefs. *CORAL REEFS*, 36, 207-212. <https://doi.org/10.1007/s00338-016-1521-1>
- Goldsworthy, N. C. (unpublished data).
- Goldsworthy, N. C., Srinivasan, M., Smallhorn-West, P., Cheah, L.-C., Munday, P. L., & Jones, G. P. (2022). Life-history constraints, short adult life span and reproductive strategies in coral reef gobies of the genus *Trimma*. *JOURNAL OF FISH BIOLOGY*. <https://doi.org/10.1111/jfb.15161>
- Green, B. S., Mapstone, B. D., Carlos, G., & Begg, G. A. (2009). Tropical fish otoliths: Information for assessment, management and ecology. In *REVIEWS: METHODS AND TECHNOLOGIES IN FISH BIOLOGY AND FISHERIES*. Springer Netherlands. <https://doi.org/10.1007/978-1-4020-5775-5>



- Greenfield, D. W., & Greenfield, T. A. (1982). Habitat and resource partitioning between two species of *Acanthemblemaria* (Pisces: Chaenopsidae), with comments on the chaos hypothesis. *SMITHSONIAN CONTRIBUTIONS TO THE MARINE SCIENCES*, 12, 499-507.
- Gwinn, D. C., Allen, M. S., & Rogers, M. W. (2010). Evaluation of procedures to reduce bias in fish growth parameter estimates resulting from size-selective sampling. *FISHERIES RESEARCH*, 105(2), 75-79. <https://doi.org/10.1016/j.fishres.2010.03.005>
- Hairston, N. G., & Hairston, N. G. (1993). Cause-effect relationships in energy flow, trophic structure, and interspecific interactions. *THE AMERICAN NATURALIST*, 142(3), 379-411. <https://doi.org/10.1086/285546>
- Hamner, Jones, Carleton, Hauri, & Williams, D. M. (1988). Zooplankton, planktivorous fish, and water currents on a windward reef face: Great Barrier Reef, Australia. *BULLETIN OF MARINE SCIENCE*, 42(3), 459-479.
- Hanken, J., & Wake, D. B. (1993). Miniaturization of body size: Organismal consequences and evolutionary significance. *ANNUAL REVIEW OF ECOLOGY AND SYSTEMATICS*, 24, 501-519. <https://doi.org/10.1146/annurev.es.24.110193.002441>
- Hartig, F. (2021). DHARMA: Residual diagnostics for hierarchical (multi-level/mixed) regression models. R package version 0.4.4. <https://CRAN.R-project.org/package=DHARMA>
- Helfman, G. S. (1989). Threat-sensitive predator avoidance in damselfish-trumpetfish interactions. *BEHAVIORAL ECOLOGY AND SOCIOBIOLOGY*, 24(1), 47-58. <https://doi.org/10.1007/BF00300117>
- Herler, J. (2007). Microhabitats and ecomorphology of coral- and coral rock-associated gobiid fish (Teleostei: Gobiidae) in the northern Red Sea. *MARINE ECOLOGY*, 28(1), 82-94. <https://doi.org/10.1111/j.1439-0485.2007.00165.x>
- Herler, J., Munday, P. L., & Hernaman, V. (2011). Gobies on coral reefs. In *THE BIOLOGY OF GOBIES* (pp. 493-529). Science Publishers.

- Hernaman, V., & Munday, P. L. (2005a). Life-history characteristics of coral reef gobies: I. Growth and life-span. *MARINE ECOLOGY PROGRESS SERIES*, 290, 207-221. <https://doi.org/10.3354/meps290207>
- Hernaman, V., & Munday, P. L. (2005b). Life-history characteristics of coral reef gobies: II. Mortality rate, mating system and timing of maturation. *MARINE ECOLOGY PROGRESS SERIES*, 290, 223-237. <https://doi.org/10.3354/meps290223>
- Hernaman, V., Munday, P. L., & Schläppy, M. L. (2000). Validation of otolith growth-increment periodicity in tropical gobies. *MARINE BIOLOGY*, 137, 715-726. <https://doi.org/10.1007/s002270000387>
- Hernaman, V., Probert, P. K., & Robbins, W. D. (2009). Trophic ecology of coral reef gobies: interspecific, ontogenetic, and seasonal comparison of diet and feeding intensity. *MARINE BIOLOGY*, 156(3), 317-330. <https://doi.org/10.1007/s00227-008-1085-x>
- Hoegh-Guldberg, O., Mumby, P. J., Knowlton, N., Eakin, C. M., Iglesias-Prieto, R., Muthiga, N., Bradbury, R. H., Dubi, A., Hatziolos, M. E., Hooten, A. J., Steneck, R. S., Greenfield, P., Gomez, E., Harvell, C. D., Sale, P. F., Edwards, A. J., & Caldeira, K. (2007). Coral reefs under rapid climate change and ocean acidification. *SCIENCE*, 318(5857), 1737-1742. <https://doi.org/10.1126/science.1152509>
- Hoegh-Guldberg, O., Pendleton, L., & Kaup, A. (2019). People and the changing nature of coral reefs. *REGIONAL STUDIES IN MARINE SCIENCE*, 30, 1-20. <https://doi.org/10.1016/j.rsma.2019.100699>
- Hoening, J. (1983). Empirical use of longevity data to estimate mortality rates. *FISHERY BULLETIN*, 81(1), 898-903.
- Hoey, A. S., & Bellwood, D. R. (2008). Cross-shelf variation in the role of parrotfishes on the Great Barrier Reef. *CORAL REEFS*, 27(1), 37-47. <https://doi.org/10.1007/s00338-007-0287-x>
- Hogan, J. D., Kozdon, R., Blum, M. J., Gilliam, J. F., Valley, J. W., & McIntyre, P. B. (2017). Reconstructing larval growth and habitat use in an amphidromous goby using

- otolith increments and microchemistry. *JOURNAL OF FISH BIOLOGY*, 90(4), 1338-1355. <https://doi.org/10.1111/jfb.13240>
- Hooper, D. U., Chapin, F. S., III, Ewel, J. J., Hector, A., Inchausti, P., Lavorel, S., Lawton, J. H., Lodge, D. M., Loreau, M., & Naeem, S. (2005). Effects of biodiversity on ecosystem functioning: a consensus of current knowledge. *ECOLOGICAL MONOGRAPHS*, 75(1), 3-35. <https://doi.org/10.1890/04-0922>
- Hughes, T. P., Baird, A. H., Bellwood, D. R., Card, M., Connolly, S. R., Folke, C., Grosberg, R., Hoegh-Guldberg, O., Jackson, J. B. C., Kleypas, J., Lough, J. M., Marshall, P., Nystrom, M., Palumbi, S. R., Pandolfi, J. M., Rosen, B., & Roughgarden, J. (2003). Climate change, human impacts, and the resilience of coral reefs. *SCIENCE*, 301(5635), 929-933. <https://doi.org/10.1126/science.1085046>
- Hughes, T. P., Kerry, J. T., Álvarez-Noriega, M., Álvarez-Romero, J. G., Anderson, K. D., Baird, A. H., Babcock, R. C., Beger, M., Bellwood, D. R., Berkelmans, R., Bridge, T. C., Butler, I. R., Byrne, M., Cantin, N. E., Comeau, S., Connolly, S. R., Cumming, G. S., Dalton, S. J., Diaz-Pulido, G., Eakin, C. M., Figueira, W. F., Gilmour, J. P., Harrison, H. B., Heron, S. F., Hoey, A. S., Hobbs, J.-P. A., Hoogenboom, M. O., Kennedy, E. V., Kuo, C.-Y., Lough, J. M., Lowe, R. J., Liu, G., McCulloch, M. T., Malcolm, H. A., McWilliam, M. J., Pandolfi, J. M., Pears, R. J., Pratchett, M. S., Schoepf, V., Simpson, T., Skirving, W. J., Sommer, B., Torda, G., Wachenfeld, D. R., Willis, B. L., & Wilson, S. K. (2017). Global warming and recurrent mass bleaching of corals. *NATURE*, 543(7645), 373-377. <https://doi.org/10.1038/nature21707>
- Hutchinson, G. E., & MacArthur, R. H. (1959). A theoretical ecological model of size distributions among species of animals. *THE AMERICAN NATURALIST*, 93(869), 117-125. <https://doi.org/10.1086/282063>
- Hyslop, E. J. (1980). Stomach contents analysis-a review of methods and their application. *JOURNAL OF FISH BIOLOGY*, 17(4), 411-429. <https://doi.org/10.1111/j.1095-8649.1980.tb02775.x>
- Jankowski, M. W., Gardiner, N. R., & Jones, G. P. (2015). Depth and reef profile: effects on the distribution and abundance of coral reef fishes. *ENVIRONMENTAL BIOLOGY OF FISHES*, 98(5), 1373-1386. <https://doi.org/10.1007/s10641-014-0365-1>

- Job, S. D., & Bellwood, D. R. (2000). Light sensitivity in larval fishes: Implications for vertical zonation in the pelagic zone. *LIMNOLOGY AND OCEANOGRAPHY*, 45(2), 362-371. <https://doi.org/10.4319/lo.2000.45.2.0362>
- Jones, G. P., & McCormick, M. I. (2002). Numerical and energetic processes in the ecology of coral reef fishes. In P. F. Sale (Ed.), *CORAL REEF FISHES* (pp. 221-238). Academic Press. <https://doi.org/https://doi.org/10.1016/B978-012615185-5/50013-X>
- Jones, G. P., McCormick, M. I., Srinivasan, M., Eagle, J. V., & Paine, R. T. (2004). Coral decline threatens fish biodiversity in marine reserves. *PROCEEDINGS OF THE NATIONAL ACADEMY OF SCIENCES*, 101(21), 8251-8253. <https://doi.org/10.1073/pnas.0401277101>
- Jones, G. P., Munday, P. L., & Julian, C., M. (2002). Rarity in coral reef fish communities. In P. F. Sale (Ed.), *CORAL REEF FISHES: DYNAMICS AND DIVERSITY IN A COMPLEX ECOSYSTEM* (pp. 81-101). Academic Press. <https://doi.org/10.1016/B978-012615185-5/50006-2>
- Jones, G. P., & Syms, C. (1998). Disturbance, habitat structure and the ecology of fishes on coral reefs. *AUSTRALIAN JOURNAL OF ECOLOGY*, 23(3), 287-297. <https://doi.org/10.1111/j.1442-9993.1998.tb00733.x>
- Kane, C. N., Brooks, A. J., Holbrook, S. J., & Schmitt, R. J. (2009). Role of microhabitat preference and social organization in determining the spatial distribution of a coral reef fish. *ENVIRONMENTAL BIOLOGY OF FISHES*, 84(1), 1-10. <https://doi.org/10.1007/s10641-008-9377-z>
- Kobayashi, Y., Nakamura, M., Sunobe, T., Usami, T., Kobayashi, T., Manabe, H., Paul-Prasanth, B., Suzuki, N., & Nagahama, Y. (2009). Sex change in the gobiid fish is mediated through rapid switching of gonadotropin receptors from ovarian to testicular portion or vice versa. *ENDOCRINOLOGY*, 150(3), 1503-1511. <https://doi.org/10.1210/en.2008-0569>
- Kobayashi, Y., Sunobe, T., Kobayashi, T., Nagahama, Y., & Nakamura, M. (2005). Gonadal structure of the serial-sex changing gobiid fish *Trimma okinawae*. *DEVELOPMENT, GROWTH AND DIFFERENTIATION*, 47(1), 7-13. <https://doi.org/10.1111/j.1440-169x.2004.00774.x>

- Kotrschal, K., & Thomson, D. A. (1986). Feeding patterns in eastern tropical Pacific blennioid fishes (Teleostei: Tripterygiidae, Labrisomidae, Chaenopsidae, Blenniidae). *OECOLOGIA*, 70(3), 367-378. <https://doi.org/10.1007/BF00379499>
- Kötter, I., Badran, M. I., Richter, C., Wunsch, M., & Rasheed, M. (2001). Endoscopic exploration of Red Sea coral reefs reveals dense populations of cavity-dwelling sponges. *NATURE*, 413(6857), 726-730. <https://doi.org/10.1038/35099547>
- Kramer, M. J., Bellwood, O., & Bellwood, D. R. (2013). The trophic importance of algal turfs for coral reef fishes: The crustacean link. *CORAL REEFS*, 32(2), 575-583. <https://doi.org/10.1007/s00338-013-1009-1>
- Kunishima, T., Saimaru, H., & Tachihara, K. (2021). Reproductive traits of the dwarf gobies *Pandaka trimaculata* and *Pandaka lidwilli* in the western Pacific Ocean: histological evidence from one of the smallest fishes in the world. *JOURNAL OF FISH BIOLOGY*, 98, 733-742. <https://doi.org/10.1111/jfb.14617>
- Kuwamura, T., Sunobe, T., Sakai, Y., Kadota, T., & Sawada, K. (2020). Hermaphroditism in fishes: an annotated list of species, phylogeny, and mating system. *ICHTHYOLOGICAL RESEARCH*, 67(3), 341-360. <https://doi.org/10.1007/s10228-020-00754-6>
- Law, C. S. W., & Sadovy de Mitcheson, Y. (2017). Reproductive biology of black seabream *Acanthopagrus schlegelii*, threadfin porgy *Evynnis cardinalis* and red pargo *Pagrus major* in the northern South China Sea with consideration of fishery status and management needs. *JOURNAL OF FISH BIOLOGY*, 91, 101-125. <https://doi.org/10.1111/jfb.13331>
- Lefèvre, C. D., Nash, K. L., González-Cabello, A., & Bellwood, D. R. (2016). Consequences of extreme life history traits on population persistence: do short-lived gobies face demographic bottlenecks? *CORAL REEFS*, 35(2), 399-409. <https://doi.org/10.1007/s00338-016-1406-3>
- Leis, J. M., & McCormick, M. I. (2002). The biology, behavior, and ecology of the pelagic, larval stage of coral reef fishes. In P. F. Sale (Ed.), *CORAL REEF FISHES: DYNAMICS AND DIVERSITY IN A COMPLEX ECOSYSTEM* (pp. 171-199). Academic Press. <https://doi.org/10.1016/B978-012615185-5/50011-6>

- Lenth, R. V. (2021). emmeans: estimated marginal means, aka least-squares means. R package version 1.7.1-1. <https://CRAN.R-project.org/package=emmeans>
- Lincoln, R. J., Boxshall, G. A., & Clark, P. F. (1982). *DICTIONARY OF ECOLOGY, EVOLUTION, AND SYSTEMATICS* (2 ed.). Cambridge University Press.
- Logan, M. (2010). *BIOSTATISTICAL DESIGN AND ANALYSIS USING R A PRACTICAL GUIDE* (1st ed. ed.). Wiley-Blackwell.
- Longenecker, K., & Langston, R. (2005). Life history of the Hawaiian blackhead triplefin, *Enneapterygius atriceps* (Blennioidei, Tripterygiidae). *ENVIRONMENTAL BIOLOGY OF FISHES*, 73, 243-251. <https://doi.org/10.1007/s10641-004-5332-9>
- Lönnstedt, O. M., & McCormick, M. I. (2013). Ultimate predators: Lionfish have evolved to circumvent prey risk assessment abilities. *PLOS ONE*, 8(10), 1-8. <https://doi.org/10.1371/journal.pone.0075781>
- Loto, O. O., Ajibare, A. O., & Abah, J. P. (2021). Gut contents, feeding ecology and condition factor of *Sarotherodon melanotheron* inhabiting Lagos Lagoon, Nigeria. *INTERNATIONAL JOURNAL OF SCIENCE FOR GLOBAL SUSTAINABILITY*, 7(2), 69.
- Lowe, J. R., Russ, G. R., Bucol, A. A., Abesamis, R. A., & Choat, J. H. (2021). Geographic variability in the gonadal development and sexual ontogeny of *Hemigymnus*, *Cheilinus*, and *Oxycheilinus* wrasses among Indo-Pacific coral reefs. *JOURNAL OF FISH BIOLOGY*, 99, 1348-1363. <https://doi.org/10.1111/jfb.14842>
- Luciani, B., Edson Fontes de, O., & Erivelto, G. (2005). Ecomorphology of fish locomotion with focus on neotropical species. *ACTA SCIENTIARUM BIOLOGICAL SCIENCES*, 27(4), 371-381. <https://doi.org/10.4025/actascibiolsci.v27i4.1271>
- MacArthur, R. H. (1958). Population ecology of some warblers of northeastern coniferous forests. *ECOLOGY*, 39(4), 599-619. <https://doi.org/10.2307/1931600>
- Magnhagen, C. (1988). Changes in foraging as a response to predation risk in two gobiid fish species, *Pomatoschistus minutus* and *Gobius niger*. *MARINE ECOLOGY PROGRESS SERIES* 49, 21-26. <https://doi.org/10.3354/meps049021>

- Magnuson, J. J. (1978). Chapter 4 - Locomotion by Scombrid fishes: Hydromechanics, morphology, and behavior. In W. S. Hoar & D. J. Randall (Eds.), *FISH PHYSIOLOGY* (Vol. 7, pp. 239-313). Academic Press. [https://doi.org/https://doi.org/10.1016/S1546-5098\(08\)60166-1](https://doi.org/https://doi.org/10.1016/S1546-5098(08)60166-1)
- Mallela, J. (2007). Coral reef encruster communities and carbonate production in cryptic and exposed habitats along a gradient of terrestrial disturbance. *CORAL REEFS*, 26, 775-785. <https://doi.org/10.1007/s00338-007-0260-8>
- Manabe, H., Ishimura, M., Shinomiya, A., & Sunobe, T. (2007). Field evidence for bi-directional sex change in the polygynous gobiid fish *Trimma okinawae*. *JOURNAL OF FISH BIOLOGY*, 70, 600-609. <https://doi.org/10.1111/j.1095-8649.2007.01338.x>
- Manabe, H., Matsuoka, M., Goto, K., Dewa, S.-I., Shinomiya, A., Sakurai, M., & Sunobe, T. (2008). Bi-directional sex change in the gobiid fish *Trimma* sp.: does size-advantage exist? *BEHAVIOUR*, 145(1), 99-113. <https://doi.org/10.1163/156853908782687214>
- Manabe, H., Toyoda, K., Nagarnoto, K., Dewa, S., Sakurai, M., Hagiwara, K., Shinomiya, A., & Sunobe, T. (2013). Bidirectional sex change in seven species of *Priolepis* (Actinopterygii: Gobiidae). *BULLETIN OF MARINE SCIENCE*, 89(2), 635-642. <https://doi.org/10.5343/bms.2012.1050>
- Marnane, M. J., & Bellwood, D. R. (2002). Diet and nocturnal foraging in cardinalfishes (Apogonidae) at One Tree Reef, Great Barrier Reef, Australia. *MARINE ECOLOGY PROGRESS SERIES* 231, 261-268. <https://doi.org/10.3354/meps231261>
- Marshall, N. J., Cortesi, F., de Busserolles, F., Siebeck, U. E., & Cheney, K. L. (2019). Colours and colour vision in reef fishes: Past, present and future research directions. *JOURNAL OF FISH BIOLOGY*, 95(1), 5-38. <https://doi.org/10.1111/jfb.13849>
- Marzluff, J. M., & Dial, K. P. (1991). Life history correlates of taxonomic diversity. *ECOLOGY*, 72(2), 428-439. <https://doi.org/10.2307/2937185>



- Maxfield, J. M., & Cole, K. S. (2019a). Patterns of structural change in gonads of the divine dwarfgoby *Eviota epiphanes* as they sexually transition. *JOURNAL OF FISH BIOLOGY*, 94, 142-153. <https://doi.org/10.1111/jfb.13883>
- Maxfield, J. M., & Cole, K. S. (2019b). Structural changes in the ovotestis of the bidirectional hermaphrodite, the blue-banded goby (*Lythrypnus dalli*), during transition from ova production to sperm production. *ENVIRONMENTAL BIOLOGY OF FISHES*, 102(11), 1393-1404. <https://doi.org/10.1007/s10641-019-00914-2>
- May, R. M. (1978). The dynamics and diversity of insect faunas. In L. A. Mound & N. Waloff (Eds.), *DIVERSITY OF INSECT FAUNAS*. Blackwell Scientific Publications. <https://doi.org/doi:10.7208/9780226115504-037>
- McCormick, M. I. (1998). Ontogeny of diet shifts by a microcarnivorous fish, *Cheilodactylus spectabilis*: Relationship between feeding mechanics, microhabitat selection and growth. *MARINE BIOLOGY*, 132(1), 9-20. <https://doi.org/10.1007/s002270050367>
- McCormick, M. I., & Holmes, T. H. (2006). Prey experience of predation influences mortality rates at settlement in a coral reef fish, *Pomacentrus amboinensis*. *JOURNAL OF FISH BIOLOGY*, 68(3), 969-974. <https://doi.org/10.1111/j.0022-1112.2006.00982.x>
- McCormick, M. I., & Manassa, R. (2008). Predation risk assessment by olfactory and visual cues in a coral reef fish. *CORAL REEFS*, 27(1), 105-113. <https://doi.org/10.1007/s00338-007-0296-9>
- McKeon, C. S., Stier, A. C., McIlroy, S. E., & Bolker, B. M. (2012). Multiple defender effects: synergistic coral defense by mutualist crustaceans. *OECOLOGIA*, 169(4), 1095-1103. <https://doi.org/10.1007/s00442-012-2275-2>
- Meekan, M. G., Steven, A. D. L., & Fortin, M. J. (1995). Spatial patterns in the distribution of damselfishes on a fringing coral reef. *CORAL REEFS*, 14(3), 151-161. <https://doi.org/10.1007/BF00367233>
- Mihalitsis, M., & Bellwood, D. R. (2017). A morphological and functional basis for maximum prey size in piscivorous fishes. *PLOS ONE*, 12(9), 1-19. <https://doi.org/10.1371/journal.pone.0184679>



- Mihalitsis, M., & Bellwood, D. R. (2019). Morphological and functional diversity of piscivorous fishes on coral reefs. *CORAL REEFS*, 38(5), 945-954. <https://doi.org/10.1007/s00338-019-01820-w>
- Mihalitsis, M., & Bellwood, D. R. (2021). Functional groups in piscivorous fishes. *ECOLOGY AND EVOLUTION*, 11(18), 12765-12778. <https://doi.org/10.1002/ece3.8020>
- Mihalitsis, M., Hemingson, C. R., Goatley, C. H. R., Bellwood, D. R., & Higham, T. (2021). The role of fishes as food: A functional perspective on predator–prey interactions. *FUNCTIONAL ECOLOGY*, 35(5), 1109-1119. <https://doi.org/10.1111/1365-2435.13779>
- Mihalitsis, M., Morais, R. A., & Bellwood, D. R. (2022). Small predators dominate fish predation in coral reef communities. *PLOS BIOLOGY*, 20(11), 1-14. <https://doi.org/10.1371/journal.pbio.3001898>
- Morais, R. A., & Bellwood, D. R. (2019). Pelagic subsidies underpin fish productivity on a degraded coral reef. *CURRENT BIOLOGY*, 29(9), 1521-1527. <https://doi.org/10.1016/j.cub.2019.03.044>
- Morais, R. A., & Bellwood, D. R. (2020). Principles for estimating fish productivity on coral reefs. *CORAL REEFS*, 39(5), 1221-1231. <https://doi.org/10.1007/s00338-020-01969-9>
- Morita, K., & Matsuishi, T. (2001). A new model of growth back-calculation incorporating age effect based on otoliths. *CANADIAN JOURNAL OF FISHERIES AND AQUATIC SCIENCES*, 58(9), 1805-1811. <https://doi.org/10.1139/cjfas-58-9-1805>
- Mouillot, D., Graham, N. A. J., Villéger, S., Mason, N. W. H., & Bellwood, D. R. (2013). A functional approach reveals community responses to disturbances. *TRENDS IN ECOLOGY & EVOLUTION*, 28(3), 167-177. <https://doi.org/10.1016/j.tree.2012.10.004>
- Moustaka, M., Langlois, T. J., McLean, D., Bond, T., Fisher, R., Fearn, P., Dorji, P., & Evans, R. D. (2018). The effects of suspended sediment on coral reef fish assemblages and feeding guilds of north-west Australia. *CORAL REEFS*, 37(3), 659-673. <https://doi.org/10.1007/s00338-018-1690-1>
- Munday, P. L. (2001). Fitness consequences of habitat use and competition among coral-dwelling fishes. *OECOLOGIA*, 128(4), 585-593. <https://doi.org/10.1007/s004420100690>

- Munday, P. L. (2004). Habitat loss, resource specialization, and extinction on coral reefs. *GLOBAL CHANGE BIOLOGY*, 10(10), 1642-1647. <https://doi.org/10.1111/j.1365-2486.2004.00839.x>
- Munday, P. L., Buston, P. M., & Warner, R. R. (2006). Diversity and flexibility of sex-change strategies in animals. *TRENDS IN ECOLOGY & EVOLUTION*, 21(1), 89-95. <https://doi.org/10.1016/j.tree.2005.10.020>
- Munday, P. L., Caley, M. J., & Geoffrey, P. J. (1998). Bi-Directional Sex Change in a Coral-Dwelling Goby. *BEHAVIORAL ECOLOGY AND SOCIOBIOLOGY* 43(6), 371-377. <https://doi.org/10.1007/s002650050504>
- Munday, P. L., Donelson, J. M., & Domingos, J. A. (2017). Potential for adaptation to climate change in a coral reef fish. *GLOBAL CHANGE BIOLOGY*, 23(1), 307-317. <https://doi.org/10.1111/gcb.13419>
- Munday, P. L., & Jones, G. P. (1998). The ecological implications of small body size among coral-reef fishes. *OCEANOGRAPHY AND MARINE BIOLOGY: AN ANNUAL REVIEW*, 36, 373-411.
- Munday, P. L., Jones, G. P., & Caley, M. J. (1997). Habitat specialisation and the distribution and abundance of coral-dwelling gobies. *MARINE ECOLOGY PROGRESS SERIES* 152, 227-239. <https://doi.org/10.3354/meps152227>
- Munday, P. L., Jones, G. P., & Caley, M. J. (2001). Interspecific competition and coexistence in a guild of coral-dwelling fishes. *ECOLOGY*, 82(8), 2177-2189. [https://doi.org/10.1890/0012-9658\(2001\)082\[2177:ICACIA\]2.0.CO;2](https://doi.org/10.1890/0012-9658(2001)082[2177:ICACIA]2.0.CO;2)
- Munday, P. L., Kuwamura, T., & Kroon, F. J. (2010). Bidirectional sex change in marine fishes. In *REPRODUCTION AND SEXUALITY IN MARINE FISHES: PATTERNS AND PROCESSES* (pp. 241-272). University of California Press. <https://doi.org/10.1525/9780520947979-011>
- Munday, P. L., & Molony, B. W. (2002). The energetic cost of protogynous versus protandrous sex change in the bi-directional sex-changing fish *Gobiodon histrio*. *MARINE BIOLOGY*, 141, 1011-1017. <https://doi.org/10.1007/s00227-002-0904-8>

- Munday, P. L., Pierce, S. J., Jones, G. P., & Larson, H. K. (2002). Habitat use, social organization and reproductive biology of the seawhip goby, *Bryaninops yongei*. *MARINE AND FRESHWATER RESEARCH*, 53, 769-775. <https://doi.org/10.1071/MF01205>
- Munday, P. L., van Herwerden, L., & Dudgeon, C. L. (2004). Evidence for sympatric speciation by host shift in the sea. *CURRENT BIOLOGY*, 14(16), 1498-1504. <https://doi.org/10.1016/j.cub.2004.08.029>
- Muñoz-Arroyo, S., Rodríguez-Jaramillo, C., & Balart, E. F. (2019). The goby *Lythrypnus pulchellus* is a bi-directional sex changer. *ENVIRONMENTAL BIOLOGY OF FISHES*, 102(11), 1377-1391. <https://doi.org/10.1007/s10641-019-00913-3>
- Naeem, S., Knops, J. M. H., Tilman, D., Howe, K. M., Kennedy, T., & Gale, S. (2000). Plant diversity increases resistance to invasion in the absence of covarying extrinsic factors. *OIKOS*, 91(1), 97-108. <https://doi.org/10.1034/j.1600-0706.2000.910108.x>
- Naeem, S., & Li, S. (1997). Biodiversity enhances ecosystem reliability. *NATURE*, 390(6659), 507-509. <https://doi.org/10.1038/37348>
- Nakamura, M., Hourigan, T. F., Yamauchi, K., Nagahama, Y., & Grau, E. G. (1989). Histological and ultrastructural evidence for the role of gonadal steroid hormones in sex change in the protogynous wrasse *Thalassoma duperrey*. *ENVIRONMENTAL BIOLOGY OF FISHES*, 24(2), 117-136. <https://doi.org/10.1007/BF00001282>
- Odum, E. P. (1968). Energy flow in ecosystems: A historical review. *AMERICAN ZOOLOGIST*, 8(1), 11-18. <https://doi.org/10.1093/icb/8.1.11>
- Odum, E. P. (1971). *FUNDAMENTALS OF ECOLOGY* (3 ed.). Saunders.
- Ogle, D. H. (2016). *INTRODUCTORY FISHERIES ANALYSES WITH R*. CRC Press.
- Ogle, D. H. (2019). RFishBC. R package version 0.2.3. <http://derekogle.com/RFishBC>
- Ogle, D. H., Brenden, T. O., & McCormick, J. L. (2017). Chapter 12 - Growth estimation: Growth models and statistical inference. In *AGE AND GROWTH OF FISHES: PRINCIPLES AND TECHNIQUES*. American Fisheries Society.

- Orpin, A. R., & Ridd, P. V. (2012). Exposure of inshore corals to suspended sediments due to wave-resuspension and river plumes in the central Great Barrier Reef: A reappraisal. *CONTINENTAL SHELF RESEARCH*, 47, 55-67. <https://doi.org/10.1016/j.csr.2012.06.013>
- Pepin, P. (1991). Effect of temperature and size on development, mortality, and survival rates of the pelagic early life history stages of marine fish. *CANADIAN JOURNAL OF FISHERIES AND AQUATIC SCIENCES*, 48(3), 503-518. <https://doi.org/10.1139/f91-065>
- Pepin, P. (2023). Feeding by larval fish: how taxonomy, body length, mouth size, and behaviour contribute to differences among individuals and species from a coastal ecosystem. *ICES JOURNAL OF MARINE SCIENCE*, 80(1), 91-106. <https://doi.org/10.1093/icesjms/fsac215>
- Peters, R. H. (1983). *THE ECOLOGICAL IMPLICATIONS OF BODY SIZE*. Cambridge University Press.
- Platt, T., Fuentes-Yaco, C., & Frank, K. T. (2003). Spring algal bloom and larval fish survival. *NATURE*, 423(6938), 398-399. <https://doi.org/10.1038/423398b>
- Pratchett, M. S., Trapon, M., Berumen, M. L., & Chong-Seng, K. (2011). Recent disturbances augment community shifts in coral assemblages in Moorea, French Polynesia. *CORAL REEFS*, 30(1), 183-193. <https://doi.org/10.1007/s00338-010-0678-2>
- Protas, M., Conrad, M., Gross, J. B., Tabin, C., & Borowsky, R. (2007). Regressive evolution in the Mexican cave Tetra, *Astyanax mexicanus*. *CURRENT BIOLOGY*, 17(5), 452-454. <https://doi.org/10.1016/j.cub.2007.01.051>
- R Core Team. (2021). R: A language and environment for statistical computing R *FOUNDATION FOR STATISTICAL COMPUTING*. <https://www.R-project.org/>
- Randall, J. E., & Delbeek, J. C. (2009). Comments on the extremes in longevity in fishes, with special reference to the Gobiidae. *PROCEEDINGS OF THE CALIFORNIA ACADEMY OF SCIENCES*, 60(13), 447-454.
- Ricklefs, R. E. (2010). Life-history connections to rates of aging in terrestrial vertebrates. *PROCEEDINGS OF THE NATIONAL ACADEMY OF SCIENCES*, 107(22), 10314-10319. <https://doi.org/10.1073/pnas.1005862107>

- Rigler, F. H. (1975). The concept of energy flow and nutrient flow between trophic levels. In W. H. van Dobben & R. H. Lowe-McConnell (Eds.), *UNIFYING CONCEPTS IN ECOLOGY: REPORT OF THE PLENARY SESSIONS OF THE FIRST INTERNATIONAL CONGRESS OF ECOLOGY*. (pp. 15-26). Springer Netherlands. [https://doi.org/10.1007/978-94-010-1954-5\\_2](https://doi.org/10.1007/978-94-010-1954-5_2)
- Rizzari, J. R., Frisch, A. J., Hoey, A. S., & McCormick, M. I. (2014). Not worth the risk: apex predators suppress herbivory on coral reefs. *OIKOS*, 123(7), 829-836. <https://doi.org/10.1111/oik.01318>
- Roberts, C. M., McClean, C. J., Veron, J. E. N., Hawkins, J. P., Allen, G. R., McAllister, D. E., Mittermeier, C. G., Schueler, F. W., Spalding, M., Wells, F., Vynne, C., & Werner, T. B. (2002). Marine biodiversity hotspots and conservation priorities for tropical reefs. *SCIENCE*, 295(5558), 1280-1285. <https://doi.org/10.1126/science.1067728>
- Roemer, M. E., & Oliveira, K. (2007). Validation of back-calculation equations for juvenile bluefish with the use of tetracycline-marked otoliths. *FISHERY BULLETIN*, 105(2), 305-309.
- Roff, D. A. (1992). *THE EVOLUTION OF LIFE HISTORIES : THEORY AND ANALYSIS*. Chapman & Hall.
- Ross, S. T. (1986). Resource partitioning in fish assemblages: A review of field studies. *COPEIA*, 1986(2), 352-388. <https://doi.org/10.2307/1444996>
- Ryer, C. H., & Olla, B. L. (1998). Shifting the balance between foraging and predator avoidance: the importance of food distribution for a schooling pelagic forager. *ENVIRONMENTAL BIOLOGY OF FISHES*, 52(4), 467-475. <https://doi.org/10.1023/A:1007433014921>
- Saeki, T., Sakai, Y., Hashimoto, H., & Gushima, K. (2005). Foraging behavior and diet composition of *Trimma caudomaculata* and *Trimma caesiura* (Gobiidae) on coral reefs in Okinawa, Japan. *ICHTHYOLOGICAL RESEARCH*, 52(3), 302-305. <https://doi.org/10.1007/s10228-005-0277-3>

- Sagar, M., Nair, R., & Gop, A. (2019). Stomach content analysis techniques in fishes. In *RECENT ADVANCES IN FISHERY BIOLOGY TECHNIQUES FOR BIODIVERSITY EVALUATION AND CONSERVATION* (Vol. Central Marine Fisheries Research Institute, pp. 104-115).
- Sakakura, Y., Soyano, K., Noakes, D. L. G., & Hagiwara, A. (2006). Gonadal morphology in the self-fertilizing mangrove killifish, *Kryptolebias marmoratus*. *ICHTHYOLOGICAL RESEARCH*, 53, 427-430. <https://doi.org/10.1007/s10228-006-0362-2>
- Sakamoto, Y., Ishiguro, M., & Kitagawa, G. (1986). *AKAIKE INFORMATION CRITERION STATISTICS*. KTK Scientific Publishers.
- Sakurai, M., Nakakoji, S., Manabe, H., Dewa, S.-i., Shinomiya, A., & Sunobe, T. (2009). Bi-directional sex change and gonad structure in the gobiid fish *Trimma yanagitai*. *ICHTHYOLOGICAL RESEARCH*, 56, 82-86. <https://doi.org/10.1007/s10228-008-0054-1>
- Sale, P. F. (2002). *CORAL REEF FISHES: DYNAMICS AND DIVERSITY IN A COMPLEX ECOSYSTEM* (2 ed.). Elsevier.
- Sambilay, V. C. (1990). Interrelationships between swimming speed, caudal fin aspect ratio and body length of fishes. *FISHBYTE*, 8(3), 16-20.
- Santos-Santos, J. H., Audenaert, L., Verheyen, E., & Adriaens, D. (2015). Divergent ontogenies of trophic morphology in two closely related haplochromine cichlids. *JOURNAL OF MORPHOLOGY*, 276, 860-871. <https://doi.org/10.1002/jmor.20385>
- Satheesh, S., & El-Sherbiny, M. M. (2022). Chapter 7 - Ecology, distribution, and biogeography of benthos. In P. S. Godson, S. G. T. Vincent, & S. Krishnakumar (Eds.), *ECOLOGY AND BIODIVERSITY OF BENTHOS* (pp. 251-285). Elsevier. <https://doi.org/https://doi.org/10.1016/B978-0-12-821161-8.00006-4>
- Savage, V. M., Gillooly, J. F., Brown, J. H., West, G. B., & Charnov, E. L. (2004). Effects of body size and temperature on population growth. *THE AMERICAN NATURALIST*, 163(3), 429-441. <https://doi.org/10.1086/381872>
- Savino, J. F., & Stein, R. A. (1989). Behavioural interactions between fish predators and their prey: effects of plant density. *ANIMAL BEHAVIOUR*, 37(2), 311-321. [https://doi.org/10.1016/0003-3472\(89\)90120-6](https://doi.org/10.1016/0003-3472(89)90120-6)

- Schemmel, E., & Cole, K. (2016). Gonad morphology of Susan's dwarfgoby *Eviota susanae*. *JOURNAL OF FISH BIOLOGY*, 89, 1839-1844. <https://doi.org/10.1111/jfb.13058>
- Schneider, C. A., Rasband, W. S., & Eliceiri, K. W. (2012). NIH Image to ImageJ: 25 years of image analysis. *NATURE METHODS*, 9(7), 671-675. <https://doi.org/10.1038/nmeth.2089>
- Schoener, T. W. (1974). Resource partitioning in ecological communities. *SCIENCE*, 185(4145), 27-39. <https://doi.org/10.1126/science.185.4145.27>
- Schoener, T. W. (1983). Field Experiments on Interspecific Competition. *THE AMERICAN NATURALIST*, 122(2), 240-285. <https://doi.org/10.1086/284133>
- Scudder, G. G. (2017). The importance of insects. *INSECT BIODIVERSITY: SCIENCE AND SOCIETY*, 9-43.
- Sebens, K. P. (1987). The ecology of indeterminate growth in animals. *ANNUAL REVIEW OF ECOLOGY AND SYSTEMATICS* 18(1), 371-407.
- Shima, J. S., & Findlay, A. M. (2002). Pelagic larval growth rate impacts benthic settlement and survival of a temperate reef fish. *MARINE ECOLOGY PROGRESS SERIES*, 235, 303-309. <https://doi.org/10.3354/meps235303>
- Shima, J. S., Osenberg, C. W., Noonburg, E. G., Alonzo, S. H., & Swearer, S. E. (2021). Lunar rhythms in growth of larval fish. *PROCEEDINGS OF THE ROYAL SOCIETY B*, 288, 1-9. <https://doi.org/10.1098/rspb.2020.2609>
- Shoji, J., Mitamura, H., Ichikawa, K., Kinoshita, H., & Arai, N. (2017). Increase in predation risk and trophic level induced by nocturnal visits of piscivorous fishes in a temperate seagrass bed. *SCIENTIFIC REPORTS*, 7(3895), 1-10. <https://doi.org/10.1038/s41598-017-04217-3>
- Shpigel, M., & Fishelson, L. (1989). Habitat partitioning between species of the genus *Cephalopholis* (Pisces, Serranidae) across the fringing reef of the Gulf of Aqaba (Red Sea). *MARINE ECOLOGY PROGRESS SERIES*, 58, 17-22. <https://www.jstor.org/elibrary/jcu.edu.au/stable/24842164>



- Silvertown, J. (2004). Plant coexistence and the niche. *TRENDS IN ECOLOGY & EVOLUTION*, 19(11), 605-611. <https://doi.org/10.1016/j.tree.2004.09.003>
- Slattery, M., Gochfeld, D. J., Easson, C. G., & O'Donahue, L. R. K. (2013). Facilitation of coral reef biodiversity and health by cave sponge communities. *MARINE ECOLOGY PROGRESS SERIES* 476, 71-86. <https://doi.org/10.3354/meps10139>
- Smedstad, O. M., & Holm, J. C. (1996). Validation of back-calculation formulae for cod otoliths. *JOURNAL OF FISH BIOLOGY*, 49(5), 973-985. <https://doi.org/10.1111/j.1095-8649.1996.tb00094.x>
- Srinivasan, M. (2003). Depth distributions of coral reef fishes: the influence of microhabitat structure, settlement, and post-settlement processes. *OECOLOGIA*, 137(1), 76-84. <https://doi.org/10.1007/s00442-003-1320-6>
- St. Mary, C. M. (1996). Sex allocation in a simultaneous hermaphrodite, the zebra goby *Lythrypnus zebra* : Insights gained through a comparison with its sympatric congener, *Lythrypnus dalli*. *ENVIRONMENTAL BIOLOGY OF FISHES*, 45, 177-190. <https://doi.org/10.1007/BF00005232>
- Stamps, J. A., Mangel, M., & Phillips, J. A. (1998). A new look at relationships between size at maturity and asymptotic size. *THE AMERICAN NATURALIST*, 152(3), 470-479. <https://doi.org/10.1086/286183>
- Starrs, D., Ebner, B. C., & Fulton, C. J. (2013). Can backcalculation models unravel complex larval growth histories in a tropical freshwater fish? *JOURNAL OF FISH BIOLOGY*, 83(1), 96-110. <https://doi.org/10.1111/jfb.12152>
- Stearns, S. C. (1992). *THE EVOLUTION OF LIFE HISTORIES*. Oxford University Press.
- Stewart, B. D., & Jones, G. P. (2001). Associations between the abundance of piscivorous fishes and their prey on coral reefs: implications for prey-fish mortality. *MARINE BIOLOGY*, 138(2), 383-397. <https://doi.org/10.1007/s002270000468>
- Sundberg, M. A., Loke, K. A., Lowe, C. G., & Young, K. A. (2009). Gonadal restructuring during sex transition in California sheephead: a reclassification three decades after



- initial studies. *BULLETIN, SOUTHERN CALIFORNIA ACADEMY OF SCIENCES*, 108(1), 16-28.  
<https://doi.org/10.3160/0038-3872-108.1.16>
- Sunobe, T. (1995). Embryonic development and larvae of three Gobiid fish, *Trimma okinawae*, *Trimma grammistes* and *Trimmatom* sp. *JAPANESE JOURNAL OF ICHTHYOLOGY*, 42(1), 11-16. <https://doi.org/10.11369/jji1950.42.11>
- Sunobe, T., Nakamura, M., Kobayashi, Y., Kobayashi, T., & Nagahama, Y. (2005). Gonadal structure and P450scc and 3 $\beta$ -HSD immunoreactivity in the gobiid fish *Trimma okinawae* during bidirectional sex change. *ICHTHYOLOGICAL RESEARCH*, 52, 27-32.  
<https://doi.org/10.1007/s10228-004-0250-6>
- Sunobe, T., & Nakazono, A. (1990). Polygynous mating system of *Trimma okinawae* (Pisces: Gobiidae) at Kagoshima, Japan with a note on sex change. *ETHOLOGY*, 84, 133-143.  
<https://doi.org/10.1111/j.1439-0310.1990.tb00790.x>
- Sunobe, T., & Nakazono, A. (1993). Sex change in both directions by alteration of social dominance in *Trimma okinawae* (Pisces: Gobiidae). *ETHOLOGY*, 94, 339-345.  
<https://doi.org/10.1111/j.1439-0310.1993.tb00450.x>
- Sunobe, T., Sado, T., Hagiwara, K., Manabe, H., Suzuki, T., Kobayashi, Y., Sakurai, M., Dewa, S., Matsuoka, M., Shinomiya, A., Fukuda, K., & Miya, M. (2017). Evolution of bidirectional sex change and gonochorism in fishes of the gobiid genera *Trimma*, *Priolepis*, and *Trimmatom*. *THE SCIENCE OF NATURE*, 104, 1-11.  
<https://doi.org/10.1007/s00114-017-1434-z>
- Sunobe, T., Sakaida, S., & Kuwamura, T. (2016). Random mating and protandrous sex change of the platycephalid fish *Thysanophrys celebica* (Platycephalidae). *JOURNAL OF ETHOLOGY*, 34, 15-21. <https://doi.org/10.1007/s10164-015-0439-3>
- Taylor, B. M., Hamilton, R. J., Almany, G. R., & Howard Choat, J. (2018). The world's largest parrotfish has slow growth and a complex reproductive ecology. *CORAL REEFS*, 37, 1197-1208. <https://doi.org/10.1007/s00338-018-1723-9>
- Taylor, B. M., Wakefield, C. B., Newman, S. J., Chinkin, M., & Meekan, M. G. (2021). Unprecedented longevity of unharvested shallow-water snappers in the Indian Ocean. *CORAL REEFS*, 40, 15-19. <https://doi.org/10.1007/s00338-020-02032-3>

- Tebbett, S. B., Goatley, C. H. R., Huertas, V., Mihalitsis, M., & Bellwood, D. R. (2018). A functional evaluation of feeding in the surgeonfish *Ctenochaetus striatus*: The role of soft tissues. *ROYAL SOCIETY OPEN SCIENCE*, 5, 1-10.  
<https://doi.org/10.1098/rsos.171111>
- Tensen, L. (2018). Biases in wildlife and conservation research, using felids and canids as a case study. *GLOBAL ECOLOGY AND CONSERVATION*, 15, 1-10.  
<https://doi.org/https://doi.org/10.1016/j.gecco.2018.e00423>
- Terborgh, J., & Estes, J. A. (2013). *TROPHIC CASCADES: PREDATORS, PREY, AND THE CHANGING DYNAMICS OF NATURE*. Island Press.
- terHorst, C. P., & Munguia, P. (2008). Measuring ecosystem function: consequences arising from variation in biomass-productivity relationships. *COMMUNITY ECOLOGY*, 9(1), 39-44. <https://doi.org/10.1556/ComEc.9.2008.1.5>
- Tokić, G., & Yue, D. K. P. (2019). Energetics of optimal undulatory swimming organisms. *PLOS COMPUTATIONAL BIOLOGY*, 15(10), 1-25.  
<https://doi.org/10.1371/journal.pcbi.1007387>
- Tomatsu, S., Ogiso, K., Fukuda, K., Deki, M., Dewa, S.-I., Manabe, H., Sakurai, M., Shinomiya, A., & Sunobe, T. (2018). Multi-male group and bidirectional sex change in the gobiid fish, *Trimma caudomaculatum*. *ICHTHYOLOGICAL RESEARCH*, 65(4), 502-506. <https://doi.org/10.1007/s10228-018-0631-x>
- Tornabene, L., Ahmadi, G. N., Berumen, M. L., Smith, D. J., Jompa, J., & Pezold, F. (2013). Evolution of microhabitat association and morphology in a diverse group of cryptobenthic coral reef fishes (Teleostei: Gobiidae: *Eviota*). *MOLECULAR PHYLOGENETICS AND EVOLUTION*, 66(1), 391-400.  
<https://doi.org/10.1016/j.ympev.2012.10.014>
- Tornabene, L., Van Tassell, J. L., Robertson, D. R., & Baldwin, C. C. (2016). Repeated invasions into the twilight zone: evolutionary origins of a novel assemblage of fishes from deep Caribbean reefs. *MOLECULAR ECOLOGY*, 25(15), 3662-3682.  
<https://doi.org/10.1111/mec.13704>

- Troyer, E. M., Coker, D. J., & Berumen, M. L. (2018). Comparison of cryptobenthic reef fish communities among microhabitats in the Red Sea. *PEERJ*, 6, 1-15.
- Tsikliras, A. C., & Stergiou, K. I. (2014). Size at maturity of Mediterranean marine fishes. *REVIEWS IN FISH BIOLOGY AND FISHERIES*, 24, 219-268. <https://doi.org/10.1007/s11160-013-9330-x>
- Tsikliras, A. C., & Stergiou, K. I. (2015). Age at maturity of Mediterranean marine fishes. *MEDITERRANEAN MARINE SCIENCE*, 16(1), 5-20. <https://doi.org/10.12681/mms.659>
- Tuset, V. M., García-Díaz, M. M., González, J. A., Lorente, M. J., & Lozano, I. J. (2005). Reproduction and growth of the painted comber *Serranus scriba* (Serranidae) of the Marine Reserve of Lanzarote Island (Central-Eastern Atlantic). *ESTUARINE, COASTAL AND SHELF SCIENCE*, 64, 335-346. <https://doi.org/10.1016/j.ecss.2005.02.026>
- Vigliola, L., Harmelin-Vivien, M., & Meekan, M. G. (2000). Comparison of techniques of back-calculation of growth and settlement marks from the otoliths of three species of *Diplodus* from the Mediterranean Sea. *CANADIAN JOURNAL OF FISHERIES AND AQUATIC SCIENCES*, 57(6), 1291-1299. <https://doi.org/10.1139/f00-055>
- Vigliola, L., & Meekan, M. G. (2009). The back-calculation of fish growth from otoliths. In *TROPICAL FISH OTOLITHS: INFORMATION FOR ASSESSMENT, MANAGEMENT AND ECOLOGY* (pp. 174-211). Springer. [https://doi.org/10.1007/978-1-4020-5775-5\\_6](https://doi.org/10.1007/978-1-4020-5775-5_6)
- Villéger, S., Brosse, S., Mouchet, M., Mouillot, D., & Vanni, M. (2017). Functional ecology of fish: current approaches and future challenges. *AQUATIC SCIENCES*, 79(4), 783-801. <https://doi.org/10.1007/s00027-017-0546-z>
- Warner, R. R. (1975). The adaptive significance of sequential hermaphroditism in animals. *THE AMERICAN NATURALIST*, 109(965), 61-82. <https://doi.org/10.1086/282974>
- Weber, D. C., & Lundgren, J. G. (2009). Assessing the trophic ecology of the Coccinellidae: Their roles as predators and as prey. *BIOLOGICAL CONTROL*, 51(2), 199-214. <https://doi.org/https://doi.org/10.1016/j.biocontrol.2009.05.013>

- West, G. B., Brown, J. H., & Enquist, B. J. (1997). A general model for the origin of allometric scaling laws in biology. *SCIENCE*, 276(5309), 122-126.  
<https://doi.org/10.1126/science.276.5309.122>
- Whiterod, N. S. (2013). The swimming capacity of juvenile Murray cod (*Maccullochella peelii*): an ambush predator endemic to the Murray-Darling Basin, Australia. *ECOLOGY OF FRESHWATER FISH*, 22(1), 117-126.  
<https://doi.org/10.1111/eff.12009>
- Willis, T. (2001). Visual census methods underestimate density and diversity of cryptic reef fish. *JOURNAL OF FISH BIOLOGY*, 59, 1408-1411.  
<https://doi.org/10.1006/jfbi.2001.1721>
- Wilson, D. T., & McCormick, M. I. (1999). Microstructure of settlement-marks in the otoliths of tropical reef fishes. *MARINE BIOLOGY*, 134, 29-41.  
<https://doi.org/10.1007/s002270050522>
- Wilson, D. T., & Meekan, M. G. (2002). Growth-related advantages for survival to the point of replenishment in the coral reef fish *Stegastes partitus* (Pomacentridae). *MARINE ECOLOGY PROGRESS SERIES* 231, 247-260. <https://doi.org/10.3354/meps231247>
- Wilson, J. A., Vigliola, L., & Meekan, M. G. (2009). The back-calculation of size and growth from otoliths: Validation and comparison of models at an individual level. *JOURNAL OF EXPERIMENTAL MARINE BIOLOGY AND ECOLOGY*, 368(1), 9-21.  
<https://doi.org/10.1016/j.jembe.2008.09.005>
- Wilson, S. (2001). Multiscale habitat associations of detritivorous blennies (Blenniidae: Salariae). *CORAL REEFS*, 20(3), 245-251. <https://doi.org/10.1007/s003380100165>
- Wilson, S. K., Dolman, A. M., Cheal, A. J., Emslie, M. J., Pratchett, M. S., & Sweatman, H. P. A. (2009). Maintenance of fish diversity on disturbed coral reefs. *CORAL REEFS*, 28(1), 3-14. <https://doi.org/10.1007/s00338-008-0431-2>

- Wilson, S. K., Fisher, R., & Pratchett, M. S. (2013). Differential use of shelter holes by sympatric species of blennies (Blenniidae). *MARINE BIOLOGY*, *160*(9), 2405-2411. <https://doi.org/10.1007/s00227-013-2235-3>
- Winterbottom, R. (2019). An illustrated key to the described valid species of *Trimma* (Teleostei: Gobiidae). *JOURNAL OF THE OCEAN SCIENCE FOUNDATION*, *34*, 1–61. <https://doi.org/https://doi.org/10.5281/zenodo.3525430>
- Winterbottom, R., Alofs, K. M., & Marseu, A. (2011). Life span, growth and mortality in the western Pacific goby *Trimma benjamini*, and comparisons with *T. nasa*. *ENVIRONMENTAL BIOLOGY OF FISHES*, *91*, 295-301. <https://doi.org/10.1007/s10641-011-9782-6>
- Winterbottom, R., Hanner, R., Burrridge, M., & Zur, M. (2014). A cornucopia of cryptic species - a DNA barcode analysis of the gobiid fish genus *Trimma* (Percomorpha, Gobiiformes). *ZOOKEYS*, *381*(381), 79-111. <https://doi.org/10.3897/zookeys.381.6445>
- Winterbottom, R., & Southcott, L. (2008). Short lifespan and high mortality in the western Pacific coral reef goby *Trimma nasa*. *MARINE ECOLOGY PROGRESS SERIES*, *366*, 203-208. <https://doi.org/10.3354/meps07517>
- Wong, M. Y. L., Munday, P. L., Buston, P. M., & Jones, G. P. (2008). Monogamy when there is potential for polygyny: tests of multiple hypotheses in a group-living fish. *BEHAVIORAL ECOLOGY*, *19*, 353-361. <https://doi.org/10.1093/beheco/arm141>
- Wootton, R. J. (1998). *ECOLOGY OF TELEOST FISHES* (2nd ed. ed.). Kluwer Academic.
- Yamaguchi, S. (2016). Time required for sex change in teleost fishes: Hormonal dynamics shaped by selection. *JOURNAL OF THEORETICAL BIOLOGY*, *407*, 339-348. <https://doi.org/10.1016/j.jtbi.2016.07.012>
- Yamaguchi, S., & Iwasa, Y. (2017). Advantage for the sex changer who retains the gonad of the nonfunctional sex. *BEHAVIORAL ECOLOGY AND SOCIOBIOLOGY*, *71*, 1-12. <https://doi.org/10.1007/s00265-017-2269-5>
- Yamaguchi, S., & Iwasa, Y. (2018). Why is bidirectional sex change rare? *JOURNAL OF THEORETICAL BIOLOGY*, *453*, 136-145. <https://doi.org/10.1016/j.jtbi.2018.05.024>

- Yodzis, P. (2001). Trophic levels. In S. A. Levin (Ed.), *ENCYCLOPEDIA OF BIODIVERSITY* (pp. 264-268). Academic Press. <https://doi.org/10.1016/B978-0-12-384719-5.00145-3>
- Yuen, Y. S., Yamazaki, S. S., Nakamura, T., Tokuda, G., & Yamasaki, H. (2009). Effects of live rock on the reef-building coral *Acropora digitifera* cultured with high levels of nitrogenous compounds. *AQUACULTURAL ENGINEERING*, 41(1), 35-43. <https://doi.org/10.1016/j.aquaeng.2009.06.004>

## Appendix 1: Supplementary Information for Chapter 2

Other data, code, and output available on request from the author

Table A1. 1a) Comparison by Akaike information criterion (AIC) of nine different generalized linear models (glms) / generalized linear mixed-effect models (glmm) of *Trimma benjamini* abundance per 20 x 1 m using AIC. All models included three fixed effects (location, aspect, and depth) and a three-way interaction term. Different random effects (site and transect number) and distributions (Poisson, Negative Binomial, and Tweedie) were tested against each other to determine if their addition significantly improved model fit. The optimum model is indicated in bold. b) Analysis of Variance table assessing the significance of interactions of the optimum model determined in a. Main effects are greyed out if there are significant interactions involving this variable. c) Pairwise comparisons for significant interaction terms in b. Estimate represents mean differences (LCL = 95% lower confidence level, UCL = 95% upper confidence level). df = degrees of freedom. \* represents significant p values ( $\alpha = 0.05$ ).

a)

Model #	Fixed effects	Random effects	Distribution	Link function	df	AIC
1		None			12	1629.70
2		Transect number	Poisson	Log	15	1300.71
3		Site			13	1367.06
4	Location X Aspect X Depth (includes 3-way interaction term)	None			13	795.41
5		Transect number	Negative Binomial	Log	14	797.41
6		Site			14	792.56
7		None			14	769.43
8		Transect number	Tweedie	Log	15	771.43
9		Site			15	<b>759.88</b>

Note: Random effects had variable intercept and fixed slope parameters. Random effects with variable intercept and variable slope parameters were not included due to model convergence issues.

b)

Term	df	Sum sq	Mean sq	F	p
Location	1	243.00	243.00	1.10	0.30

Aspect	1	22360.33	22360.33	100.96	0.00
Depth	2	3270.17	1635.08	7.38	0.00
Location : Aspect	1	249.04	249.04	1.12	0.29
Location : Depth	2	20.17	10.08	0.05	0.96
<b>Aspect : Depth</b>	<b>2</b>	<b>2035.39</b>	<b>1017.69</b>	<b>4.59</b>	<b>0.01*</b>
Location : Aspect : Depth	2	391.69	195.84	0.88	0.42

c)

<i>Interaction</i>		<i>Contrast</i>	<i>Estimate</i>	<i>LCL</i>	<i>UCL</i>	<i>p</i>
<b>Aspect:Depth</b>	<b>Wall</b>	<b>6 m - 4 m</b>	<b>21.56</b>	<b>7.12</b>	<b>35.99</b>	<b>0.00*</b>
Aspect:Depth	Wall	10 m - 6 m	-10.94	-25.38	3.49	0.24
Aspect:Depth	Wall	10 m - 4 m	10.61	-3.83	25.05	0.28
Aspect:Depth	Slope	6 m - 4 m	3.28	-11.16	17.72	0.99
Aspect:Depth	Slope	10 m - 6 m	7.61	-6.83	22.05	0.64
Aspect:Depth	Slope	10 m - 4 m	10.89	-3.55	25.33	0.25
<b>Aspect:Depth</b>	<b>4 m</b>	<b>Wall - Slope</b>	<b>22.78</b>	<b>8.34</b>	<b>37.22</b>	<b>0.00*</b>
<b>Aspect:Depth</b>	<b>6 m</b>	<b>Wall - Slope</b>	<b>41.06</b>	<b>26.62</b>	<b>55.49</b>	<b>0.00*</b>
<b>Aspect:Depth</b>	<b>10 m</b>	<b>Wall - Slope</b>	<b>22.50</b>	<b>8.06</b>	<b>36.94</b>	<b>0.00*</b>



Table A1. 2 a) Comparison by Akaike information criterion (AIC) of six different generalized linear models (glms) / generalized linear mixed-effect models (glmms) of *Trimma capostriatum* abundance per 20 x 1 m using AIC. All models included three fixed effects (location, aspect, and depth) and a three-way interaction term. Different random effects (site and transect number) and distributions (Poisson and Negative Binomial) were tested against each other to determine if their addition significantly improved model fit. Note the Tweedie distribution was not assessed due to model convergence issues. The optimum model is indicated in bold. b) Analysis of Variance table assessing the significance of interactions of the optimum model determined in a. Main effects are greyed out if there are significant interactions involving this variable. c) Pairwise comparisons for significant interaction terms in b. Estimate represents mean differences (LCL = 95% lower confidence level, UCL = 95% upper confidence level). df = degrees of freedom. \* represents significant p values ( $\alpha = 0.05$ ).

a)

<i>Model #</i>	<i>Fixed effects</i>	<i>Random effects</i>	<i>Distribution</i>	<i>Link function</i>	<i>df</i>	<i>AIC</i>
1		None			12	508.05
2		Transect number	Poisson	Log	13	461.31
3	Location X Aspect X Depth	Site			13	482.24
4	(includes 3-way interaction term)	None			13	458.36
5		Transect number	Negative Binomial	Log	14	460.36
6		Site			14	<b>455.64</b>

Note: Random effects had variable intercept and fixed slope parameters. Random effects with variable intercept and variable slope parameters were not included due to model convergence issues.

b)

<i>Term</i>	<i>df</i>	<i>Sum sq</i>	<i>Mean sq</i>	<i>F</i>	<i>p</i>
Location	1	1.33	1.33	0.13	0.71
Aspect	1	313.48	313.48	31.59	0.00
Depth	2	32.91	16.45	1.66	0.20
<b>Location:Aspect</b>	<b>1</b>	<b>327.26</b>	<b>327.26</b>	<b>32.98</b>	<b>0.00*</b>
Location:Depth	2	56.06	28.03	2.82	0.06
<b>Aspect:Depth</b>	<b>2</b>	<b>120.13</b>	<b>60.06</b>	<b>6.05</b>	<b>0.00*</b>

---

Location:Aspect:Depth	2	15.35	7.68	0.77	0.46
-----------------------	---	-------	------	------	------

---

c)

---

<i>Interaction</i>		<i>Contrast</i>	<i>Estimate</i>	<i>LCL</i>	<i>UCL</i>	<i>p</i>
<b>Location:Aspect</b>	<b>Wall</b>	<b>Offshore - Inshore</b>	<b>-3.70</b>	<b>-5.95</b>	<b>-1.46</b>	<b>0.00*</b>
<b>Location:Aspect</b>	<b>Slope</b>	<b>Offshore - Inshore</b>	<b>3.26</b>	<b>1.02</b>	<b>5.50</b>	<b>0.00*</b>
Location:Aspect	Inshore	Wall - Slope	0.07	-2.17	2.32	1.00
<b>Location:Aspect</b>	<b>Offshore</b>	<b>Wall - Slope</b>	<b>-6.89</b>	<b>-9.13</b>	<b>-4.65</b>	<b>0.00*</b>
Aspect:Depth	Wall	6 m – 4 m	-0.39	-3.45	2.67	1.00
Aspect:Depth	Wall	10 m – 6 m	-0.94	-4.00	2.11	0.95
Aspect:Depth	Wall	10 m – 4 m	-1.33	-4.39	1.72	0.80
Aspect:Depth	Slope	6 m – 4 m	-0.56	-3.61	2.50	0.99
<b>Aspect:Depth</b>	<b>Slope</b>	<b>10 m – 6 m</b>	<b>3.61</b>	<b>0.55</b>	<b>6.67</b>	<b>0.01</b>
Aspect:Depth	Slope	10 m – 4 m	3.06	-0.00	6.11	0.05
Aspect:Depth	4 m	Wall - Slope	-2.00	-5.06	1.06	0.41
Aspect:Depth	6 m	Wall - Slope	-1.83	-4.89	1.22	0.51
<b>Aspect:Depth</b>	<b>10 m</b>	<b>Wall - Slope</b>	<b>-6.39</b>	<b>-9.45</b>	<b>-3.33</b>	<b>0.00</b>

---

Table A1. 3 a) Comparison by Akaike information criterion (AIC) of six different generalized linear models (glms) / generalized linear mixed-effect models (glmm) of *Trimma yanoi* abundance per 20 x 1 m using AIC. All models included three fixed effects (location, aspect, and depth) and a three-way interaction term. Different random effects (site and transect number) and distributions (Poisson and Negative Binomial) were tested against each other to determine if their addition significantly improved model fit. Note the Tweedie distribution was not assessed due to model convergence issues. The optimum model is indicated in bold. b) Analysis of Variance table assessing the significance of interactions of the optimum model determined in a. Main effects are greyed out if there are significant interactions involving this variable. c) Pairwise comparisons for significant interaction terms in b. Estimate represents mean differences (LCL = 95% lower confidence level, UCL = 95% upper confidence level). df = degrees of freedom. \* represents significant p values ( $\alpha = 0.05$ ).

a)

<i>Model #</i>	<i>Fixed effects</i>	<i>Random effects</i>	<i>Distribution</i>	<i>Link function</i>	<i>df</i>	<i>AIC</i>
1		None			12	1209.05
2		Transect number	Poisson	Log	13	471.99
3	Location X Aspect X Depth	Site			13	1122.79
4	(includes 3-way interaction term)	None			13	<b>469.15</b>
5		Transect number	Negative Binomial	Log	14	473.99
6		Site			14	470.94

Note: Random effects had variable intercept and fixed slope parameters. Random effects with variable intercept and variable slope parameters were not included due to model convergence issues.

b)

<i>Term</i>	<i>df</i>	<i>Sum sq</i>	<i>Mean sq</i>	<i>F</i>	<i>p</i>
Location	1	2966.26	2966.26	10.50	0.00
Aspect	1	16975.15	16975.15	60.09	0.00
Depth	2	7293.85	3646.93	12.91	0.00
<b>Location : Aspect</b>	<b>1</b>	<b>2966.26</b>	<b>2966.26</b>	<b>10.50</b>	<b>0.00*</b>
Location : Depth	2	1668.07	834.04	2.95	0.06
<b>Aspect : Depth</b>	<b>2</b>	<b>7293.85</b>	<b>3646.93</b>	<b>12.91</b>	<b>0.00*</b>

Location : Aspect : Depth	2	1668.07	834.04	2.95	0.06
---------------------------	---	---------	--------	------	------

c)

<i>Interaction</i>		<i>Contrast</i>	<i>Estimate</i>	<i>LCL</i>	<i>UCL</i>	<i>p</i>
<b>Location:Aspect</b>	<b>Wall</b>	<b>Offshore - Inshore</b>	<b>20.96</b>	<b>9.00</b>	<b>32.92</b>	<b>0.00*</b>
Location:Aspect	Slope	Offshore - Inshore	0.00	-11.96	11.96	1.00
<b>Location:Aspect</b>	<b>Inshore</b>	<b>Wall - Slope</b>	<b>14.59</b>	<b>2.63</b>	<b>26.55</b>	<b>0.01*</b>
<b>Location:Aspect</b>	<b>Offshore</b>	<b>Wall - Slope</b>	<b>35.56</b>	<b>23.60</b>	<b>47.52</b>	<b>0.00*</b>
<b>Aspect:Depth</b>	<b>Wall</b>	<b>6 m - 4 m</b>	<b>24.67</b>	<b>8.37</b>	<b>40.96</b>	<b>0.00*</b>
Aspect:Depth	Wall	10 m - 6 m	15.22	-1.07	31.51	0.08
<b>Aspect:Depth</b>	<b>Wall</b>	<b>10 m - 4 m</b>	<b>39.89</b>	<b>23.60</b>	<b>56.18</b>	<b>0.00*</b>
Aspect:Depth	Slope	6 m - 4 m	0.00	-16.29	16.29	1.00
Aspect:Depth	Slope	10 m - 6 m	0.00	-16.29	16.29	1.00
Aspect:Depth	Slope	10 m - 4 m	0.00	-16.29	16.29	1.00
Aspect:Depth	4 m	Wall - Slope	3.56	-12.74	19.85	0.99
<b>Aspect:Depth</b>	<b>6 m</b>	<b>Wall - Slope</b>	<b>28.22</b>	<b>11.93</b>	<b>44.51</b>	<b>0.00*</b>
<b>Aspect:Depth</b>	<b>10 m</b>	<b>Wall - Slope</b>	<b>43.44</b>	<b>27.15</b>	<b>59.74</b>	<b>0.00*</b>

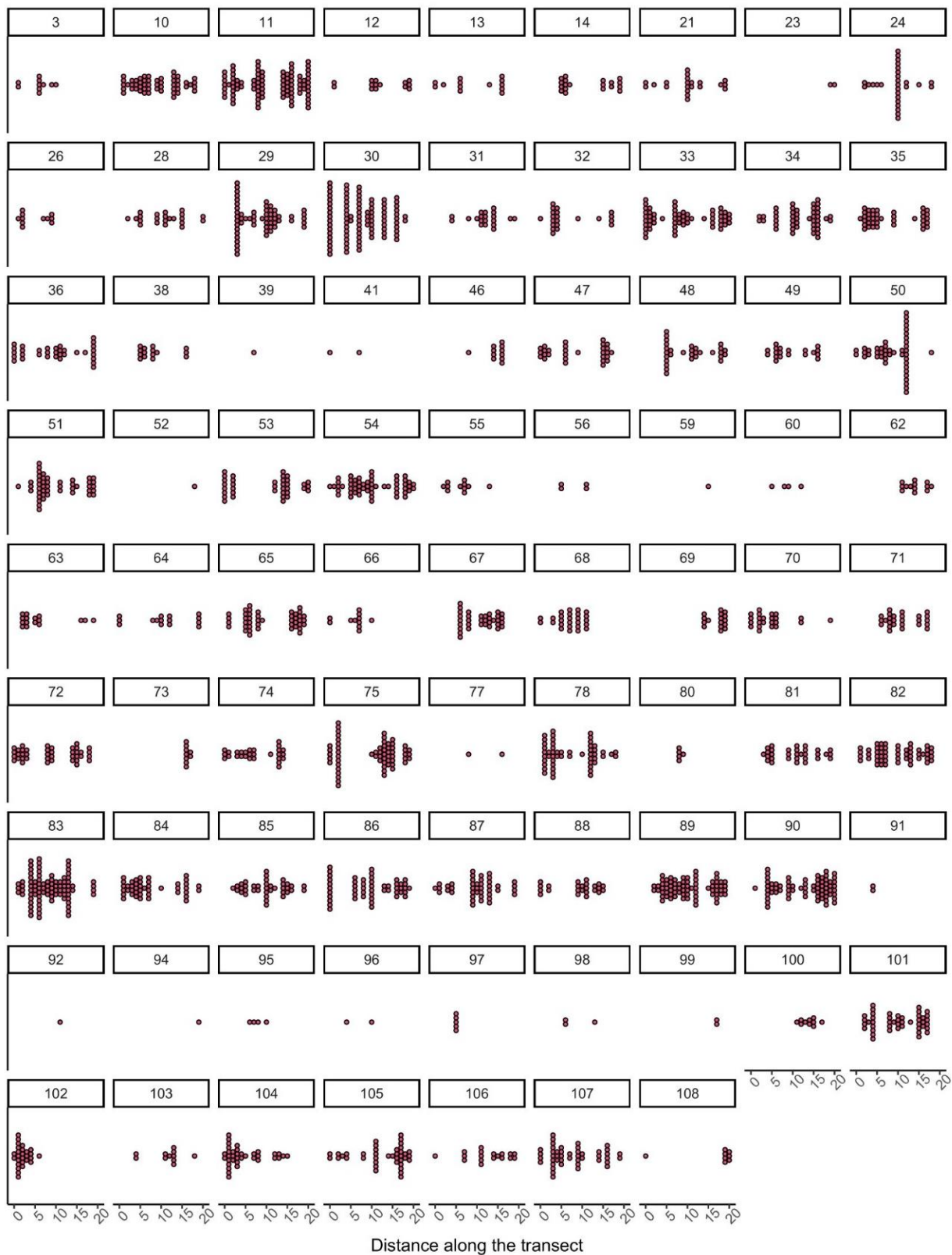


Figure A1. 1 Visual representation of clustering in *T. benjamini*. Each point represents an individual fish. On the x axis is the distance along the transect where each fish was found. Single points represent solitary individuals. The number above each plot is the transect number. Empty transects are not included.

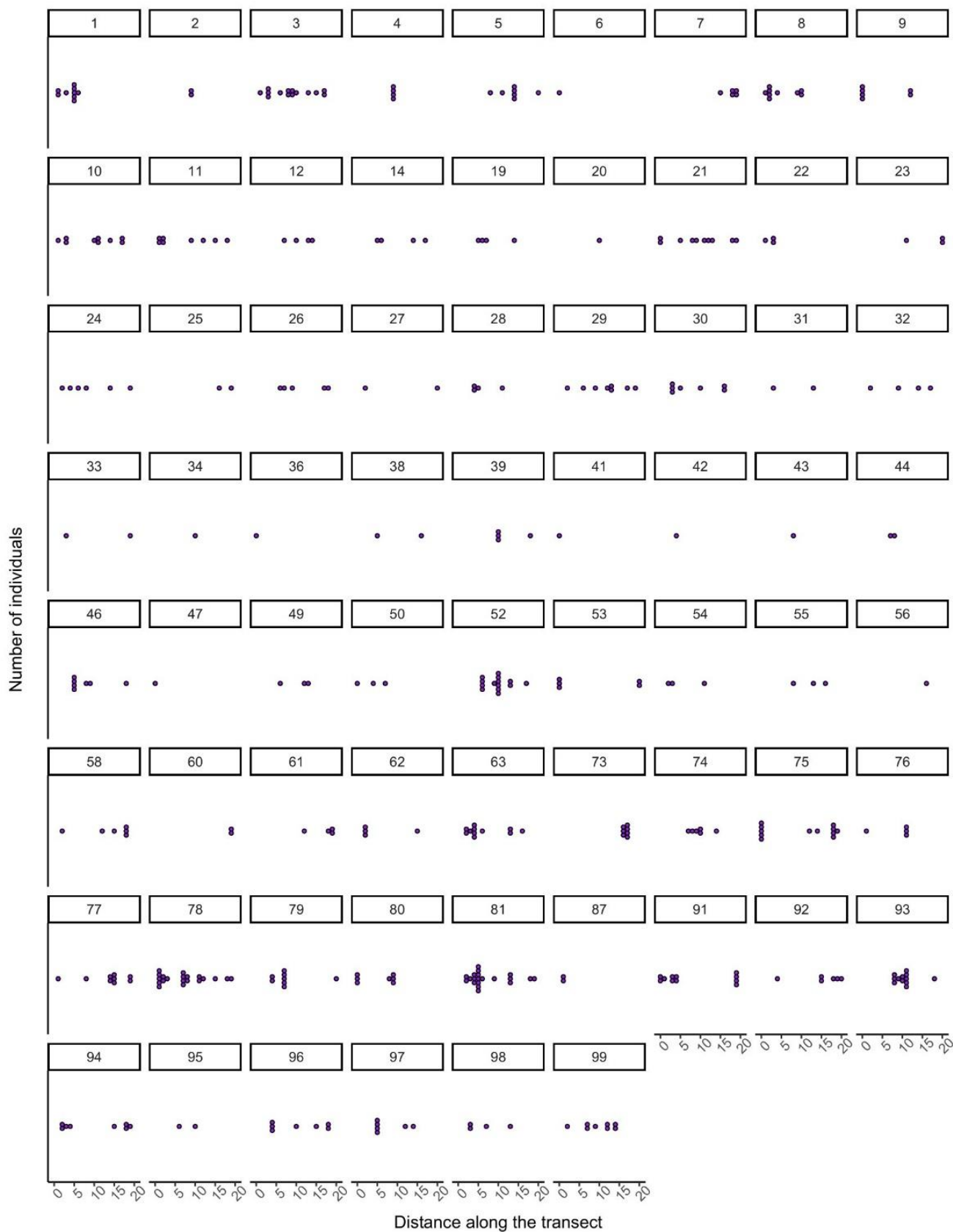


Figure A1. 2 Visual representation of group structure in *T. capostriatum*. Each point represents an individual fish. On the x axis is the distance along the transect where each fish was found. Single points represent solitary individuals. The number above each plot is the transect number. Empty transects are not included.

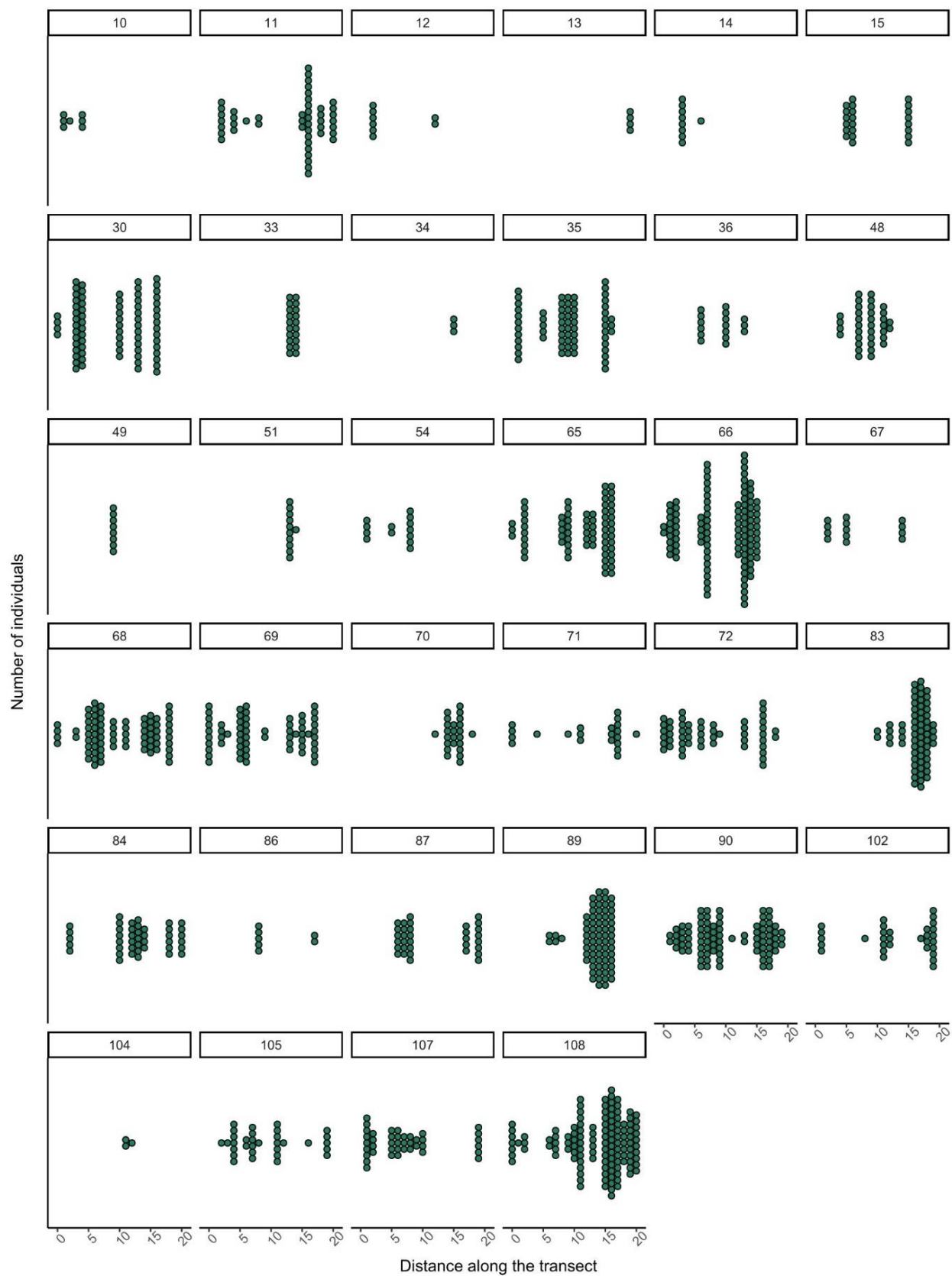


Figure A1. 3 Visual representation of group structure in *T. yanoi*. Each point represents an individual fish. On the x axis is the distance along the transect where each fish was found. Single points represent solitary individuals. The number above each plot is the transect number. Empty transects are not included.

Table A1. 4 a) Comparison by Akaike information criterion (AIC) of 14 different generalized linear models (glms) / generalized linear mixed-effect models (glmms) to model mean cluster size in each species. Different random effects (cluster number, transect number and site) and distributions (Poisson and Negative Binomial) were tested against each other to determine if their addition significantly improved model fit. The optimum model is indicated in bold. b) Pairwise comparisons of cluster size between species, determined using the optimum model in a. Mean differences are represented on a ratio scale (LCL = 95% lower confidence level, UCL = 95% upper confidence level). \* represents significant p values ( $\alpha = 0.05$ ).

a)

<i>Model #</i>	<i>Response ~ Fixed effects</i>	<i>Random effects</i>	<i>Distribution</i>	<i>Link function</i>	<i>df</i>	<i>AIC</i>	
1		None	Poisson	Log	3	4181.45	
2		Cluster number (variable intercept & fixed slope parameters)			4	3081.49	
3		Cluster number (variable intercept & variable slope parameters)			9	<b>2571.91</b>	
4		Transect number (variable intercept & fixed slope parameters)			4	3597.30	
5		Transect number (variable intercept & variable slope parameters)			9	3417.79	
6	Cluster size ~ Species	Site (variable intercept & fixed slope parameters)			4	4107.04	
7		Site (variable intercept & variable slope parameters)			9	4071.04	
8			None	Negative Binomial	Log	4	2646.01
9			Cluster number (variable intercept & fixed slope parameters)			5	2630.58
10			Cluster number (variable intercept & variable slope parameters)			10	2574.01
11			Transect number (variable intercept & fixed slope parameters)			5	2624.05
12			Transect number (variable intercept & variable slope parameter)			10	2623.26
13			Site (variable intercept & fixed slope parameters)			5	2641.00



14	Site (variable intercept & variable slope parameters)	10	2649.59
----	-------------------------------------------------------	----	---------

b)

<i>Contrast</i>	<i>Ratio</i>	<i>LCL</i>	<i>UCL</i>	<i>df</i>	<i>t</i>	<i>p</i>
<i>Trimma benjamini / Trimma capostriatum</i>	2.09	426	1.73	2.52	9.23	<b>0.00*</b>
<i>Trimma benjamini / Trimma yanoi</i>	0.77	426	0.61	0.98	-2.52	<b>0.03*</b>
<i>Trimma capostriatum / Trimma yanoi</i>	0.37	426	0.28	0.49	-8.59	<b>0.00*</b>

Table A1. 5 a) Comparison by Akaike information criterion (AIC) of 10 different generalized linear models (glms) / generalized linear mixed-effect models (glmms) to model mean cluster density (number of individuals per cluster per m<sup>2</sup>) in each species. Different random effects (transect number and site) and distributions (Poisson and Negative Binomial) were tested against each other to determine if their addition significantly improved model fit. The optimum model is indicated in bold. b) Pairwise comparisons of cluster density between species, determined using the optimum model in a. Mean differences are represented on a ratio scale (LCL = 95% lower confidence level, UCL = 95% upper confidence level). \* represents significant p values ( $\alpha = 0.05$ ).

a)

Model #	Response ~ Fixed effects	Random effects	Distribution	Link function	df	AIC
1		None	Poisson	Log	3	1932.43
2		Transect number (variable intercept & fixed slope parameters)			4	1878.60
3		Transect number (variable intercept & variable slope parameters)			9	NA <sup>†</sup>
4	Cluster density ~ Species	Site (variable intercept & variable slope parameters)			4	1923.47
5		Site (variable intercept & fixed slope parameters)			9	1925.14
6		None	Negative Binomial	Log	4	1893.49
7		Transect number (variable intercept & fixed slope parameters)			5	<b>1868.48</b>
8		Transect number (variable intercept & variable slope parameters)			10	NA <sup>†</sup>
9		Site (variable intercept & variable slope parameters)			5	1890.78
10		Site (variable intercept & fixed slope parameters)			10	NA <sup>†</sup>

<sup>†</sup> Model convergence issue

b)

Contrast	Ratio	LCL	UCL	df	t	p
----------	-------	-----	-----	----	---	---

<i>Trimma benjamini</i> / <i>Trimma capostriatum</i>	1.79	1.44	2.21	430	6.44	<b>0.00 *</b>
<i>Trimma benjamini</i> / <i>Trimma yanoi</i>	0.67	0.58	0.78	430	-6.39	<b>0.00 *</b>
<i>Trimma capostriatum</i> / <i>Trimma yanoi</i>	0.38	0.30	0.48	430	-9.87	<b>0.00 *</b>

Table A1. 6 a) Comparison by Akaike information criterion (AIC) of 5 different generalized linear models (glms) / generalized linear mixed-effect models (glmms) to model the proportion of individuals that were solitary in each species. Different random effects (transect number and site) were tested against each other to determine if their addition significantly improved model fit. The optimum model is indicated in bold. b) Pairwise comparisons of the proportion of solitary individuals between species, determined using the optimum model. Mean differences are represented on an odds ratio scale (LCL = 95% lower confidence level, UCL = 95% upper confidence level). df = degrees of freedom. \* represents significant p values ( $\alpha = 0.05$ ).

a)

Model #	Response ~ Fixed effects	Random effects	Distribution	Link Function	df	AIC
1		None	Binomial	Logit	3	925.77
2	Proportion of solitary individuals ~ Species	Transect number (variable intercept & fixed slope parameters)			4	906.60
3		Transect number (variable intercept & variable slope parameters)			9	<b>884.48</b>
4		Site (variable intercept & fixed slope parameters)			4	910.25
5		Site (variable intercept & variable slope parameters)			9	913.59

b)

Contrast	Odds Ratio	LCL	UCL	df	t	p
<i>Trimma benjamini</i> / <i>Trimma capostriatum</i>	0.04	0.01	0.13	3827	-6.72	<b>0.00*</b>
<i>Trimma benjamini</i> /	4.92	0.77	31.66	3827	2.01	0.11

*Trimma yanoi*

<i>Trimma capostriatum</i> / <i>Trimma yanoi</i>	114.59	24.23	541.87	3827	7.16	<b>0.00*</b>
-----------------------------------------------------	--------	-------	--------	------	------	--------------

Table A1. 7 a) Comparison by Akaike information criterion (AIC) of 3 different generalized linear models (glms) / generalized linear mixed-effect models (glmms) to model the proportion of individuals that were present in each microhabitat category in each species. Different random effects (transect number and site) were tested against each other to determine if their addition significantly improved model fit. The optimum model is indicated in bold. b) Analysis of Variance table assessing the significance of interactions of the optimum model determined in a. Main effects are greyed out if there are significant interactions involving this variable. c) Pairwise comparisons for significant interaction terms in b. Mean differences are shown on an odds ratio scale (LCL = 95% lower confidence level, UCL = 95% upper confidence level). df = degrees of freedom. \* represents significant p values ( $\alpha = 0.05$ ).

a)

<i>Model #</i>	<i>Response ~ Fixed effects</i>	<i>Random effects</i>	<i>Distribution</i>	<i>Link Function</i>	<i>df</i>	<i>AIC</i>
1	Proportion of individuals per m <sup>2</sup> ~ Species X Microhabitat	None	Binomial	Logit	18	<b>11504.22</b>
2		Transect number			19	11506.22
3		Site			19	11506.22

Note: Models with random effects with variable intercept & variable slope parameters did not converge and are therefore not included

b)

<i>Term</i>	<i>df</i>	<i>Sum sq</i>	<i>Mean sq</i>	<i>F</i>	<i>p</i>
Species	2	0.00	0.00	0.00	1.00
Microhabitat category	5	325.58	65.12	233.54	0.00
Species : Microhabitat category	10	610.44	61.04	218.93	<b>0.00*</b>

c)

<i>Species</i>	<i>contrast</i>	<i>Odds ratio</i>	<i>LCL</i>	<i>UCL</i>	<i>df</i>	<i>t</i>	<i>p</i>
----------------	-----------------	-------------------	------------	------------	-----------	----------	----------

<i>Trimma benjamini</i>	Overhang / Vertical	0.02	0.01	0.03	6066	-26.98	<b>0.00*</b>
	Overhang / Sloping inwards	0.12	0.08	0.18	6066	-14.03	<b>0.00*</b>
	Overhang / Sloping outwards	0.09	0.06	0.14	6066	-15.93	<b>0.00*</b>
	Overhang / Mounding coral	3.99	1.64	9.73	6066	4.44	<b>0.00*</b>
	Overhang / Other 3D structure	1.78	0.91	3.47	6066	2.45	0.14
	Vertical / Sloping inwards	6.40	5.22	7.86	6066	25.80	<b>0.00*</b>
	Vertical / Sloping outwards	4.91	4.04	5.97	6066	23.26	<b>0.00*</b>
	Vertical / Mounding coral	218.22	97.79	486.99	6066	19.12	<b>0.00*</b>
	Vertical / Other 3D structure	97.09	56.17	167.83	6066	23.83	<b>0.00*</b>
	Sloping inwards / Sloping outwards	0.77	0.61	0.96	6066	-3.40	<b>0.01*</b>
	Sloping inwards / Mounding coral	34.08	15.17	76.58	6066	12.42	<b>0.00*</b>
	Sloping inwards / Other 3D structure	15.16	8.68	26.48	6066	13.91	<b>0.00*</b>
	Sloping outwards / Mounding coral	44.41	19.81	99.55	6066	13.40	<b>0.00*</b>
	Sloping outwards / Other 3D structure	19.76	11.36	34.38	6066	15.36	<b>0.00*</b>
	Mounding coral / Other 3D structure	0.44	0.17	1.16	6066	-2.42	0.15
<i>Trimma capostriatum</i>	Overhang / Vertical	14.31	6.98	29.31	6066	10.57	<b>0.00*</b>
	Overhang / Sloping inwards	5.78	3.38	9.87	6066	9.34	<b>0.00*</b>
	Overhang / Sloping outwards	99.83	18.64	534.60	6066	7.82	<b>0.00*</b>

	Overhang / Mounding coral	1.84	1.19	2.83	6066	4.02	<b>0.00*</b>
	Overhang / Other 3D structure	8.95	4.87	16.46	6066	10.26	<b>0.00*</b>
	Vertical / Sloping inwards	0.40	0.18	0.89	6066	-3.26	<b>0.01*</b>
	Vertical / Sloping outwards	6.98	1.18	41.27	6066	3.12	<b>0.02*</b>
	Vertical / Mounding coral	0.13	0.06	0.27	6066	-8.04	<b>0.00*</b>
	Vertical / Other 3D structure	0.63	0.27	1.46	6066	-1.58	0.61
	Sloping inwards / Sloping outwards	17.28	3.12	95.75	6066	4.75	<b>0.00*</b>
	Sloping inwards / Mounding coral	0.32	0.18	0.55	6066	-5.94	<b>0.00*</b>
	Sloping inwards / Other 3D structure	1.55	0.77	3.11	6066	1.79	0.47
	Sloping outwards / Mounding coral	0.02	0.00	0.10	6066	-6.77	<b>0.00*</b>
	Sloping outwards / Other 3D structure	0.09	0.02	0.51	6066	-3.96	<b>0.00*</b>
	Mounding coral / Other 3D structure	4.87	2.62	9.06	6066	7.26	<b>0.00*</b>
<i>Trimma yanoi</i>	Overhang / Vertical	22.20	14.75	33.40	6066	21.63	<b>0.00*</b>
	Overhang / Sloping inwards	1.41	1.13	1.76	6066	4.35	<b>0.00*</b>
	Overhang / Sloping outwards	347.97	82.76	1463.12	6066	11.62	<b>0.00*</b>
	Overhang / Mounding coral	1395.15	80.21	24266.42	6066	7.23	<b>0.00*</b>
	Overhang / Other 3D structure	1395.11	80.21	24264.74	6066	7.23	<b>0.00*</b>
	Vertical / Sloping inwards	0.06	0.04	0.10	6066	-19.21	<b>0.00*</b>

Vertical / Sloping outwards	15.68	3.58	68.61	6066	5.31	<b>0.00*</b>
Vertical / Mounding coral	62.85	3.54	1115.68	6066	4.10	<b>0.00*</b>
Vertical / Other 3D structure	62.85	3.54	1115.61	6066	4.10	<b>0.00*</b>
Sloping inwards / Sloping outwards	247.07	58.75	1039.00	6066	10.93	<b>0.00*</b>
Sloping inwards / Mounding coral	990.58	56.95	17230.89	6066	6.88	<b>0.00*</b>
Sloping inwards / Other 3D structure	990.55	56.95	17229.70	6066	6.88	<b>0.00*</b>
Sloping outwards / Mounding coral	4.01	0.17	97.29	6066	1.24	0.82
Sloping outwards / Other 3D structure	4.01	0.17	97.28	6066	1.24	0.82
Mounding coral / Other 3D structure	1.00	0.02	56.42	6066	-0.00	1.00

---

Table A1. 8 Comparison by Akaike information criterion (AIC) of 3 different generalized linear models (glms) / generalized linear mixed-effect models (glmms) to model the proportion of m<sup>2</sup> quadrats that were occupied by lone species relative to the proportion of m<sup>2</sup> quadrats occupied by multiple species. Different random effects (transect number and site) were tested against each other to determine if their addition significantly improved model fit. The optimum model is indicated in bold.

<i>Model #</i>	<i>Response ~ Fixed effects</i>	<i>Random effects</i>	<i>Distribution</i>	<i>Link Function</i>	<i>df</i>	<i>AIC</i>
1	Presence/ absence per m <sup>2</sup> quadrat ~ Lone and co-existing species	None			7	<b>3724.96</b>
2	categories (i.e., B, C, Y, B&C, B&Y, C&Y and B&C&Y)*	Transect number	Binomial	<u>Logit</u>	8	3739.38
3		Site			8	3739.38

Note: Models with random effects with variable intercept & variable slope parameters did not converge and are therefore not included

\*B = *Trimma benjamini*, C = *T. capostriatum*, Y = *T. yanoi*

Table A1. 9 Comparison by Akaike information criterion (AIC) of 5 different generalized linear models (glms) / generalized linear mixed-effect models (glmms) to model the proportion of individuals per m<sup>2</sup> quadrats that inhabited the same microhabitat category (overlap) vs different (no overlap) in m<sup>2</sup> quadrats where species co-existed. Different random effects (transect number and site) were tested against each other to determine if their addition significantly improved model fit. The optimum model is indicated in bold.

<i>Model #</i>	<i>Response ~ Fixed effects</i>	<i>Random effects</i>	<i>Distribution</i>	<i>Link Function</i>	<i>df</i>	<i>AIC</i>
1		None			3	<b>353.90</b>
2	Individuals inhabit the same microhabitat category	Transect number (variable intercept & fixed slope parameters for each species)			4	357.90
3	(overlap) vs different (no overlap)	Transect number (variable intercept & variable slope parameters for each species)	Binomial	<u>Logit</u>	9	367.57
4	~ co-existing species categories (i.e., B&C, B&Y, C&Y)*	Site (variable intercept & fixed slope parameters for each species)			4	356.67
5		Site (variable intercept & variable slope parameters for each species)			9	363.25



Table A1. 10 Comparison by Akaike information criterion (AIC) of 3 different generalized linear models (glms) / generalized linear mixed-effect models (glmms) to model the proportion of individuals that interacted vs did not interact with another *Trimma* species, for each species examined. The random effect of site was tested to determine if their accounting for its variation significantly improved model fit. The optimum model is indicated in bold.

<i>Model #</i>	<i>Response ~ Fixed effects</i>	<i>Random effects</i>	<i>Distribution</i>	<i>Link Function</i>	<i>df</i>	<i>AIC</i>
1		None			3	<b>84.32</b>
2	Proportion of individuals that interacted vs did not interact with another <i>Trimma</i> species	Site (variable intercept & fixed slope parameters for each species)	Binomial	Logit	4	86.29
3	Species ~ Species	Site (variable intercept & variable slope parameters for each species)			9	96.24

**Appendix 2: Supplementary Information for Chapter 3**

Other data, code, and output available on request from the author

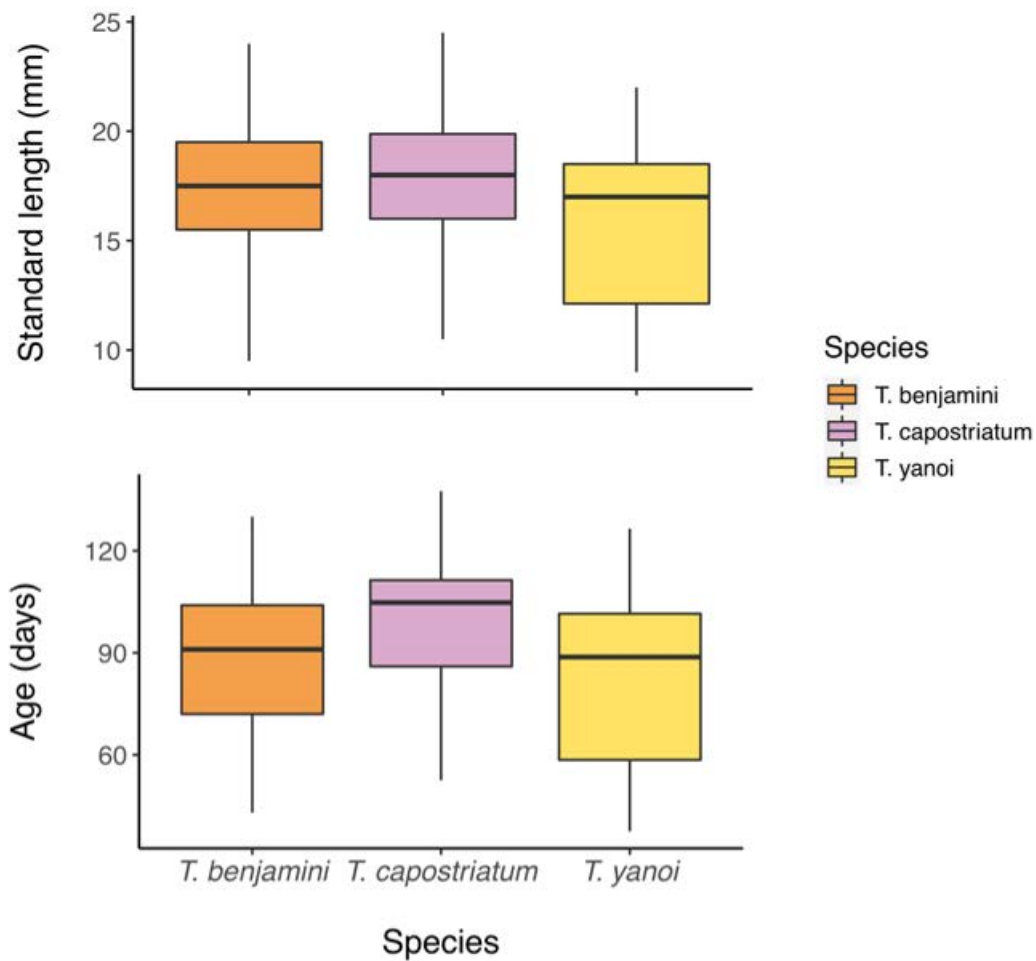


Figure A2. 1 Boxplots of standard length (mm) and age (days) of *Trimma benjamini*, *T. capostriatum* and *T. yanoi*.

### Appendix 3: Supplementary Information for Chapter 4

Other data, code, and output available on request from the author

Table A3. 1 Model equations, explanation of model *terms*, and R functions and packages used

Model and equation	Explanation of terms	R function() R Package
1. Generational turnover  $GT = AM \pm \left( \frac{T_{max} - AM}{2} \right)$	<ul style="list-style-type: none"> <li>• <math>GT</math>: Generational turnover: The potential number of generations able to be produced annually.</li> <li>• <math>AM</math>: The female age at maturity.</li> <li>• <math>T_{max}</math>: The maximum age recorded.</li> </ul>	Base R (R Core Team, 2021)
2. Generalised linear model  $L_i = \beta_0 + \beta_1 x_i$	<ul style="list-style-type: none"> <li>• <math>L_i</math>: The response variable, standard length at age <math>i</math>.</li> <li>• <math>x_i</math>: The predictor variable (age or otolith radius) at observation <math>i</math>.</li> <li>• <math>\beta_0</math> and <math>\beta_1</math>: The coefficients for the intercept and the linear term of <math>x_i</math>.</li> </ul>	glm() stats (R Core Team, 2021)
3. Polynomial model  $L_i = \beta_0 + \beta_1 x_i + \beta_2 x_i^2 \dots + \beta_n x_i^n$	<ul style="list-style-type: none"> <li>• <math>L_i</math>: The response variable (standard length at age <math>i</math>).</li> <li>• <math>x_i</math>: The predictor variable (age or otolith radius) at observation <math>i</math>.</li> <li>• <math>\beta_0, \beta_1, \dots, \beta_n</math>: The coefficients for the intercept and polynomial terms of <math>x_i</math>, where <math>n</math> is The degree of polynomial.</li> </ul>	poly() glm() stats (R Core Team, 2021)  glmTMB() glmTMB (Brooks et al., 2017)

<p>4. Akaike information criterion</p> $AIC = 2k - 2 \ln(\hat{L})$	<ul style="list-style-type: none"> <li>• AIC: Akaike information criterion.</li> <li>• <math>k</math>: The number of parameters in the model, penalising models with more parameters to prevent overfitting.</li> <li>• <math>\hat{L}</math>: The maximum likelihood of the model and is a measure of how well the model predicts the observed data.</li> <li>• <math>\ln</math>: The natural logarithm</li> </ul> <p>A difference in AIC scores of &gt;2 units indicated a significant difference in model fit, with a lower AIC score indicated a better fitting model. If AIC scores were equal, the most conservative model was used.</p>	<p>AIC() stats (R Core Team, 2021)</p>
<p>5. Experimental Modified Fry (MF) model</p> $L_i = a + \exp\left(\frac{\ln(L_{op} - a)}{\frac{[\ln(L_{cpt} - a) - \ln(L_{op} - a)] [\ln(R_i) - \ln(R_{op})]}{[\ln(R_{cpt}) - \ln(R_{op})]}}\right)$	<p>The MF model (Vigliola et al., 2000) has an allometric growth component that allows the otolith–somatic growth relationship to vary with size and includes biologically determined parameters.</p> <ul style="list-style-type: none"> <li>• <math>L_i</math> and <math>R_i</math>: Fish length and otolith radius at age <math>i</math>.</li> <li>• <math>L_{cpt}</math> and <math>R_{cpt}</math>: Fish length and otolith radius at the time of capture.</li> <li>• <math>L_{op}</math> and <math>R_{op}</math>: The biologically determined intercepts of fish length and otolith radius at hatch. <math>L_{op}</math> was taken as 1.855 mm, which is the mean size of <i>T. okinawae</i> (2.01 mm) and <i>T. grammistes</i> (1.7 mm) at hatching (Sunobe, 1995). <math>R_{op}</math> was taken as the mean radius of the first increment for each species.</li> <li>• <math>a</math>: The regression parameter. The experimental version of the model was utilised therefore <math>a</math> was taken as <math>0.75L_{op}</math> (Vigliola &amp; Meekan, 2009).</li> </ul>	<p>backCalc() RfishBC (Ogle, 2019).</p>

<p>6. Biological Intercept (BI) model</p> $L_i = L_{cpt} + (R_i + R_{cpt}) \frac{(L_{cpt} - L_{op})}{(R_{cpt} - R_{op})}$	<ul style="list-style-type: none"> <li>• <math>ln</math>: The natural logarithm</li> </ul> <p>The BI model (Campana, 1990) assumes each individual has a unique length–radius relationship that passes through fish length and otolith radius at hatching and capture.</p> <ul style="list-style-type: none"> <li>• <math>L_i</math> and <math>R_i</math>: Fish length and otolith radius at age <math>i</math>.</li> <li>• <math>L_{cpt}</math> and <math>R_{cpt}</math>: Fish length and otolith radius at the time of capture.</li> <li>• <math>L_{op}</math> and <math>R_{op}</math>: The biologically determined intercepts of fish length and otolith radius at hatch. <math>L_{op}</math> was taken as 1.855 mm, which is the mean size of <i>T. okinawae</i> (2.01 mm) and <i>T. grammistes</i> (1.7 mm) at hatching (Sunobe, 1995). <math>R_{op}</math> was taken as the mean radius of the first increment for each species.</li> </ul>	<p>backCalc() RFishBC (Ogle, 2019).</p>
<p>7. Linear Body Proportional Hypothesis (BPH)</p> $L_i = (a + bR_i) \frac{L_{cpt}}{(a + bR_{cpt})}$	<p>The BPH model (Francis, 1990) assumes there is a constant proportional deviation from the mean body size, and the length – otolith radius lines for each individual passes through fish length and radius at capture</p> <ul style="list-style-type: none"> <li>• <math>L_i</math> and <math>R_i</math>: Fish length and otolith radius at age <math>i</math>.</li> <li>• <math>L_{cpt}</math> and <math>R_{cpt}</math>: Fish length and otolith radius at the time of capture.</li> <li>• <math>a</math> and <math>b</math>: The regression parameters statistically estimated from the fish length – otolith radius regression.</li> </ul>	<p>backCalc() RFishBC (Ogle, 2019).</p>
<p>8. Growth rate</p> $G_i = \frac{dL_i}{dx_i} = \beta_1 + 2\beta_2x_i + 3\beta_3x_i^2 \dots + n\beta_nx_i^{n-1}$	<p>Growth rate was determined by differentiating the optimum growth equation (Vigliola et al., 2000), which followed the formula <math>L_i = \beta_0 + \beta_1x_i + \beta_2x_i^2 \dots + \beta_nx_i^n</math></p>	<p>glmTMB() glmTMB (Brooks et al., 2017)</p>

	<ul style="list-style-type: none"> <li>• <math>x_i</math>: The predictor variable age at observation <math>i</math></li> <li>• <math>G_i</math>: Growth rate at age <math>i</math>, representing the instantaneous rate of change of standard length with respect to age <math>x_i</math>.</li> <li>• <math>\frac{dL_i}{dx_i}</math>: Derivative of length <math>L_i</math> with respect to age <math>x_i</math></li> <li>• <math>\beta_1, \beta_2, \dots, \beta_n</math>: The coefficients of the polynomial terms of <math>x_i</math>, where <math>n</math> is the degree of polynomial</li> </ul>	
--	------------------------------------------------------------------------------------------------------------------------------------------------------------------------------------------------------------------------------------------------------------------------------------------------------------------------------------------------------------------------------------------------------------------------------------------------------------------------------------------------------------------------------------------------------------------------------------------------------	--

Table A3. 2 AIC scores and consumed degrees of freedom for otolith radius and somatic growth models. The optimum model is indicated in bold.

Species	Model	df	AIC
<i>Trimma benjamini</i> (n = 128)	Generalised linear	3.0	402.1
	<b>2<sup>nd</sup> degree polynomial</b>	<b>4.0</b>	<b>398.0</b>
<i>Trimma capostriatum</i> (n = 95)	<b>Generalised linear</b>	<b>3.0</b>	<b>340.9</b>
	2 <sup>nd</sup> degree polynomial	4.0	341.9
<i>Trimma yanoi</i> (n = 116)	Generalised linear	3.0	352.9
	<b>2<sup>nd</sup> degree polynomial</b>	<b>4.0</b>	<b>341.6</b>

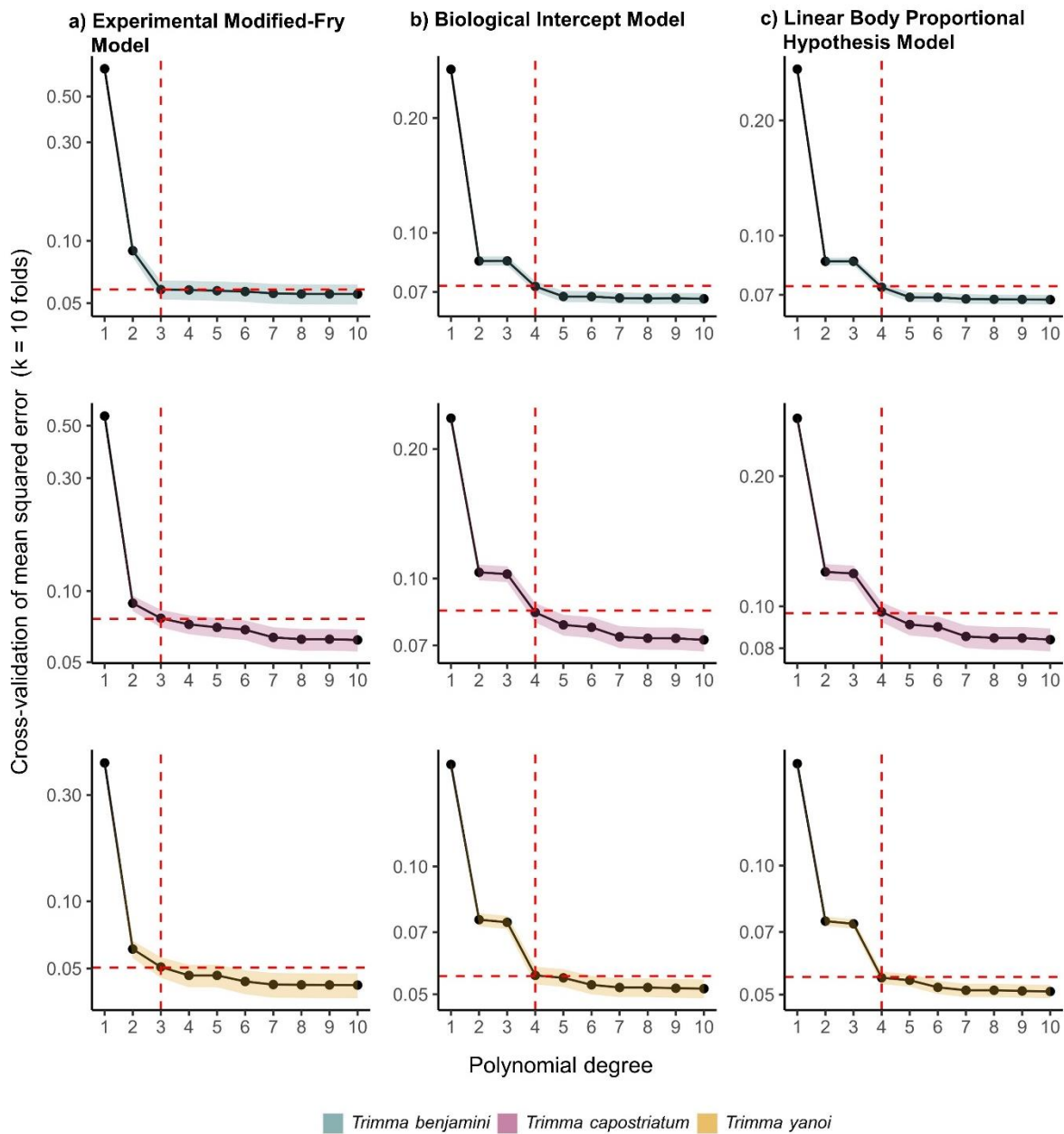


Figure A3. 1 Cross validated mean squared error MSE (k = 10 folds) for linear and polynomial population growth models for MF, BI, and BPH back calculated datasets for *Trimma benjamini*, *T. capostriatum*, and *T. yanoi*. On the x-axis,  $n = 1$  signifies a generalised linear model with no polynomial terms (Table A3. 1.2), while  $n = 2 : 10$  represents polynomial models of the  $n^{th}$  degree (Table A3. 1.3). Red dashed lines indicate the selected optimal polynomial degree along the x-axis and the corresponding MSE on the y-axis. Decreases in MSE greater than 0.01 between polynomial degrees suggest a more suitable model. Note: The y-axis is presented on a logarithmic scale to better visualize the substantial differences in MSE between linear and higher polynomial degrees.

Table A3. 3 Difference in cross-validated mean squared error (MSE) between polynomial degrees for the Experimental Modified Fry model (MF), Biological Intercept model (BI), and the Body Proportional Hypothesis model (BPH). Decreases in MSE greater than 0.01 between polynomial degrees suggest a more suitable model, highlighted in bold.

Species	Polynomial Degree	Difference in MSE between polynomial degrees		
		MF model	BI model	BPH model
<i>Trimma benjamini</i>	1-2	-0.5904	-0.1841	-0.1869
	2-3	<b>-0.0315</b>	0.0000	0.0000
	3-4	-0.0002	<b>-0.0120</b>	<b>-0.0124</b>
	4-5	-0.0005	-0.0043	-0.0043
	5-6	-0.0005	-0.0000	-0.0001
	6-7	-0.0012	-0.0006	-0.0007
	7-8	-0.0003	-0.0002	-0.0001
	8-9	0.0000	0.0001	-0.0000
	9-10	-0.0000	-0.0002	-0.0001
<i>Trimma capostriatum</i>	1-2	-0.4607	-0.1324	-0.1520
	2-3	<b>-0.0121</b>	-0.0010	-0.0010
	3-4	-0.0045	<b>-0.0190</b>	<b>-0.0220</b>
	4-5	-0.0021	-0.0054	-0.0063
	5-6	-0.0016	-0.0010	-0.0011
	6-7	-0.0049	-0.0038	-0.0045
	7-8	-0.0011	-0.0006	-0.0007
	8-9	0.0000	-0.0001	-0.0000
	9-10	-0.0004	-0.0006	-0.0007
<i>Trimma yanoi</i>	1-2	-0.3570	-0.0990	-0.0987
	2-3	<b>-0.0103</b>	-0.0011	-0.0011
	3-4	-0.0042	<b>-0.0185</b>	<b>-0.0184</b>



4-5	0.0000	-0.0007	-0.0007
5-6	-0.0028	-0.0020	-0.0020
6-7	-0.0014	-0.0008	-0.0008
7-8	-0.0001	-0.0000	0.0000
8-9	-0.0001	-0.0002	-0.0002
9-10	-0.0001	-0.0001	-0.0001

---

---

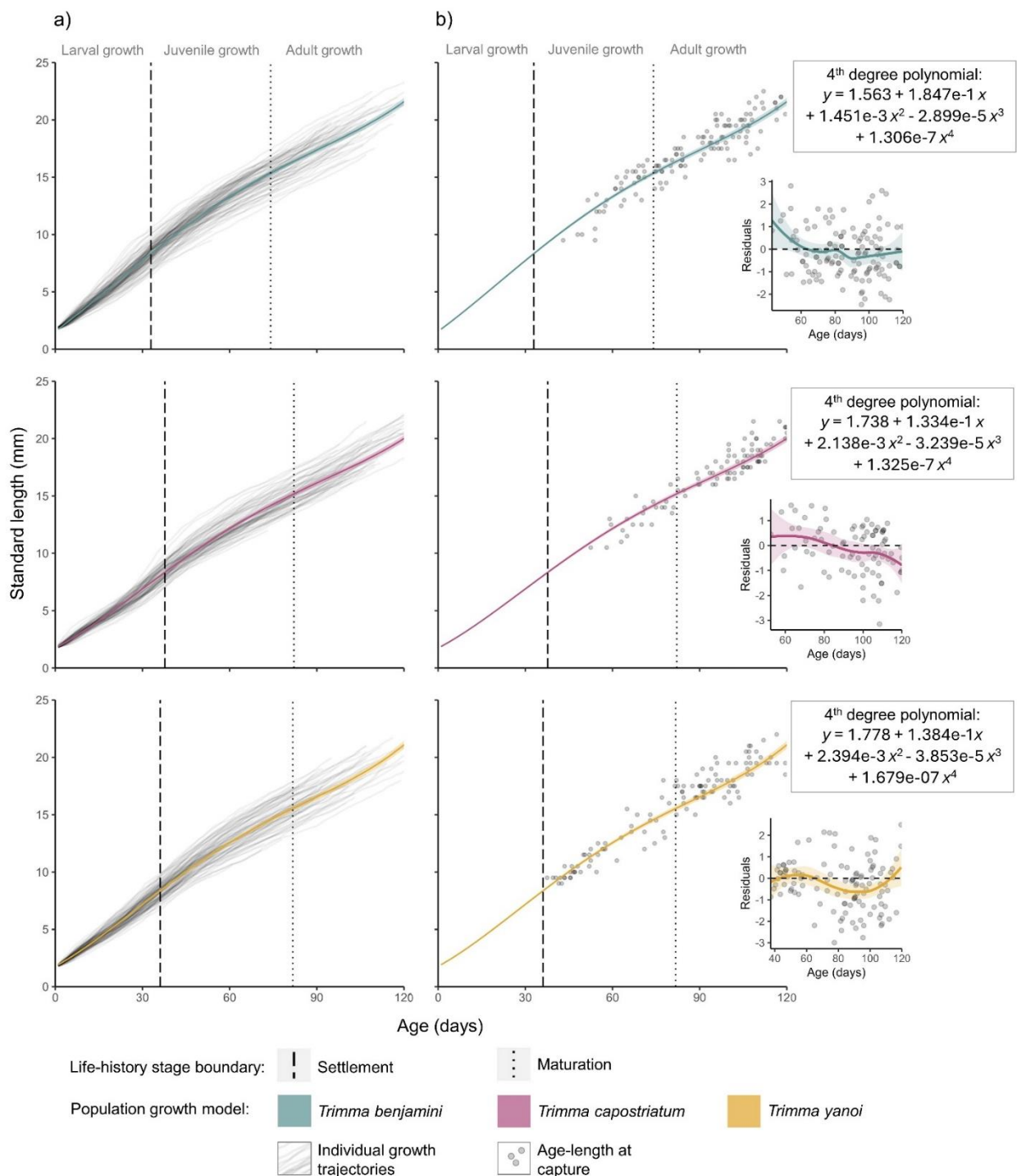


Figure A3. 3 a & b) Modelled population growth curves across larval, juvenile, and adult life history stages for *Trimma benjamini*, *T. capostriatum*, and *T. yanoi*. Solid regression lines and shaded ribbons represent polynomial mixed-effects models of the 4<sup>th</sup> degree  $\pm$  95% confidence intervals (model equations for each species are displayed in a box). Dashed and dotted lines represent the age at settlement and maturity for each species, respectively. a) Displays growth curves fitted to individual fish growth trajectories, back-calculated using the Biological Intercept model. b) Illustrates growth curves against the ages (days) and standard lengths (mm) of individuals at the time of capture. Residual plots depict the deviations between the population growth model and observed ages and lengths at capture, with lines showing a locally weighted regression smoother applied to these residuals.

Table A3. 4 Residual sum of squares (RSS) and mean squared error (MSE) of modelled population growth curves compared to ages and standard lengths at capture, for the Experimental Modified Fry model (MF), the Biological Intercept model (BI), and the Body Proportional Hypothesis model (BPH). *Trimma benjamini* (n = 128), *T. capostriatum* (n = 95) and *T. yanoi* (n = 116).

	Residual sum of squares			Mean squared error		
	MF	BI	<b>BPH</b>	MF	BI	<b>BPH</b>
<i>Trimma benjamini</i>	388.35	164.21	<b>162.43</b>	3.01	1.27	<b>1.26</b>
<i>Trimma capostriatum</i>	284.50	123.81	<b>106.41</b>	2.79	1.21	<b>1.04</b>
<i>Trimma yanoi</i>	296.47	150.67	<b>149.81</b>	2.43	1.24	<b>1.23</b>

Table A3. 5 Pairwise comparisons of growth rate among life history stages (Larvae, Juvenile, and Adult). Estimate represents mean differences (LCL = 95% lower confidence level, UCL = 95% upper confidence level). df = degrees of freedom. \* Represents significant p values ( $\alpha = 0.05$ ).

<i>Species</i>	<i>contrast</i>	<i>estimate</i>	<i>df</i>	<i>LCL</i>	<i>UCL</i>	<i>t</i>	<i>p</i>
<i>Trimma benjamini</i>	Adult - Juvenile	-0.020	129	-0.032	-0.007	-3.707	0.001*
	Adult - Larvae	-0.056	129	-0.070	-0.043	-9.928	0.000*
	Juvenile - Larvae	-0.037	129	-0.051	-0.022	-6.058	0.000*
<i>Trimma capostriatum</i>	Adult - Juvenile	-0.014	124	-0.024	-0.003	-3.102	0.007*
	Adult - Larvae	-0.061	124	-0.072	-0.050	-13.100	0.000*
	Juvenile - Larvae	-0.047	124	-0.058	-0.036	-10.167	0.000*
<i>Trimma yanoi</i>	Adult - Juvenile	-0.014	125	-0.025	-0.003	-2.990	0.009*

Adult - Larvae	-0.059	125	-0.071	-0.048	-11.918	0.000*
Juvenile - Larvae	-0.045	125	-0.057	-0.034	-9.203	0.000*

---

---

### Appendix 4: Supplementary Information for Chapter 5

Other data, code, and output available on request from the author

Table A4. 1 Comparison by Akaike information criterion (AIC) of 5 different generalized linear models (glms) / generalized linear mixed-effect models (glmm) to model the proportion of individuals that were actively feeding in each species. Different random effects were tested against each other to determine if their addition significantly improved model fit. The optimum model is indicated in bold.

<i>Model #</i>	<i>Fixed effects</i>	<i>Random effects</i>	<i>Distribution</i>	<i>Link function</i>	<i>df</i>	<i>AIC</i>
1		None			3	<b>578.3</b>
2		Site (variable intercept & fixed slope parameters for each species)			4	580.1
3	Proportion of individuals that were actively feeding vs. not feeding ~ Species	Depth (variable intercept & fixed slope parameters for each species)	Binomial	Logit	4	580.0
4		Site (variable intercept & variable slope parameters for each species)			9	NA <sup>†</sup>
5		Depth (variable intercept & variable slope parameters for each species)			9	588.4

<sup>†</sup> Model convergence issue

Table A4. 2 Comparison by Akaike information criterion (AIC) of 10 different generalized linear models (glms) / generalized linear mixed-effect models (glmms) to model feeding rate per minute in each species. Different random effects and different distributions were tested against each other to determine if their addition significantly improved model fit. The optimum model is indicated in bold.

<i>Model #</i>	<i>Fixed effects</i>	<i>Random effects</i>	<i>Distribution</i>	<i>Link function</i>	<i>df</i>	<i>AIC</i>
1		None			4	2927.0
2		Site (variable intercept & fixed slope parameters for each species)			5	2907.5
3		Depth (variable intercept & fixed slope parameters for each species)	Gaussian	Identity	5	2912.7
4		Site (variable intercept & variable slope parameters for each species)			10	NA <sup>†</sup>
5		Depth (variable intercept & variable slope parameters for each species)			10	2920.3
6	Feeding rate per minute ~ Species	None			3	2814.3
7		Site (variable intercept & fixed slope parameters for each species)			4	2787.5
8		Depth (variable intercept & fixed slope parameters for each species)	Poisson	Log	4	2792.6
9		Site (variable intercept & variable slope parameters for each species)			5	2786.8
10		Depth (variable intercept & variable slope parameters for each species)			5	2912.7
11		None		Log	4	2801.4

12	Site (variable intercept & fixed slope parameters for each species)		5	<b>2780.6</b>
13	Depth (variable intercept & fixed slope parameters for each species)		5	2786.8
14	Site (variable intercept & variable slope parameters for each species)	Negative Binomial	4	2792.6
15	Depth (variable intercept & variable slope parameters for each species)		10	2794.5

† Model convergence issue

Table A4. 3 Comparison by Akaike information criterion (AIC) of 5 different generalized linear models (glms) / generalized linear mixed-effect models (glmm) to model the proportion pelagic vs benthic feeding events in each species. Different random effects were tested against each other to determine if their addition significantly improved model fit. The optimum model is indicated in bold.

<i>Model #</i>	<i>Fixed effects</i>	<i>Random effects</i>	<i>Distribution</i>	<i>Link function</i>	<i>df</i>	<i>AIC</i>
1		None			3	<b>215.5</b>
2		Site (variable intercept & fixed slope parameters for each species)			4	217.3
3	Proportion of pelagic vs benthic feeding events ~ Species	Depth (variable intercept & fixed slope parameters for each species)	Binomial	Logit	4	215.1
4		Site (variable intercept & variable slope parameters for each species)			9	222.5
5		Depth (variable intercept & variable slope parameters for each species)			9	218.6

Table A4. 4 Proportion of feeding events where food items were pelagic (items floating in the water column captured) or benthic (items picked from the benthos). Predicted proportions are shown in bold and 95 % LCL (lower confidence level) and UCL (upper confidence levels) positioned below were derived from a Binomial distribution (logit link). n represents the number of feeding events observed

Species	Proportion of feeding events (95% LCL, UCL)	
	Pelagic	Benthic
<i>Trimma benjamini</i> (n = 2152)	99.6 % (99.3 %, 99.8 %)	0.4 % (0.7 %, 0.2 %)
<i>Trimma capostriatum</i> (n = 974)	99.8 % (99.2 %, 99.9 %)	0.2 % (0.8 %, 0.1 %)
<i>Trimma yanoi</i> (n = 1178)	99.5 % (98.9 %, 99.8 %)	0.5 % (1.1 %, 0.2 %)

Table A4. 5 Comparison of 3 different generalized linear models (glms) / generalized linear mixed-effect models (glms) for each species to model the proportion of individuals in each interference category. Different random effects were tested against each other to determine if their addition significantly improved model fit. The optimum model is indicated in bold.

Model #	Species	Fixed effects	Random effects	Distribution	Link function	df	AIC
1	<i>Trimma benjamini</i>	Proportion of individuals ~ interference categories	None	Binomial	Logit	4	<b>930.0</b>
2		‘Conspecifics’, ‘Labridae’, or ‘Other’	Site			5	932.0
3			Depth			5	932.0
1	<i>Trimma capostriatum</i>	Proportion of individuals ~ interference category	None	Binomial	Logit	3	<b>242.3</b>
2		“Labridae”	Site			4	244.3
3			Depth			4	242.9
1	<i>Trimma yanoi</i>	Proportion of individuals ~ interference categories	None	Binomial	Logit	4	<b>696.3</b>
2		‘Conspecifics’, ‘Labridae’, or ‘Other’	Site			5	698.3
3			Depth			5	698.3

Note: Random effects had variable intercept and fixed slope parameter. Random effects with variable intercept and variable slope parameters were not included due to model convergence issues.



Table A4. 6 a) Comparison by Akaike information criterion (AIC) of 9 different generalized linear models (glms) / generalized linear mixed-effect models (glmms) for each species to model the feeding rate of individuals in each interference category. Different random effects and distributions were tested against each other to determine if their addition significantly improved model fit. The optimum model is indicated in bold. b) Pairwise comparisons of feeding rate of *Trimma* individuals that were interfered with by a conspecific, Labridae, or other animal, compared to the feeding rate of individuals that did not experience interferences by other animals. Ratio represents fold differences (LCL = 95% lower confidence level, UCL = 95% upper confidence level). df = degrees of freedom. \* Represents significant p values ( $\alpha = 0.05$ ).

a)

Model #	Species	Fixed effects	Random effects	Distribution	Link function	df	AIC
1			None			5	1582.3
2			Site	Gaussian	Identity	6	1580.0
3			Depth			6	1583.4
4	<i>Trimma benjamini</i>	Feeding rate ~ interference categories 'Conspecific', 'Labridae', 'Other' and baseline category 'No interferences'	None			4	1525.4
5			Site	Poisson	Log	5	1518.5
6			Depth			5	1516.4
7			<b>None</b>			5	<b>1503.5</b>
8			Site	Negative Binomial	Log	6	1501.5
9			Depth			6	1504.5
1			None			3	705.9
2			Site	Gaussian	Identity	4	706.5
3			Depth			4	696.7
4	<i>Trimma capostriatum</i>	Feeding rate ~ interference category 'Labridae' and baseline category 'No interferences'	None			2	680.9
5			Site	Poisson	Log	3	678.9
6			Depth			3	672.2
7			None			3	675.2
8			Site	Negative Binomial	Log	4	675.2
9			<b>Depth</b>			4	<b>666.5</b>
1			None			5	1058.1

2		Site	Gaussian	Identity	6	1053.5
3		Depth			6	1058.5
4		None			4	964.4
5	<i>Trimma yanoi</i>	Site	Poisson	Log	5	954.5
6		Depth			5	954.1
7		None			5	948.4
8		Site	Negative Binomial	Log	6	<b>944.9</b>
9		Depth			6	949.0

Note: Random effects had variable intercept and fixed slope parameter. Random effects with variable intercept and variable slope parameters were not included due to model convergence issues.

b)

<i>Species</i>	<i>Contrast</i>	<i>Ratio</i>	<i>df</i>	<i>LCL</i>	<i>UCL</i>	<i>t</i>	<i>p</i>
<i>Trimma benjamini</i>	Conspecific	0.80		0.37	1.74	-0.73	0.88
	<b>Labridae</b>	0.47	364	0.34	0.65	-5.97	<b>0.00*</b>
	Other	0.80		0.52	1.23	-1.34	0.54
<i>Trimma capostriatum</i>	<b>Labridae</b>	0.55	163	0.37	0.84	-2.80	<b>0.01*</b>
<i>Trimma yanoi</i>	Conspecific	1.36		0.80	2.33	1.49	0.44
	<b>Labridae</b>	0.18	253	0.10	0.32	-7.70	<b>0.00*</b>
	Other	0.69		0.28	1.70	-1.06	0.72

Table A4. 7 a) Comparison by Akaike information criterion (AIC) of 6 different generalized linear models (glms) / generalized linear mixed-effect models (glmms) per trait to model the mean relative eye diameter (%  $L_S$ ), relative horizontal gape, elongation index, and caudal fin aspect ratio among species. Different random effects and distributions were tested against each other to determine if their addition significantly improved model fit. The optimum model for each trait is indicated in bold. b) Pairwise comparisons the four traits among *Trimma* species. Estimate represents mean differences (LCL = 95% lower confidence level, UCL = 95% upper confidence level). df = degrees of freedom. \* Represents significant p values ( $\alpha = 0.05$ ).

a)

Model #	Fixed effects	Random effects	Distribution	Link function	df	AIC	
1		None			4	<b>649.8</b>	
2		Site	Gaussian	Identity	5	651.8	
3	Relative eye diameter (% $L_S$ ) ~ Species	None			3	1183.0	
4		Site	Poisson	Log	4	1185.0	
5		None			4	1185.0	
6		Site	Negative Binomial	Log	5	1187.0	
1			None			4	736.3
2			Site	Gaussian	Identity	5	<b>731.3</b>
3	Relative horizontal gape (% $L_S$ ) ~ Species	None			3	1091.0	
4		Site	Poisson	Log	4	1093.0	
5		None			4	1093.0	
6		Site	Negative Binomial	Log	5	1095.0	
1			None			4	18.2
2			Site	Gaussian	Identity	5	<b>9.6</b>
3	Elongation index ~ Species	None			3	978.0	
4		Site	Poisson	Log	4	980.0	
5		None			4	980.0	
6		Site	Negative Binomial	Log	5	982.0	
1		Caudal fin aspect ratio ~ Species	None			4	-109.1
2			Site	Gaussian	Identity	5	<b>-195.1</b>

3	None	Poisson	Log	3	641.0
4	Site			4	643.1
5	None	Negative Binomial	Log	4	643.1
6	Site			5	645.1

Note: Random effects had variable intercept and fixed slope parameter. Random effects with variable intercept and variable slope parameters were not included due to model convergence issues.

b)

<i>Trait</i>	<i>Contrast</i>	<i>Estimate</i>	<i>df</i>	<i>LCL</i>	<i>UCL</i>	<i>t</i>	<i>p</i>
Relative eye diameter (% $L_S$ )	<i>T. benjamini/ T. capostriatum</i>	0.12	264	-0.17	0.42	0.99	0.59
	<b><i>T. benjamini/ T. yanoi</i></b>	-1.18	264	-1.46	-0.91	-10.16	<b>0.00*</b>
	<b><i>T. capostriatum/ T. yanoi</i></b>	-1.31	264	-1.60	-1.02	-10.52	<b>0.00*</b>
Relative horizontal gape (% $L_S$ )	<i>T. benjamini/ T. capostriatum</i>	0.12	264	-0.23	0.46	0.78	0.71
	<b><i>T. benjamini/ T. yanoi</i></b>	-1.14	264	-1.47	-0.82	-8.35	<b>0.00*</b>
	<b><i>T. capostriatum/ T. yanoi</i></b>	-1.26	264	-1.61	-0.92	-8.62	<b>0.00*</b>
Elongation index	<b><i>T. benjamini/ T. capostriatum</i></b>	-0.35	298	-0.43	-0.26	-9.65	<b>0.00*</b>
	<b><i>T. benjamini/ T. yanoi</i></b>	0.21	298	0.13	0.28	6.35	<b>0.00*</b>
	<b><i>T. capostriatum/ T. yanoi</i></b>	0.55	298	0.47	0.63	16.02	<b>0.00*</b>
Caudal fin aspect ratio	<i>T. benjamini/ T. capostriatum</i>	0.01	298	-0.06	0.08	0.27	0.96
	<i>T. benjamini/ T. yanoi</i>	-0.03	298	-0.09	0.04	-0.97	0.60
	<i>T. capostriatum/ T. yanoi</i>	-0.03	298	-0.10	0.03	-1.20	0.46

